

NASA Contractor Report 187213

1N-20

40350

P.191

Reusable Rocket Engine Intelligent Control System Framework Design

(NASA-CR-187213) REUSABLE ROCKET ENGINE
INTELLIGENT CONTROL SYSTEM FRAMEWORK DESIGN,
PHASE 2 Final Report (Rockwell
International Corp.) 191 p

N91-31219

CSCL 21H

Unclass
G3/20 0040350

E. Nemeth, R. Anderson, J. Ols, and M. Olsasky
Rockwell International
Canoga Park, California

September 1991

Prepared for
Lewis Research Center
Under Contract NAS3-25557

NASA
National Aeronautics and
Space Administration

REPORT DOCUMENTATION PAGE			Form Approved OMB No. 0704-0188	
Public reporting burden for this collection of information is estimated to average 1 hour per response, including the time for reviewing instructions, searching existing data sources, gathering and maintaining the data needed, and completing and reviewing the collection of information. Send comments regarding this burden estimate or any other aspect of this collection of information, including suggestions for reducing this burden, to Washington Headquarters Services, Directorate for Information Operations and Reports, 1215 Jefferson Davis Highway, Suite 1204, Arlington, VA 22202-4302, and to the Office of Management and Budget, Paperwork Reduction Project (0704-0188), Washington, DC 20503.				
1. AGENCY USE ONLY (Leave blank)		2. REPORT DATE September 1991		3. REPORT TYPE AND DATES COVERED Final Contractor Report Phase II
4. TITLE AND SUBTITLE Reusable Rocket Engine Intelligent Control System Framework Design			5. FUNDING NUMBERS WU-582-01-41 C-NAS3-25557	
6. AUTHOR(S) E. Nemeth, R. Anderson, J. Ols, and M. Olsasky				
7. PERFORMING ORGANIZATION NAME(S) AND ADDRESS(ES) Rockwell International Rocketdyne Division Canoga Park, California			8. PERFORMING ORGANIZATION REPORT NUMBER None	
9. SPONSORING/MONITORING AGENCY NAMES(S) AND ADDRESS(ES) National Aeronautics and Space Administration Lewis Research Center Cleveland, Ohio 44135-3191			10. SPONSORING/MONITORING AGENCY REPORT NUMBER NASA CR-187213 RI/RD91-158	
11. SUPPLEMENTARY NOTES Project Manager, Walter Merrill, Instrumentation and Control Technology Division, NASA Lewis Research Center, (216) 433-6328.				
12a. DISTRIBUTION/AVAILABILITY STATEMENT Unclassified - Unlimited Subject Category 20			12b. DISTRIBUTION CODE	
13. ABSTRACT (Maximum 200 words) Elements of an advanced functional framework for reusable rocket engine propulsion system control are presented for the space shuttle main engine (SSME) demonstration case. Functional elements of the baseline functional framework are defined in detail. SSME failure modes are evaluated and specific failure modes identified for inclusion in the advanced functional framework diagnostic system. Active control of the SSME start transient is investigated, leading to the identification of a promising approach to mitigating start transient excursions. Key elements of the functional framework are simulated and demonstration cases are provided. Finally, the advanced functional framework for control of reusable rocket engines is presented.				
14. SUBJECT TERMS Intelligent controls; Reusable rocket engines; Space station main engine			15. NUMBER OF PAGES	
			16. PRICE CODE	
17. SECURITY CLASSIFICATION OF REPORT Unclassified	18. SECURITY CLASSIFICATION OF THIS PAGE Unclassified	19. SECURITY CLASSIFICATION OF ABSTRACT Unclassified	20. LIMITATION OF ABSTRACT	

CONTRACT NAS3-25557

**REUSABLE ROCKET ENGINE INTELLIGENT
CONTROL SYSTEM FRAMEWORK DESIGN**

Phase II

FINAL REPORT

RI/RD91-158

21 JUNE, 1991

PREPARED FOR NASA-LEWIS RESEARCH CENTER
CLEVELAND, OHIO 44135



ED NEMETH
RON ANDERSON
JOE OLS
MARK OLSASKY

APPROVED BY



J. M. MARAM
Manager
Advanced Launch System Avionics



A. M. NORMAN
Program Manager
Control and Monitoring Systems

ABSTRACT

Elements of an advanced functional framework for reusable rocket engine propulsion system control are presented for the space shuttle main engine (SSME) demonstration case. Functional elements of the baseline functional framework are defined in detail. SSME failure modes are evaluated and specific failure modes identified for inclusion in the advanced functional framework diagnostic system. Active control of the SSME start transient is investigated, leading to the identification of a promising approach to mitigating start transient excursions. Key elements of the functional framework are simulated and demonstration cases are provided. Finally, the advanced functional framework for control of reusable rocket engines is presented.

Table of Contents

Section 1 Program Overview	1
Section 2 Introduction	2
Section 3 Detailed Baseline Functional Framework	4
3.1 Baseline Functional Framework Revision 2.3	4
3.2 Baseline Functional Framework Descriptions	4
3.3 Conclusions About the Baseline Functional Framework	10
Section 4 Diagnostic Subsystem Definition	11
4.1 Failure Mode Database	11
4.2 Selection of Failure Modes	11
4.3 Failure Accommodation Tables	12
4.4 Excluded Volumes	12
4.5 Failure Accommodation Discussion	13
4.6 Informational Architecture	15
4.7 Diagnostic Subsystem Conclusions	16
Section 5 Investigation of SSME Start Transient Control	17
5.1 The Current SSME Startup Sequence	18
5.2 Overview of Proposed Approaches	22
5.3 Conclusions of the Closed Loop Start Sequence Investigation	33
5.4 Recommendations for Further Study	33
Section 6 ICS Functional Framework Simulation	35
6.1 Engine Level Controller Simulations	35
6.2 Propulsion Level Controller Simulations	39
6.3 ICS Simulation Conclusions	46
Section 7 ICS Advanced Functional Framework	47
7.1 Controller Adaptation Functions	47
7.2 Real Time Control Loop Functions	50
7.3 Advanced Functional Framework Conclusions	52
References	53
Appendix 1 SSME Start Transient Simulation Results - Nominal Case	
Appendix 2 SSME Start Transient Simulation Results - FPOV 1st Notch @ 0.60 sec.	
Appendix 3 SSME Start Transient Simulation Results - FPOV 1st Notch @ 0.75 sec.	
Appendix 4 Listing of SSME Start Transient Control Actions	
Appendix 5 ICS Propulsion Level Simulation - BASIC code listing	

List of Figures

Figure 3-1 ICS Baseline Functional Framework - Revision 2.3

Figure 3-2 Thrust Vector Coordinator

Figure 3-3 Fuel Utilization Coordinator

Figure 3-4 Tank Pressure Coordinator

Figure 3-5 Propulsion Diagnostics and Status

Figure 3-6 Engine Command Generator

Figure 3-7 Primary Actuator Command Generator

Figure 3-8 Thrust and Mixture Ratio Estimator

Figure 3-9 Engine Coordinator

Figure 3-10 Engine Diagnostics

Figure 3-11 Actuator Diagnostics

Figure 3-12 Engine Status

Figure 3-13 Valve Sequence Coordinator

Figure 4-1 Combustion Devices

Figure 4-2 Fuel Turbopumps

Figure 4-3 Oxidizer Turbopumps

Figure 4-4 Pneumatic Controls

Figure 4-5 Propellant Valves

Figure 4-6 Igniters and Sensors

Figure 5-0 SSME Start Sequence

Figure 5-1 SSME Startup Stages of Controllability

Figure 5-2 SSME FPB Temperature During Startup

Figure 5-3 SSME HPFT Discharge Temperature

Figure 5-4 SSME Fuel Preburner Temperature

Figure 5-5 SSME FPB Mixture Ratio

Figure 5-6 FPB Ignition Temperature for Off-Nominal Fuel Inlet Pressures

Figure 5-7 SSME Start Sequence FPOV Position

Figure 5-8 SSME Start Sequence HPFTP Speed

Figure 5-9 FPOV Offset Used to Investigate Engine Controllability

Figure 5-10 OPOV Offset Used to Investigate Engine Controllability

Figure 5-11 Engine Response to FPOV and OPOV Flow Area Offsets

Figure 5-12 Changes in FPOV Notch Timing Used to Investigate Engine Controllability

Figure 5-13 Simulation of Fuel Inlet Pressure Anomaly

Figure 5-14 Summary of Fuel Pressure Anomaly and Accommodation

Figure 5-15 Simulation of MOV Anomaly

Figure 5-16 Summary of MOV Anomaly and Accommodation

Figure 6-1 Overview of ICS Engine Level Simulation

Figure 6-2 Proof of Concept Controller Simulation

Figure 6-3 Multiple Input/Multiple Output Controller Simulation

Figure 6-4 Downthrust Factor Characterization

Figure 6-5 ICS Propulsion Level Simulation - MatrixX Version

Figure 6-6 ICS Propulsion Level Simulation - PC Version

Figure 6-7 ICS Propulsion Level Controller Simulation

Figure 6-8 ICS Propulsion Level Controller Simulation, Case 1 w/o Downthrust Factor

Figure 6-9 ICS Propulsion Level Controller Simulation, Case 1 w/o gn Function

Figure 6-10 ICS Propulsion Level Controller Simulation, Case 1

Figure 6-11 ICS Propulsion Level Controller Simulation, Case 2

Figure 6-12 HPFT Temperature Recorded During SSME Test 902-249

Figure 6-13 ICS Propulsion Level Controller Simulation, Test 902-249

Figure 7-1 ICS Advanced Functional Framework
Figure 7-2 Allowable Thrust Range
Figure 7-3 Weighted Engine Thrust
Figure 7-4 Engine Efficiency Modification to Weighted Engine Thrust
Figure 7-5 Remaining Engine Life Modification to Weighted Engine Thrust
Figure 7-6 Three Engine Thrust Control Strategy
Figure 7-7 Possible Solutions
Figure 7-8 Estimated Engine Parameters
Figure 7-9 Weighted Cost of Each Solution

List of Tables

Table 4-1 FMEA Summary - Combustion Devices
Table 4-2 FMEA Summary - Fuel Turbopumps
Table 4-3 FMEA Summary - Oxidizer Turbopumps
Table 4-4 FMEA Summary - Pneumatic Controls
Table 4-5 FMEA Summary - Propellant Valves
Table 4-6 FMEA Summary - Igniters and Sensors

Table 5-1 Start Transient Changes for Offsets in FPOV and OPOV Flow Areas
Table 5-2 Start Transient Changes for Changes in FPOV Notch Time

Table 6-1 SSME Characterization Results
Table 6-2 Relationship Between Control Valves and Controlled Parameters

SECTION 1 PROGRAM OVERVIEW

The objective of this program is to develop a functional framework for control of reusable rocket engine propulsion systems used on future launch vehicles. The framework applies to a variety of of propulsion systems and provides, in the design, the capability to enhance engine performance with increased reliability, durability, and maintainability. This capability is achieved through improved control algorithms, additional instrumentation, and additional actuation hardware. Specific details of the framework functional elements are based on an SSME derivative engine to facilitate validation on the SSME technology testbed.

The Reusable Rocket Engine Intelligent Control System Framework Design (RREICS) program was funded by the NASA Lewis Research Center in Cleveland, Ohio and was monitored by Dr. W. Merrill.

The RREICS framework design program is one element of an integrated program undertaken by NASA-LeRC to develop an advanced control system for future reusable rocket engine propulsion systems. Other related efforts include the development of a real-time diagnostic system framework (NASA-LeRC), development of specific diagnostic capabilities (under contract to NASA-LeRC), development of detailed fatigue damage models (NASA-LeRC), and advanced control concepts for reusable rocket engines (NASA-LeRC).

The RREICS program is divided into two phases. In the phase I program (Re:1), the requirements for a RREICS functional framework were defined and candidate functional capabilities were identified. The candidate functional capabilities were then evaluated using a figure of merit developed in the RREICS program. Based on the figure of merit evaluations, functional capabilities for the framework were selected and an integrated functional framework was synthesized. The phase I program resulted in a functional framework for control of reusable rocket engine propulsion systems within the constraints of near term capabilities.

The Reusable Rocket Engine Intelligent Control System Framework Design phase II program was a 12 month continuation of the phase I contract. The objectives of the RREICS Phase II program were to demonstrate and further define elements of a functional framework for integrated, adaptable control of reusable rocket engines.

The ICS phase II program consisted of five relatively independent tasks:

1. Definition of the baseline functional framework (BFF) to the next level of detail,
2. Definition of specific SSME diagnostic capabilities,
3. A feasibility study of closed loop control during the SSME start transient,
4. Demonstration of fundamental ICS concepts using dynamic system simulations, and
5. Definition of an ICS advanced functional framework (AFF).

SECTION 2 INTRODUCTION

Conventional rocket engine propulsion systems are a collection of independent engines. Each engine is controlled to the same commanded power level and is operated autonomously. In this configuration, the reliability and useful life of the engine cluster is completely dictated by the "weak link" in the system. The objective of the Reusable Rocket Engine Intelligent Control System (RREICS) functional framework design is to increase the reliability, extend the useful life, and increase the performance of the engine cluster through new control schemes, diagnostic capabilities, and actuation.

The RREICS framework describes a controller that controls the rocket engine cluster as a single system rather than as a collection of independent engines and allows for accommodation of engine degradations at the engine level without affecting the propulsion system output. Control of the engine cluster as a single system enables shortcomings in the operation of an individual engine to be mitigated by offloading some of the workload to other engines. The result is that the "weak link" is operated at lower stress levels, effectively increasing the reliability and useful life of the rocket engine cluster. Engine stress levels are further reduced by functional elements at the engine level that respond to the engine operating conditions.

The effectiveness of engine level functions to increase engine reliability, extend engine life, and increase engine performance is limited by the highly coupled engine configuration. Only relatively minor adjustments to the engine are possible within the constraints of thrust and mixture ratio control. However, propulsion level coordination of the engine cluster enables significant increases in the overall propulsion system reliability, useful life, and performance as described in this report. This report demonstrates fundamental concepts used in the framework and describes the benefits and limitations expected of each functional element.

Section 3 describes the baseline functional framework at the tier two level of detail. The function of each element in the framework is illustrated and a description is included.

Section 4 evaluates the SSME failure modes and effects analysis (FMEA) and critical items list (CIL). Specific diagnostic capabilities for the RREICS are identified and characterized to include required engine measurements, failure severity, and failure likelihood.

Section 5 discusses the feasibility of closed loop control during the SSME start sequence to:

- desensitize the system to engine parameter variations
- desensitize the system to external perturbations or noise
- improve the system performance
- increase the engine reliability
- reduce the SSME maintenance costs

Several approaches by which closed loop control may be used to increase the SSME performance and safety during startup are evaluated to determine if such closed loop control is possible.

Section 6 uses a dynamic model of the SSME and simplified RREICS functions to demonstrate the feasibility and utility of several fundamental concepts in the framework. Concepts demonstrated are: 1) the ability to control engine variables other than thrust and mixture ratio while maintaining a specified thrust and mixture ratio, 2) the ability to rapidly and smoothly change engine variables using a multivariable controller, and 3) the ability to coordinate a three engine cluster using downthrust factors as feedback. Since the goal of the simulation effort is to demonstrate feasibility, no effort to optimize the control gains was expended beyond that required to demonstrate the control feasibility.

Finally, in Section 7, the advanced functional framework is presented and each functional element is described.

SECTION 3 DETAILED BASELINE FUNCTIONAL FRAMEWORK

The baseline functional framework (BFF) defined in Phase I of this contract [Re:1] was modified in Phase II to clearly delineate the ICS diagnostic functions. Additionally, each functional element of the modified BFF was further defined to identify the functional level one tier below that presented in the phase I BFF framework.

3.1 Baseline Functional Framework Revision 2.3

In the BFF Rev. 2.2 (Re:1), the engine level diagnostics are distributed between the Engine Diagnostics and Status (EDS) and Life Extension Coordinator (LEC) functions. The BFF Rev 2.2 EDS and LEC functions are replaced by three functional elements in the BFF Rev. 2.3: 1) Engine Diagnostics, 2) Engine Coordination, and 3) Engine Status. The modified BFF, identified as Revision 2.3, is shown in Figure 3-1. The changes made to create BFF Rev. 2.3 do not alter the overall function of the phase I BFF Rev. 2.2. The only difference is that a distinct and complete engine diagnostic function has been defined.

The Engine Diagnostics function represents all of the engine level diagnostics. Two distinct categories of diagnostics are identified in the BFF: 1) diagnostics of conditions which the engine can resolve or mitigate without changing thrust or mixture ratio (denoted by a C prefix in Figure 3-1), and 2) diagnostics of conditions that cannot be successfully mitigated without a change in thrust or mixture ratio (denoted by an F prefix in Figure 3-1). The distinction between diagnostic functions is made since the C class of conditions can be handled by the engine level while the F class of conditions require intervention by the propulsion level coordinator.

The Engine Coordinator functions interprets the C class diagnostic information and engine variables to identify control actions that optimize the engine operating state according to a set of adaptable rules. The Engine Coordinator has authority over the F7V, CCV, and LPOTV valves only. In addition to directly controlling the F7V, CCV, and LPOTV, the Engine Coordinator modifies the engine state by issuing a high pressure turbine temperature error to the Primary Actuator Command Generator.

The Engine Status function interprets F class diagnostic information and issues an indication of overall engine risk/stress to the propulsion level coordinator. Additionally, the Engine Status function interprets C class diagnostic information since a severe C class condition would require intervention by the propulsion level coordinator to mitigate the problem.

3.2 Tier 2 Baseline Functional Framework Descriptions

The ICS framework is hierarchical in nature with major functional elements divided between a single propulsion level subsystem and engine level subsystems at each engine as shown in Figure 3-1.

The propulsion level ICS acts to maintain vehicle propulsion parameters under both nominal and degraded conditions. Parameters include the overall vehicle thrust, thrust vector, and overall vehicle mixture ratio. Each of these parameters is held to the value commanded by the mission coordinator (a higher level control function) by reconfiguring individual engine operating states to accommodate propulsion system degradations. In addition, the propulsion level ICS is responsible for managing overall propulsion system concerns such as propellant tank pressurization.

The engine level ICS implements the propulsion level commands (thrust, mixture ratio, gimbal angle) in the manner that is least stressful to the engine. In addition, alternate control modes are employed, at the engine level, to meet propulsion level commands in the event of a degraded control system. Details of each functional element are provided in the following descriptions.

PROPULSION LEVEL FUNCTIONS

Thrust Vector Coordinator (Figure 3-2)

The thrust vector coordinator is responsible for achieving and maintaining the vehicle thrust vector required for mission completion. To achieve the required thrust vector, the coordinator commands the thrust level and gimbal angles of each engine. The thrust vector is maintained by comparing the required thrust vector to the estimated thrust vector and modifying the engine commands to resolve any discrepancies.

Since the mission is dependent on the total thrust vector (not individual engine thrust vectors) the coordinator has some degree of flexibility in the position and thrust assigned to each engine. For example, three engines at 100% are equivalent to two engines at 109% and one at 82% (as far as the vehicle is concerned). Therefore, the primary coordination role of the thrust vector coordinator can be described as ensuring that the vector sum of individual engine thrust vectors equals the required vehicle thrust vector.

The thrust vector coordinator has control of all aspects of engine operation that influence the thrust vector, including: thrust, gimbal position, engine lockups, and cutoffs. However, to avoid continuous, minor changes in engine levels, a threshold must generally be exceeded before any action is taken. If an engine degraded status flag indicates that an engine is unable to implement thrust level changes, the thrust vector coordinator will freeze the thrust command for that engine at its current level. This becomes an additional constraint to be considered in the thrust vector calculations.

Relative engine thrusts are based on minimizing the downthrust factors and maximizing specific impulse for the engine cluster while still achieving the required thrust vector. Both the total thrust magnitude and direction of the thrust vector constrain the possible thrust distribution among the cluster. For example, it may be possible to meet the thrust magnitude requirement and still downthrust an engine but a failed gimbal actuator could make it impossible to downthrust the engine and still meet the directional requirement. Therefore, the status of each gimbal actuator, estimated engine thrusts, downthrust factor of each engine, and specific impulse of each engine contribute to the thrust distribution commands.

Decisions to allow an engine to run, lockup an engine, or cutoff an engine are based on the relative risk to the mission. The coordinator risk assessment considers the cutoff factors of other engines, engine redlines, results of upthrusting other engines, time of flight remaining, and the ability to maintain commanded thrust vector (gimbal status, available upthrust capabilities). For example, the risk associated with engine cutoff is significantly higher after the first engine has been cutoff. Therefore, it is expected that a more serious degradation (i.e. higher failure risk) would be required before a second engine was cutoff.

Engine cutoff signals are issued if the engine cutoff factor is sufficiently large that the risk of catastrophic failure outweighs the potential benefits of continued operation. If an engine indicates a failure risk (large cutoff factor) the coordinator compares it to an estimated risk associated with engine cutoff and chooses the less risky option. The coordinator also has the option of locking the engine in its current state if the cutoff factor is trending towards an unacceptable limit. For example, if an engine redline measurement is approaching its cutoff

limit, the thrust vector coordinator may elect to lockup the engine rather than allowing it to be cutoff. Once locked, the thrust value may change, due to changing inlet conditions, and the estimated engine thrust becomes a constraint to be considered while maintaining the required thrust vector. Additionally, if the estimated risk associated with engine cutoff is so large that engine cutoff directly results in a loss of mission, the thrust vector coordinator issues a redline inhibit command to the engine level diagnostics to eliminate the possibility of cutoff under any circumstances.

Fuel Utilization Coordinator (Figure 3-3)

The coordination task is one of maintaining the weighted average of engine mixture ratios (weighted by thrust) equal to the commanded vehicle mixture ratio.

The fuel utilization coordinator is responsible for achieving and maintaining the vehicle mixture ratio at its commanded value. To achieve the commanded mixture ratio, the coordinator issues mixture ratio commands to each engine. The mixture ratio is maintained by comparing the commanded mixture ratio to the estimated mixture ratio and modifying the engine commands to resolve any discrepancies. If an engine degraded status flag indicates that an engine is unable to implement mixture ratio changes, the fuel utilization coordinator will freeze the mixture ratio command for that engine at its current level. The basic strategy is to identify engines that cannot change mixture ratio. These include engines that have been locked or those indicating a degraded status. The weighted mixture ratio for each of these engines is determined. Then, the mixture ratio required to make the weighted average of the cluster equal to the vehicle mixture ratio command is calculated for the remaining engines. The appropriate mixture ratio command is issued to each engine.

Tank Pressure Coordinator (Figure 3-4)

The tank pressure coordinator is responsible for maintaining the vehicle propellant tank pressures at their predetermined values. The tank pressure is maintained by comparing the desired tank pressure to the measured tank pressure and issuing FTV and OTV commands to resolve any discrepancies. The coordination task consists of determining the pressure error in each tank, estimating the change in recirculation flow required to resolve the error, and determining the FTV and OTV commands required to implement the change in total recirculation flow. The contribution to the total recirculation flow, for a given change in the FTV or OTV position, is dependent on the thrust of the associated engine. Therefore, the tank pressure coordinator considers the required recirculation flow, thrust of each engine, current position of FTV and OTV for each engine, lockup status of each engine, and FTV and OTV status for each engine in determining the required actuator commands.

Propulsion Diagnostics and Status (Figure 3-5)

The propulsion diagnostics and status function provides estimates of the measured vehicle thrust vector and mixture ratio to the appropriate coordinators. Diagnostic and status information required for mission level decisions are passed to the mission coordinator. These include: vehicle thrust, mixture ratio, propellant utilization rate, remaining propellents, and a propulsion system risk factor. In addition, the propulsion diagnostic and status function responds to risk assessment requests from the mission coordinator.

The vehicle thrust vector is estimated by the vector sum of individual engine thrust vectors. Individual thrust vectors are determined using the estimated thrust from each engine and measured gimbal angles. The rate of propellant utilization is directly measured by vehicle propellant flowmeters. Mixture ratio is determined by the ratio of the measured propellant flowrates. If a vehicle flowmeter fails, the sum of the engine flowrates is used to estimate the

missing data. Remaining propellents are determined from tank level measurements. If level indicators are lost, subsequent data is estimated by subtracting the integral of the the measured flowrate from the last known value of remaining propellant.

A propulsion system risk factor is used to estimate the risk of operating at the current thrust vector relative to possible abort modes. Issues that impact the risk factor for a specified thrust vector include: the ability to achieve that thrust vector (gimbal and engine statuses), and the thrust, cutoff factor, degraded status, lockup status, and cutoff status for each engine. For example, a configuration where one engine has already been cutoff and a second is indicating an increasing cutoff factor would have a high risk factor. An abort mode in which the second engine could be cutoff, if the cutoff factor continues to increase, would have a much lower risk factor.

Thrust vectors required to implement the possible abort modes are received from the mission coordinator and a propulsion system risk factor is determined for the current thrust vector and each abort mode. These values are sent to the mission coordinator. It is expected that other major vehicle subsystems (e.g. GNC, Payload Management) would also provide estimates of the relative risk associated with possible abort modes and thereby enable the mission coordinator to maximize the likelihood of mission success by minimizing the overall vehicle risk. For example, if a possible abort mode somewhat reduces the risk of catastrophic engine failure but greatly increases the risk of missing an acceptable orbit it would not be implemented.

ENGINE LEVEL FUNCTIONS

Engine Command Generator (Figure 3-6)

The engine command generator is responsible for maintaining the local engine thrust and mixture ratio required by the propulsion level. Propulsion level commands to the engine are each compared to estimates of local thrust and mixture ratio and appropriate commands are issued for the turbopump discharge pressures. The discharge pressures influence propellant flows into the MCC. The commands are sent to the primary actuator command generator and are the fundamental control parameters for the engine.

Primary Actuator Command Generator (Figure 3-7)

The primary actuator command generator implements the turbopump discharge pressure commands. In addition, HPFT temperature is implemented as a secondary control variable since the OPFV enables a tradeoff between HPOT and HPFT temperatures. Based on the errors in each of these variables; FPOV, OPOV, and OPFV positions are determined and issued to the actuators. The control strategy calculates actuator positions resulting in no turbopump discharge pressure errors and minimizing the HPFT temperature error. If an actuator fails, HPFT temperature control is forfeited since it does not impact current mission success. The remaining two actuators are used to maintain turbopump discharge pressure control. For example, if the OPOV fails, turbopump discharge pressure errors are resolved using the FPOV and OPFV at the possible expense of the resulting turbine temperature.

Thrust and Mixture Ratio Estimator (Figure 3-8)

The thrust estimate is based on MCC pressure and is corrected for MCC mixture ratio (estimated by MCC temperature). Redundant transducers are used in the MCC so that no alternate estimation technique is required for thrust. The primary estimate of engine mixture ratio is the ratio of measured oxidizer mass flow rate to fuel mass flow rate into the engine.

Both flows are corrected for propellant temperatures as needed. Since redundant flowmeters pose additional risk to the engine, only single measurements are baselined. If a flowmeter fails, the mixture ratio is estimated analytically using the remaining flowmeter (this is the estimation technique currently used on the SSME).

Engine Coordinator (Figure 3-9)

The Engine Coordinator function controls the F7V, CCV, and LPOTV to maintain certain engine parameters within specified ranges. The parameters selected for coordination, as well as the valves used to control the parameters, can be controlled with relatively little effect on the engine thrust and mixture ratio. The small perturbations in thrust and mixture ratio caused by the Engine Coordination function are accounted for by the Engine Command Generator and are therefore transparent to the propulsion level.

Each parameter is compared to its current acceptable range and an error signal is generated to quantify the compliance with that range. If the parameter falls within its specified range, an error signal of 0.0 is issued. The response of each valve is determined by the weighted sum of the measured errors. The errors are weighted according to the relative change in the coinciding parameter effected by each valve.

A nominal set of parameter ranges are defined to optimize engine performance, minimize wear and damage, and reduce the risk of engine failure. Alternate acceptable ranges are selected based on engine conditions indicated by the Engine Diagnostics function.

The error weighting factors are different if the errors are resolved without using all three valves (F7V, CCV, LPOTV). To accommodate changes in error weighting factors, an alternate set of factors is selected if the F7V, CCV, or LPOTV are locked up by the Actuator Diagnostics function.

Engine Diagnostics (Figure 3-10)

The Engine Diagnostics function reduces engine measurements to quantified conditions and/or degradations of engine components that the Engine Status Function and Engine Coordinator can interpret. Examples of the diagnostic capabilities required are shown in Figure 3-1b, while a more complete list is developed in Section 4.0.

Actuator Diagnostics, Gimbal Diagnostics (Figure 3-11)

The status of each actuator is monitored by the actuator diagnostics module. Actuator commands from the primary actuator command generator, the life extension coordinator, the tank pressure coordinator, and the valve sequence coordinator are used to drive actuator models. The model response is compared to the measured actuator response (monitored using position indicators). Unresponsive actuators are identified as "failed" and locked in their current positions. If a lockup command is received from the thrust vector coordinator, all engine control actuators are locked at their current positions. The gimbal actuator diagnostics are also model based and are the same as the actuator diagnostic functions described above.

Engine Status (Figure 3-12)

The engine status function evaluates key engine health indicators, reports the engine status to the propulsion level controller, and handles engine redlines. Key status indicators sent to the propulsion level are the estimated mixture ratio, the estimated thrust, the specific impulse of the engine, the heat exchanger status, and health indicators (cutoff factor, downthrust factor, and degraded status flag).

Redlines are handled by the Engine Status function. If a redline value is exceeded, a cutoff command is directly issued to the valve sequence coordinator. This is the only engine level cutoff capability and serves as an engine saving "reflex" in the event of rapid engine failures. However, this reflex can be inhibited by the thrust vector coordinator to prevent engine cutoffs that result in a loss of mission.

In addition, the Engine Status functions calculates engine health parameters that act as recommendations to the propulsion level ICS functions. The intention of this feature is to reduce the large amounts of engine data and send only "status" type parameters to the propulsion level. Values sent to the propulsion level include: 1) specific impulse, 2) degraded status, 3) downthrust factor, and 4) cutoff factor. The engine diagnostic function also sends estimated thrust and mixture ratio to the propulsion level where they are used to verify that commands are implemented.

Specific impulse is estimated using the thrust estimate and the measured propellant flowrates. This parameter provides an indication of how efficiently the engine is operating.

The degraded status indicates that the engine is no longer capable of full thrust and mixture ratio throttling. For example, if the FPOV fails, the engine can still maintain closed loop control over the thrust and mixture ratio with the OPOV and the OPFV but can not implement "large" changes in either variable. This parameter is a pass/fail type status and alerts the thrust vector and mixture ratio coordinators that the engine commands should not be changed.

The downthrust factor is a measure that reflects the expected benefit of reducing thrust. Primarily, downthrusting relieves strain on the high pressure turbopumps. Therefore, this factor is defined by measurements indicative of excessive turbopump strain, in other words: speed, torque, turbine temperature, and vibration. These measurements are evaluated for both high pressure turbopumps (HPOTP and HPFTP) and are related to the benefit realized by downthrusting the engine. The overall benefits of incorporating the downthrust factor in the RREICS framework include degraded engine accommodation, risk minimization, and life extension issues.

The cutoff factor is a measure that reflects the risk associated with continued engine operation. Other studies [Re: Health Management System For Rocket Engines, NASA-LeRC] have shown that engine failures are often indicated well before the failure occurs by changes in key engine parameters. The weighted sum of these changes generally increases as the degradation (impending failure) progresses and propagates through the system. It is expected that these values can be roughly correlated to the relative "risk" of engine failure and therefore provide a good source of information for an intelligent system to make engine cutoff decisions.

Valve Sequence Coordinator (Figure 3-13)

The valve sequence coordinator is responsible for safely starting and stopping the engine. When a start command is received from the propulsion level, actuator commands are issued in a preset sequence designed to minimize adverse affects associated with the start transient (e.g. the CCV is throttled down during early stages of the start sequence to provide additional cooling to the MCC). During mainstage, the valve sequence coordinator prepares for cutoff by updating the scheduled cutoff sequence in response to actuator failures. For example, if the FPOV fails (and is therefore locked in its current position) the actuator commands are resequenced to minimize the risk of catastrophic failure at cutoff. Initially, an alternate cutoff is selected from a set of predetermined sequences to ensure a timely response. Then this sequence is optimized to determine if a "better" sequence can be identified and validated (using a system model). The new sequence replaces the predetermined one. Therefore, upon receipt

of a cutoff command, the "best" cutoff sequence is issued for the current engine status. Actuators continue to be monitored during the cutoff and the sequence is altered, according to predetermined rules, in response to actuator failures.

3.2 Conclusions About the Baseline Functional Framework

The ICS baseline functional framework (BFF) identifies control capabilities that result in increased engine reliability, increased engine performance, and greater engine life by adapting the engine control in response to measured conditions. However, several significant limitations exist in the BFF. They are: 1) optimization of thrust, mixture ratio, and health parameters at the engine level is limited by using only the OPOV, FPOV, and OPFV to implement thrust and mixture ratio control, 2) life extension and performance optimization are implemented independently of the primary control objectives (thrust and MR) and have only a relatively minor impact on the engine, 3) feedback to the propulsion level is limited to calculated parameters (e.g. the downthrust factor) that describe the global engine condition but hide detailed engine information from the propulsion level. The BFF limitations result from the inability to process and evaluate large amounts of engine data in real time and the lack of detailed diagnostic and prognostic engine health algorithms. For the advanced functional framework described in Section 5.0, the data processing and engine health algorithm limitations are assumed to no longer exist.

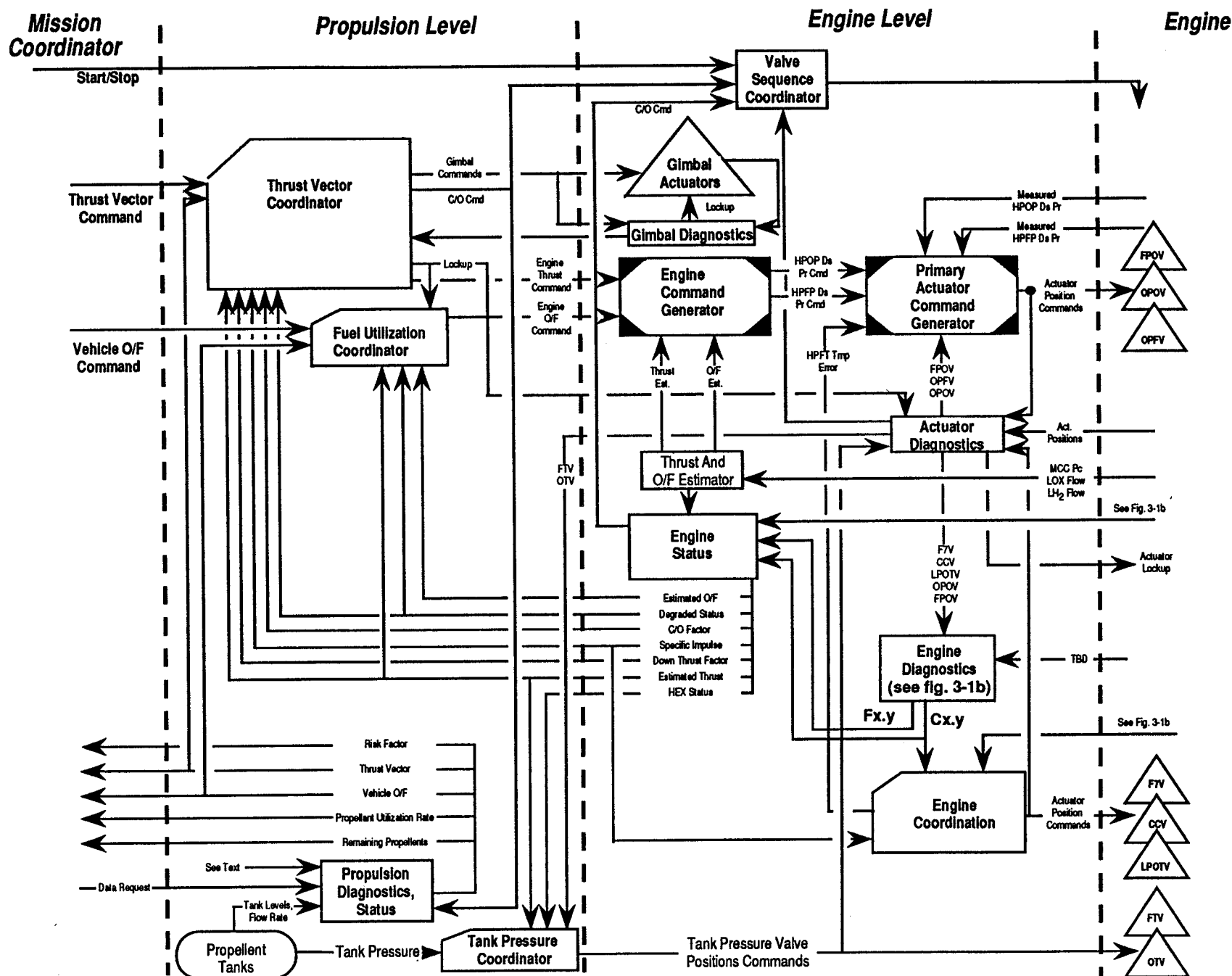


Figure 3-1a ICS Baseline Functional Framework - Rev. 2.3

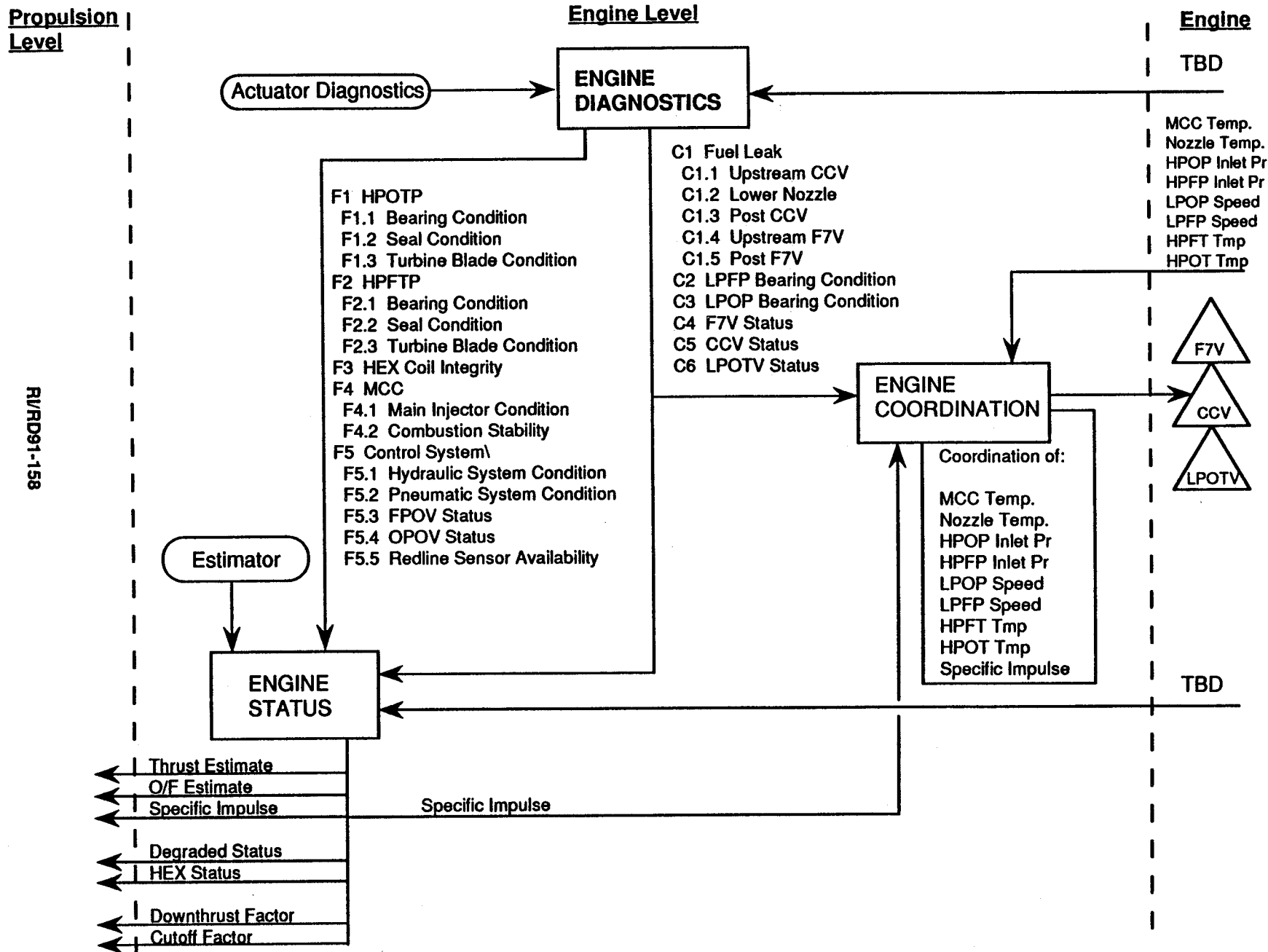


Figure 3-1b Diagnostic Function Interfaces

INPUTS

OUTPUTS

RI/RD91-158

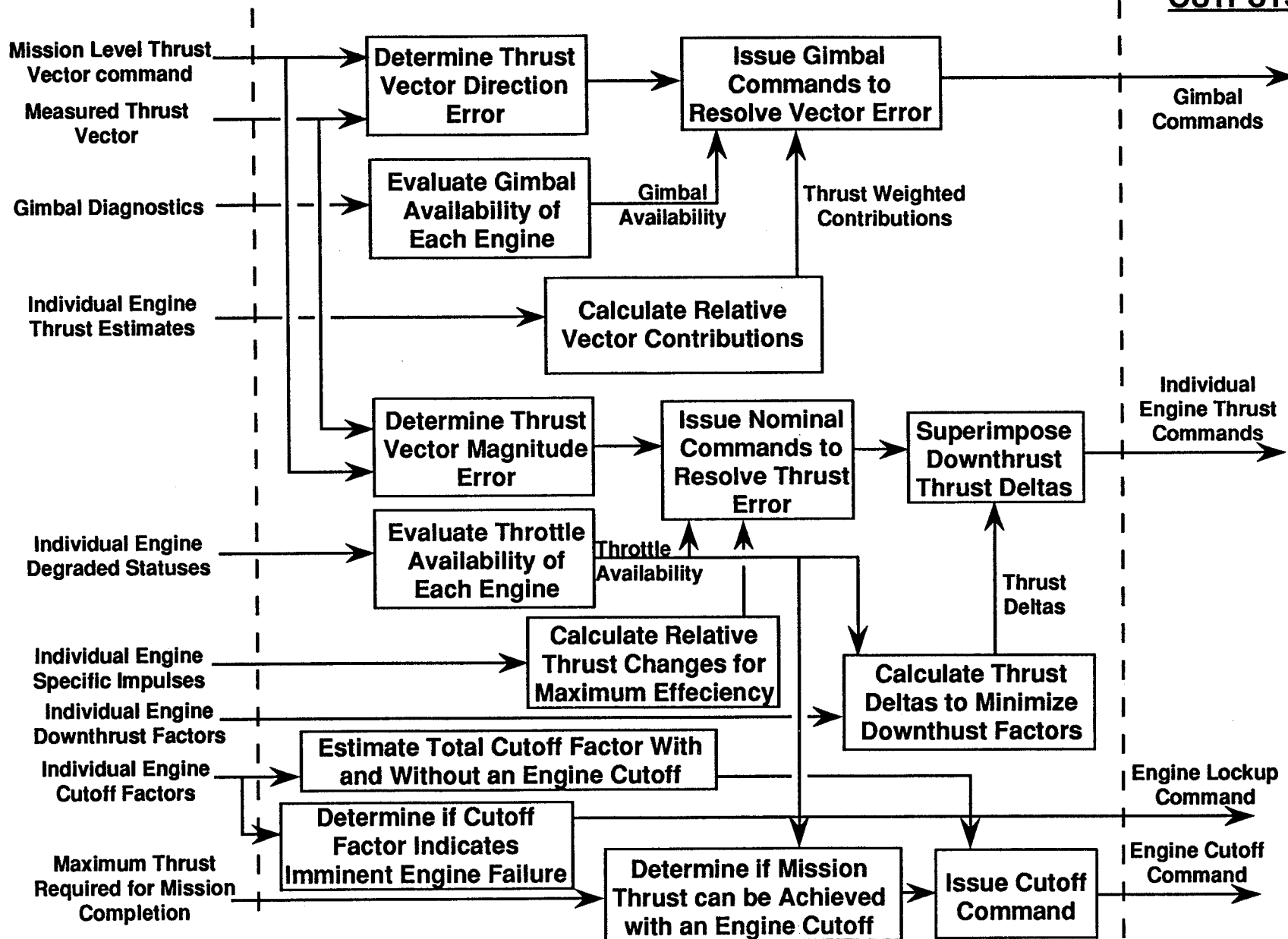


Figure 3-2 Thrust Vector Coordinator

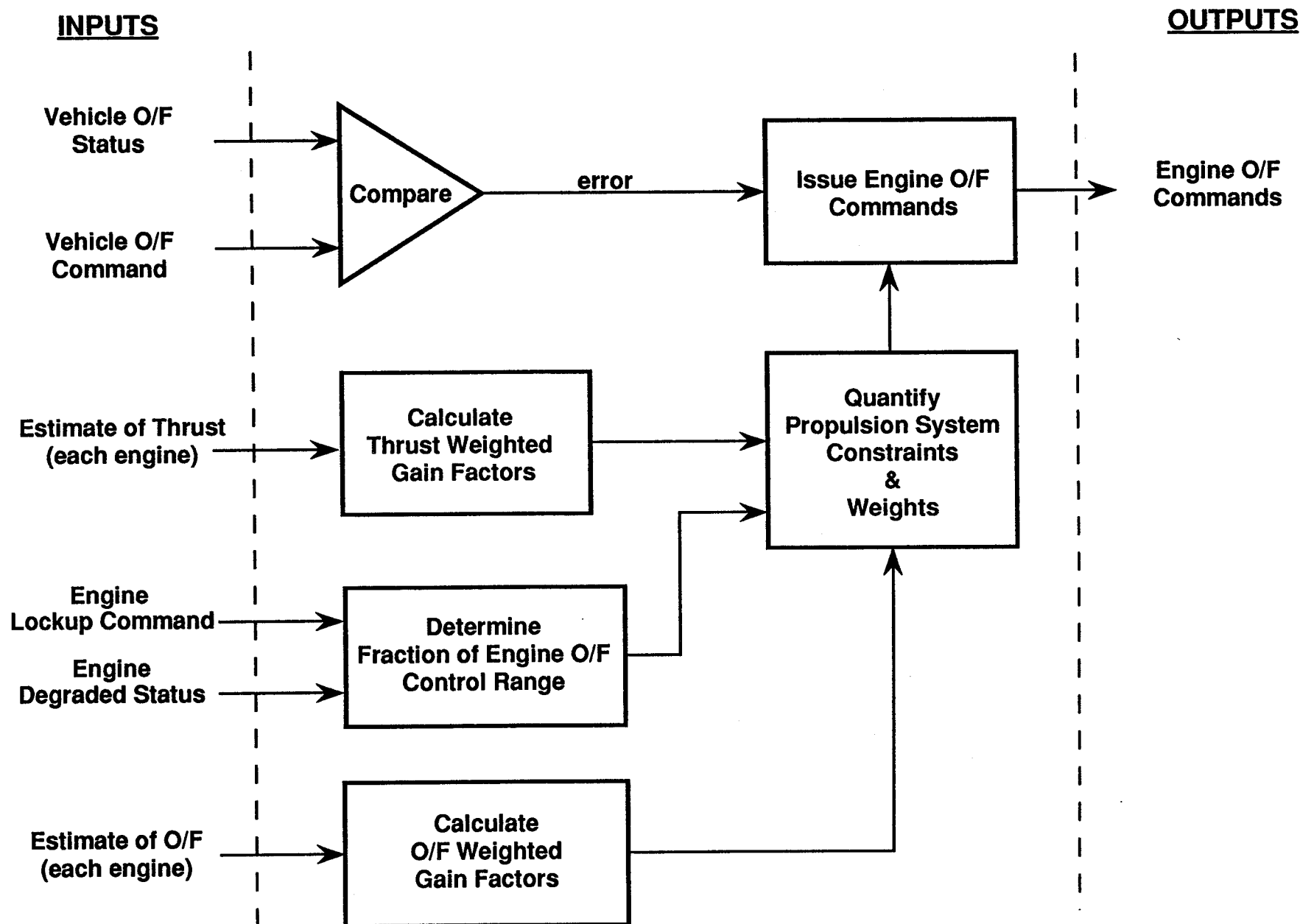


Figure 3-3 Fuel Utilization Coordinator

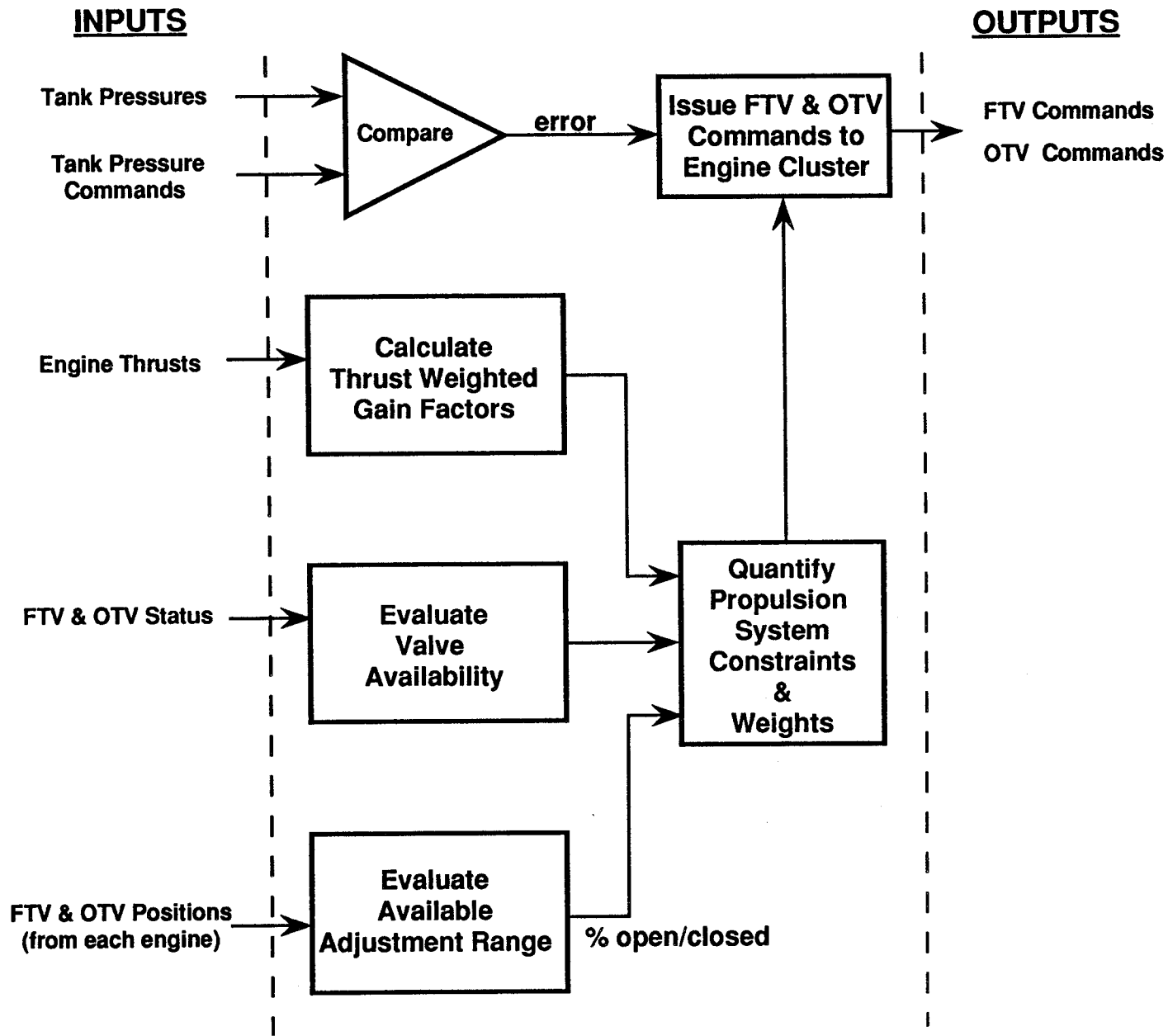


Figure 3-4 Tank Pressure Coordinator

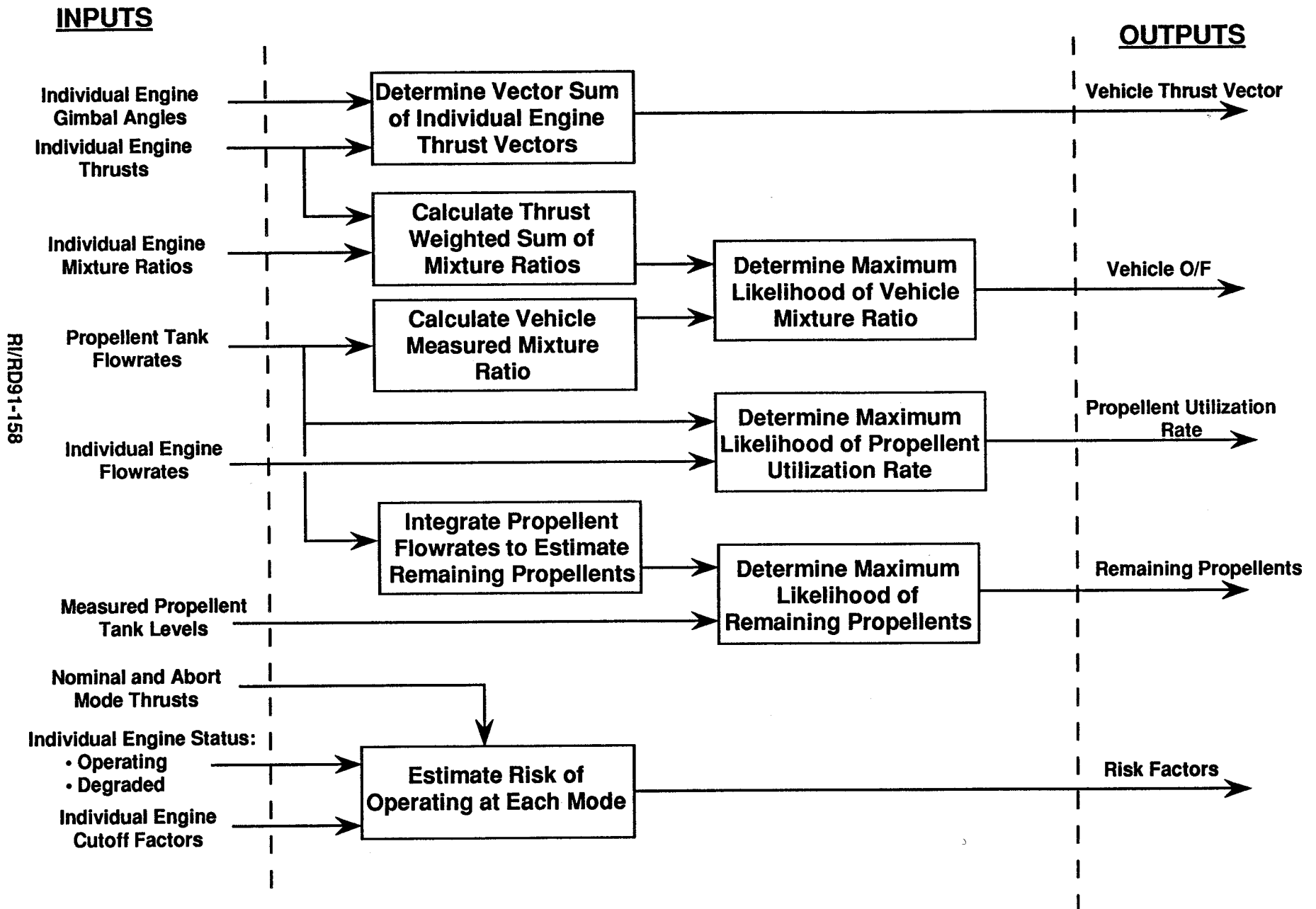


Figure 3-5 Propulsion Diagnostics and Status

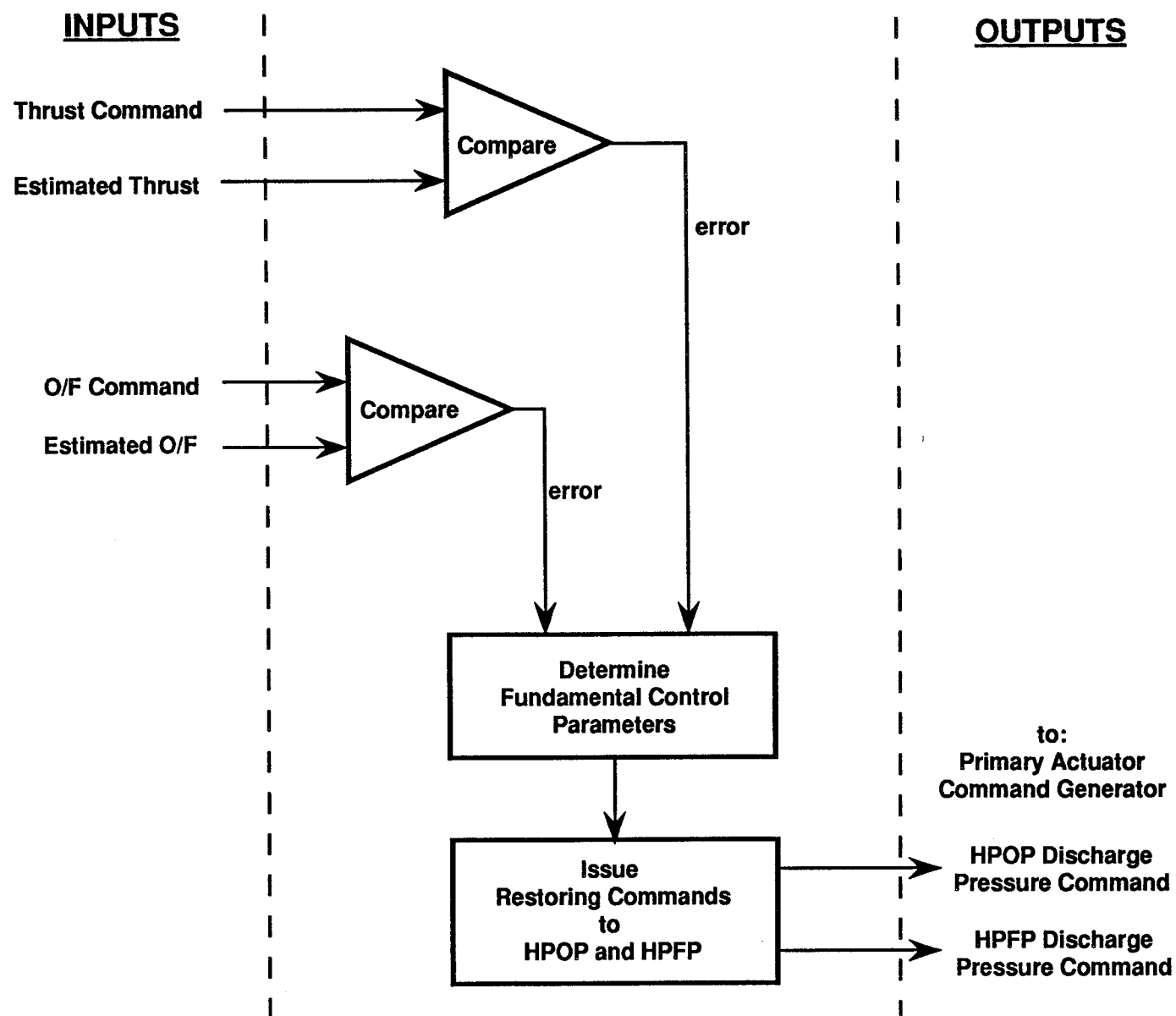


Figure 3-6 Engine Command Generator

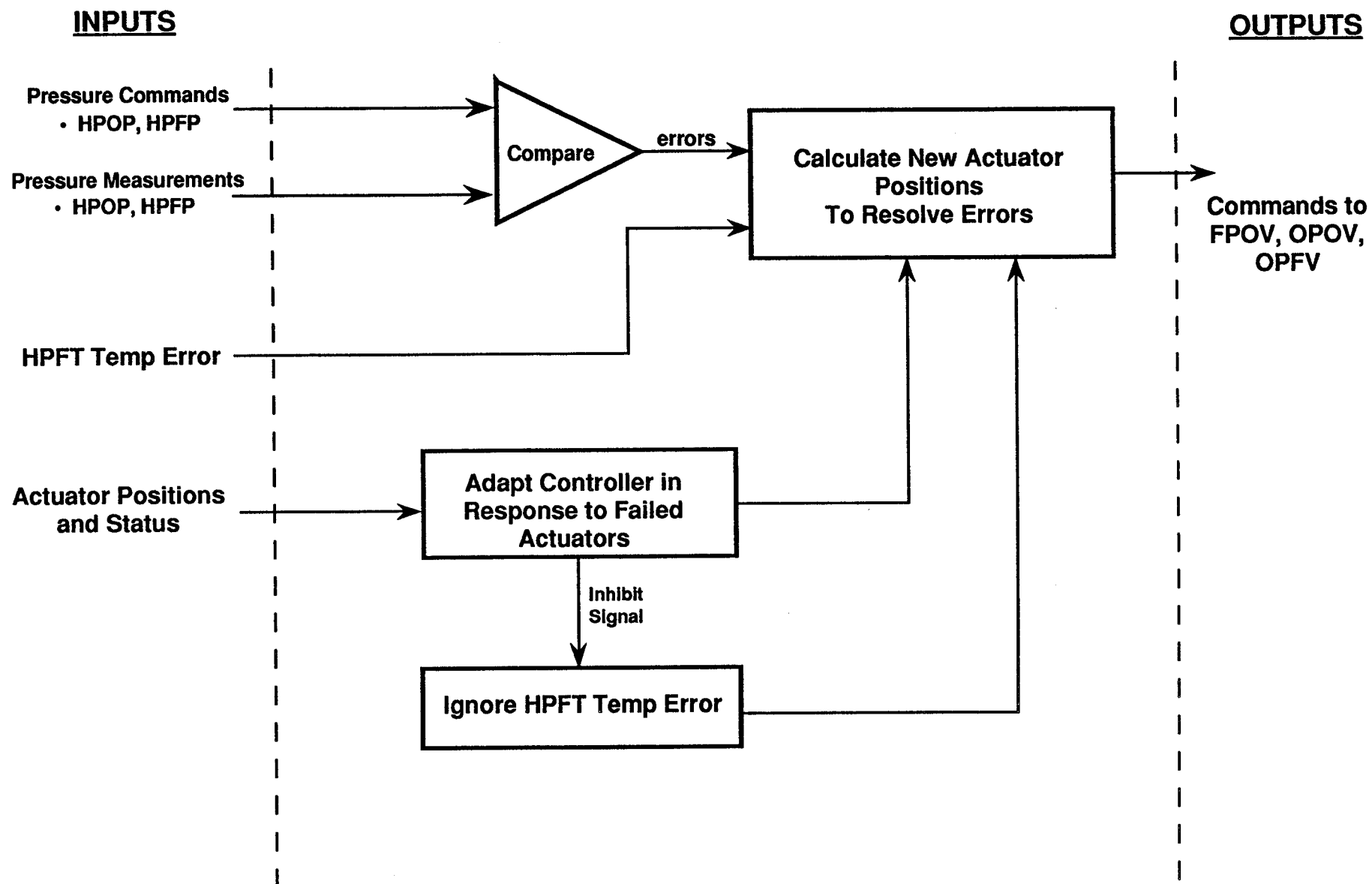


Figure 3-7 Primary Actuator Command Generator

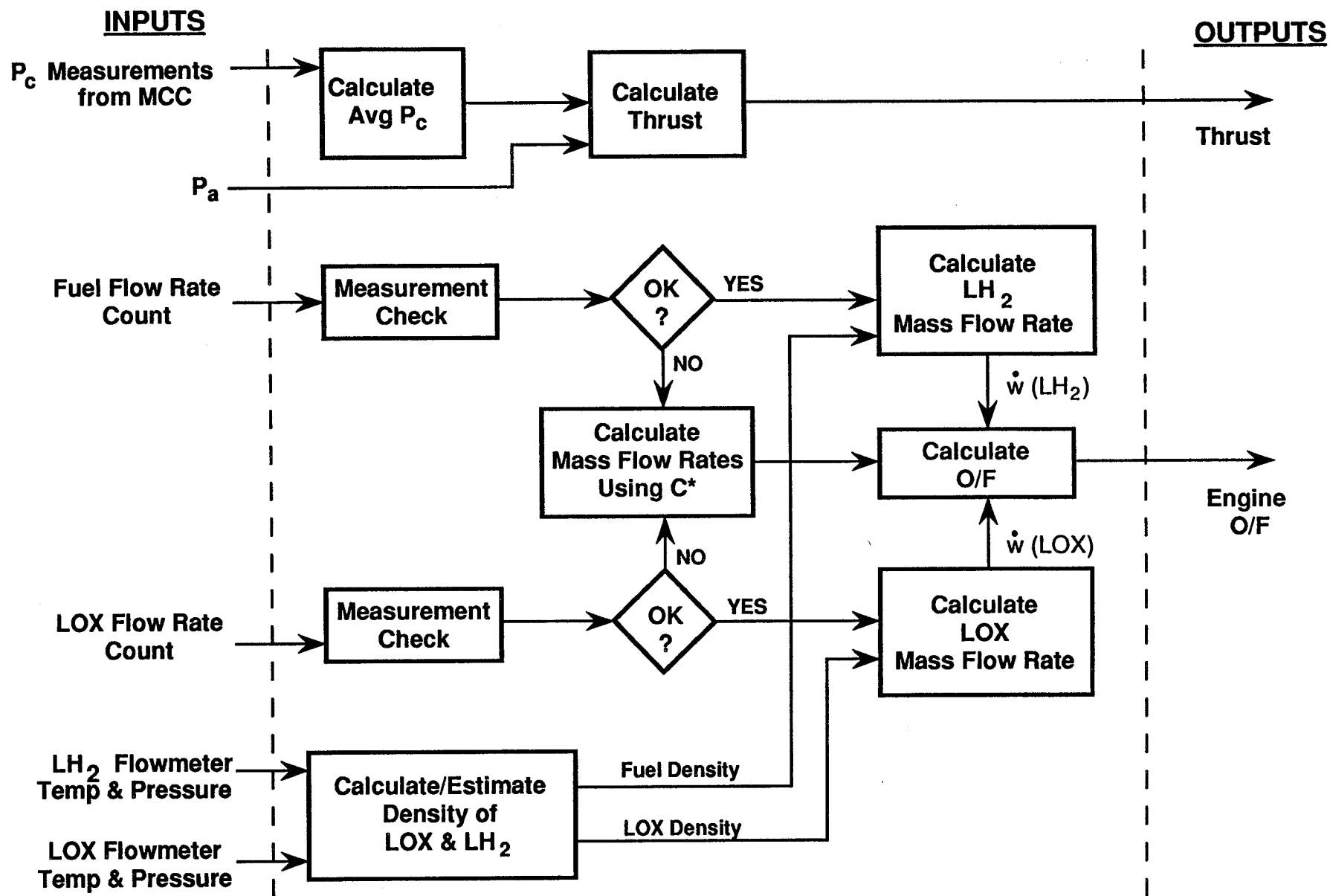


Figure 3-8 Thrust and Mixture Ratio Estimator

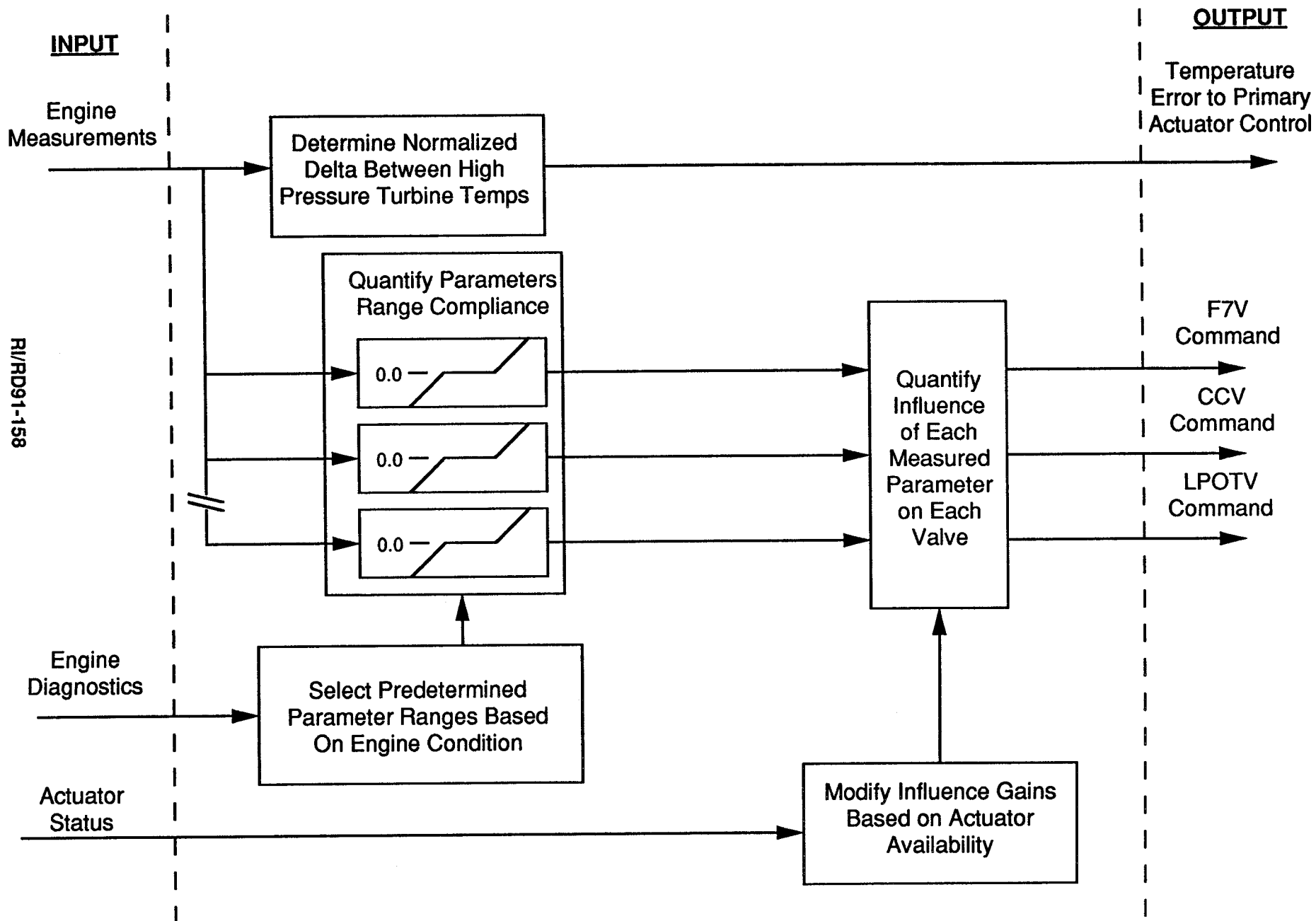


Figure 3-9 Engine Coordinator

INPUTS

PRIMARY DIAGNOSTICS (F-Class)

SECONDARY DIAGNOSTICS (C-Class)

OUTPUTS

Engine
Measurement
Parameters

- Temps
- Pressures
- Bearing Wear
- Vibration
etc.

Actuator
Diagnostics

Actuator/Valve Positions

To
Engine
Status

To
Engine
Coordination

Determine
HPOTP Condition

Determine
HPFTP Condition

Determine
HEX Coil Integrity

Determine
Main Inj. Condition

Verify
Control System
Condition

Verify
Redline Sensor
Integrity

Determine
Fuel Leakage Status

Determine
LPFP Bearing
Condition

Determine
LPOP Bearing
Condition

Verify
Secondary Valve
Status

Figure 3-10 Engine Diagnostics

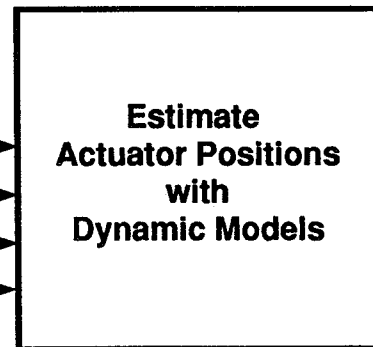
INPUTS

Actuator Position Commands

- from PACG
- from Engine Coordination
- from Valve Seq. Coord.
- from Propulsion Level

Measured Actuator Positions

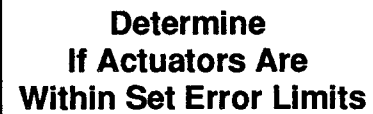
External Lockup Command



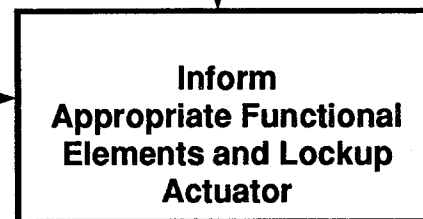
Measured
Positions

Predicted
Positions

Compare



Actuator Not
Within Limits



OUTPUTS

Actuator
Within Limits

Actuator
Positions

Issue Actuator
Lockup Command

Actuator
Status

Lock
Actuators

Figure 3-11 Actuator Diagnostics

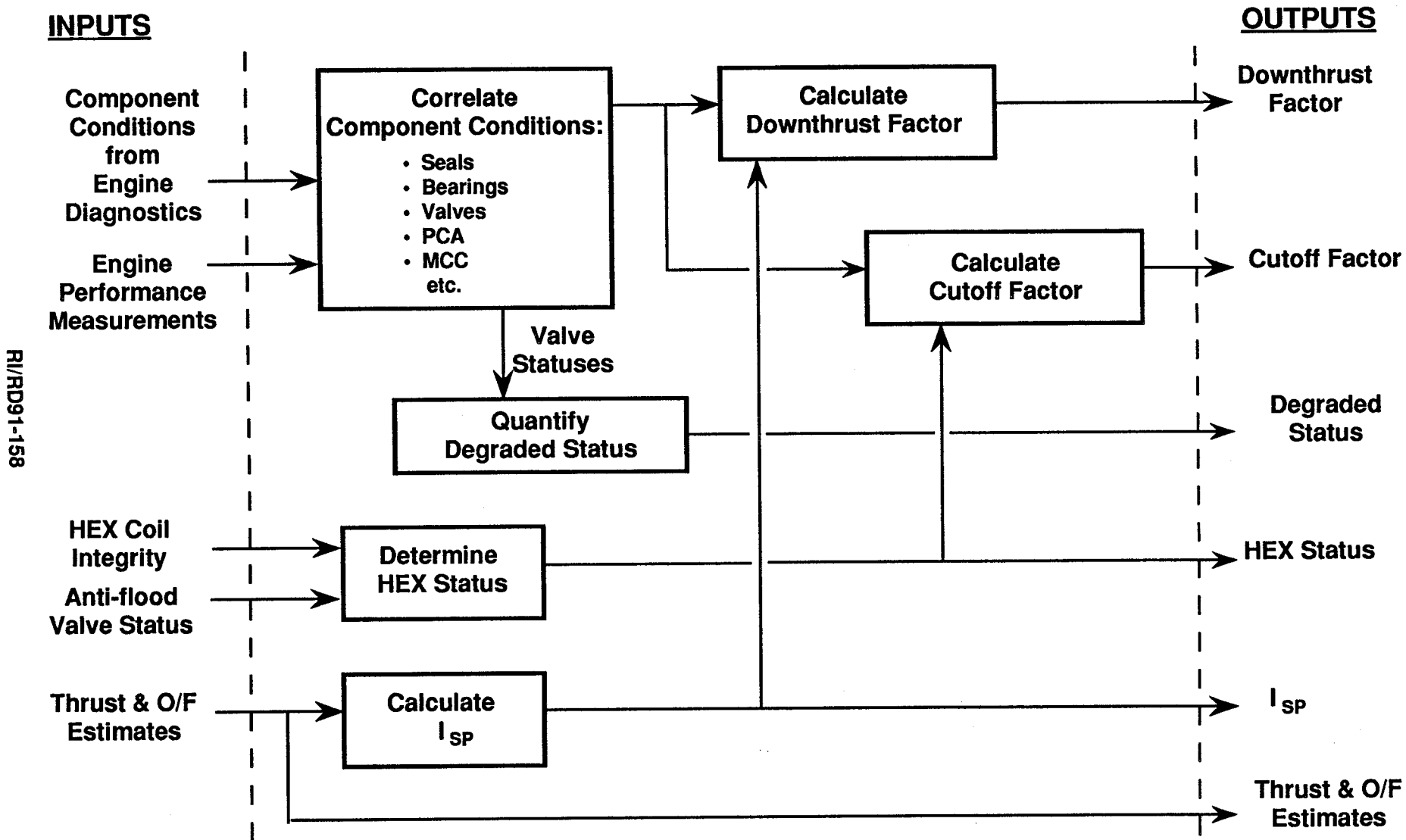


Figure 3-12 Engine Status

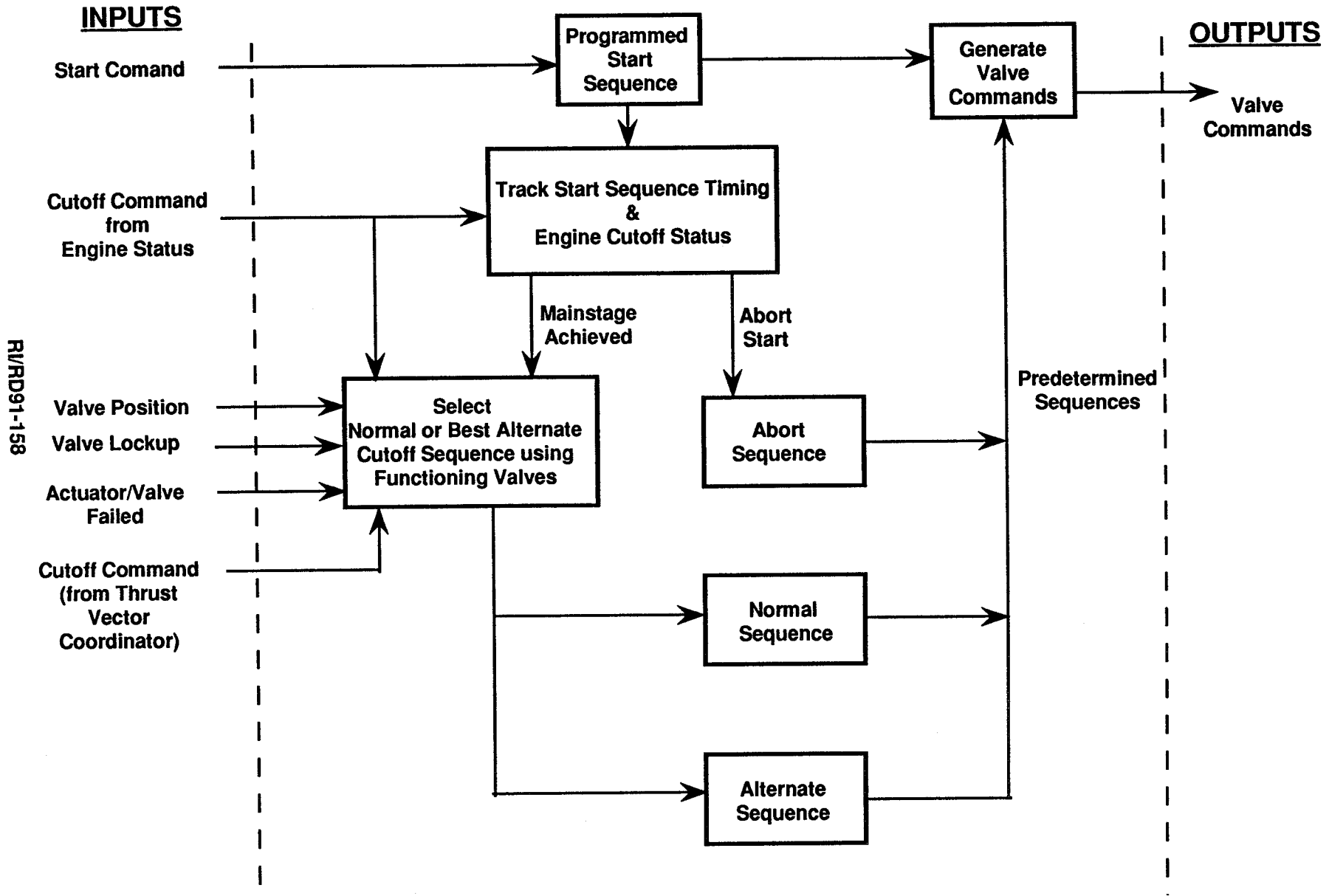


Figure 3-13 Valve Sequence Coordinator

SECTION 4 DIAGNOSTIC SUBSYSTEM DEFINITION

This section further defines the diagnostics function to include a description of the failure modes to be covered by the diagnostic system. The informational architecture, including required sensed information and engine status output information (failure severity, failure likelihood, etc.) is described. The rationale for failure mode selection is outlined below.

4.1 Failure Mode Database

Failure modes to be covered by the diagnostics system have been taken from the SSME FMEA-CIL documents, RSS-8553-11 and RSS-8740-11, dated 15 July 1988. The SSME FMEA was accomplished using a component functional analysis approach to identify the potential failure modes. The failure modes were then evaluated to determine the worst-case effect on engine, vehicle, crew and mission. The criticality code is determined by the worst-case effects statement. The current (for this referenced document) SSME flight and software configuration were analyzed. The depth of analysis is down to Line Replaceable Unit (LRU)/black box to identify all credible failure modes for that component. Failure mode causes were identified by the FMEA to the piece-part level for critical failures. Criticality 1R items were also analyzed to the lowest level necessary to verify that redundancy exists. Failure likelihood for each mode is not available from the FMEA as a statistical quantity. The CIL quotes number of seconds of operation for fleet leaders for various components including the number of failure free starts.

The FMEA consists of the following volumes:

Volume I	Executive Summary
Volume II	Combustion Devices
Volume III	Fuel Turbopumps
Volume IV	Oxidizer Turbopumps
Volume V	Pneumatic Controls
Volume VI	Propellant Valves
Volume VII	Actuators
Volume VIII	Controller
Volume IX	Harnesses
Volume X	Igniters and Sensors
Volume XI	Lines, Ducts, Joints and Orifices
Volume XII	Flight Accelerometer Safety Cutoff System (FASCOS)

4.2 Selection of failure modes

Several cycles of screening have been used to extract candidate modes from the documentation as follows:

A preliminary list of failure modes was extracted from the data base of greater than 400 items. Emphasis was placed on modes amenable to corrective or mitigating action. Specific types of failure modes excluded for the diagnostics system were:

- Failures occurring in too short a time to take corrective action
- Failures where no corrective action is possible
- Failures leading to unconditional engine cutoff.

This list of about 120 items was then reviewed in more detail for consideration of the various phases of the launch and ascent profile to generate failure accommodation tables (as described below). Some deletions were made, and the list was reduced to about 100 items.

Some failure modes where no corrective action can presently be taken will still be considered where it may be possible to use new or additional sensors or where the candidate ICS valves may be used for corrective action. Exceptions to other criteria will always be made when there is some way the ICS may be used to accommodate, correct, or lessen the effect of a failure.

Additional modes that could apply to generic engine diagnostics may be added.

4.3 Failure Accommodation Tables

The phases of operation covered are indicated in the failure accommodation tables. These are the same as indicated in the FMEA. An example is \emptyset = SMC. The five possible letters are defined as follows:

Propellant Conditioning Phase (P) - Start of Purge Sequence 1 through Purge Sequence 4, ending with Start Command.

Start Phase (S) - Start Command to SRB Ignition (~ 5 seconds).

Mainstage Phase (M) - Starts at SRB Ignition and ends with Cutoff Command at end of ascent phase.

Cutoff Phase (C) - Starts at MECO Command and ends with Zero Thrust (includes on-pad cutoff following an aborted start and any unique failure effect).

Dump (Post-Cutoff) Phase (D) - Begins with Zero Thrust and ends with completion of propellant dump including vacuum inerting.

Item numbers for the various components are the FMEA item numbers, which in most cases are the same as the CIL reference numbers. Criticality codes (Crit =) are included in the tables for quick reference and the timing (t =) is noted where:

I = Immediate -- less than one second

S = Seconds -- 1 to 60 seconds

M = Minutes -- 60 seconds to 60 minutes

N/A = No set timing (damage may occur during cutoff) --
Igniters and sensors generally have this timing

Notes concerning failure mode history included in the CIL may also be found in the Failure Accommodation Tables. Tables for the volumes covered are found in Tables 4-1 through 4-6.

4.4 Excluded Volumes

The following volumes of the SSME FMEA were not included as ICS diagnostic candidates for the reasons listed:

Actuators -- Volume VII

None of the actuator failure modes in the FMEA appear to be amenable to accommodation or resolution by the diagnostic system functions. Most failures result

in hydraulic or pneumatic lockup through redundancy and fail-safe mechanisms that are built into the actuators.

Controller -- Volume VIII

The FMEA for the Controller will not be used because it is specific to the Block I Controller for the SSME. The design of the ICS has not yet been accomplished and may have significantly different architecture, packaging scheme and unique set of failure modes.

Ducts/Lines, Joints and Orifices -- Volume XI

Failure modes associated with ducts/lines, joints and orifices will not be accommodated by the diagnostic system directly. Large failures in these components will, in general, lead very quickly to catastrophic engine failure. Minor leaks that do not lead to fire/explosion or overpressurization of the aft compartment may be covered indirectly by pressure or flow anomalies detected by various sensors. If optical or other leak detection systems are employed in the future, their measurement data would be analyzed by the diagnostic system.

FASCOS -- Volume XII

The Flight Accelerometer Safety Cutoff System (FASCOS) is an integral part of the SSME Controller. It interfaces directly to the address and data bus of the controller. ICS designs may or may not use this approach. Future turbopump designs may incorporate bearing wear detection sensors capable of detecting/predicting bearing failure modes (a major source of excessive vibration) much earlier and more definitively than the present FASCOS. Thus, the way accelerometers are used may change significantly. Severe vibration indicates that enough mechanical damage has already occurred to make shutdown imperative.

4.5 Failure Accommodation Discussion

4.5.1 Combustion Devices

The main failure modes in this category involve the blockage of a fuel, oxidizer, or hot gas flow. The failure of Augmented Spark Igniters (ASI) is also included. The failure of the ASIs is not very likely. The Main Injector Fleet Leader has accumulated over 19,000 seconds and 60 starts without any anomalies (as of July, 1988). One in-flight failure occurred in 1984, when a drill chip lodged in an Oxidizer Preburner fuel line (Item # A700-2). ASI chamber erosion was discovered during post flight inspection, but no engine failure occurred because the erosion was limited in scope.

No corrective action appears possible for the ICS other than engine shutdown if erosion is present. There is no present or planned method for quantifying erosion. If erosion were detected late in the ascent profile, downthrusting or increasing the coolant flow might be an option for propulsion or mission level decision. Early detection by plume spectrometry would help ensure shutdown before severe erosion caused major structural failures.

4.5.2 Fuel Turbopumps

The failure accommodation tables show that the method of detection and control system action are very nearly the same for many of the failure modes. This is because of the method of control used for the staged combustion cycle type of engine with variable thrust. Fuel pump

output flow and pressure must be maintained to ensure proper mixture ratio and cooling. Any anomaly that reduces output causes an increase in oxidizer to the fuel turbopump preburner to increase turbine power. If the anomaly is a developing failure mode, pump output may continue to decrease, and oxidizer input to the fuel preburner will be increased further. This can escalate rapidly, and rising turbine discharge temperature may exacerbate the problem, causing the failure mode to develop even more quickly. Rates at which the OPFV is modulated to control mixture ratio during anomalous operation, however detected, should be carefully monitored.

Correlation of rising turbine discharge temperature on the HPFTP with other measurement parameters should be made wherever possible to determine the specific failure mode. Degraded status and updated downthrust factor must be relayed to the propulsion level of the functional framework as quickly as possible to insure that potential engine cut-off actions are timely while still being based on overall mission objectives. Additional sensors such as bearing wear detectors and plume spectrometers that may give advance warning of turbopump failures are highly recommended.

4.5.3 Oxidizer Turbopumps

As with the fuel turbopumps, the failure accommodation tables show that the method of detection and control system action are very nearly the same for many of the failure modes. Oxidizer pump output flow and pressure must be maintained to ensure that the proper thrust levels for the mission profile are satisfied. Any anomaly that reduces output (as determined by thrust calculations) causes an increase in oxidizer to the oxidizer turbopump preburner to increase turbine power. A developing failure mode may cause output to continue to decrease, and oxidizer input to the oxidizer preburner will be increased further by opening the OPOV. Rapid escalation of failure modes is also possible (and likely) in the HPOTP.

Again, the earliest possible detection of a failure mode is very important and newer sensors and diagnostic methods should be employed.

4.5.4 Pneumatic Controls

This group of components has a very good history of reliability. Purge check valves are simple in design compared with propellant valves and generally operate under less severe conditions (no cryogenic fluid flow through the valve). Other components are somewhat more complex, but they have been carefully designed and evolved through extensive testing. The components are active mainly during Prestart, Start and Cutoff.

Only limited time for analysis/accommodation is available during Start and Cutoff. One exception is the HPOTP Intermediate Seal Purge PAV that is very important during Mainstage to maintain separation of LOX and fuel rich hot gas in the pump turbine. This seal purge pressure is monitored by a pressure transducer whereas some other purge pressures are not directly monitored. In general, this group may be of limited interest to the ICS except for engine status.

4.5.5 Propellant Valves

The valves selected as candidates for ICS have demonstrated good reliability for the failure modes described. The main propellant valves were not selected because they are moved on a predefined schedule to either fully open or fully closed positions, and are not used for thrust or mixture ratio control. Opening rates and relative timing affect Start and Cutoff transients.

Control is effected through the two valves (FPOV and OPOV) that control the flow of oxidizer to the preburners, and the Chamber Coolant Valve (CCV) is scheduled linearly with thrust reference such that it will be partially open at minimum power level (65%) and fully open at the 100% thrust level. Heat transfer loads on the MCC and Nozzle do not decrease at a rate that matches the decrease in total hydrogen flow when thrust is decreased. Therefore, the CCV, which acts as a bypass valve, must be partially closed to force more of the available hydrogen flow through these components at the lower thrust levels.

The preburner oxidizer valves may be opened or closed when the controller attempts to compensate for other failure modes (such as loss of impeller head rise in the HPFTP). This may cause turbine discharge temperature to exceed redline limits. The bleed valves are not operated by servoactuators, but they do have position feedback.

4.5.6 Igniters and Sensors

This group of components should receive close attention in considering failure mode candidates for the ICS. The use of analytical redundancy should be considered wherever it is possible to compensate for sensor failures. At present, temperature and pressure sensors are dual channel devices, and critical measurements, e.g., MCC pressure, have redundant sensors.

The more important sensors may be categorized into three groups as defined in the following tables. Thus, some measurements are more important during one phase of the mission than another. HPFTP shaft speed, for example, is of secondary interest during Mainstage and Cutoff.

Engine Ready Sensors:

- | | |
|---|--------------------------------|
| a. LPFTP Discharge Pressure | e. Emergency Shutdown Pressure |
| b. LPFTP Discharge Temperature | f. Preburner Purge Pressures |
| c. Preburner Pump Discharge Temperature | g. MOV Hydraulic Temperature |
| d. LPOTP Discharge Pressure | h. MFV Hydraulic Temperature |

Performance Control Sensors:

- a. MCC Pressure
- b. LPFTP Discharge Pressure
- c. LPFTP Discharge Temperature
- d. Fuel Flowrate

Engine Limit Control Sensors:

- | | |
|---|--------------------------------------|
| a. HPFTP Turbine Discharge Temperature | f. HPFTP Coolant Liner Pressure |
| b. HPOTP Intermediate Seal Purge Pressure | g. Ignition Confirm, MCC Pressure |
| c. HPOTP Secondary Seal Cavity Pressure | h. Ignition Confirm, Antiflood Valve |
| d. HPOTP Turbine Discharge Temperature | i. Ignition Confirm, HPFTP Speed |
| e. Preburner Shutdown Purge Pressure | |

Sensors not in these groups may be considered as flight data sensors only.

4.6 Informational Architecture

Block diagrams illustrating a proposed "informational architecture" have been prepared for each of the FMEA volumes used for the data base. The diagrams may be found in Figure 4-1 through Figure 4-6. Intermediate actions that may be taken to accommodate or lessen the effect of incipient failures, before a decision to cutoff, are shown for groups of failure modes that

cause similar symptoms (e.g., increase in turbine discharge temperature). The three main actions identified are: downthrust, decrease O/F, and increase coolant flow.

4.7 Diagnostic Subsystem Conclusions

The majority of FMEA criticality 1 failures for the SSME eventually lead to an engine shutdown. However, the useful life of an engine can be extended by downthrusting the engine if the failure is detected in the early stages. For combustion device failures, minor improvements in the engine life can be made by changing the engine mixture ratio and by redistributing available coolant through the affected area of the engine.

Table 4-1 FMEA Summary - Combustion Devices

Failure	Description		Detected by	Control System Action
A050-1 Ø = SMC	Powerhead -- Liner failure	Crit = 1 t = S	Rapid rise of turbopump discharge temps	If not severe, may be able to downthrust or decrease O/F to increase cooling. No failure history.
A200-1 Ø = S	Main Injector -- ASI fails to ignite	Crit = 1R t = S	MCC pressure low	Engine shutdown during start phase -- quick detection will minimize potential engine damage. No failure history
A200-2 Ø = SMC	Main Injector --- Loss of fuel to ASI	Crit = 1 t = S	Erosion may be detected by plume spectrometry	If detectable, engine shutdown before high mixture ratio erosion leads to injector burnout. No failure history.
A200-3 Ø = SMC	Main Injector -- Blockage of one LOX ASI passage	Crit = 1 t = S	Erosion may be detected by plume spectrometry	If detectable, engine shutdown before erosion leads to injector burnout. No failure history.
A200-5 Ø = SMC	Main Injector -- Partial blockage of an oxidizer orifice	Crit = 1 t = S	Erosion may be detected by plume spectrometry	If detectable, engine shutdown before erosion leads to injector burnout. Two cases (1979) - no effect during hotfire.
A330-5 Ø = M	MCC Lee Jet is blocked	Crit = 1R t = S	MCC pressure sensor qualification limit exceeded	Disqualify sensor -- may choose not to allow electrical lockup if other MCC pressure sensor fails. No failure history.
A340-1 Ø = M	Nozzle Assembly -- Multiple internal tube fuel leakage	Crit = 1R t = S	Turbine discharge temps increase	Engine shutdown. If redlines not exceeded, try to adjust the mixture ratio by modulation of the FPOV. Two cases (1979)
A600-1 Ø = S	Fuel Preburner -- ASI fails to ignite	Crit = 1R t = S	HPOTP speed will not reach lower limit	Engine shutdown -- redline on lower limit of HPFTP speed during Start. No failure history.
A600-2 Ø = SMC	Fuel Preburner -- Loss of fuel to ASI	Crit = 1 t = S	Erosion may be detected by plume spectrometry	If detectable, engine shutdown before high mixture ratio erosion leads to injector burnout. No failure history.
A600-3 Ø = SMC	Fuel Preburner -- Blockage of one LOX ASI passage	Crit = 1 t = S	Erosion may be detected by plume spectrometry	If detectable, engine shutdown before erosion leads to injector burnout. No failure history.
A700 Ø = S	Oxidizer Preburner -- ASI fails to ignite	Crit = 3 t = S	Turbine discharge temp below lower limit	Engine shutdown -- redline on lower limit of HPOTP turbine discharge temp. No failure history.
A700-2 Ø = SMC	Oxidizer Preburner -- Loss of fuel to ASI	Crit = 1 t = S	Erosion may be detected by plume spectrometry	If detectable, engine shutdown before high mixture ratio erosion leads to injector burnout. One failure (1984)
A700-3 Ø = SMC	Oxidizer Preburner -- Blockage of one LOX ASI passage	Crit = 1 t = S	Erosion may be detected by plume spectrometry	If detectable, engine shutdown before erosion leads to injector burnout. No failure history.

Table 4-2 FMEA Summary - Fuel TurboPumps (1 of 3)

Failure	Description	Detected by	Control System Action
B200-1 Ø = SM	High Pressure Fuel TP -- Crit = 1R Leakage past preburner G5 seal into the HGM t = I	HPFTP turbine discharge temp increase toward redline limit and pump speed decreases	Initially, a decrease in turbine power causes an increase in preburner oxidizer to maintain pump flow and pressure but this may increase turbine discharge temp beyond the redline limit and engine must be shutdown. No failure history.
B200-2 Ø = SM	High Pressure Fuel TP -- Crit = 1R Energy loss at turbine inlet t = I	HPFTP turbine discharge temp increase toward redline limit and pump speed decreases	Initially, a decrease in turbine power causes an increase in preburner oxidizer to maintain pump flow and pressure but this may increase turbine discharge temp beyond the redline limit and engine must be shutdown. No failure history.
B200-5 Ø = SM	High Pressure Fuel TP -- Crit = 1R Rotor tip seal leakage t = I	HPFTP turbine discharge temp increase toward redline limit and pump speed decreases	Initially, a decrease in turbine power causes an increase in preburner oxidizer to maintain pump flow and pressure but this may increase turbine discharge temp beyond the redline limit and engine must be shutdown. No failure history.
B200-6 Ø = SM	High Pressure Fuel TP -- Crit = 1R Platform seal leakage t = I	HPFTP turbine discharge temp increase toward redline limit and pump speed decreases	Initially, a decrease in turbine power causes an increase in preburner oxidizer to maintain pump flow and pressure but this may increase turbine discharge temp beyond the redline limit and engine must be shutdown. No failure history.
B200-9 Ø = SM	High Pressure Fuel TP -- Crit = 1R Pressure drop or flow distortion at Impeller inlet t = I	HPFTP turbine discharge temp increase toward redline limit and pump speed decreases	Initially, a decrease in turbine power causes an increase in preburner oxidizer to maintain pump flow and pressure but this may increase turbine discharge temp beyond the redline limit and engine must be shutdown. No failure history.
B200-10 Ø = SM	High Pressure Fuel TP -- Crit = 1R Loss of Impeller head rise t = I	HPFTP turbine discharge temp increase toward redline limit and vibration may increase	Initially, a decrease in turbine output causes an increase in preburner oxidizer to maintain pump flow and pressure but this may increase turbine discharge temp beyond the redline limit and engine must be shutdown. Early test failure (1984).
B200-11 Ø = SM	High Pressure Fuel TP -- Crit = 1R Excessive Impeller bypass leakage t = I	HPFTP turbine discharge temp increase toward redline limit and pump speed decreases	Initially, a decrease in turbine power causes an increase in preburner oxidizer to maintain pump flow and pressure but this may increase turbine discharge temp beyond the redline limit and engine must be shutdown. No failure history.

Table 4-2 FMEA Summary - Fuel TurboPumps (2 of 3)

Failure	Description	Detected by	Control System Action
B200-12 Ø = SM	High Pressure Fuel TP -- Crit = 1R Excessive pump interstage seal leakage t = I	HPFTP turbine discharge temp increase toward redline limit and pump speed decreases	Initially, a decrease in turbine power causes an increase in preburner oxidizer to maintain pump flow and pressure, but this may increase turbine discharge temp beyond the redline limit and engine must be shut down. No failure history.
B200-13 Ø = SM	High Pressure Fuel TP -- Crit = 1R Energy loss in diffusers and housing t = I	HPFTP turbine discharge temp increase toward redline limit and pump speed decreases	Initially, a decrease in turbine power causes an increase in preburner oxidizer to maintain pump flow and pressure, but this may increase turbine discharge temp beyond the redline limit and engine must be shut down. No failure history.
B200-15 Ø = SMC	High Pressure Fuel TP -- Crit = 1 Loss of support or position control t = I	Pump speed decrease and increased level of vibration. May use spectrometry to detect bearing wear	Early detection of this mode by plume spectrometry or other means is imperative to prevent vehicle loss by engine shutdown. No action is possible if turbopump fails quickly. Two isolated failures (1985, 1983).
B200-16 Ø = SMC	High Pressure Fuel TP -- Crit = 1 Loss of coolant flow to turbine bearings t = I	Excessive wear of races or bearings may be detected by plume spectrometry	Early detection of this mode by plume spectrometry or other means is imperative to prevent vehicle loss by engine shutdown. No action is possible if turbopump fails quickly. No failure history.
B200-17 Ø = SM	High Pressure Fuel TP -- Crit = 1 Loss of coolant flow to turbine discs t = I	None at present	TBD No failure history.
B200-20 Ø = SM	High Pressure Fuel TP -- Crit = 1R Excessive coolant flow t = I	Rise in coolant liner pressure	Engine shutdown if coolant liner pressure exceeds the redline limit. One failure --coolant liner buckle. Leakage at lift-off seal caused overpressurization.
B200-21 Ø = SM	High Pressure Fuel TP -- Crit = 1R Excessive hot gas leakage into coolant circuit t = I	Rise in coolant liner pressure	Engine shutdown if coolant liner pressure exceeds the redline limit. No failure history.
B200-24 Ø = S	High Pressure Fuel TP -- Crit = 1R Shaft movement not restrained during Start (shaft speeds below 12,000 rpm) t = S	Fast rise in turbine discharge temp. Rubbing or wearing may be detected by plume spectrometry.	Engine shutdown if turbine discharge temp exceeds the redline limit. No failure history.

Table 4-2 FMEA Summary - Fuel TurboPumps (3 of 3)

Failure	Description	Detected by	Control System Action
B600-1 Ø = SM	Low Pressure Fuel TP -- Crit = 1R Energy loss at turbine inlet t = I	Rise in HPFTP turbine discharge temp Low shaft speed	Initially, a decrease in turbine power causes an increase in preburner oxidizer to maintain pump flow and pressure, but this may increase turbine discharge temp beyond the redline limit and engine must be shutdown. No failure history.
B600-2 Ø = SM	Low Pressure Fuel TP -- Crit = 1R Power loss in rotor t = I	Rise in HPFTP turbine discharge temp Low shaft speed	Initially, a decrease in turbine power causes an increase in preburner oxidizer to maintain pump flow and pressure, but this may increase turbine discharge temp beyond the redline limit and engine must be shutdown. No failure history.
B600-4 Ø = SM	Low Pressure Fuel TP -- Crit = 1R Loss of head rise t = I	Rise in HPFTP turbine discharge temp	Initially, a decrease in turbine power causes an increase in preburner oxidizer to maintain pump flow and pressure, but this may increase turbine discharge temp beyond the redline limit and engine must be shutdown. No failure history.
B600-5 Ø = SM	Low Pressure Fuel TP -- Crit = 1R Loss of support or position control t = I	Pump speed decrease and increased level of vibration. May use spectrometry to detect bearing wear	Early detection of this mode by plume spectrometry or other means is imperative to prevent vehicle loss by engine shutdown. No action is possible if turbopump fails quickly. No failure history.
B600-8 Ø = SM	Low Pressure Fuel TP -- Crit = 1R Turbine seal leakage t = S	Cavitation, if present, will cause increase in HPFTP turbine discharge temp	Engine shutdown if turbine discharge temp increases to redline limit. May shut down before limit if high vibration is also present. No failure history.

Table 4-3 FMEA Summary - Oxidizer TurboPumps (1 of 3)

Failure	Description	Detected by	Control System Action
B400-1 Ø = SM	High Pressure Oxid. TP – Leakage past outboard OPB/HPOTP seal Crit = 1R t = I	HPOTP turbine discharge temp increase toward redline limit and pump speed decreases	Initially, a decrease in turbine power causes an increase in preburner oxidizer to maintain pump flow and pressure, but this may increase turbine discharge temp beyond the redline limit and engine must be shutdown. No failure history.
B400-2 Ø = SM	High Pressure Oxid. TP – Energy loss at turbine inlet due to excessive flow distortion Crit = 1R t = I	HPOTP turbine discharge temp increase toward redline limit and pump speed decreases	Initially, a decrease in turbine power causes an increase in preburner oxidizer to maintain pump flow and pressure, but this may increase turbine discharge temp beyond the redline limit and engine must be shutdown. No failure history.
B400-4 Ø = SM	High Pressure Oxid. TP – Turbine blade tip seal leakage Crit = 1R t = I	HPOTP turbine discharge temp increase toward redline limit and pump speed decreases	Initially, a decrease in turbine power causes an increase in preburner oxidizer to maintain pump flow and pressure, but this may increase turbine discharge temp beyond the redline limit and engine must be shutdown. One test failure (1985).
B400-5 Ø = SM	High Pressure Oxid. TP – Turbine interstage seal leakage Crit = 1R t = I	HPOTP turbine discharge temp increase toward redline limit and pump speed decreases	Initially, a decrease in turbine power causes an increase in preburner oxidizer to maintain pump flow and pressure, but this may increase turbine discharge temp beyond the redline limit and engine must be shutdown. No failure history.
B400-6 Ø = SM	High Pressure Oxid. TP – Turbine discharge flow blockage Crit = 1R t = I	HPOTP turbine discharge temp increase toward redline limit and pump speed decreases	Initially, a decrease in turbine power causes an increase in preburner oxidizer to maintain pump flow and pressure, but this may increase turbine discharge temp beyond the redline limit and engine must be shutdown. No failure history.
B400-8 Ø = SM	High Pressure Oxid. TP – Flow distortion at main pump inlet Crit = 1R t = I	HPOTP turbine discharge temp increase toward redline limit and vibratoion may increase	Initially, a decrease in turbine output causes an increase in preburner oxidizer to maintain pump flow and pressure, but this may increase turbine discharge temp beyond the redline limit and engine must be shutdown. No failure history.
B400-9 Ø = SM	High Pressure Oxid. TP – Loss of Inducer/Impeller head rise Crit = 1R t = I	HPOTP turbine discharge temp increase toward redline limit and pump speed decreases	Initially, a decrease in turbine power causes an increase in preburner oxidizer to maintain pump flow and pressure, but this may increase turbine discharge temp beyond the redline limit and engine must be shutdown. No failure history.

Table 4-3 FMEA Summary - Oxidizer TurboPumps (2 of 3)

Failure	Description	Detected by	Control System Action
B400-10 Ø = SM	High Pressure Oxid. TP -- Crit = 1R Energy loss at main pump difuser t = I	HPOTP turbine discharge temp increase toward redline limit and pump speed decreases	Initially, a decrease in turbine power causes an increase in preburner oxidizer to maintain pump flow and pressure, but this may increase turbine discharge temp beyond the redline limit and engine must be shut down. No failure history.
B400-11 Ø = SM	High Pressure Oxid. TP -- Crit = 1R Inadequate preburner pump impeller head rise t = I	HPOTP turbine discharge temp increase toward redline limit and pump speed decreases	Initially, a decrease in turbine power causes an increase in preburner oxidizer to maintain pump flow and pressure, but this may increase turbine discharge temp beyond the redline limit and engine must be shut down. No failure history.
B400-13 Ø = SMC	High Pressure Fuel TP -- Crit = 1 Loss of support or position control t = I	Pump speed decrease and increased level of vibration. May use spectrometry to detect bearing wear	Early detection of this mode by plume spectrometry or other means is imperative to prevent vehicle loss by engine shutdown. No action is possible if turbopump fails quickly. Four failures during engine test
B400-15 Ø = SMC	High Pressure Oxid. TP -- Crit = 1 Loss of purge pressure barrier t = I	None at present	TBD No failure history
B400-18 Ø = SM	High Pressure Oxid. TP -- Crit = 1 Loss of coolant flow to bearings t = S	None at present Excessive wear of races or bearings may be detected by plume spec- trometry	Early detection of this mode by plume spectrometry or other means is imperative to prevent vehicle loss by engine shutdown. No action is possible if turbopump fails quickly. No failure history.
B400-19 Ø = SM	High Pressure Oxid. TP -- Crit = 1R Loss of coolant flow to turbine seals t = S	Turbine secondary seal cavity pressure meas. Metallurgical deterioration may be detected by plume spectrometer	Engine shutdown if redline is exceeded. If correlated with plume measurements, shutdown with more safety margin may be possible. No failure history.
B400-20 Ø = SMC	High Pressure Oxid. TP Crit = 1 Coolant loss to 1st and 2nd stage turbine components t = S	None at present Metallurgical deterioration may be detected by plume spectrometer	TBD Early failures found only on disassembly and the causes corrected (1985, 1983, 1982)

Table 4-3 FMEA Summary - Oxidizer TurboPumps (3 of 3)

Failure	Description	Detected by	Control System Action
B800-1 Ø = SM	Low Pressure Oxid. TP -- Crit = 1R Seal leakage at turbine inlet t = I	HPOTP turbine discharge temp increase toward redline limit and pump speed decreases	Initially, a decrease in turbine power causes an increase in preburner oxidizer to maintain pump flow and pressure, but this may increase turbine discharge temp beyond the redline limit and engine must be shutdown. No failure history.
B800-2 Ø = SM	Low Pressure Oxid. TP -- Crit = 1R Loss of turbine power t = I	HPOTP turbine discharge temp increase toward redline limit and pump speed decreases	Initially, a decrease in turbine power causes an increase in preburner oxidizer to maintain pump flow and pressure, but this may increase turbine discharge temp beyond the redline limit and engine must be shutdown. One test failure (1984).
B800-4 Ø = SM	Low Pressure Oxid. TP -- Crit = 1R Loss of Inducer head rise t = I	HPOTP turbine discharge temp increase toward redline limit and pump speed decreases	Initially, a decrease in turbine power causes an increase in preburner oxidizer to maintain pump flow and pressure, but this may increase turbine discharge temp beyond the redline limit and engine must be shutdown. No failure history.
B800-5 Ø = SM	Low Pressure Oxid. TP -- Crit = 1R Loss of dynamic head recovery/guidance t = I	HPOTP turbine discharge temp increase toward redline limit and pump speed decreases	Initially, a decrease in turbine power causes an increase in preburner oxidizer to maintain pump flow and pressure, but this may increase turbine discharge temp beyond the redline limit and engine must be shutdown. No failure history.
B800-6 Ø = SMC	Low Pressure Oxid. TP -- Crit = 1 Loss of support and position control t = I	Pump speed decrease and increased level of vibration. May use spectrometry to detect bearing wear	Early detection of this mode by plume spectrometry or other means is imperative to prevent vehicle loss by engine shutdown. No action is possible if turbopump fails quickly. One case of excessive vibration observed -- no attributable cause found during extensive inspections (1985)

Table 4-4 FMEA Summary - Pneumatic Controls (1 of 2)

Failure	Description	Detected by	Control System Action
C111 Ø = S	FPB Purge Check Valve -- Crit = 3 Check valve leaks t = N/A	Fuel and oxidizer preburner shutdown purge pressure	Controller monitors pressure from Start to Start +2.3 seconds. If redline limit is exceeded, engine is shutdown. No failure history.
C112 Ø = S	OPB Purge Check Valve -- Crit = 3 Check valve leaks t = N/A	Fuel and oxidizer preburner shutdown purge pressure	Controller monitors pressure from Start to Start +2.3 seconds. If redline limit is exceeded, engine is shutdown. No failure history.
C113-1 Ø = PS	Oxidizer Dome Purge Check Valve -- Crit = 1 Fails to open or restricts flow t = S	None at present	TBD No failure history.
C114 Ø = PS	Fuel Purge Check Valve -- Crit = 3 Fails to open or restricts flow KT = 1 t = 1	HPOTP or HPFTP turbine discharge temperature	Engine shutdown if redline exceeded. No failure history.
C116-1 Ø = PSC	FPB ASI Purge Check Valve -- Crit = 1, 3 Fails to open or restricts flow t = S	None at present	TBD No failure history
C117-2 Ø = S	OPB ASI Purge Check Valve -- Crit = 3 Check valve leaks t = 1	Fuel and oxidizer preburner shutdown purge pressure	Controller monitors pressure from Start to Start +2.3 seconds. If redline limit is exceeded, engine is shutdown. No failure history.
C200-7 Ø = PS	PCA oxidizer system purge -- Crit = 1 Insufficient or no N ₂ purge flow during conditioning t = M	None at present	TBD Two failures: 1982, contamination; 1984, failed poppet
C200-8 Ø = PSMC	PCA HPOTP Intermediate Seal Purge -- Crit = 1 Insufficient or no He purge flow t = 1	HPOTP intermediate seal pressure	Controller monitors intermediate seal pressure for out of limit condition. Start inhibit during Phase P. Engine shutdown during SMC (redline). No failure history.

Table 4-4 FMEA Summary - Pneumatic Controls (2 of 2)

Failure	Description	Detected by	Control System Action
C200-11 Ø = S	PCA Emergency Pneumatic Shutdown -- Failure to supply helium pressurant Crit = 1 t = 1	None at present	TBD One failure on vehicle prelaunch test, 1984, contamination
C200-16 Ø = SMC	PCA -- Fails to contain helium Crit = 1 t = 1	HPOTP intermediate seal pressure	Controller monitors intermediate seal pressure for out of limit condition. Start inhibit during Phase P. Engine shutdown during SMC (redline). No failure history.
C300-1 Ø = PSC	Helium Precharge Valve -- Insufficient or no He flow to Pogo Accumulator Crit = 3,1 t = 1	Pogo precharge pressure	Inhibit Start in Phase P Engine shutdown in Phase S TBD in Phase C -- cavitation/overspeed of oxidizer turbopumps possible at zero G and minimum NPSP. No failure history.
C300-7 Ø = PSMC	Helium Precharge Valve -- Fails to contain oxidizer Crit = 1 t = 1	None at present	TBD No failure history.

Table 4-5 FMEA Summary - Propellant Valves

Failure	Description	Detected by	Control System Action
D130-2 Ø = SM	Fuel Preburner Oxidizer Valve -- Fails to move or moves slowly. No SEII. t = S Crit = 1R	HPFTP or HPOTP turbine discharge temperature	Engine cutoff if redline is exceeded. See Note below: No Failure history.
D140-2 Ø = SM	Oxidizer Preburner Oxidizer Valve -- Fails to move or moves slowly. No SEII. t = S Crit = 1R	HPFTP or HPOTP turbine discharge temperature	Engine cutoff if redline is exceeded. See Note below: No Failure history.
D150-1 Ø = SM	Coolant Control Valve -- Fails to move or moves slowly. t = I No SEII. Crit = 1R	HPFTP Or HPOTP turbine discharge temperature	Engine cutoff if redline is exceeded. See Note below: No Failure history.
D210-4 Ø = P	Fuel Bleed Valve -- Erroneous position feedback. t = I Crit = 1R	None at present	TBD One failure, 1983 -- manufacturing procedure changed.
D220-4 Ø = P	Oxidizer Bleed Valve -- Erroneous position feedback. t = I Crit = 1R	None at present	TBD No failure history. Fleet leader has over 26,450 seconds hot fire time.
			Note: One servoactuator failure is permitted with no change in performance. Switching to redundant backup is automatic. Continued presence of SEII initiates various shutdown scenarios. When no SEII is present, turbine discharge temperatures are the failure indication parameters. SEII = Servoacutator Error Indication Interrupt

Table 4-6 FMEA Summary - Igniters and Sensors (1 of 5)

Failure	Description	Detected by	Control System Action
J201-1 & J202-1 Ø = M	MCC Pressure Transducer Crit = 1R t = S All sensors drift in the same direction	HPFTP or HPOTP turbine discharge temperatures and OPOV command limit	Present action is shutdown if temps or command limit exceeded. It may be possible to synthesize P _C based on other measurements and compare to detect erroneous drift. Three failures: 1977; port plugged with ice -- added Lee Jet purge 1985; erroneous output, broken lead wire -- new process 1987; zero shift due to link pin weld -- new weld controls
J203-1 Ø = PSMCD	LPOTP Discharge Pressure Transducer -- Crit = 3 t = N/A No output or erroneous output	None at present for erroneous output	No action required at present. Loss of data only No failure history.
J205-1 Ø = PSMCD	FPB Chamber Pressure Transducer -- Crit = 3 t = N/A No output or erroneous output	None at present for erroneous output	No action required at present. Loss of data only No failure history.
J207-1 Ø = PSMCD	Oxidizer Tank Pressurant Transducer -- Crit = 3 t = N/A No output or erroneous output	None at present for erroneous output	No action required at present. Loss of data only No failure history.
J208-1 Ø = PSMCD	HPFTP Discharge Pressure Transducer -- Crit = 3 t = N/A No output of erroneous output	None at present for erroneous output	No action required at present. Loss of data only No failure history.
J209-1 Ø = PSMCD	HPOTP Boost Pump Pressure Transducer -- Crit = 3 t = N/A No output of erroneous output	None at present for erroneous output	No action required at present. Loss of data only No failure history.
J210-1 Ø = PSMCD	Fuel Injection Pressure Transducer -- Crit = 3 t = N/A No output of erroneous output	None at present for erroneous output	No action required at present. Loss of data only No failure history.

Table 4-6 FMEA Summary - Igniters and Sensors (2 of 5)

Failure	Description	Detected by	Control System Action
J211-1 Ø = SMCD	Hydraulic Supply Pressure Transducer -- Crit = 3 t = N/A	None at present for erroneous output.	No action required at present. Loss of data only. No failure history.
J213-1 Ø = SMCD	Fuel System Purge Pressure Transducer -- Crit = 3 t = N/A	None at present for erroneous output.	No action required at present. Loss of data only. No failure history.
J216-1 Ø = SM	HPOTP IMSI Purge Pressure Transducer -- Crit = 1R t = 1	HPOTP IMSL purge pressure qualification limit.	If one channel only, it is disqualified. If both channels, redline is deleted. Two failures: 1985, 1986 ; zero shift -- link pin weld.
J218-1 Ø = SM	LPFTP Discharge Pressure Transducer -- Crit = 3 t = 1	LPFTP discharge pressure qualification limits.	If one channel only, it is disqualified. If both channels, fixed density will be used for mixture ratio control. No failure history (not listed in CIL).
J220-1 Ø = PSMCD	HPOTP Discharge Pressure Transducer -- Crit = 3 t = N/A	None at present for erroneous output.	No action required at present. Loss of data only. No failure history.
J221-1 Ø = PSMCD	MCC Coolant Outlet Pressure Transducer -- Crit = 3 t = N/A	None at present for erroneous output.	No action required at present. Loss of data only. No failure history.
J222-1 Ø = SM	Pogo Precharge Pressure Transducer -- Crit = 3 t = 1	Pogo precharge pressure and ancillary monitoring or qualification limits.	Engine shutdown, if in Start phase. No action during mainstage (loss of data only). No failure history.

Table 4-6 FMEA Summary - Igniters and Sensors (3 of 5)

Failure	Description	Detected by	Control System Action
J223-1 & 224-1 Ø = SMCD	FPB & OPB Purge Pressure Transducers -- Crit = 3 t = 1 No output or erroneous output	Preburner purge pressure redline limit	Engine shutdown, if in Start phase. No action during mainstage (loss of data only). Failure 1985; erroneous output -- broken gold leadwire. Two Failures 1985, 1986; zero shift -- link pin weld.
J225-1 Ø = SMCD	Emergency Shutdown Pressure Transducer -- Crit = 3 t = 1 No output or erroneous output	Emergency shutdown pressure purge and ancillary limits	Controller posts an MCF and vehicle will command shutdown if failure occurs during Start phase. Loss of data only during MCD phases. No failure history.
J228-1 Ø = PSM	Seal Cavity Pressure Transducer -- Crit = 3, 1R t = 1 No output or erroneous output	HPOTP secondary seal cavity pressure qualification limits	Engine shutdown, if during Start phase. If one channel only, it is disqualified. If both channels, redline is deleted during mainstage. No failure history.
J230 Ø = SM	HPFTP Coolant Liner Pressure Transducer -- Crit = 3 t = 1 No output or erroneous output	HPFTP coolant liner pressure qualification or redline limits	Engine shutdown, if during Start phase. If one channel only, it is disqualified. If both channels, redline is deleted during mainstage. No failure history.
J237 Ø = PSMCD	Pogo Pressure Transducer -- Crit = 3 t = N/A No output or erroneous output	None at present for erroneous output.	No action required at present. Loss of data only. No failure history (No CIL reference).
J301-1 & J302-1 Ø = SM	HPFTP Turbine Discharge Temperature Transducer -- Crit = 1R t = 1 Erroneous output	HPFTP Turbine discharge temperature qualification limits.	Failure of one channel during Start phase causes controller to post MCF and the vehicle will command shutdown. During mainstage, both channels bad deletes redline. Failure, 1987; probe structural failure -- changed tap location
J303-1 & J304-1 Ø = SM	HPOTP Turbine Discharge Temperature Transducer -- Crit = 1R t = 1 Erroneous output	HPOTP Turbine discharge temperature qualification limits.	Failure of one channel during Start phase causes controller to post MCF and the vehicle will command shutdown. During mainstage, both channels bad deletes redline. No failure history.

Table 4-6 FMEA Summary - Igniters and Sensors (4 of 5)

Failure	Description	Detected by	Control System Action
J306-1 Ø = SM	LPFTP Discharge Temperature Transducer -- Erroneous output Crit = 3,1R t = S	LPFTP Discharge temperature qualification limits.	Failure of one channel during Start phase causes controller to post MCF and the vehicle will command shutdown. During mainstage, both channels bad deletes redline. Two failures,1982; intermittent signal -- wet connector
J309 Ø = SMCD	MCC Coolant Outlet Temperature Transducer -- Erroneous output Crit = 3 t = N/A	None at present for erroneous output.	No action required at present Loss of data only. No failure history.
J310 Ø = SMCD	MOV Hydraulic Temperature Transducer -- Erroneous output Crit = 3 t = N/A	None at present for erroneous output.	No action required at present Loss of data only. No failure history.
J311 Ø = SMCD	MFV Hydraulic Temperature Transducer -- Erroneous output Crit = 3 t = N/A	None at present for erroneous output.	No action required at present Loss of data only. No failure history.
J312 Ø = SMCD	HPOTP Boost Stage Discharge Temperature Transducer -- Erroneous output Crit = 3 t = N/A	None at present for erroneous output.	No action required at present Loss of data only. No failure history.
J313 Ø = SM	MCC Oxidizer Injection Temperature Transducer -- Erroneous output Crit = 3 t = N/A	None at present for erroneous output.	No action required at present Loss of data only. No failure history.
J350 & J351 & J352 Ø = P	MFV/OPV/AFV Skin Temperature Transducers -- Erroneous output Crit = 3,1R t = S	Skin temperature launch temperature commit criteria limits. No detection if within limits.	Launch delay if out of limits TBD if within limits but erroneous. No failure history

Table 4-6 FMEA Summary - Igniters and Sensors (5 of 5)

Failure	Description	Detected by	Control System Action
J601-1 & 602-1 Ø = M	Fuel Flow Transducer -- Intermittent or no output Crit = 1R t = S	Fuel Flowmeter qualification limits.	Loss of one channel results in disqualification of that channel. Loss of both channels precludes mixture ratio control and the controller initiates electrical lockup. No failure history.
J607 Ø = SMCD	LPFTP Shaft Speed Transducer -- Intermittent or no output Crit = 3 t = N/A	None at present	No action required at present. Loss of data only. No failure history (no CIL entry).
J608 Ø = SMCD	HPFTP Shaft Speed Transducer -- Intermittent or no output Crit = 3,1R t = N/A	HPFTP shaft speed ignition confirmed limit.	Engine shutdown if no confirmation during Start phase. Loss of data only during MCD phases. One failure, 1985; bridge open -- Isolated failure.
J609 Ø = SMCD	LPOTP Shaft Speed Transducer -- Intermittent or no output Crit = 3 t = N/A	None at present	No action required at present. Loss of data only. No failure history.
J701-1 Ø = SM	Fuel Flowmeter -- Erroneous flowmeter turbine speed Crit = 3,1R t = S	HPFTP or HPOTP turbine temperature redline limits.	Engine shutdown if temperatures exceed redline limits. No failure history.

Exceptions:
330-5 MCC Lee Jet blocked
Detected by redundant sensors

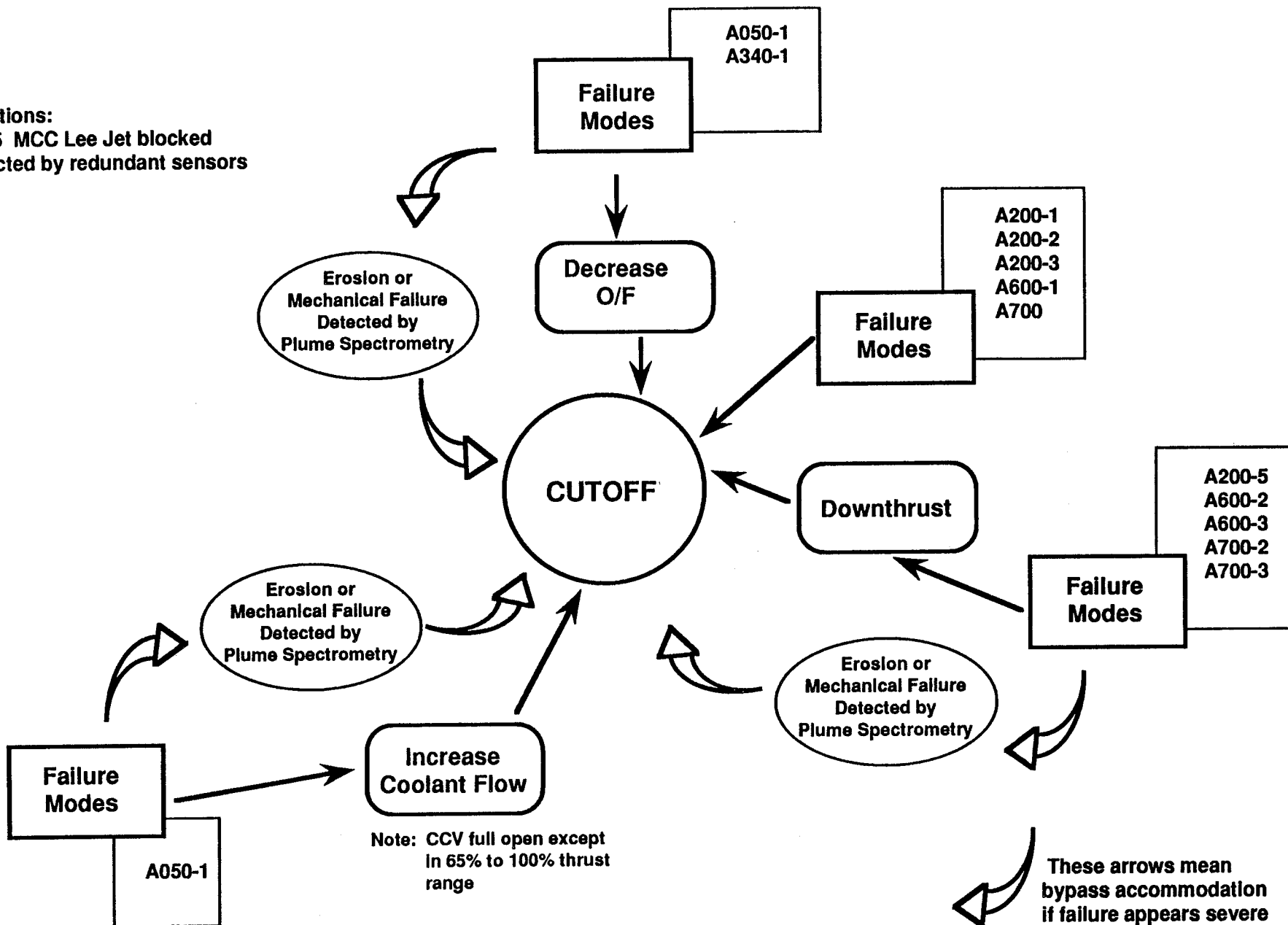


Figure 4-1 Combustion Devices

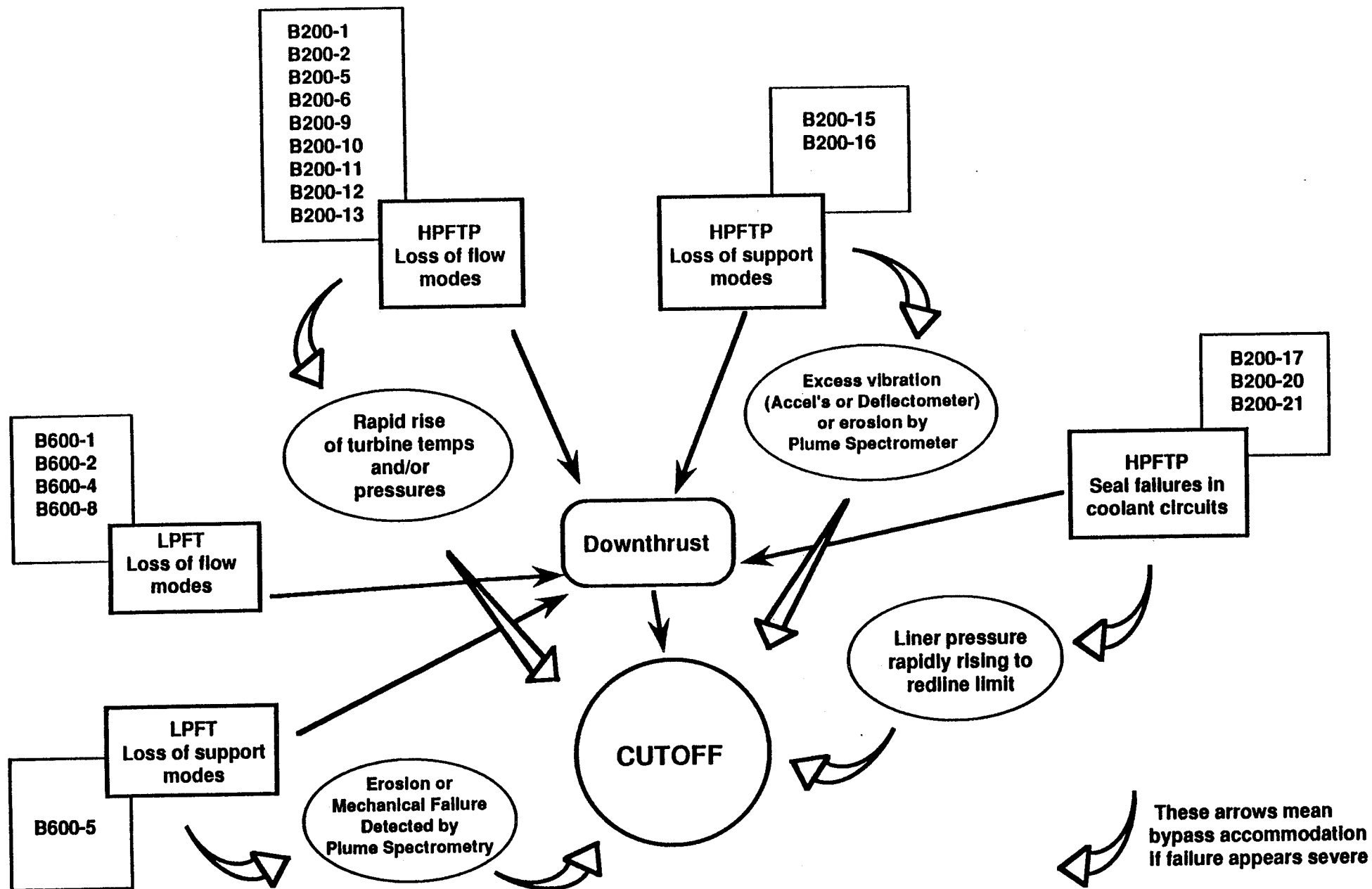
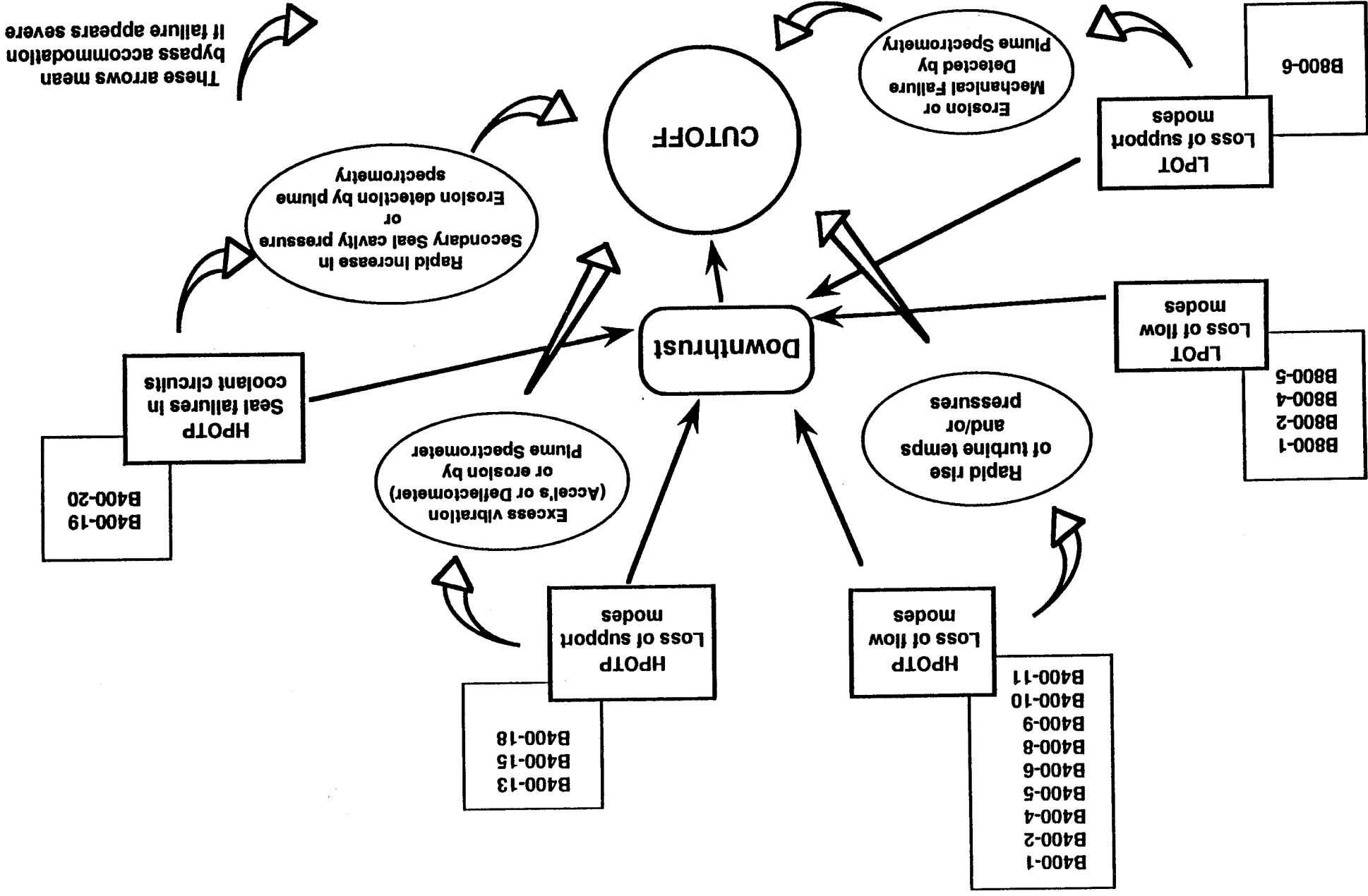


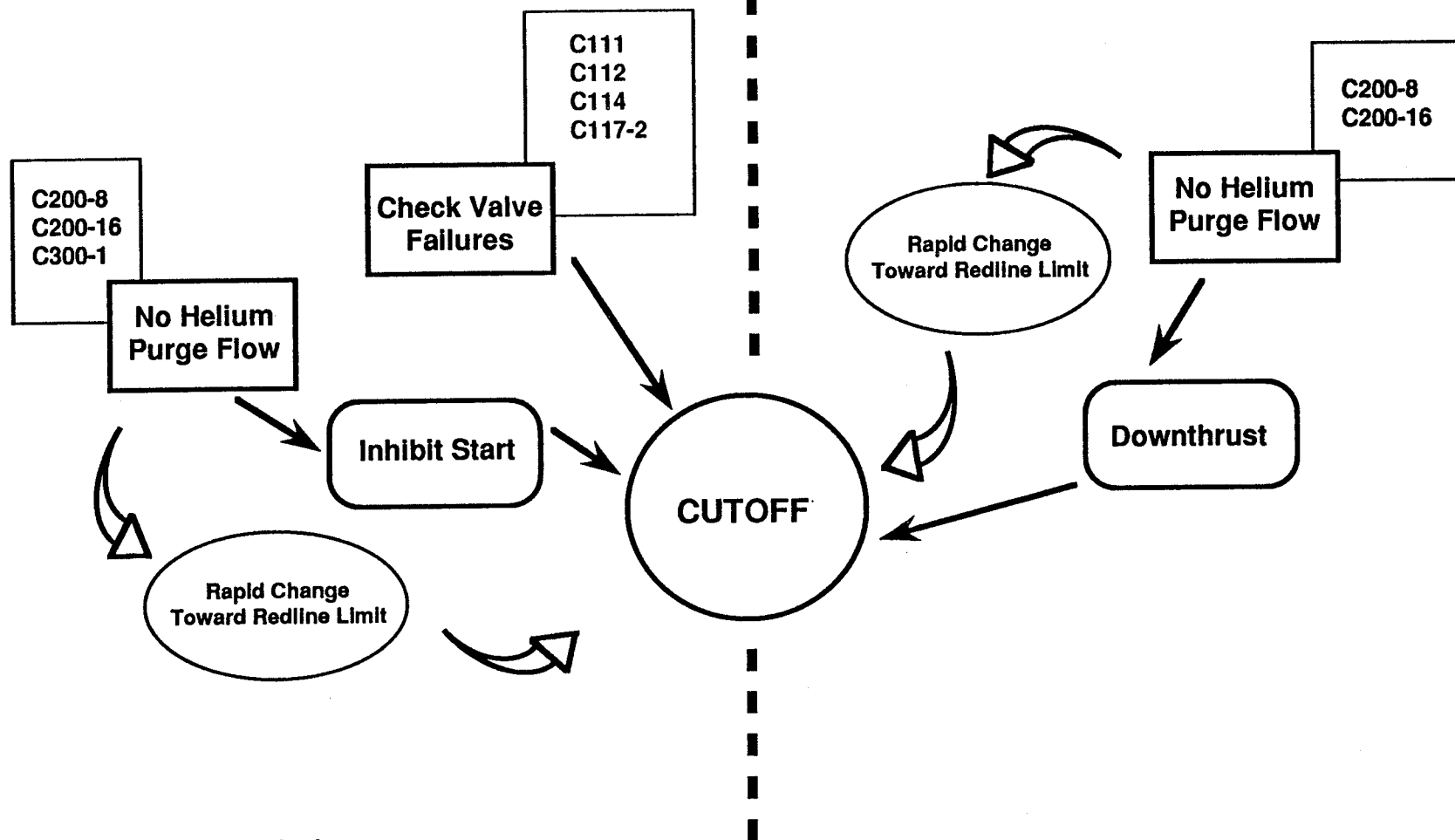
Figure 4-2 Fuel Turbopumps

Figure 4-3 Oxidizer Turbopumps



Prestart, Start, & Cutoff

Mainstage

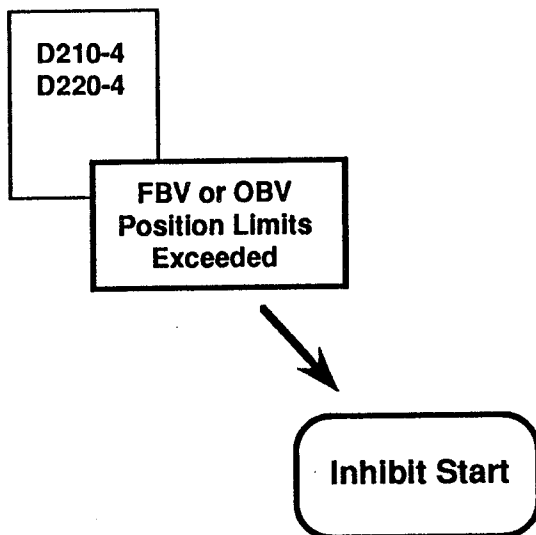


Exceptions: No detection method at present

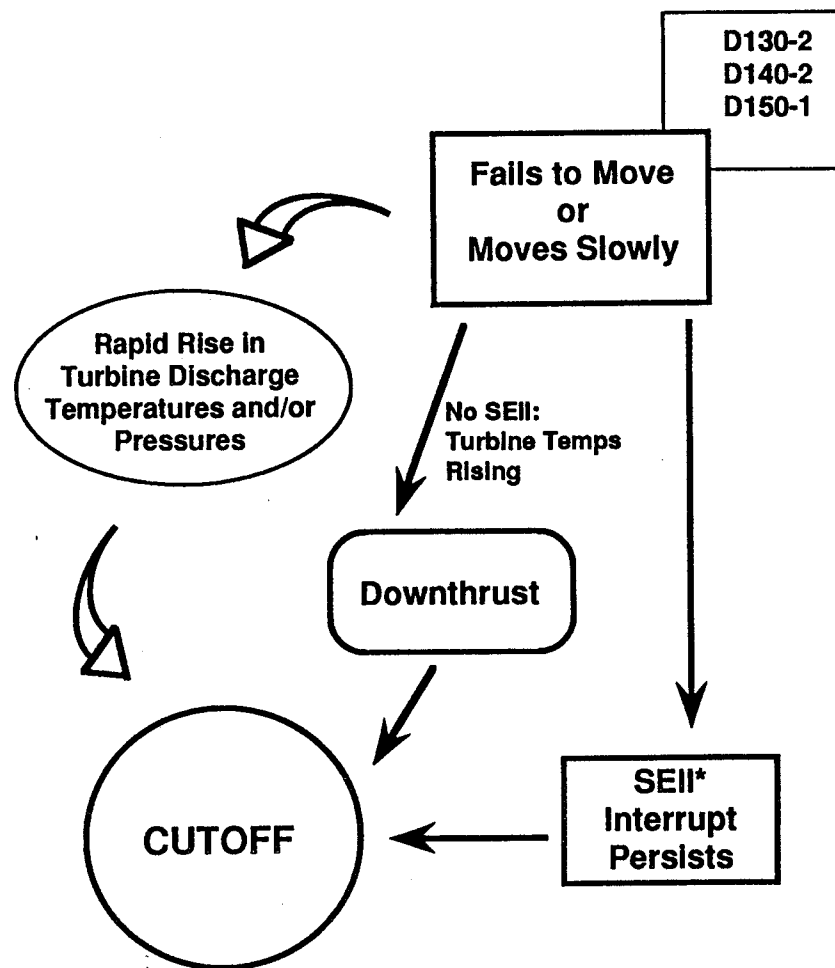
C113-1
C116-1
C200-7
C200-11
C300-7

Figure 4-4 Pneumatic Controls

Prestart



Start & Mainstage



* Note: SEII = Servoactuator Error Indication Interrupt ---
Interrupt persists if redundancy fails


 These arrows mean
bypass accommodation
if failure appears severe

Figure 4-5 Propellant Valves

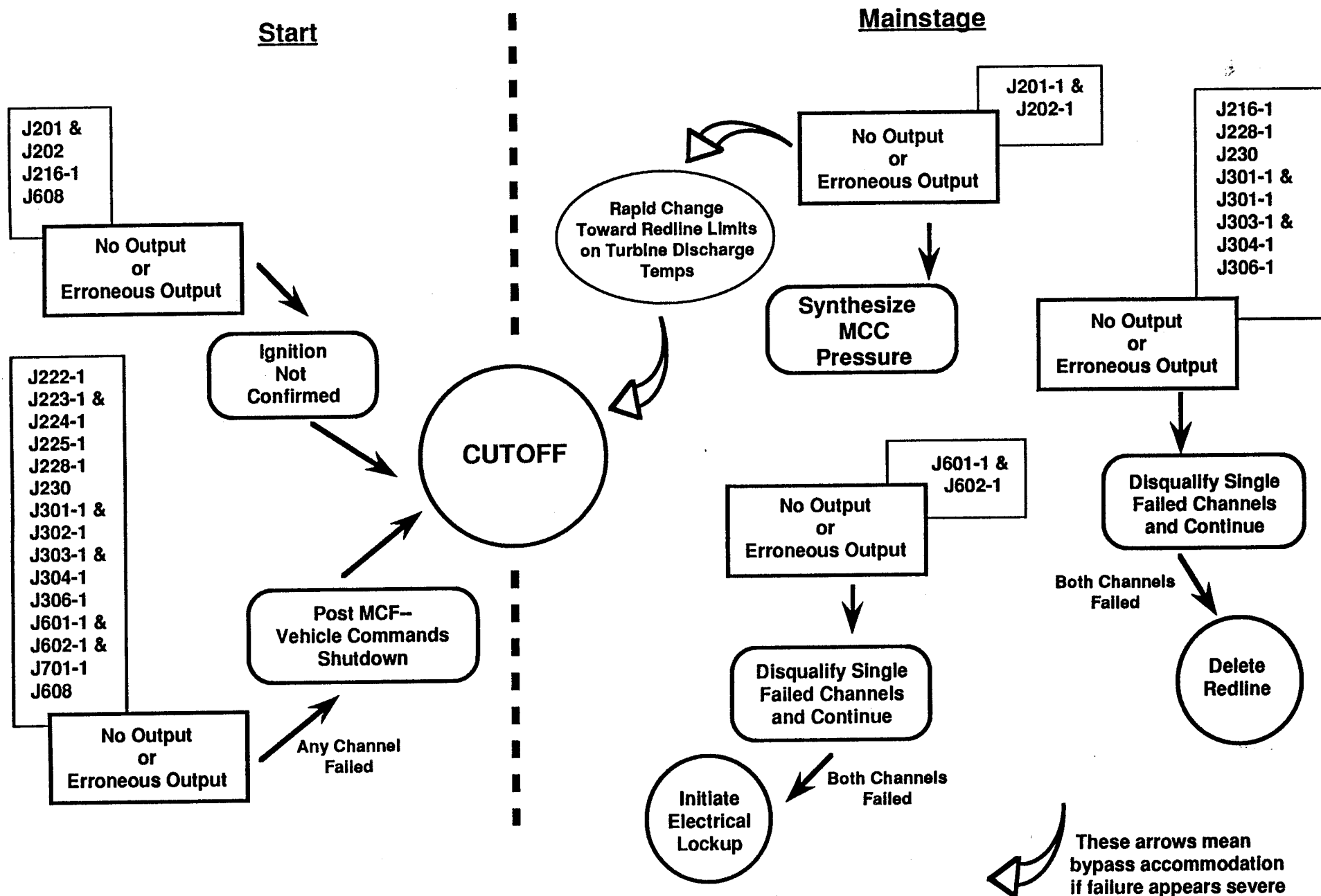


Figure 4-6 Igniters & Sensors

SECTION 5 INVESTIGATION OF SSME START TRANSIENT CONTROL

In the current SSME startup, open loop valve control, redline aborts, and closed loop valve control are used to safely start the engine. Initially, the engine is operated in an open loop mode with the valves responding to scheduled commands. Proportional and integral thrust control begins at 2.40 seconds. Proportional and Integral control of the mixture ratio is initiated at 3.6 seconds.

The valve sequence was developed for a nominal SSME start. For each perturbation about the nominal engine parameters (e.g. nominal breakaway torques, nominal propellant pressures, etc.) a slightly different valve sequence would best ensure engine start and minimize damaging transient effects. To successfully start the SSME requires that engine characteristics are measured between each flight to ensure nominal values and that external conditions (e.g. propellant conditions) are tightly controlled.

The SSME start sequence has been developed and refined to the point where the current start sequence represents a near optimal tradeoff between starting the engine and minimizing engine damaging transients. There is, therefore, little interest in exploring alternate startup techniques to improve the nominal startup characteristics.

However, the sequence of engine phenomena (governed by the startup sequence) that successfully start the engine is highly sensitive to external conditions, such as propellant temperatures, and to internal engine characteristics, such as turbine breakaway torques. Relatively minor changes in propellant conditions or engine characteristics result in large transient events (e.g. temperature spikes) or can inhibit the successful start of an engine. The sensitivity of the engine startup to external conditions and engine characteristics is attributed to: 1) the highly coupled and non-linear phenomena occurring during startup, and 2) the limited closed loop control of the engine during startup. In this task, the possibility of reducing engine startup sensitivities by using additional closed loop control during startup is investigated. The desired result of such a control strategy is a more robust and reliable engine system.

The goal of this task is to explore the means by which closed loop control may be used to increase the SSME performance and safety during startup and to determine if such closed loop control is possible. The objectives of additional closed loop control during startup, as part of the Advanced Functional Framework, include:

- desensitizing the system to engine parameter variations
- desensitizing the system to external perturbations or noise
- improving the system performance by:
 - expanding the performance envelope by stabilizing unstable engine modes
 - ensuring safe operation nearer the performance envelope boundary
- increasing the engine reliability
- reducing the SSME maintenance costs

Additional closed loop SSME startup control would achieve these advantages by monitoring and controlling all parameters of the engine which are critical to the performance and health of the engine. The current state of the SSME is a function of the prior engine state and the fuel and oxidizer flow rates throughout the engine. Thus, the state of the engine is ultimately defined by the valves, the original engine state, and engine perturbations. Since the latter two contributors cannot be directly controlled without modifications to the engine, valve control is the object of this study.

This section includes: 1) a description of the current SSME startup sequence, constraints, and failure history, 2) an overview of the approaches investigated, 3) the conclusions of this investigation, and 4) recommendations for further study.

5.1 The Current SSME Startup Sequence

5.1.1 Nominal SSME Startup

The current SSME start transient is controlled by opening the engine propellant valves in a predetermined sequence and providing limited closed loop control. This sequence was developed and optimized over the course of years with the aid of hundreds of hardware firings and thousands of simulations. A thorough description of the SSME startup valve commands and resulting engine responses are described by Bob Biggs, SSME Systems Analysis Project Engineer, in a paper presented to the American Astronautical Society in 1989 titled Space Shuttle Main Engine The First Ten Years. The SSME startup as described by Mr. Biggs is given in the next paragraphs.

When a start command is received, the MFV is immediately ramped to its full open position in two-thirds of a second (see Figure 5-0). This enables the liquid hydrogen (LH2) to fill the downstream system and begin to power the high pressure turbines. The latent heat of the hardware imparts enough energy to the hydrogen to operate as an 'expander-cycle' engine for the early part of the start sequence. This eliminates the need for any auxiliary power to initiate the start sequence, however it also creates a thermodynamic instability which is referred to as the fuel system oscillations. When the cold LH2 begins to flow into the thrust chamber nozzle, the hardware latent heat causes the hydrogen to expand rapidly, creating a flow blockage and momentary flow reversal. The result is a pulsating fuel flow rate with an unstable pressure oscillation at a frequency of approximately 2 Hz. The oscillations continue to increase in magnitude with dips (reductions in pressure) occurring at approximately 0.25, 0.75, and 1.25 seconds, until the establishment of MCC chamber pressure causes it to stabilize after 1.5 seconds. Events prior to stabilization had to be made to conform to the idiosyncrasies of the fuel system oscillations.

Simultaneously with the opening of the MFV, electrical power is provided to the spark plugs in the augmented spark igniters (ASI) included in each of the three combustors. The ASI will then ignite the combustors when both fuel and oxidizer are present in the proper mixture ratio. The fuel is provided first by the MFV being opened and then the oxidizer is provided later for each combustor separately through the three oxidizer valves. Each valve has an ASI liquid oxygen (LOX) supply line that allows LOX to flow to the ASI upon initial valve motion (about 5 percent). The proper mixture ratio for ignition is achieved by the second dip in pressure caused by the fuel system oscillations.

After the MFV starts to open, the three oxidizer valves are separately subjected to a series of position commands intended to precisely control the oxidizer system priming times for the three combustors. Priming is the process of filling the system with liquid, as with the old hand cranked water pump. An oxidizer system is said to be 'primed' when it is filled with liquid down to the combustor such that the flow rate entering the injector is equal to the flow rate leaving the injector to be burned in the combustor. This event generally results in a rapid rise in combustion chamber pressure. The target priming times for the three combustors are a tenth of a second apart; FPB prime at 1.4 seconds, MCC prime at 1.5 seconds, and OPB prime at 1.6 seconds. Although part of the valve positioning is accomplished under a limited form of closed loop control, it is merely a convenient method of commanding the valves to a predetermined position and therefore will be treated as if it were all done an open loop commanded positions as a function of time.

The first oxidizer valve to be commanded is the FPOV. After a delay of 0.10 seconds, the FPOV is ramped to 56 percent open at its maximum slew rate. At 0.72 seconds, the FPOV is given a 'notch' command to close to about 10 percent and then reopen. This is done to compensate for the second pressure dip caused by the fuel system oscillations and avoid damaging temperature spikes in the HPFTP turbine. During this dip, the FPB is ignited and the additional power causes a slight acceleration in the HPFTP speed. Just prior to the third fuel system oscillation pressure dip, the FPOV is given another notch command which is maintained throughout the priming sequence.

A safety check is made at 1.25 seconds to ensure that the HPFTP speed is high enough to safely proceed through the priming sequence. The speed must be high enough at MCC prime to be able to pump hydrogen through the downstream system against the backpressure rise created by the MCC prime, or an engine burnout will occur due to the resulting oxygen-rich combustion. It was determined from test experience that if the speed were to be less than 4600 RPM at 1.25 seconds (Figure 5-0a), then it would likely be too low at MCC prime to maintain pumping capability. The engine must be shutdown at 1.25 seconds because, if the speed is discovered to be too low later in the start sequence, there is insufficient time to react and shut down safely.

When the FPB prime occurs at 1.4 seconds, there is a rapid rise of pressure at the inlet to the HPFTP turbine. Since the turbine back pressure is not provided until MCC prime, this pressure rise causes a high turbine pressure ratio and a significant acceleration in the HPFTP speed (Figure 5-0b). The higher HPFTP speed is desirable for a cool fuel rich start, however the turbine back pressure must be applied (MCC prime) soon to prevent a runaway condition.

MCC prime is primarily controlled by positioning of the MOV. After an initial delay of 0.20 seconds, the MOV is slowly ramped to just under 60 percent open. This combination of time delay, ramp rate, and position provides a LOX flow rate that causes MCC prime to occur at 1.5 seconds and creates an engine system balance that will produce a safe low mixture ratio (between 3 and 4) for the stabilized operation just prior to activating the closed loop thrust control system at 2.4 seconds. When MCC prime occurs at 1.5 seconds, it causes a rapid rise in MCC chamber pressure (Figure 5-0c) which, because it increases the turbine back pressure, acts as a brake to decelerate the HPFTP (Figure 5-0b).

The OPOV is used to control OPB prime. Its initial opening is after a delay of 0.12 seconds, however, the opening only retracts the valve inlet seal which is designed to provide sufficient oxygen to ignite the ASI and to have a small leakage flow into the OPB injector. The valve is designed so that the major flow path does not start to open until an indicated position of 46 percent. The slow ramp shown in Figure 5-0d has no effect on the OPB LOX flow rate except to delay until 0.84 seconds when the main flow path through the valve starts to open. This flow path is partially open for about a third of a second before it recloses and the OPB is again run on valve leakage flow. The timing for this opening is scheduled to provide sufficient oxygen to allow the ASI to ignite the OPB before the second fuel oscillation pressure dip recovers and causes a significant decrease in mixture ratio. The next opportunity for ignition would be about half a second later. With valve leakage flow, OPB prime occurs at 1.6 seconds and causes an increase in drive power to both high pressure turbines. The power increase stabilizes at about 2 seconds with the MCC chamber pressure at approximately 25 percent of rated power level (RPL). During this time the chamber coolant valve (CCV), which was full open at start, is throttled down to 70 percent in order to force additional coolant flow through the MCC. The engine is allowed to run at this condition until 2.4 seconds to assure stable operation. The additional time period of 0.4 seconds is to allow for and absorb normal variations in propellant pressures and temperatures.

By using the engine mounted sensors, the main engine controller (MEC) verifies proper ignition and operation of the three combustors at 1.7 seconds and again at 2.3 seconds. If no malfunctions are discovered the closed loop thrust control system is activated at 2.4 seconds. The MEC compares the measured MCC chamber pressure to a pre-programmed chamber pressure ramp to RPL and modulates the OPOV in an attempt to zero out any differences. During this time, the FPOV is simply moved by the MEC with position changes that are proportional to the amount of OPOV movement, and the CCV is commanded open at a rate commensurate with the commanded chamber pressure ramp rate. Because of the engine dynamic response characteristics, the resulting chamber pressure lags behind the command by about 0.2 seconds. At 3.8 seconds the closed loop mixture ratio control system is activated using the FPOV to adjust fuel flow rate until the commanded mixture ratio is achieved. At 5 seconds the engine has achieved stabilized operation at RPL with a mixture ratio of 6.

A detailed listing of the events that are initiated, monitored, and controlled by the SSME controller during engine startup is provided as Appendix 4.

5.1.2 SSME Startup Constraints

Certain physical constraints of the SSME startup define the minimal conditions necessary to safely start the engine and define the boundaries that new control strategies must work within. These constraints have been identified based on analytical analysis of the SSME, the results of SSME hot fire tests, and the results of early development testing. Each of these constraints, and failures which have resulted from their violation, are summarized below.

Preburner Ignition Time: The high pressure fuel and oxidizer turbine preburners must ignite between 0.75 and 0.80 seconds from start-up to produce the required turbopump acceleration to achieve satisfactory start and plateau (the phase during which the engine has settled to an intermediate level prior to initiation of closed loop MCC pressure control at $t=2.4$ seconds) performance. Ignition time is governed by the fuel system oscillations and sufficient oxidizer flow must be available during the fuel flow pressure dip for ignition at this time. If ignition is delayed, the fuel density and fuel flow increase as the hardware chills and the resulting mixture ratios and propellant injection flow velocities are not proper for complete and evenly distributed combustion in the preburners resulting in combustion fluctuations and local temperature excursions.

Fuel and Oxidizer Preburner Oxidizer Flow at Ignition: The preburner oxidizer flow-rates must be sufficient at ignition time to achieve ignition and ensure total combustion. If partial combustion occurs, plateau performance is low and ignition of the remaining injection elements does not take place until the engine is approaching or has already achieved mainstage. This results in large preburner "pops" (e.g. test 902-081 to 902-084, Engine 0002) and temperature spikes as the inlet injection elements are ignited which may cause turbine damage (e.g. test 902-068, Engine 0002).

An indication of the oxidizer flow limits can be obtained by examining results of early ignition tests. For the initial Integrated Subsystem Test Bed (ISTB, early developmental SSME) tests, the Oxidizer Preburner Oxidizer Valve (OPOV) was commanded open at 300 milliseconds after engine start command with a 200 percent per second (%/sec.) ramp rate with satisfactory preburner ignition. The time at which the OPOV starts to open was subsequently changed to 120 milliseconds after engine start command with no change in preburner ignition time since fuel side oscillations govern the ignition. On the other hand, on test 901-034, when the OPOV initial opening ramp was reduced to 100%/sec. (starting at 300 milliseconds after the start command) ignition did not occur.

Fuel Preburner Priming Time: The fuel preburner oxidizer manifold must prime between 1.45 and 1.55 seconds (nominal) after engine start command. If the fuel preburner primes early, fuel flow may be low due to fuel side oscillations, resulting in a high mixture ratio and overtemperature of the High Pressure Fuel Turbine (HPFT). For example, the FPB primed early on test 901-178 and 901-179, Engine 0005, with erosion of the HPFT. Prime occurred at approximately 1.25 seconds after engine start on both of these tests. This time is at the minimum fuel flow caused by the fuel system oscillations. Delay of prime to 1.5 (+/- 0.05) seconds after engine start will result in FPB priming at the maximum fuel flow condition produced by the fuel system oscillations.

Sequential Order of Combustor Primes: Priming of the SSME combustors must occur in a specified sequential order to achieve minimum turbine discharge temperatures. The FPB must prime first, then the main chamber and, finally, the OPB. Priming of the FPB first is required to ensure continued acceleration of the HPFP during start and to insure that the HPFP speed is high enough to maintain fuel flow with the increased pump head required at MCC prime. If the FPB primes too late, i.e., after the MCC has primed, HPFP speed and, consequently, fuel flow may not be sufficient at preburner prime to prevent damage to the high pressure turbines. On test 901-166, Engine 0002, the FPB primed at 1.67 seconds, approximately 100 milliseconds after the main chamber primed. When the fuel preburner did prime (at the same time as the OPB), HPFP speed was not high enough resulting in a low fuel flow condition with excessive HPFT and HPOT temperature.

Approximately 100 milliseconds after the FPB primes, the MCC should prime. This time delay is used to accelerate the HPFP and provide the desired fuel flow margin. At MCC prime, the HPFT and HPOT pressure ratios are significantly decreased (increasing back pressure) and the turbopump acceleration slows down. The effect on the HPOP is much greater since the OPB is not primed and its acceleration is essentially stopped until OPB prime. The loss of HPOP acceleration and continued acceleration of the HPFP increases fuel flow to each preburner. Finally, the OPB prime should occur approximately 100 milliseconds after the MCC prime. The increased fuel flow and fuel density to the OPB prevents an overtemperature condition at prime. After prime, the HPOP starts to accelerate until the plateau speed levels are reached. If the OPB primes too early, fuel flow is not adequate and a HPOT overtemperature condition will result with turbine damage. On test 901-164, Engine 0002, the OPB primed 30 milliseconds before the MCC. Fuel flow to the OPB was not sufficient at this time and extensive turbine damage resulted. A similar condition occurred on test 902-107, Engine 0101, with the OPB priming immediately after the MCC. To provide the required fuel flow, the OPB should prime approximately 100 milliseconds after the main chamber has primed.

MCC Priming Time: The MCC should prime no later than 1.7 seconds after engine start. Priming of the main chamber results in increasing the fuel system pressure above critical pressure so that the fuel flow oscillations are terminated. The fuel flow oscillations get bigger with time and, therefore, MCC prime is required between the second (FPB prime) and third oscillation. In addition, priming of the MCC increases fuel density so that the effect of the reduced fuel system pressure drop on flowrate is minimized.

HPFP Speed at MCC Prime: The HPFP speed should be a minimum of 8000 RPM at MCC prime. This speed is required so that the reduction in HPFP fuel flow at MCC prime does not decay below the pump throttle limit line (which may result in boilout). In addition, this speed level insures adequate fuel flow to each preburner during the MCC and OPB priming sequence.

Turbopump Speed Ratio: The ratio of HPFP speed to HPOP speed should be a minimum of 1.2 at the time of MCC prime. The increased HPFP speed relative to the HPOP speed results in increased preburner fuel flow and minimized the possibility of turbine overtemperature. A speed ratio of 1.04 at MCC prime occurred on test 902-166, Engine 0002, with HPOT

damage. Ratios of approximately 1.0 to 1.1 have also been experienced on the early OPB prime tests with HPOT turbine damage. An earlier FPB prime relative to the MCC prime results in achieving speed ratios in excess of 1.2.

Plateau Mixture Ratio: The engine mixture ratio should be between 3.0 and 4.0 to provide the desired transition into mainstage. Low plateau mixture ratio caused by poor HPOT performance also results in low main combustion chamber pressure producing high HPOT discharge temperatures and/or pressure oscillations during the transition into mainstage.

Mixture ratios above 4.0 may result in a mixture ratio overshoot until the MR loop is closed. The thrust ramp into mainstage is controlled by the OPOV only with a cross-feed gain to the FPOV. Therefore if mixture ratio is high on the plateau, this condition could result in an overshoot in mixture ratio during the upthrust with possible MCC overheating.

Hardware Conditioning: The engine hardware upstream of the fuel and oxidizer valves must be pre-conditioned prior to engine start so that all latent heat in excess of propellant temperature equilibrium is removed. If the oxidizer side hardware is not conditioned properly, the engine start transients will be slow. The slow start transients cause low HPFP speed at prime and high turbine discharge temperature (test 901-027, ISTB). If the fuel side hardware is not conditioned properly, the liquid hydrogen may vaporize causing cavitation of the HPFP and turbine overtemperature.

5.2 Overview of Proposed Approaches

Several approaches were investigated to evaluate the feasibility and potential benefits of implementing closed loop control during the SSME startup.

For closed loop control to be successful, the SSME must satisfy three important control conditions: the SSME must be observable, modelable, and controllable. Observability is the ability to discern what state the engine is in. Sensors to directly measure the variables associated with each component are not necessary for observability, if that variable can be reconstructed from other measurements through observers, models, or filters. However, the more complete and more accurate the engine measurements, the higher the performance an engine controller may attain since control actions are taken on reliable and trusted data. Modelability reflects the degree to which the engine variables making up the desired state vector can be accurately described. Controllability is, strictly speaking, the ability to control the engine state to arbitrary values in finite time. However, in this investigation the requirements for controllability are relaxed to include "improvements" in the engine startup transient. Therefore the engine is considered controllable if the ability exists to mitigate adverse effects of external influences, factors inherent to engine startup, or engine anomalies.

Four stages of engine controllability were defined for the SSME startup as shown in Figure 5-1. Stage 1 begins when the engine start command is received and continues until the engine is established as a continuous system. During stage 1, the engine propellant system (ducts, LOX domes, etc.) fill with propellant, combustible mixtures are established in the combustion chambers, the combustible mixtures are ignited, and the high pressure turbopumps begin to speed up. The goal of the stage 1 start transient is to establish the engine as a continuous system in a state suitable for the start sequence to continue and to minimize engine damaging transient affects. The discrete events that are characteristic of stage 1 include the ignition of propellant gasses in the combustion chambers, the temperature resulting from combustion chamber ignitions, the timing and sequence of LOX dome primes, the temperatures resulting from the sudden increase in LOX flow when the domes prime, and the speed of the HPFTP when the MCC LOX dome primes. The transient nature of stage 1 is indicated by the FPB temperature as shown in Figure 5-2. Stage 2 begins after the discrete events related to

establishing the engine as a continuous system have occurred and continues until the thrust buildup phase of the start sequence (stage 3) is reached. During stage 2, the engine state is transitioned to an equilibrium and allowed to "settle out". The goal of the stage 2 start transient is to transition the engine parameters to a suitable state to enable a safe and reliable thrust buildup to mainstage values. Stage 3 is the thrust buildup phase of the start transient and is characterized by the initiation of closed loop control of the MCC pressure in the current SSME start sequence. Stage 4 starts when the current SSME start sequence initiates closed loop control of the engine mixture ratio and represents the mainstage control case.

The start transient stage which has the highest potential for improvement by using closed loop control is stage 1 since the primary engine damaging transients occur during this stage. Therefore, the efforts of the start transient investigation are concentrated on the stage 1 start transient. Additionally, some consideration is given to resolving anomalies that occur in stage 2, primarily those resulting from conditions during stage 1. Stages 3 and 4 were not investigated as part of the start transient investigation since some form of closed loop control is currently used during these stages of the start sequence.

The SSME is not easily observable or controllable and is not perfectly modeled during the stage 1 start transient. Most engineers in the SSME program, and others who have studied startup control of the SSME engine, have made this observation. Because of this, SSME experts have had to rely on test firings to support analytical approaches to determine an acceptable SSME startup procedure. Therefore, much of the knowledge related to the SSME startup is in the form of engineering expertise gained through this endeavor. This investigation relies heavily on that expertise to supplement and clarify the results obtained with the SSME transient model.

Three approaches were investigated for the SSME stage 1 start transient. These are:

- a) Extended start sequence
- b) Robust nominal sequence - continuous control of critical engine start variables
- c) Robust nominal sequence - influence coefficient, model-based valve control

The initial approach for using closed loop control during the stage 1 start transient was to extend the start sequence and thereby reduce adverse transient effects. The investigation of the extended start sequence provided no indications that any benefit would be realized and the approach was abandoned. Within the constraints of the SSME, the nominal start sequence provides a near optimal tradeoff between engine startup reliability and adverse transient effects. Therefore, the investigation turned to closed loop control approaches that provide a startup that is more robust to external influences and engine conditions. The first, continuous multiple input/multiple output control, failed due to a lack of observable/controllable variables during the SSME start transient. The second approach, an influence model based controller, indicated some promise and was the most thoroughly investigated approach.

5.2.1 Extended Start Sequence

The initial approach investigated is extending the start sequence while attempting to control critical SSME startup parameters such as turbine speeds and temperatures. The philosophy is to smoothly bring the SSME up to mainstage, avoiding severe transient effects inherent to the current startup. The basic argument for this approach is that the most severe normal start transient effect is the potentially turbine blade damaging temperature spikes that occur in the preburner at preburner ignition and when the FPB LOX dome primes (Figure 5-3 to 5-4).

The test data shown in Figure 5-3a indicates an ignition temperature spike of about 80 R. However, this value is somewhat misleading since: 1) the temperature measured is the fuel turbine discharge temperature, not the preburner temperature, and 2) the temperature sensor

used on the engine has a relatively slow time constant. The fuel turbine discharge temperature is lower than the preburner temperature since the hot gasses generated in the preburner (and incident on the first stage turbine blades) pass through a labyrinth of relatively cool hardware before exiting the turbine. Once these cooled gasses exit the turbine, the temperature is measured with a slow sensor that further attenuates the true reading. Ground tests which included a preburner temperature sensor indicate a much higher temperature spike than is indicated by the SSME flight sensors. The SSME system dynamics group evaluated this data and determined that the true preburner temperature excursion during the ignition spike is about 25 to 27 times greater than that indicated by the HPFT discharge temperature sensors. Using a conversion factor of 25, the temperature spike shown in Figure 5-3a would be expected to correspond to a maximum preburner temperature of about 2500R ($500 + 25 \cdot 80$).

Figure 5-3b shows the fuel turbine discharge temperature calculated by the SSME transient model. The transient model results agree with the actual test data in both magnitude and time of the ignition spike as indicated by the fuel turbine discharge sensor. The transient model also provides an estimate of the actual preburner temperature as shown in Figure 5-4. The calculated fuel preburner temperatures during the ignition spike agree with the maximum value estimated using SSME test data. The agreement between transient model results and measured test data provides a degree of confidence that the temperature transients indicated by the transient model accurately reflect the true SSME FPB temperature transients during startup.

Investigation of the extended start sequence identified two major flaws in the approach: 1) the transient effects with the current SSME startup that are most critical to engine damage, fuel preburner temperature spikes, are not reduced, and 2) other potentially damaging transient effects, most notably sidelading on the engine nozzle, are significantly increased.

Initially, extending the duration of the fuel preburner temperature transients was investigated. Two fuel preburner temperature spikes, the ignition spike and the priming spike, are indicated in Figure 5-4. The ignition spike is caused by the ignition of the propellant gasses in the preburner when an ignitable mixture ratio is reached. The priming spike is caused by the sudden increase in oxidizer flowrate into the preburner that occurs when the fuel preburner LOX dome is primed. Both fuel preburner temperature spikes are the result of discrete events, i.e. ignition and LOX dome priming. The risetime and duration of the temperature spikes are then governed solely by the physical characteristics of the event. For example, when the combustible mixture of propellant gasses is ignited, the only time limitation is the propagation of the flamefront. Therefore, while modifying the propellant flows in the engine may change the time at which the fuel preburner ignites and the fuel preburner LOX dome primes, the risetime and duration of the resulting temperature spikes will be unchanged.

Reducing the magnitude of the fuel preburner temperature spikes was then investigated. The preburner temperature is directly related to the preburner mixture ratio as demonstrated by comparing the fuel preburner temperature (Figure 5-4) with the fuel preburner mixture ratio (Figure 5-5). Both the fuel and oxidizer preburners are run very fuel rich and all of the oxidizer injected into the preburners is burned. Since the fuel/oxidizer combustion is the source of energy in the combustion gasses, the energy (heat) imparted per unit of combustion gasses is directly proportional to the ratio of oxidizer to fuel (mixture ratio). No method of reducing the fuel preburner mixture ratio at ignition or LOX dome prime that was related to extending the start sequence could be identified.

Therefore, based on the above arguments, it is concluded that extending the engine start sequence provides no mechanism for reducing the adverse effects of the fuel preburner temperature spikes.

Additionally, the effect of extending the start sequence on other engine startup transients was investigated. No additional potential benefits were identified. However, several adverse effects were noted. The most severe of these are: 1) additional transverse loading of the high pressure turbopump bearings, 2) additional thermal loading of the MCC, and 3) additional side loading of the engine nozzle.

Transverse loading of the high pressure turbopump bearings is caused by the vibration of the turbopump which increases as its speed passes through the turbopump natural frequencies. Slowly bringing the turbopump up to its mainstage operating speed, which is a requirement for an extended start sequence, increases the time spent near each natural frequency and consequently increases the overall turbopump vibrations.

Additional thermal loading of the MCC is caused by lower fuel flowrates during startup. During startup, the combustion temperature in the MCC is nearly equal to the mainstage combustion temperature; 5000R at 1.8 seconds compared to a mainstage value of about 6000R. However, the fuel flowrate during startup is significantly less than the fuel flowrate during mainstage. Since the fuel flow acts as a coolant for the MCC wall, during startup there is less available coolant to the MCC walls than during mainstage operation. The disparity between startup and mainstage conditions is accommodated somewhat by closing the chamber coolant valve (CCV) and forcing a higher percentage of the available fuel through the MCC coolant circuit, but the MCC thermal balance is not achieved until mainstage flowrates are reached.

Side loading of the engine nozzle is caused by the turbulent flow conditions that exist in the nozzle until the engine thrust reaches 80% - 85% of the rated power level (RPL) at sea level. Even though the engine is at a reduced thrust level, the flowrates and associated forces are still considerable. The combustion gas flow rate through the nozzle at 80% - 85% of RPL is in excess of 850 lbm/sec. Nozzle side loading during startup is strikingly indicated during an SSME ground test or a space shuttle launch. The SSME visibly "jumps" and jerks from side to side during the startup until the nozzle flow becomes laminar at about 85% of RPL. An extended start sequence requires that the engine thrust increases to 85% of RPL over a longer time period than with the current startup resulting in increased nozzle side loading.

The investigation of additional transient effects associated with an extended start sequence, leads to the conclusion that an extended start sequence is expected to increase the stress levels of several major engine components - the high pressure turbopumps, the MCC, and the nozzle.

The results of the extended start sequence investigation are threefold:

- 1) No improvement in fuel preburner startup temperature transients were identified,
 - 2) No beneficial transient effects on other major engine components were identified,
- and
- 3) Several adverse transient effects were identified for major engine components.

Therefore, it is concluded that any form of closed loop control designed to extend the SSME start sequence has no potential to extend engine life, increase engine reliability, or reduce engine maintenance.

5.2.2 Continuous Control of Critical Engine Start Variables

The results of Section 5.2.1 indicate that the nominal SSME start transients cannot be improved upon within the constraints of the existing SSME configuration. However, the nominal start transients are extremely sensitive to external influences and engine conditions. For example, Figure 5-6 shows the expected increase in the fuel preburner ignition temperature spike for several off-nominal fuel inlet pressures. The FPB ignition spike reaches temperatures of about

6500R for fuel inlet pressures significantly less than the nominal 45 psi. Further insight into the start transient sensitivities is provided in Section 5.1.

An approach to make the current start sequence more robust to external influences and engine conditions was proposed. The proposed approach was to provide continuous closed loop control over the engine variables that are critical to successfully starting the engine and the variables that affect engine damaging transients. Each variable would be controlled to mimic (or at least approach) the time varying values observed during a nominal startup.

Based on the startup phenomena and constraints described in Section 5.1, the following events and conditions were identified as critical to a nominal engine startup (the proposed engine variables to implement the required control are included in parentheses):

- 1) the time of FPB ignition
(fuel flow rate and oxidizer flow rate into the FPB)
- 2) the time of OPB ignition
(fuel flow rate and oxidizer flow rate into the OPB)
- 3) the time of FPB LOX dome prime
(FPB LOX dome oxidizer level)
- 4) the time of MCC LOX dome prime
(MCC LOX dome oxidizer level)
- 5) the time of OPB LOX dome prime
(OPB LOX dome oxidizer level)
- 6) the speed of the HPFTP when the MCC primes
(HPFTP speed)

In addition, the following conditions were identified as critical to minimizing adverse transient effects:

- 7) the FPB temperature (mixture ratio) at FPB ignition
(fuel flow rate and oxidizer flow rate into the FPB)
- 8) the FPB temperature (mixture ratio) when the FPB LOX dome primes
(fuel flow rate and oxidizer flow rate into the FPB)
- 9) the OPB temperature (mixture ratio) at OPB ignition
(fuel flow rate and oxidizer flow rate into the OPB)
- 10) the OPB temperature (mixture ratio) when the OPB LOX dome primes
(fuel flow rate and oxidizer flow rate into the OPB)

If the identified engine variables (fuel flowrate into the FPB and OPB, oxidizer flowrate into the FPB and OPB, the three LOX dome levels, and the HPFTP speed) can be controlled to replicate the values observed during a nominal startup, then the critical engine startup events and transients should mimic those of a nominal engine startup.

Problems with continuous closed loop control of the start sequence arise due to the actual observability and controllability of the proposed variables. Each of the proposed variables is theoretically observable and controllable. However, measuring or estimating and controlling some of the variables to the accuracy required for useful engine control is extremely difficult or impossible within realistic constraints imposed by the SSME configuration (with the exception of measuring the HPFTP speed).

First consider the fuel flowrate into the FPB and OPB. Observability can be readily achieved with flowmeters incorporated into the fuel lines leading to each of the preburners. This statement is based on the premise that a flowmeter can be designed that accurately measures small gaseous hydrogen flowrates at low pressures and also measures (or at least survives)

gaseous hydrogen flowrates up to 86 lbm/sec at over 6000 psi during mainstage operation. A difficult task, but one that is seemingly realistic. Optical flow measuring techniques exist (Laser induced pulse/echo techniques) that technically should be able to measure the low level flowrates if cost and reliability issues are acceptable.

Controllability of the fuel flow into the FPB and OPB is not available with the existing SSME configuration, but limited control can be achieved with valves incorporated into the fuel lines leading to each preburner. Control is limited by the availability of gaseous hydrogen in the system. The MFV is open to 100% at the beginning of the start transient and fuel flowrates through the system oscillate as described in Section 5.1. If a pressure dip occurs at a time that more fuel is required in a preburner, it may simply not be available no matter how far the preburner fuel valve is opened. Theoretically, during start, the fuel path upstream of the preburner fuel valves can be operated so that the pressure is always above the minimum required to supply the maximum nominal flowrate to the preburners, but this results in a certain amount of stagnation in that part of the system. The stagnation causes more of the engine hardware latent heat to be expended in warming up gaseous hydrogen rather than expanding liquid hydrogen (the driving force responsible for starting the engine). The feasibility of providing positive pressure in this manner while extracting sufficient energy from the engine hardware to power the early start transient is not clear. Therefore, controllability of the fuel flow into the preburners is left an open issue.

The amount of oxidizer actually flowing into the FPB and OPB during engine startup is very difficult, perhaps impossible with the existing SSME configuration, to observe. Liquid oxygen is introduced into a labyrinth of relatively hot hardware through the LOX dome and injector assembly. The oxygen boils and some of the oxygen remains in the LOX dome while some of the oxygen flows through the injector into the preburner. No realistic means of directly measuring the oxygen flowrate actually entering the preburner could be identified. Estimating the oxidizer flowrate into the preburner has difficulties that appear prohibitive. Reliable models of the oxidizer dome filling and the corresponding oxidizer expulsion into the preburner are not available and are not likely due to the complexities of the reaction and sensitivity to a multitude of parameters (LOX temperature, hardware temperature, oxidizer inlet pressure, preburner backpressure, time history of oxidizer flow into the cavity, engine orientation, etc.). Therefore, to estimate the oxidizer flowrate into the preburner, the oxidizer entering the LOX dome and the oxidizer remaining in the LOX dome must be measured. Measuring the oxidizer flow into the LOX dome requires either a flowmeter downstream of the preburner oxidizer valve, since some of the oxidizer entering the valve is rerouted to supply oxidizer to the ASI, or another flowmeter on the ASI line. A flowmeter downstream of the preburner oxidizer valve introduces additional hot hardware for the oxidizer to encounter. The preburner oxidizer flowmeter must be able to accurately measure the mass flowrate of two-phase, boiling, cryogenic oxygen for low flowrates and still measure (or at least survive) liquid oxygen flow rates up to 79 lbm/sec at 6800 psi during mainstage. It seems unlikely that such a flowmeter could be designed that meets the engine reliability requirements. The original LOX flowmeter was removed from the SSME because it presented too great a risk. Even allowing that such a flowmeter can be designed, severe difficulties still exist with measuring the oxidizer level in the LOX dome.

The oxidizer flowrate into the preburner is entirely dictated by (and effects) events occurring in the preburner LOX dome, therefore the oxidizer flowrate into the preburner cannot be controlled independently from the LOX dome priming event. Additionally, the same sensitivities that inhibit estimating LOX dome filling inhibit reliable control of the oxidizer flowrate into the preburner since the only mechanism for getting oxidizer into the preburner is through the LOX dome. Therefore, for the purpose of continuous closed loop start sequence control, the oxidizer flowrate into the preburners lacks the required controllability.

The LOX dome oxidizer level is not reliably modellable as described above. Therefore, a means of directly measuring the oxidizer level was considered. It is critical to note that the oxidizer level that must be measured refers to the amount of liquid oxidizer in the LOX dome cavity, not the height of the two phase fluid. Therefore, the required measuring device must be capable of measuring the volume of the LOX dome cavity occupied by liquid oxygen under boiling conditions. No such device or technique could be identified that is realistic for application to the LOX dome.

Controllability of the LOX dome filling appear inadequate for continuous closed loop control of the start sequence by the same arguments that discount controllability of the oxidizer flow into the preburner.

HPFTP speed is directly measurable to a high degree of accuracy during the start transient. However, controllability of the HPFTP speed is not achieved until the fuel preburner lox dome primes and enables some degree of control over the amount of energy available to the high pressure fuel turbine. The lack of controllability until the fuel preburner LOX dome primes is shown by Figures 5-7 and 5-8. Figure 5-7 indicates the position of the FPOV during the start transient. The FPOV is the actuation that most strongly affects the HPFTP speed. Figure 5-8 shows the HPFTP speed during the start transient. Changes in the FPOV position have no detectable affect on the HPFTP speed until after 1.4 seconds when the fuel preburner LOX dome primes. After 1.4 seconds, changes in the FPOV position cause noticeable changes in the HPFTP speed.

Therefore:

- 1) the fuel flowrate into the preburners is observable and somewhat controllable
- 2) the oxidizer flowrate into the preburners is not observable and not controllable
- 3) the LOX dome oxidizer levels are not observable and not controllable
- 4) the HPFTP speed is observable and controllable

Based on the limited observability and controllability of the identified variables, it was concluded that closed loop control of the SSME start sequence based on measurement and control of the critical engine start variables was not feasible.

5.2.3 Influence Model Based Controller

The investigation of continuous control of critical engine start variables, described in Section 5.2.2, indicates that the engine variables that need to be controlled to ensure a safe and reliable engine startup are inadequately observable and controllable during the stage 1 start transient. Therefore, any feasible closed loop control strategy for the stage 1 start transient cannot rely on observation and control of the engine variables primarily responsible for the start transient phenomena described in Section 5.2.2. Therefore, a control strategy based on relating only observable variables to the stage 1 start transient phenomena was investigated. The selected approach to implementing the control strategy was to base the start transient control on the influence that observable external factors, engine conditions, and control variables are expected to have on the start phenomena - an influence model. The control strategy investigated is to quantify the influence of external factors and engine conditions, combine the individual influences of each factor and condition, and then determine changes in the engine control variables that offset the non-control influences.

A simple example of the influence model based control strategy is brewing a pot of coffee using an automatic drip coffee maker. Assume 3 scoops of coffee grounds and 10 cups of water produce the nominal pot of coffee. Further assume that 8 cups of nominal coffee are required for a given purpose. The "correct" amount of coffee grounds for the off-nominal

amount of water is estimated by an operator that has used the machine before and knows that 2 cups less water requires 1/2 scoop fewer coffee grounds. The relationship between cups of water and scoops of coffee is a simple influence model. The external factor (2 cups less water) is observed, the expected influence (strong coffee) is estimated, and the control response (1/2 scoop fewer coffee grounds) to offset the external influence is implemented. It is important to note that the operator generally has little knowledge of the chemistry associated with brewing coffee or even the events occurring within the coffee maker and is still able to control the coffee state (temperature, taste) to near nominal, for a variety of water levels. It is equally important to note that if the coffee maker has an unobservable failure (e.g. heating coil burns out) the resultant coffee state will be far from nominal (cold). Additionally, if asked to make 1 cup of coffee, the amount of coffee grounds used by the operator (based on an influence model developed around a nominal 10 cup water level) is likely to be far from the "correct" value.

The example used above illustrates three important features of an influence model: 1) a useful model can be developed without observation or complete understanding of the interactions that relate the external influence to the desired output, 2) unobservable anomalies are not accounted for, and 3) the model is useful only over the range of observed (or simulated) influences used to develop the model. Generally, for a complex system, the observed influences consist of limited perturbations to the nominal system. To explore all combinations of external influences and internal conditions is not feasible because of the large number of off-nominal combinations that must be considered. Therefore, practical influence models are limited to perturbations around a nominal system.

For the SSME stage 1 start transient, the influence model is a model of the start transient in which the influence of external factors (e.g. propellant inlet pressures), engine conditions (e.g. high pressure turbine torques), and control variables (e.g. FPOV position) on the controlled engine phenomena are characterized by observation and simulation.

Investigation of the influence model based control strategy consisted of 1) identifying stage 1 start transient phenomena to be controlled, 2) evaluating the controllability of the selected phenomena, 3) developing a limited influence model for the SSME start transient, 4) simulating an anomaly in an external influence (low fuel inlet pressure), and 5) simulating an anomaly in an internal engine condition (MOV error)

5.2.3.1 Stage 1 Start Transient Control Phenomena

The stage 1 start transient phenomena selected as control parameters are those identified in Section 5.2.2 as critical to a safe and reliable engine startup

The critical stage 1 start transient phenomena (as described in Section 5.1) were identified as:

- 1) the time of FPB ignition
- 2) the time of OPB ignition
- 3) the time of FPB LOX dome prime
- 4) the time of MCC LOX dome prime
- 5) the time of OPB LOX dome prime
- 6) the speed of the HPFTP when the MCC primes
- 7) the FPB temperature at FPB ignition
- 8) the FPB temperature when the FPB LOX dome primes
- 9) the OPB temperature at OPB ignition
- 10) the OPB temperature when the OPB LOX dome primes

5.2.3.2 Controllability and the Influence Model

The SSME digital transient model was used to evaluate several off-nominal FPOV and OPOV start sequences. The results of this evaluation were used to assess the controllability of the selected start transient phenomena. Additionally, the results were used to develop a limited influence model for the stage 1 start transient. The limitations on the influence model are: 1) only the FPOV and OPOV are used as control valves, 2) no multiple influences were investigated, and 3) influences were quantified only over a limited range around the nominal engine state. The limitations result from the desire to limit the number of simulation runs and the inability (within the scope of this effort) to modify the SSME digital transient model. No fundamental limit exists on the capability to develop a comprehensive influence model for the stage 1 start transient.

Four test cases were run: 1) a positive offset in the FPOV flow area [approx. 0.003 in^2], 2) a positive offset in the OPOV flow area [approx. 0.002 in^2], 3) a positive offset in the first FPOV notch time [+0.05 seconds], and 4) a negative offset in the FPOV first notch time [-0.10 seconds].

The FPOV and OPOV flow area offsets are shown in Figures 5-9 and 5-10. The offsets were implemented by increases the valve leakage value in the digital transient model and are labeled as "FPOV leak" and "OPOV leak" in the subsequent data plots. The relevant digital transient model data resulting from the FPOV and OPOV flow area offsets is shown in Figure 5-11. Changes in critical start transient phenomena resulting from the FPOV and OPOV flow area offsets are listed in Table 5-1. Table 5-1 lists the nominal value for each phenomena in the "Nominal" column and lists the changes from nominal in the "FPOV" and "OPOV" columns.

The FPB ignition time is measured as the time that the main spike of the first temperature transient occurs in the fuel preburner (Figure 5-11d). The OPB ignition time is measured as the time that the main spike of the first temperature transient occurs in the oxidizer preburner (Figure 5-11b). The FPB prime time is measured as the time when the fuel preburner pressure begins to rise rapidly (Figure 5-11c). The OPB prime time is measured as the time when the oxidizer preburner pressure begins to rise rapidly (Figure 5-11a). The MCC prime time is measured as the time when the main combustion chamber pressure begins to rise rapidly (Figure 5-11f). The HPFTP speed at the first plateau is measured where the HPOTP speed levels out after MCC prime (Figure 5-11e). The FPB temperature at ignition is measured as the

maximum temperature reached during the first fuel preburner temperature transient (Figure 5-11d). The FPB temperature at FPB LOX dome prime is measured as the maximum temperature reached during the second fuel preburner temperature transient (Figure 5-11d). The OPB temperature at ignition is measured as the maximum temperature reached during the first oxidizer preburner temperature transient (Figure 5-11b). The OPB temperature at OPB LOX dome prime is measured as the maximum temperature reached during the second oxidizer preburner temperature transient (Figure 5-11b)

The offsets in the first FPOV notch time are shown in Figure 5-12. Changes in critical start transient phenomena resulting from the offset first FPOV notch time are listed in Table 5-2. Table 5-2 lists the nominal value for each phenomena in the "Nominal" column and lists the changes from nominal in the "0.60" and "0.75" columns. The complete set of digital transient model data plots for each case is provided in the appendices. Appendix 1 contains the nominal simulation. Appendix 2 contains the data plots for an FPOV first notch time of 0.60 seconds. Appendix 3 contains the data plots for an FPOV notch time of 0.75 seconds. The data summarized in Table 5-2 was measured from the data plots in the appendices in the manner described for the offset FPOV and OPOV flow area simulations.

The digital transient model indicates that each of the selected start transient phenomena is controllable. Furthermore, the data summarized in Tables 5-1 and 5-2 define a simple influence model for the stage 1 start transient. The influence on controlled phenomena (FPB ignition, FPB prime time, etc.) by control variables (OPOV and FPOV position/time) are clearly defined for a limited range of control options.

5.2.3.3 Simulation of a Low Fuel Inlet Pressure Anomaly

The nominal fuel inlet pressure during SSME startup is 45 psi, with an allowable window of 43 to 47 psi for successful SSME startup. The stage 1 and 2 start transient was simulated with the digital transient model using a fuel inlet pressure of 42 psi to represent a degrading external influence on the start transient. The most notable and potentially damaging anomaly in the engine is a large increase in the magnitude of the FPB ignition temperature transient (Figure 5-13c).

If the influence model were completed, the fuel inlet pressure (an external factor) would be measured and the corresponding start transient influence would be estimated as a 2400 R increase in the FPB ignition temperature. Then an offsetting control action would be determined. In this case, the anomaly was manually evaluated and determined to be a 2400 R increase in the magnitude of the FPB ignition temperature. As indicated by the influence data shown in Table 5-1, an increase of 0.003 in² in the FPOV flow area is expected to result in a 100 R increase in FPB ignition temperature. The ratio of delta FPOV flow area to delta FPB ignition temperature results in an influence coefficient of 0.00003 in²/R. Therefore, the influence data indicates that a reduction in valve area of 0.072 in² is required to reduce the FPB ignition temperature to its nominal value. By manually evaluating the start transient anomalies and using the influence data to estimate effective control actions, the influence model based control strategy is replicated.

Figure 13 shows the data plots from three digital transient model runs: 1) the nominal case - fuel inlet pressure of 45 psi, 2) the anomalous case - fuel inlet pressure of 42 psi, and 3) the anomalous case with a modified valve sequence.

Figure 5-14 summarizes the digital transient data by providing bar graphs of the selected start transient phenomena for the nominal simulation, simulation with a fuel inlet pressure of 42 psi, and the simulation with a fuel inlet pressure of 42 psi and a modified valve sequence.

Figures 5-13 and 5-14 indicate that the FPB ignition temperature is the only start phenomena to significantly differ from the nominal case when the fuel inlet pressure is reduced and the original start sequence is used. A FPB ignition temperature of 4800 R is indicated. When the control action determined manually from the influence data is incorporated into the simulation, the simulation shows a decrease in the FPB ignition temperature from 4800 R to about 2700 R. The decrease in FPB ignition temperature is close to that estimated with the influence data. However, severe transient affects were generated in other start transient phenomena by the control action as shown in Figure 5-14.

The simulation of the influence model based control strategy seems worse than the open loop case. However, the anomaly upon which the control action was based is significantly improved. These facts indicate that the influence model based control strategy has the potential to reduce stage 1 start transient anomalies, but requires a more extensive influence model to be effective.

5.2.3.4 Simulation of a Main Oxidizer Valve Anomaly

The digital transient model was used to simulate an anomalous engine condition, a misaligned main oxidizer valve (MOV). The valve resistance was changed in the model so that at a position of 60% open the valve resistance was equivalent to a normal MOV at 55% open. Additionally, a simulation was run with the misaligned MOV and an influence model based control strategy employed.

For the influence model based control strategy used to determine the modified start sequence in the final simulation the following parameters are relevant:

- 1) The observable engine condition is the oxidizer system effective resistance (OSER) defined as:

$$\text{Oxidizer System (OSER) Effective Resistance} = \frac{\text{High Pressure Oxidizer Discharge Pressure}}{(\text{Oxidizer Flow})^2}$$

- 2) The start transient phenomenon to be addressed is the HPFTP speed at MCC LOX dome prime time.
- 3) The control action considered is a change in the MOV position.

The control strategy consists of measuring the amount that the OSER is away from nominal, estimating the affect the off-nominal value of OSER will have on the HPFTP speed when the MCC LOX dome primes, and determining the change in MOV position required to counteract the estimated HPFTP speed anomaly.

The influence coefficients were defined from the simulation results as:

$$\text{Influence Coefficient (1)} = \frac{\Delta \text{HPFTP Speed at MCC LOX Dome Prime}}{\Delta \text{OSER}} = \frac{300 \text{ RPM}}{-0.04} = -7500$$

$$\text{Influence Coefficient (2)} = \frac{\Delta \text{MOV Position}}{\Delta \text{HPFTP Speed at MCC LOX Dome Prime}} = \frac{+5\%}{-300 \text{ RPM}} = -0.0167$$

Figure 15 shows the data plots from three digital transient model runs: 1) the nominal case, 2) the anomalous case - MOV misaligned, and 3) the anomalous case with a modified valve sequence.

Figure 5-14 summarizes the digital transient data by providing bar graphs of the selected start transient phenomena for the nominal simulation, simulation with misaligned MOV, and the simulation with a misaligned MOV and a modified valve sequence.

The results indicate that the HPFTP speed when the MCC LOX dome primes is much closer to the nominal value of 14500 RPM in the controlled case than in the open loop case (Figure 5-15f).

5.2.3.5 Summary of Influence Model Controller Investigation

The fuel inlet pressure anomaly and the MOV anomaly simulations indicate that the control strategy is effective at bringing single start transient phenomena closer to their nominal values under anomalous conditions. However, other aspects of the start sequence were significantly degraded during the low fuel inlet pressure anomaly.

The study was performed as a feasibility demonstration and only single start transient phenomena were considered in evaluating a control response using only a specific valve. To fully evaluate the utility of the influence model based control strategy, a complete influence model needs to be developed that evaluates the influence on all of the start phenomena when determining the control response and determines the response for all of the control valves.

5.3 Conclusions of The Closed Loop Start Sequence Investigation

It appears that any form of control designed to slow down the SSME start sequence has no potential to extend engine life, increase engine reliability, or reduce engine maintenance. Investigation of extending the duration of the start sequence shows no improvement in fuel preburner startup temperature transients, no beneficial transient effects on other major engine components, an increase in MCC thermal loading, an increase in transverse loading of the high pressure turbopump bearings, and an increase in nozzle side loading.

Continuous control of the engine critical start variables during the early start sequence (0.0 to 1.6 seconds) is not feasible because the critical engine variables (ignitions, priming, flowrates) have limited observability and controllability during this period.

Closed loop control based on an influence model appears to hold some potential for improving the robustness of the current start sequence. Simulations with limited influence models resolve single transient anomalies but seem to cause larger anomalies elsewhere in the start sequence.

A full influence model that takes into account all of the critical startup events and evaluates the influence of each valve is required for a more thorough evaluation.

5.4 Recommendations for Further Study

Two areas for further study are suggested by the results of the investigation performed under this contract.

1. Development and evaluation of a full influence model for control of the early start sequence.
2. Evaluation of a modified engine in which observability and controllability of critical start transient variables is possible. The limitation with the current engine configuration seems to be the time before the LOX domes prime, it is therefore recommended that an investigation along this path include simulation of an engine in which the oxidizer system is fully primed prior to initiating engine start.

Table 5-1 Start Transient Changes for Offsets in FPOV and OPOV Flow Areas

Change in Flow Area	None (nominal)	FPOV	OPOV
FPB Ignition Time, @ Main Spike (seconds)	0.73	0	0
OPB Ignition Time, @ Main Spike (seconds)	1.0	0	0
FPB Prime Time (seconds)	1.41	-0.02	-0.02
OPB Prime Time (seconds)	1.70	-0.04	-0.09
MCC Prime Time (seconds)	1.48	0	-0.01
HPFTP Speed @ Plateau (RPM)	14500	+500	+100
FPB Temperature, Maximum @ FPB Ignition (°R)	2400	+100	0
FPB Temperature, Maximum @ FPB Prime °R)	2200	+100	0
OPB Temperature, Maximum @ OPB Ignition (°R)	760	-20	+240
OPB Temperature, Maximum @ OPB Prime (°R)	630	0	+70

Table 5-2 Start Transient Changes for Changes in FPOV Notch Time

1st FPOV Notch Time (seconds)	0.70 (nominal)	0.60	0.75
FPB Ignition Time, @ Main Spike (seconds)	0.73	-0.03	+0.01
OPB Ignition Time, @ Main Spike (seconds)	1.0	+0.03	0
FPB Prime Time (seconds)	1.40	+0.02	-0.02
OPB Prime Time (seconds)	1.65	+0.03	+0.01
MCC Prime Time (seconds)	1.47	-0.05	+0.01
HPFTP Speed @ Plateau (RPM)	14500	-500	+200
FPB Temperature, Maximum @ FPB Ignition (°R)	2400	-200	+200
FPB Temperature, Maximum @ FPB Prime (°R)	2200	-350	-1150
OPB Temperature, Maximum @ OPB Ignition (°R)	720	+200	-60
OPB Temperature, Maximum @ OPB Prime (°R)	580	0	0

Figure 5-0 SSME Start Sequence

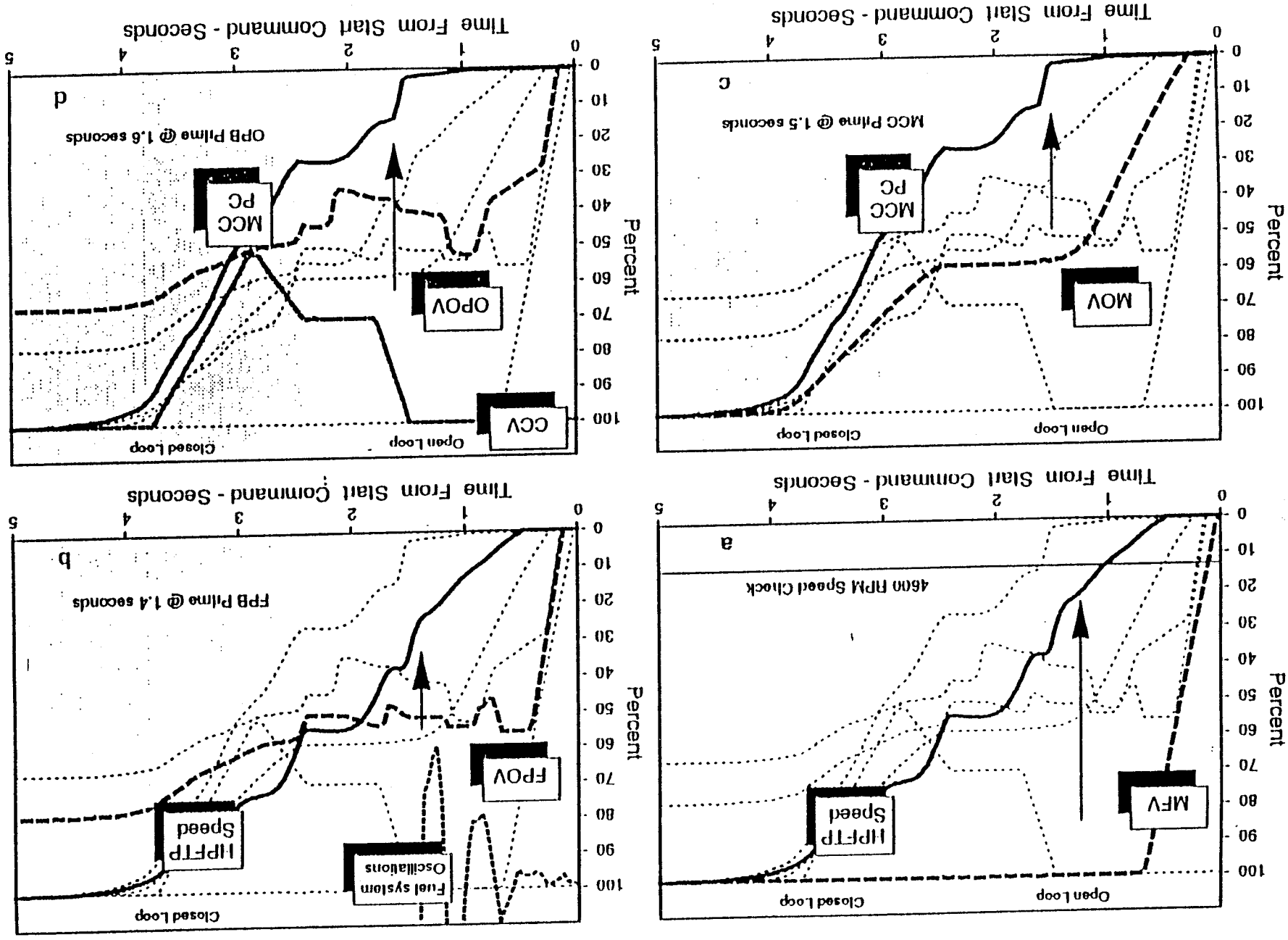
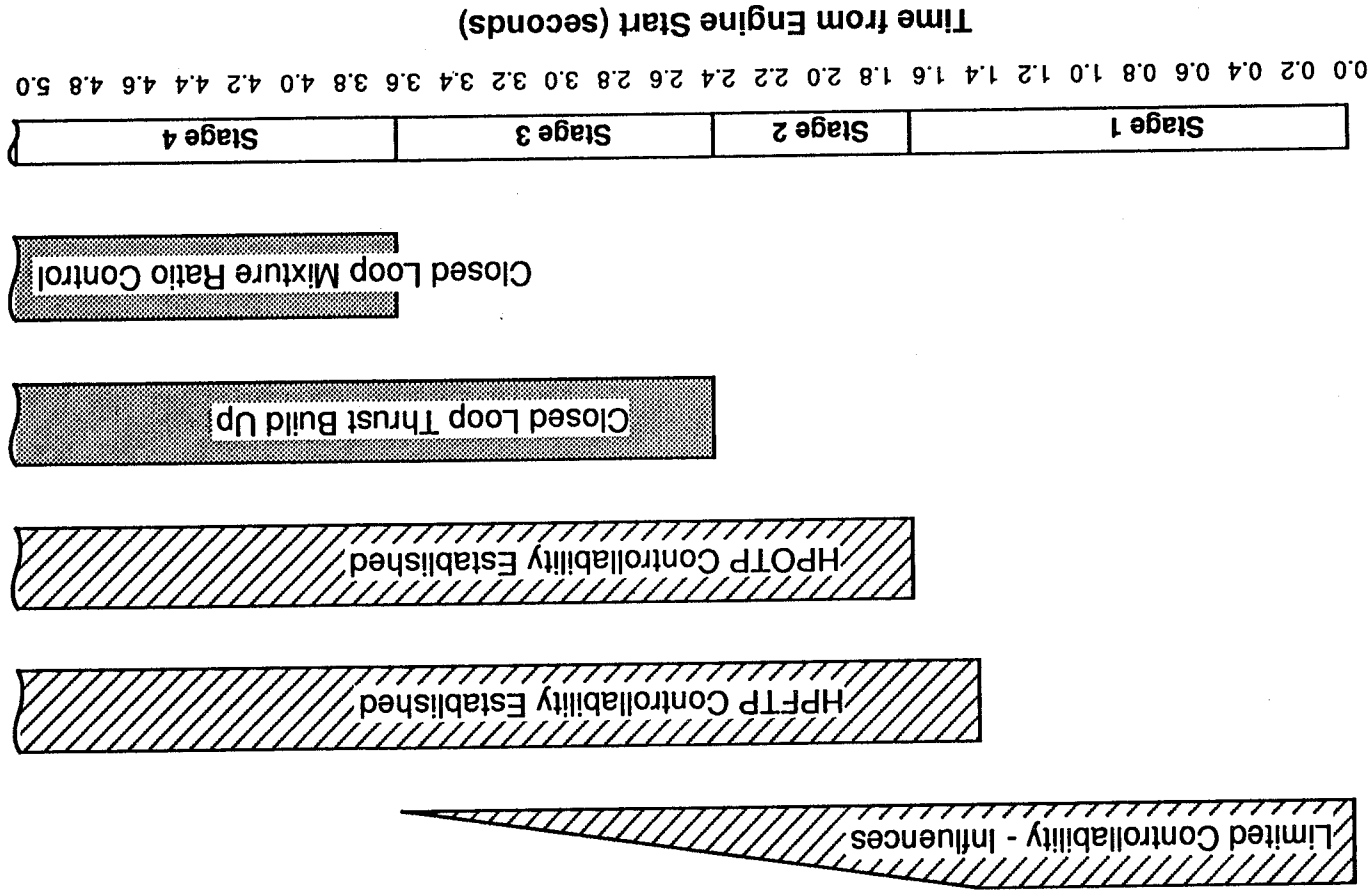


Figure 5-1 SSME Startup Stages of Controllability



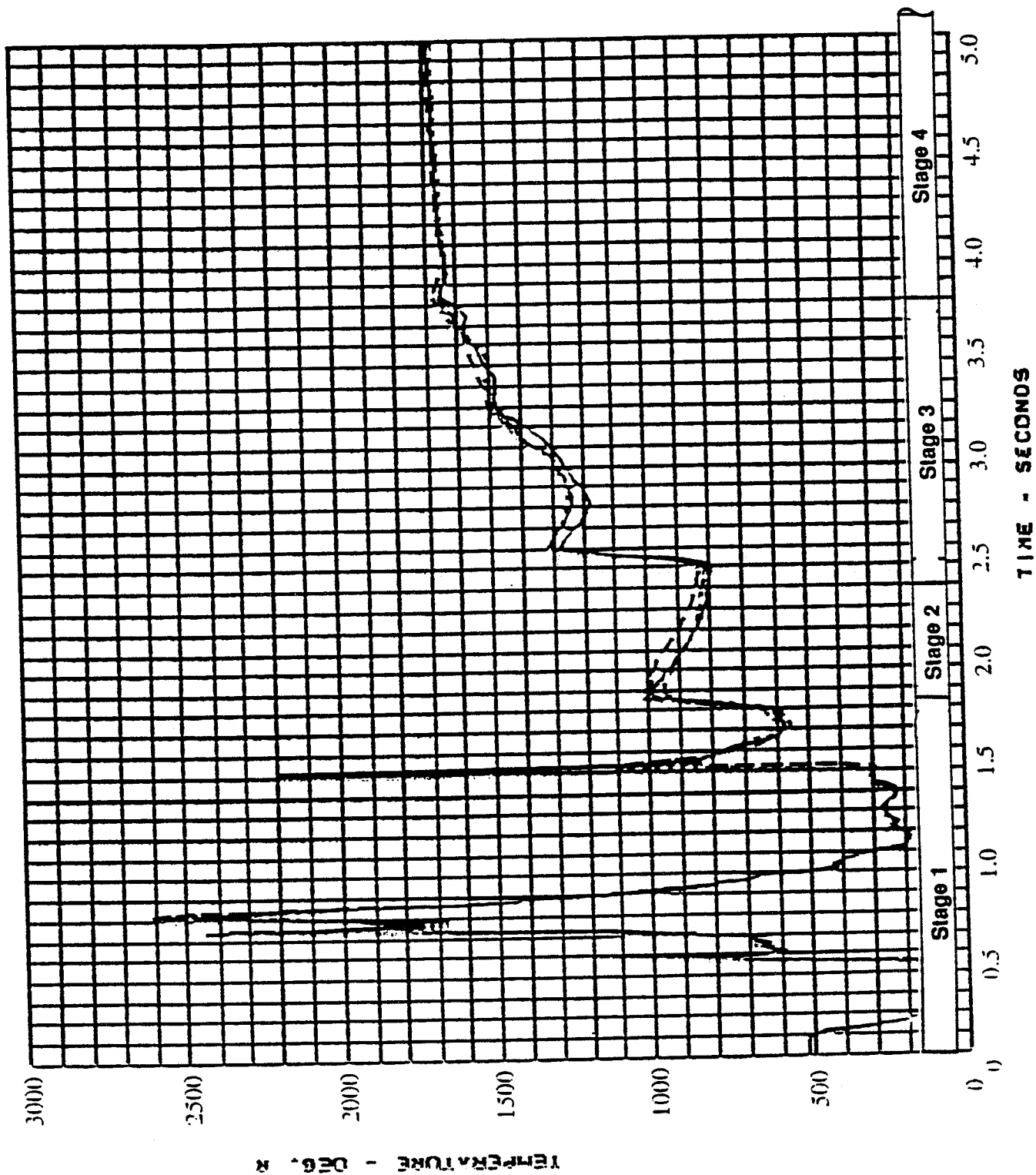


Figure 5-2 SSME FPB Temperature During Startup

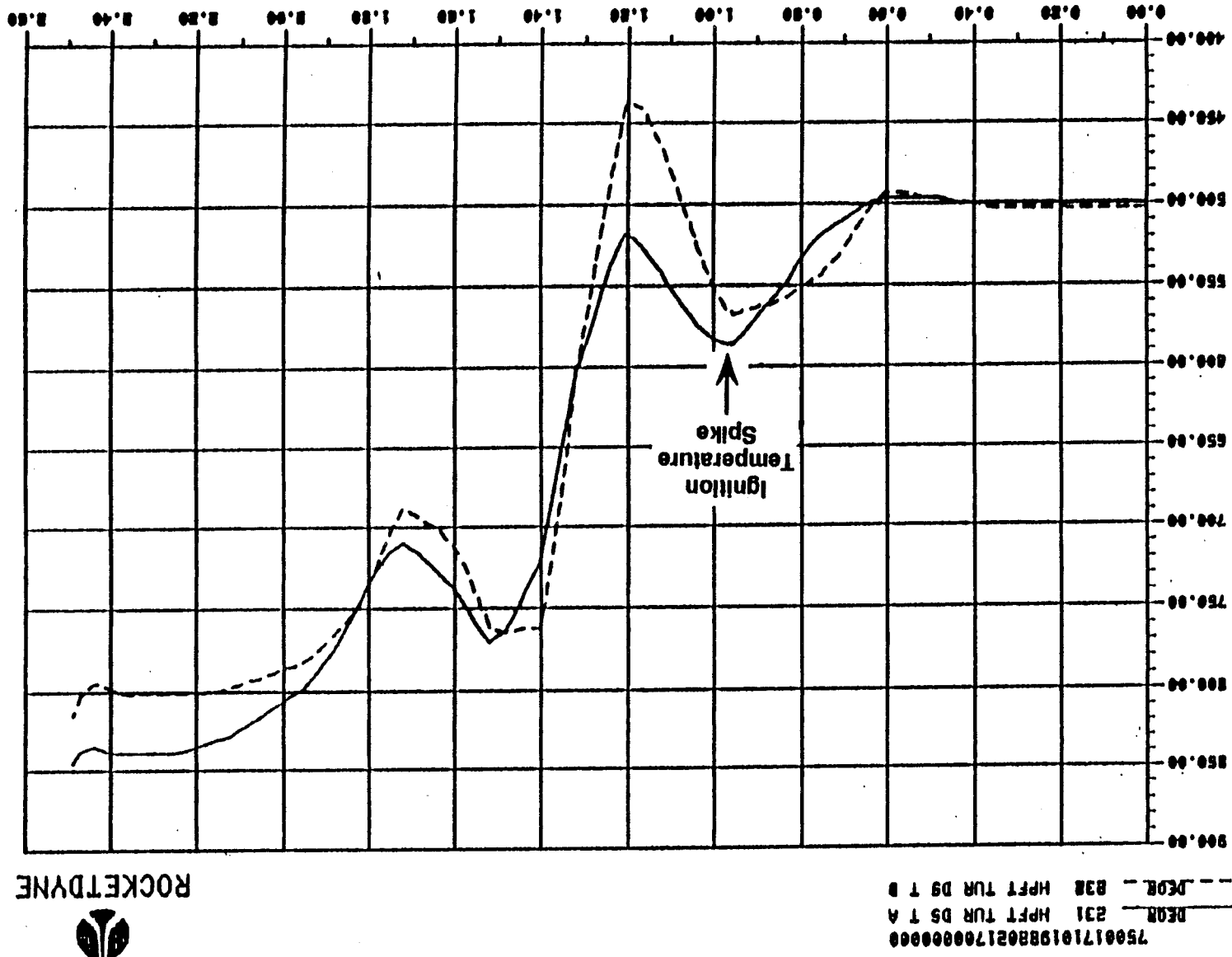


Figure 5-3a SSME HPFT Discharge Temperature
 (Hot Fire Test Data)

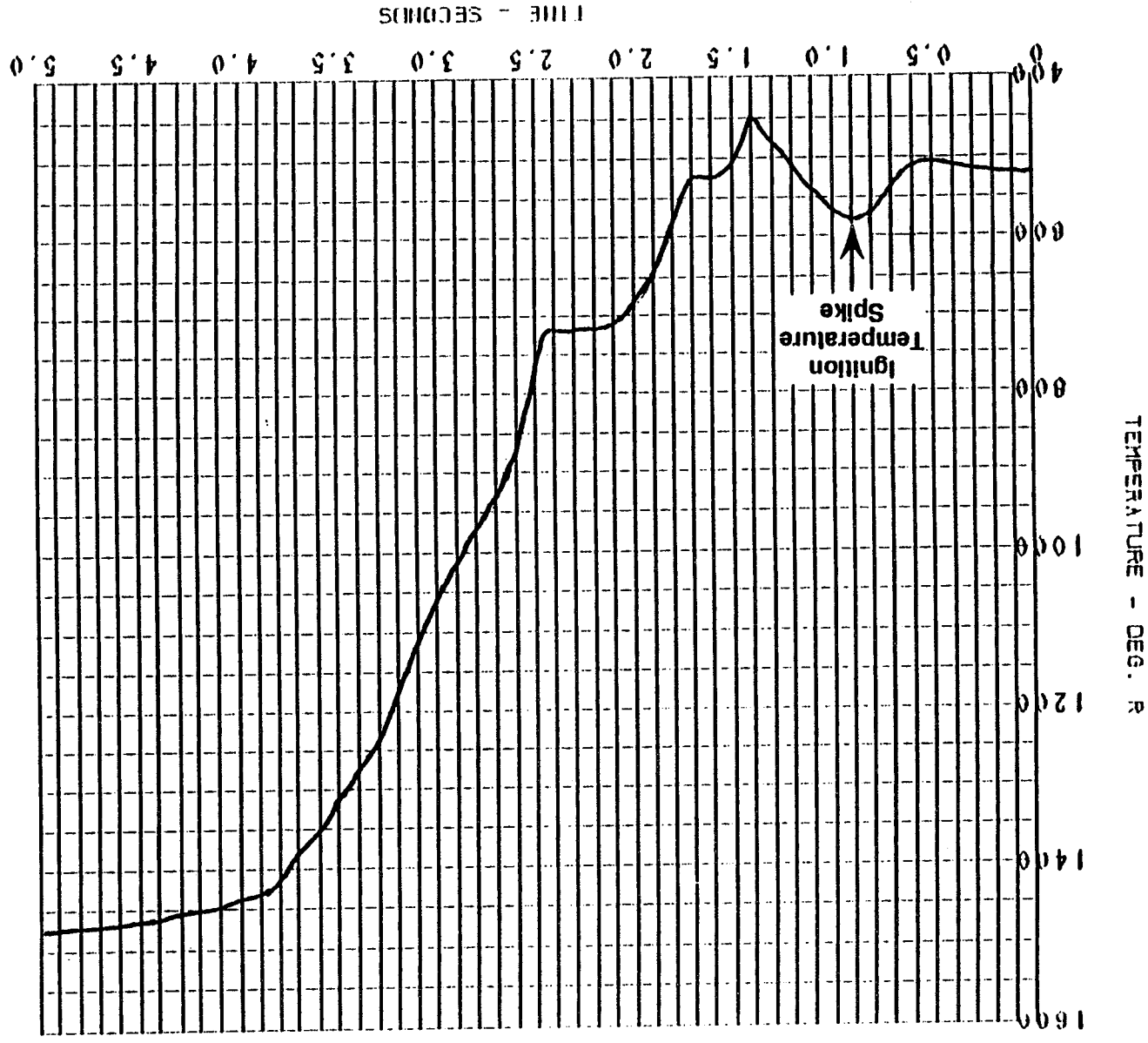


Figure 5-3b SSME HPFT Discharge Temperature
(SSME Transient Model)

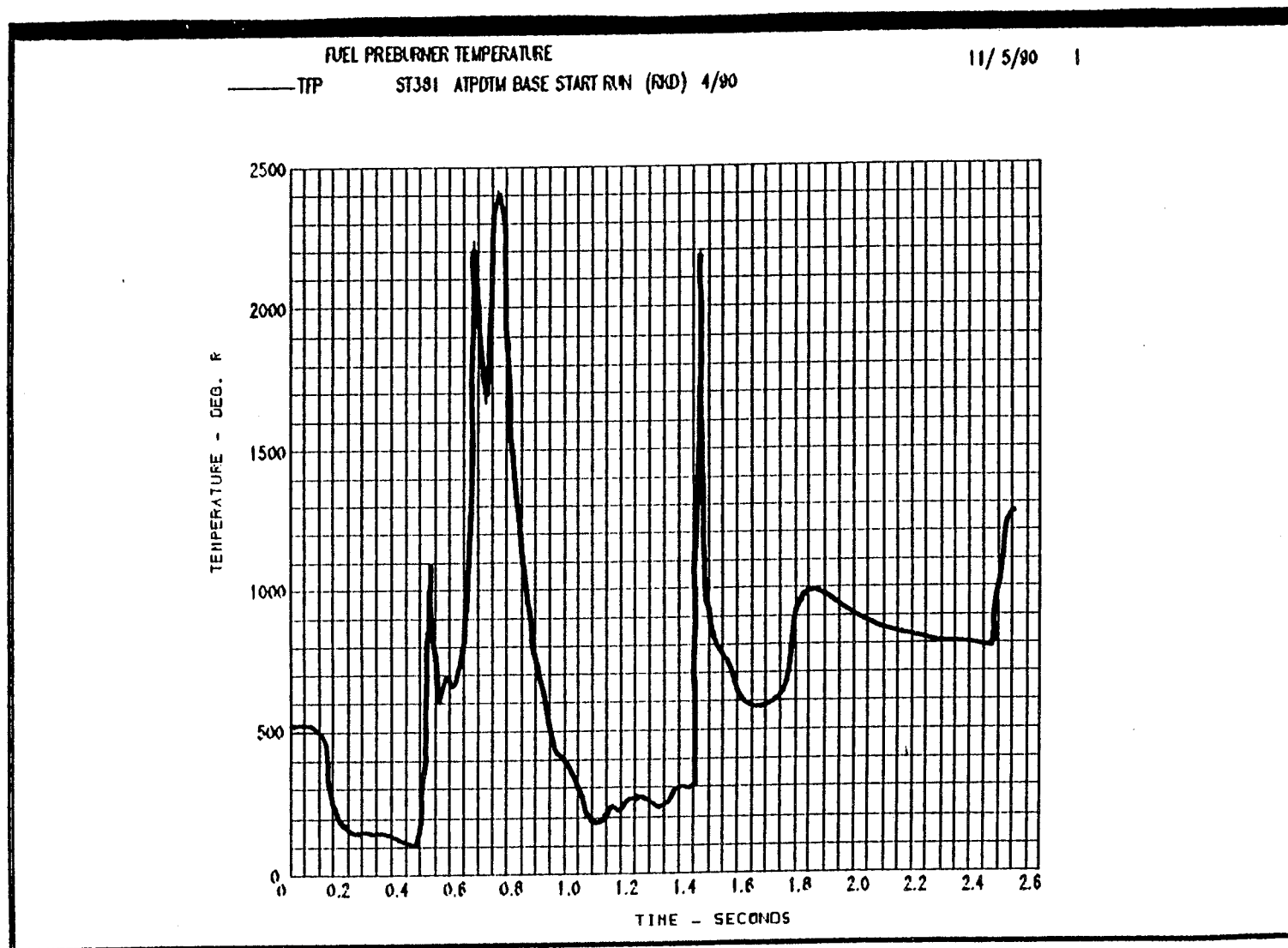


Figure 5-4 SSME Fuel Preburner Temperature
(SSME Transient Model)

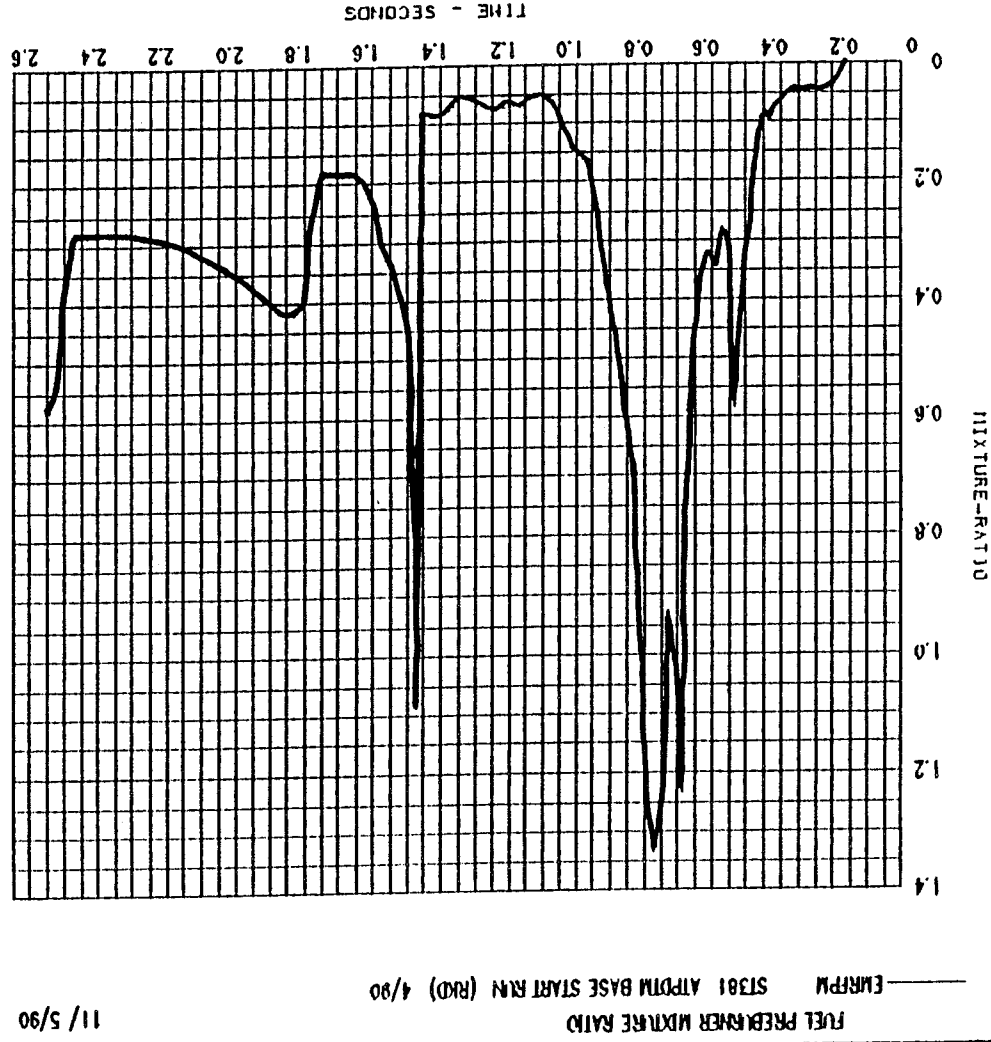


Figure 5-5 SSME FPB Mixture Ratio
(SSME Transient Model)

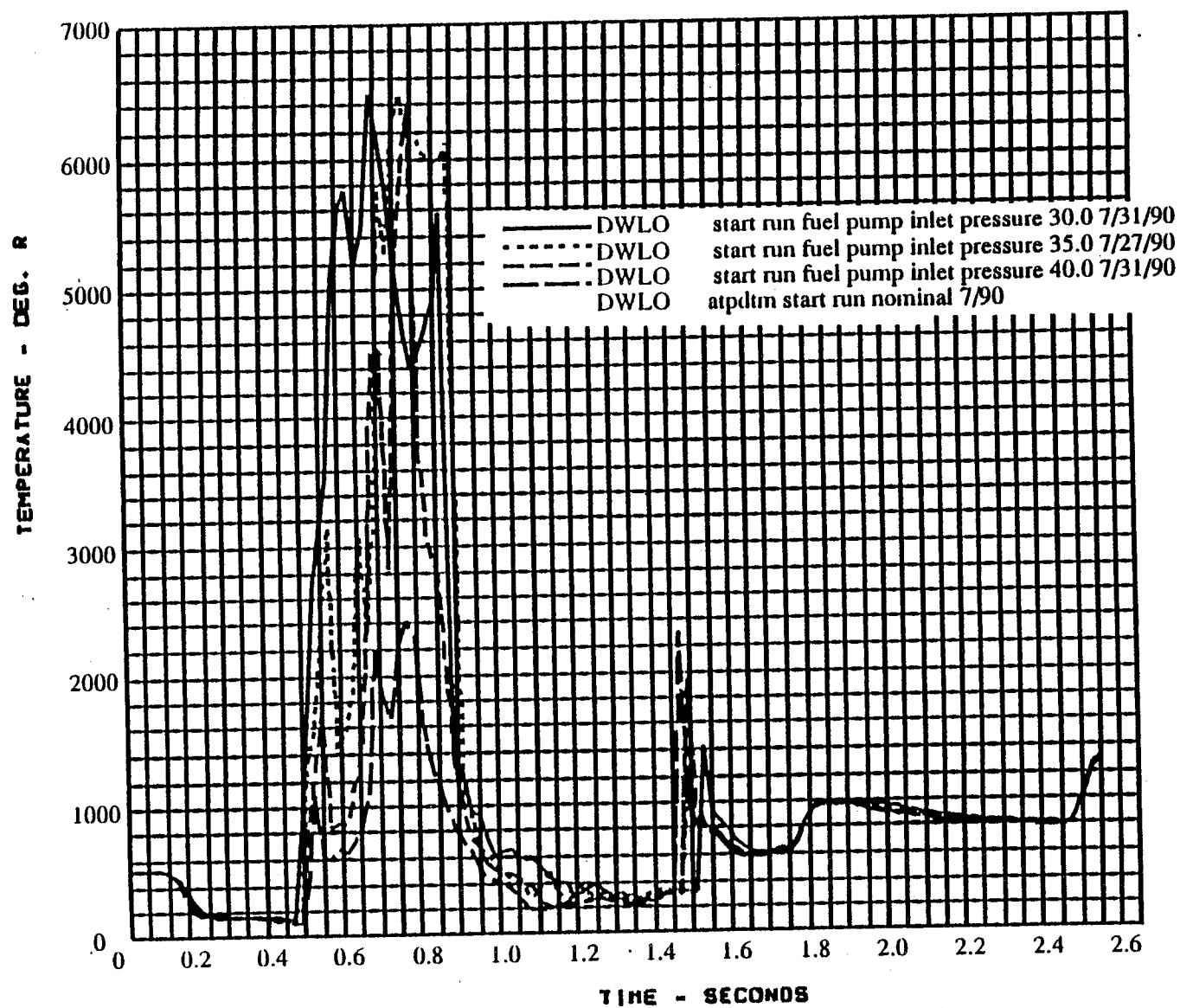


Figure 5-6 FPB Ignition Temperature for Off-Nominal Fuel Inlet Pressures

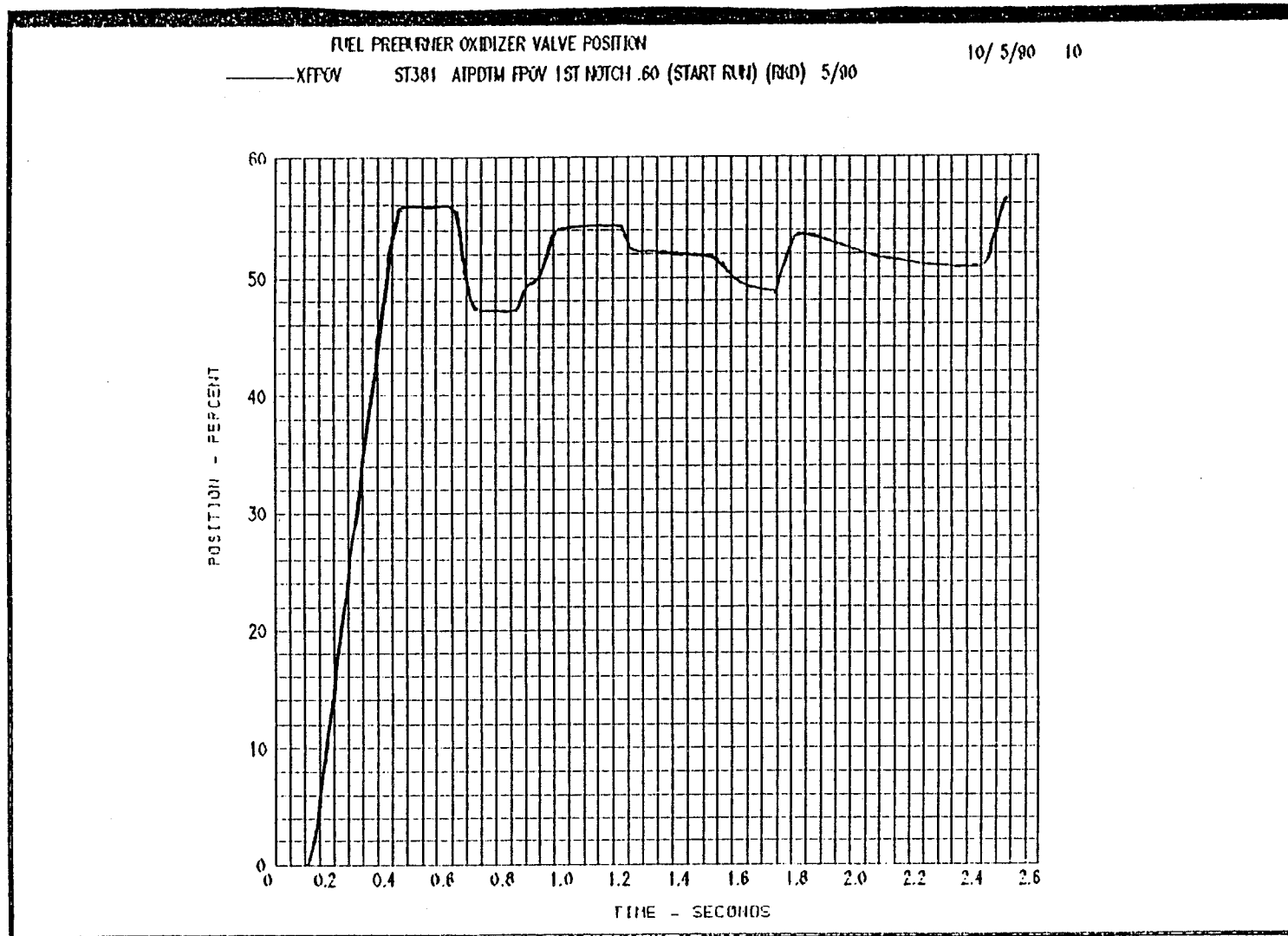


Figure 5-7 SSME Start Sequence FPOV Position

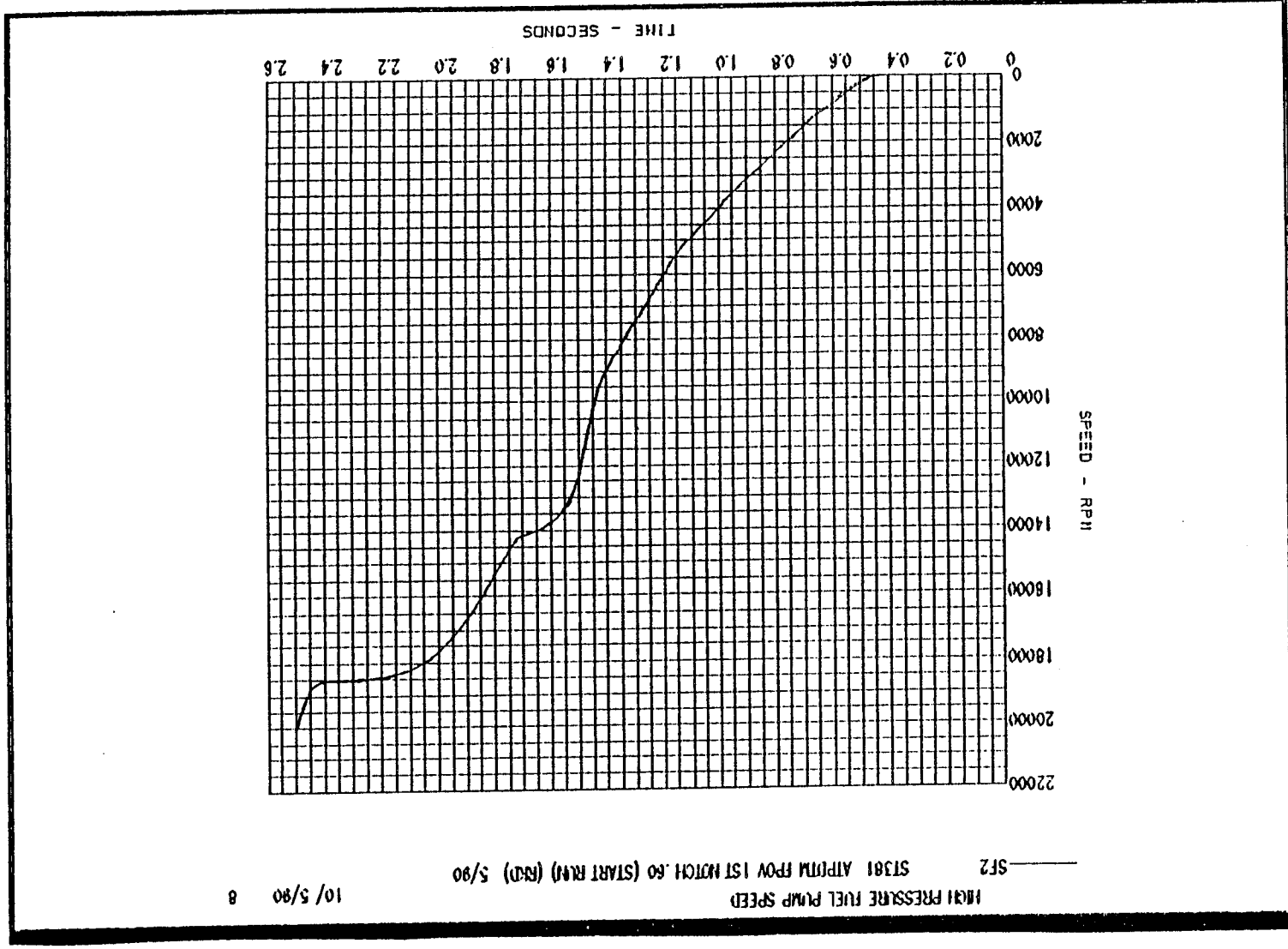


Figure 5-8 SSME Start Sequence HPFTP Speed

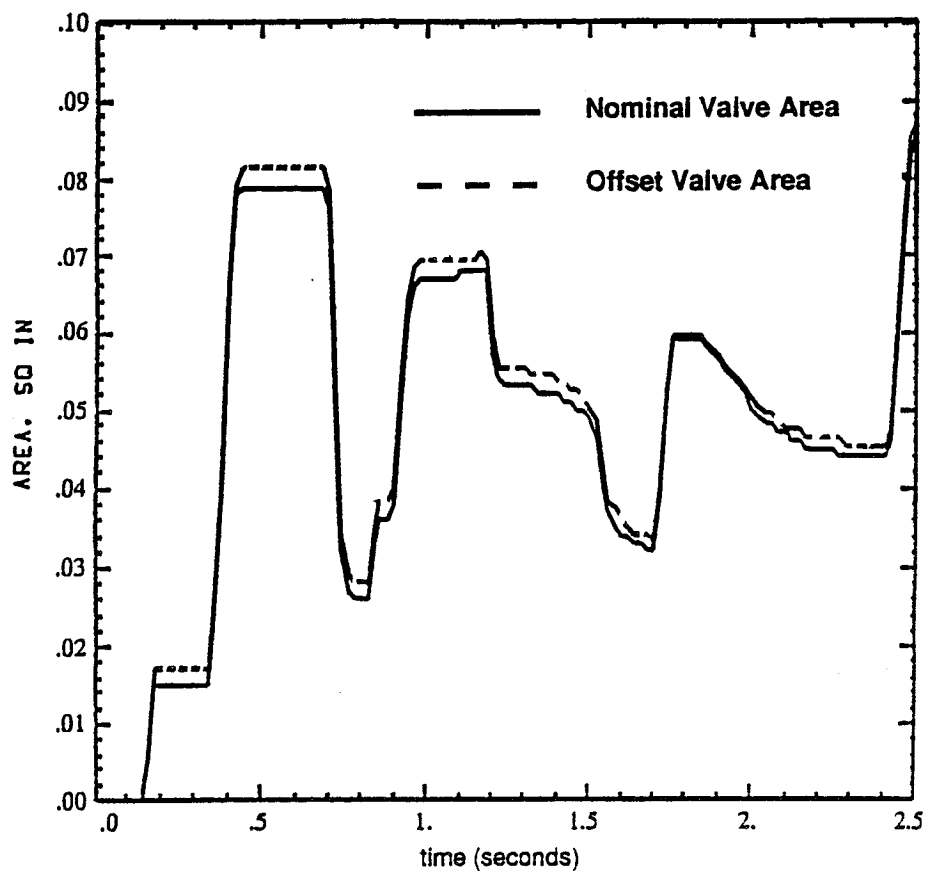


Figure 5-9 FPOV Offset used to Investigate Engine Controllability

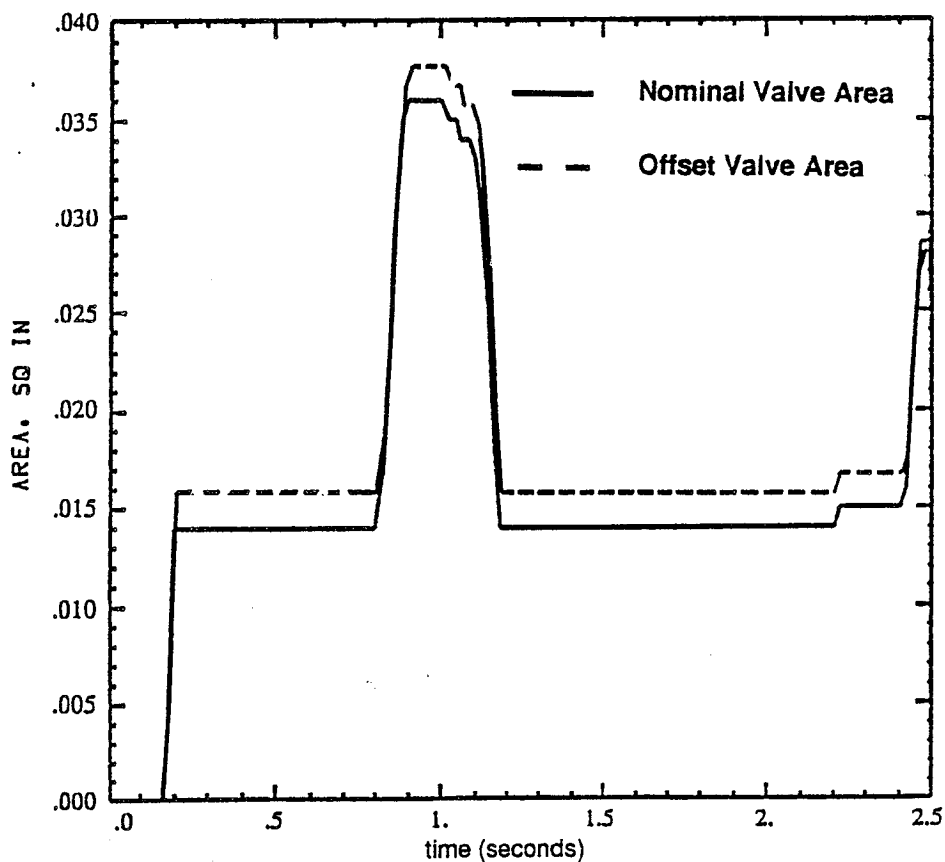


Figure 5-10 OPOV Offset used to Investigate Engine Controllability

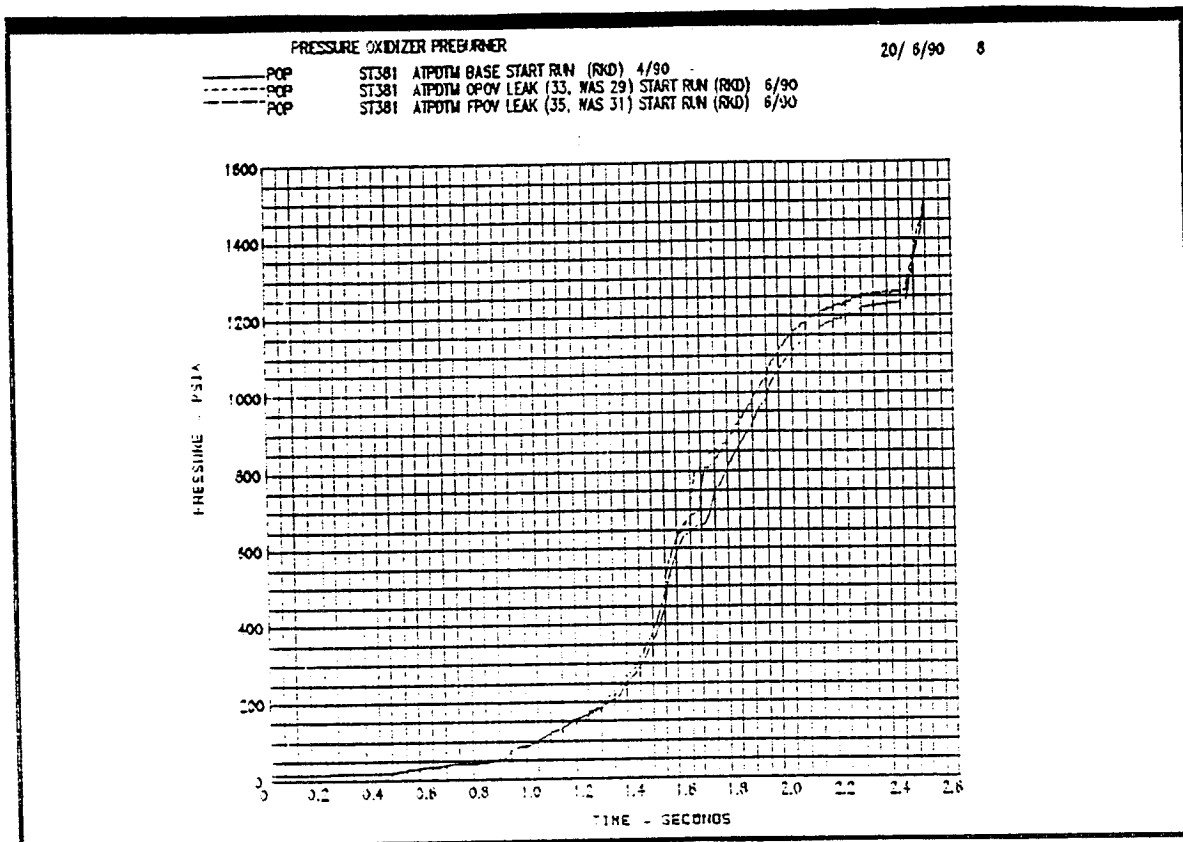


Figure 5-11a Engine Response to FPOV and OPOV Flow Area Offsets

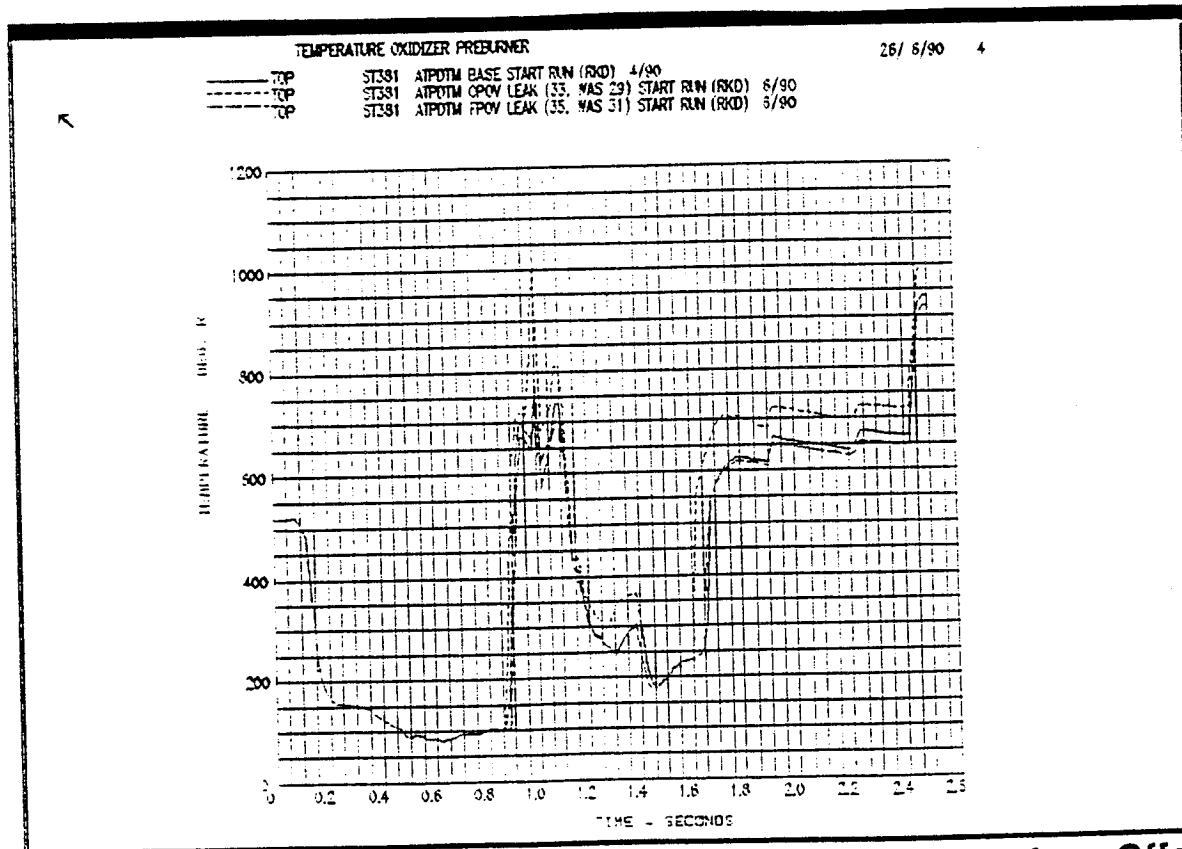


Figure 5-11b Engine Response to FPOV and OPOV Flow Area Offsets

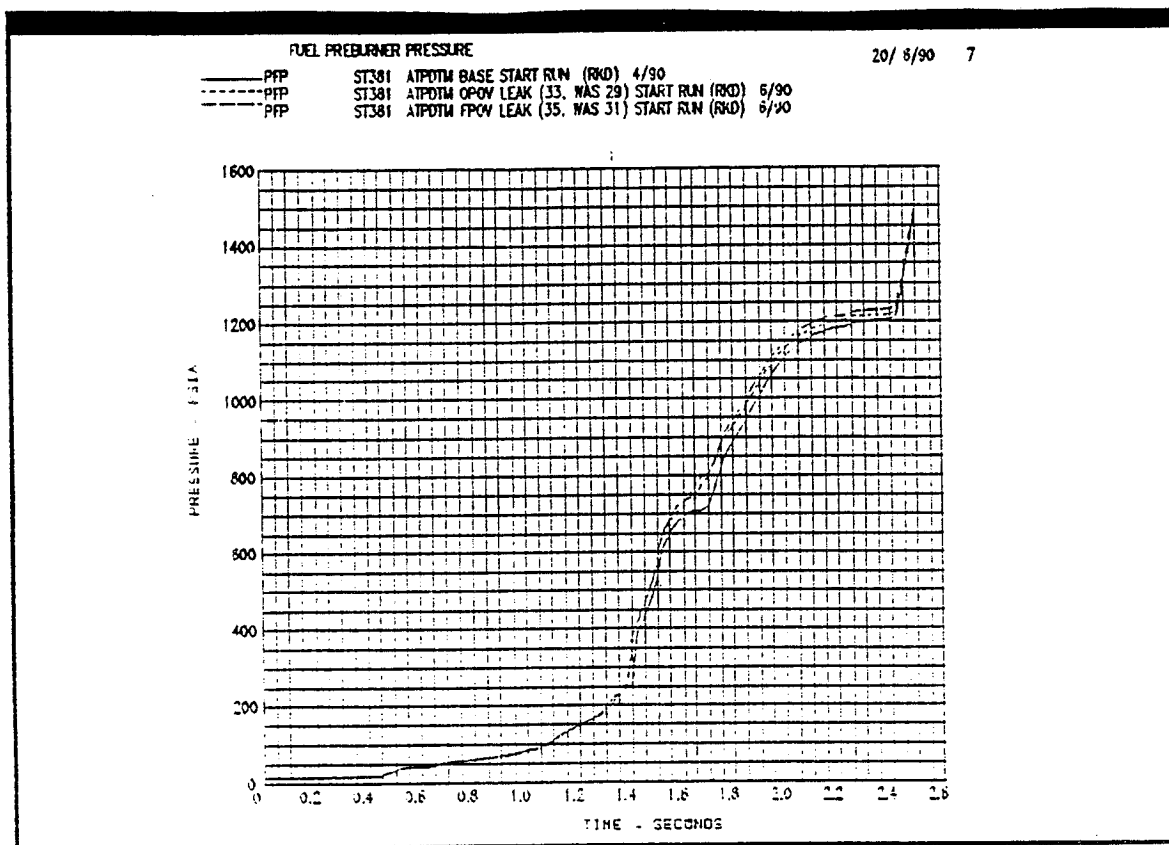


Figure 5-11c Engine Response to FPOV and OPOV Flow Area Offsets

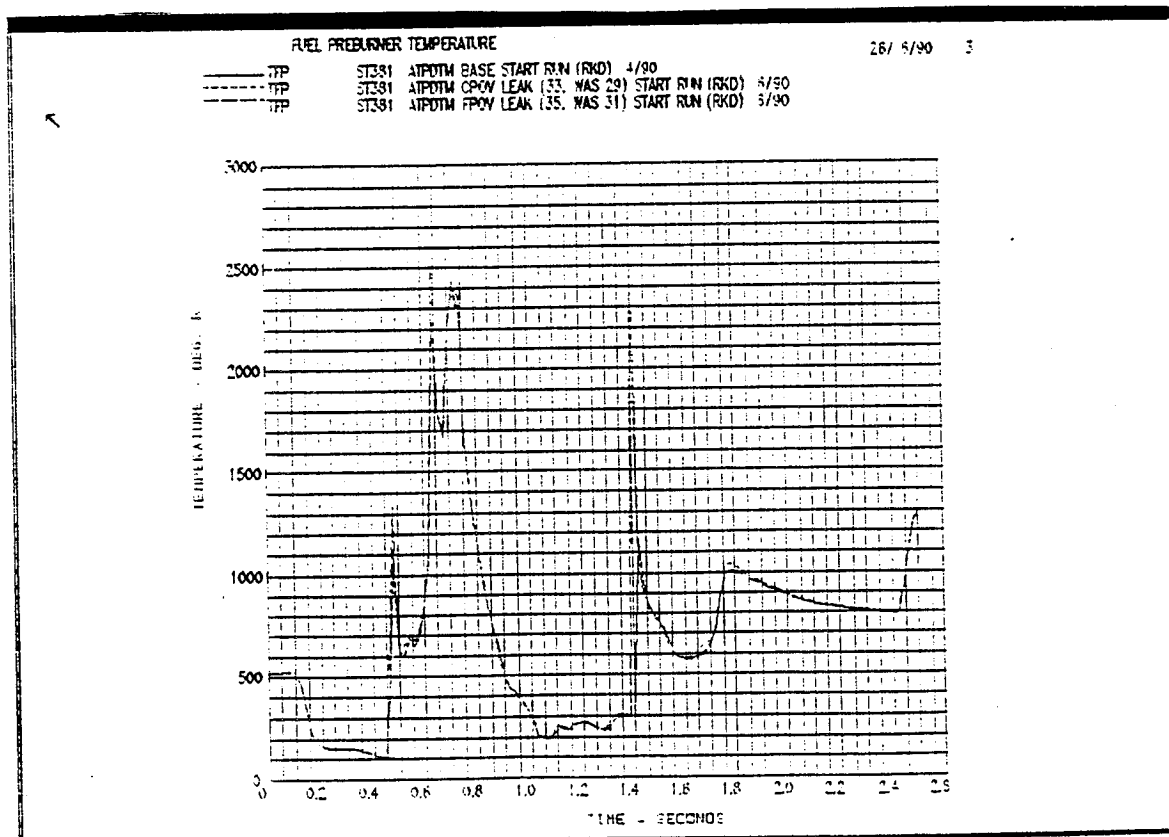


Figure 5-11d Engine Response to FPOV and OPOV Flow Area Offsets

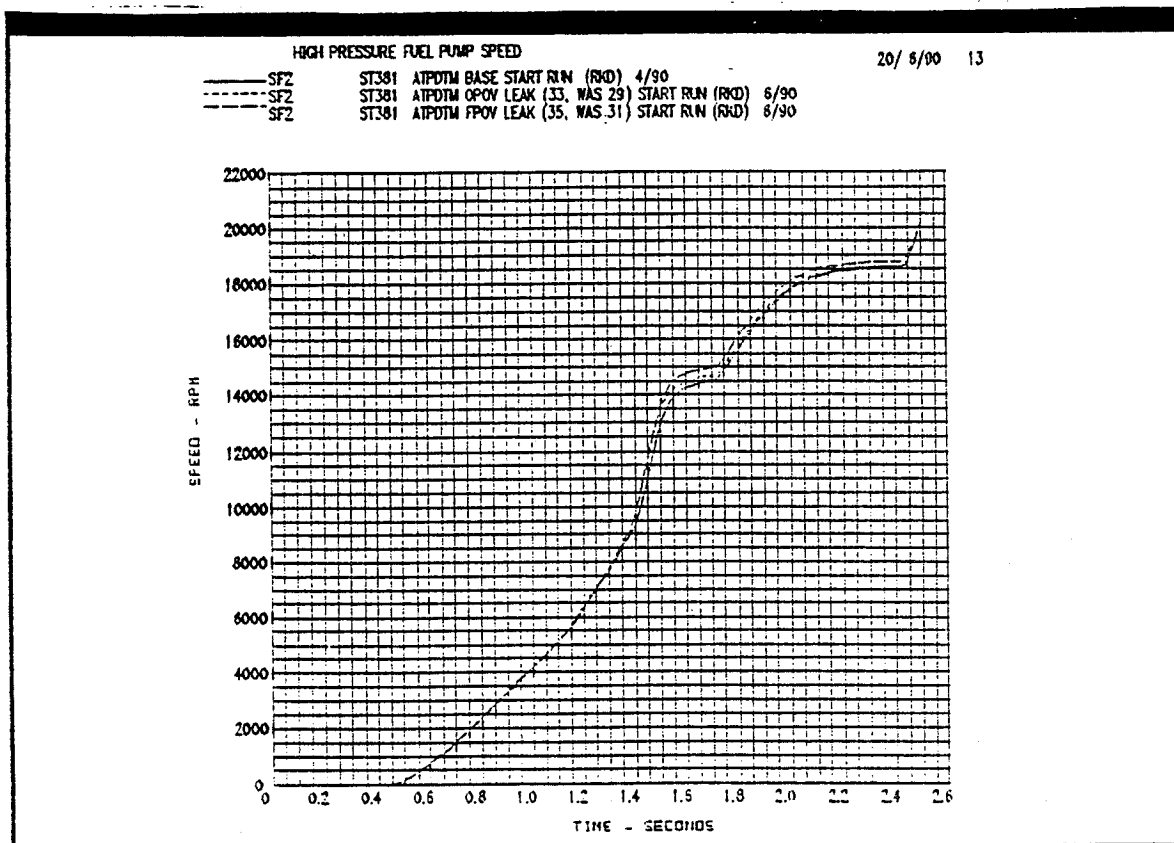


Figure 5-11e Engine Response to FPOV and OPOV Flow Area Offsets

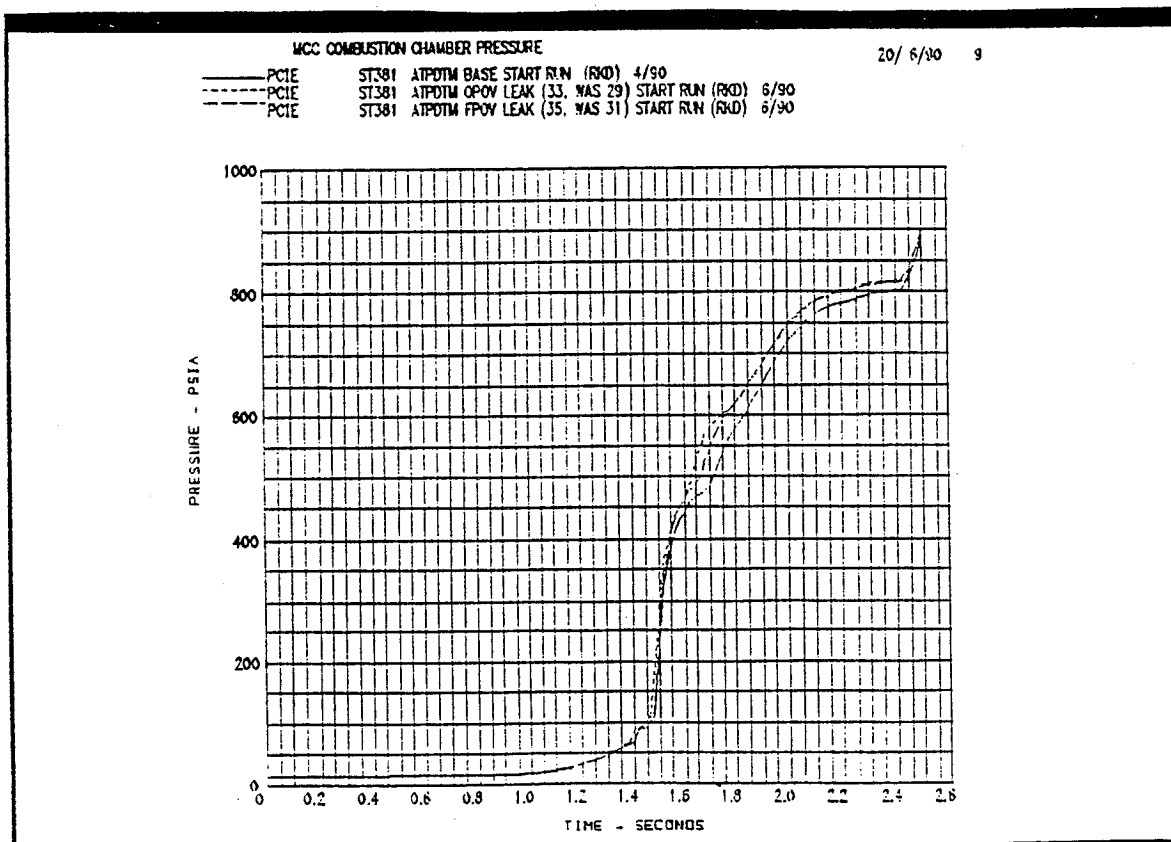
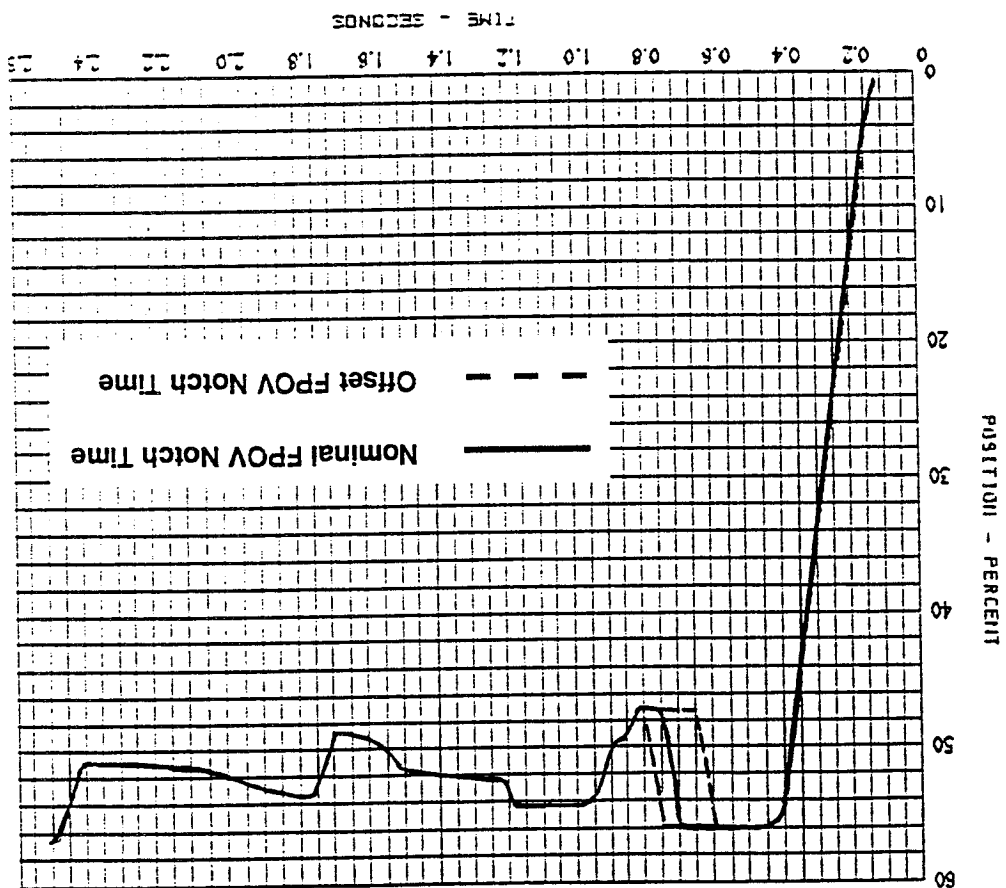


Figure 5-11f Engine Response to FPOV and OPOV Flow Area Offsets

Figure 5-12 Changes in FPOV Notch Timing used to Investigate Engine Controllability



FUEL PREBURNER OXIDIZER VALVE POSITION

29/ 8/90

- OI atpdtm start run nominal 7/90
- - - OI start run 42.0 fuel in pr 8/17/90
- - - OI start run 42.0 fuel in pr with valve changes 8/17/90

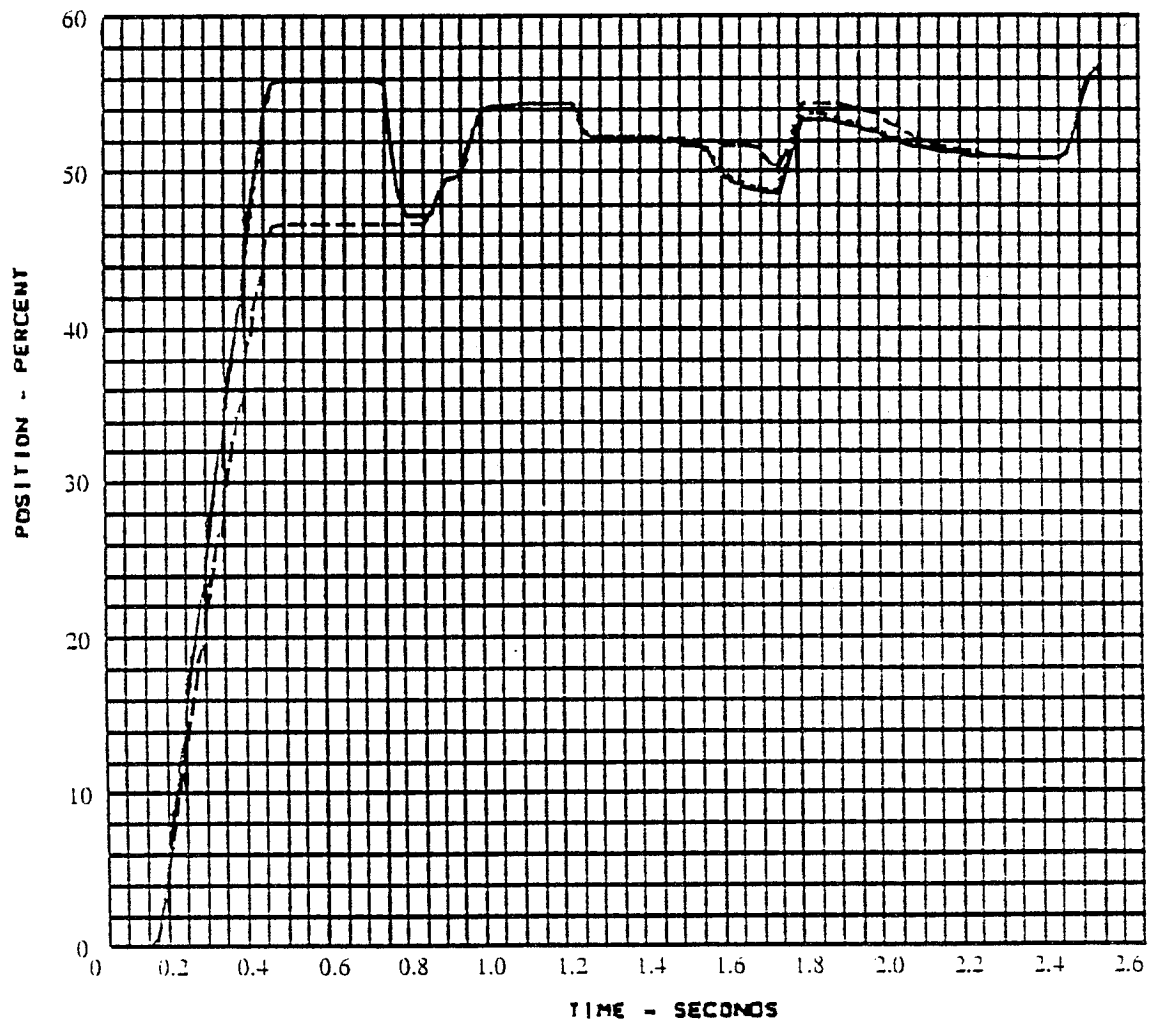


Figure 5-13a Simulation of Fuel Inlet Pressure Anomaly

OXIDIZER PREBURNER OXIDIZER VALVE POSITION

29/ 8/90



atpdtm start run nominal 7/90

start run 42.0 fuel in pr 8/17/90

start run 42.0 fuel in pr with valve changes 8/17/90

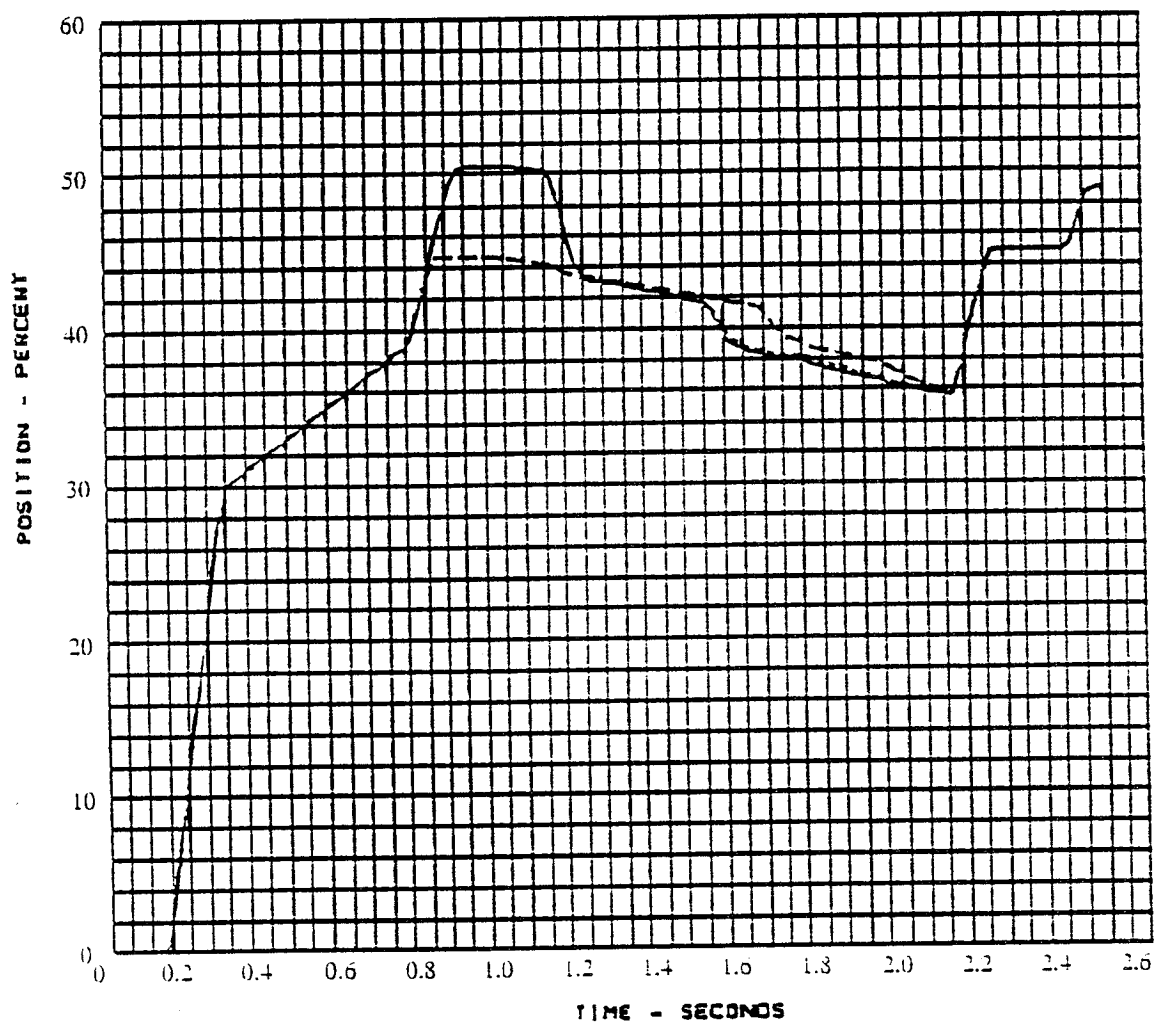


Figure 5-13b Simulation of Fuel Inlet Pressure Anomaly

FUEL PREBURNER TEMPERATURE

29/ 8/90

- DWLO arpdtn start run nominal 7/90
- - - DWLO start run 42.0 fuel in pr 8/17/90
- - - DWLO start run 42.0 fuel in pr with valve changes 8/17/90

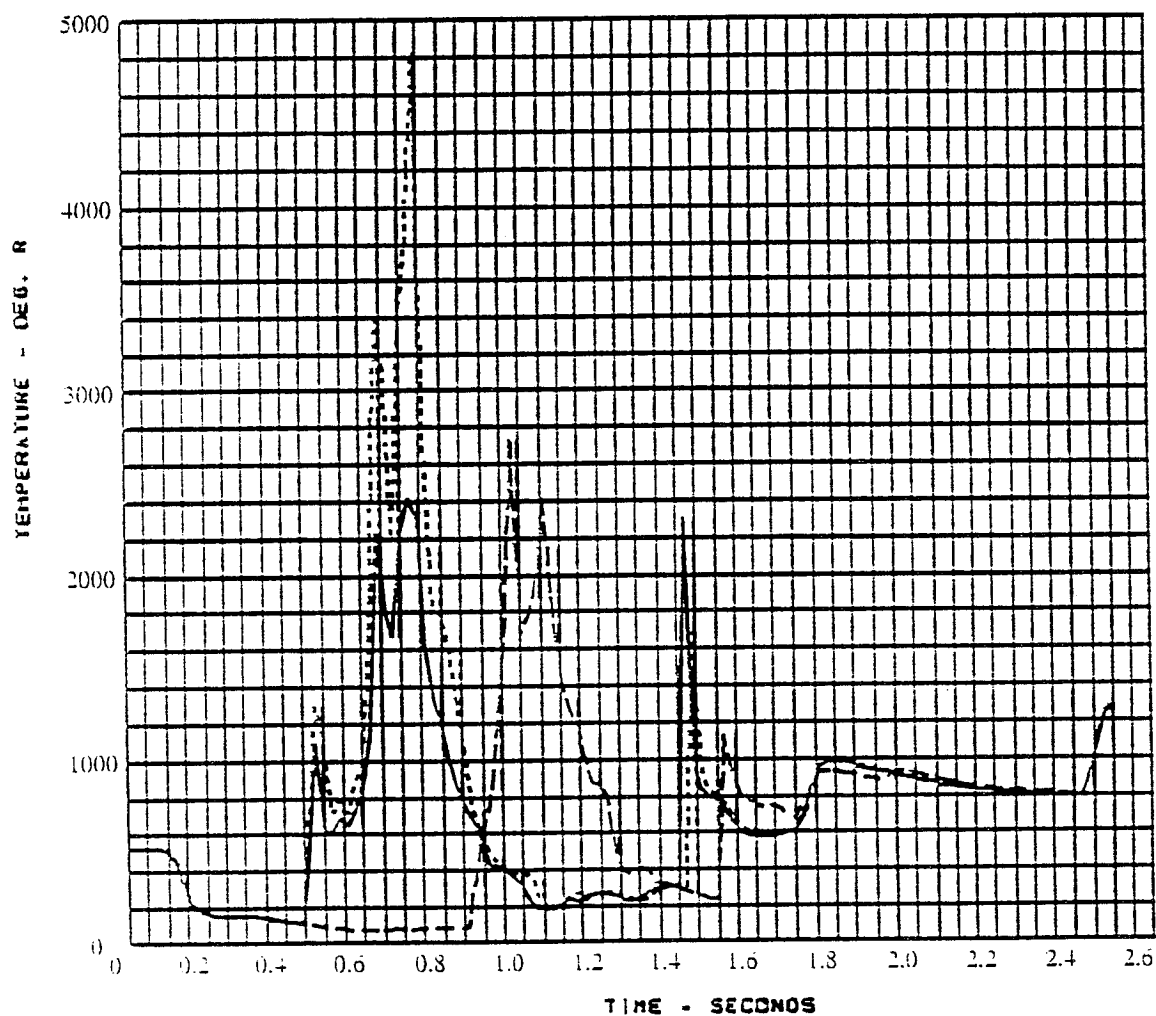


Figure 5-13c Simulation of Fuel Inlet Pressure Anomaly

FUEL PREBURNER PRESSURE

29/8/90

- DWFP arpdtn start run nominal 7/90
- - - DWFP start run 42.0 fuel in pr 8/17/90
- · - DWFP start run 42.0 fuel in pr with valve changes 8/17/90

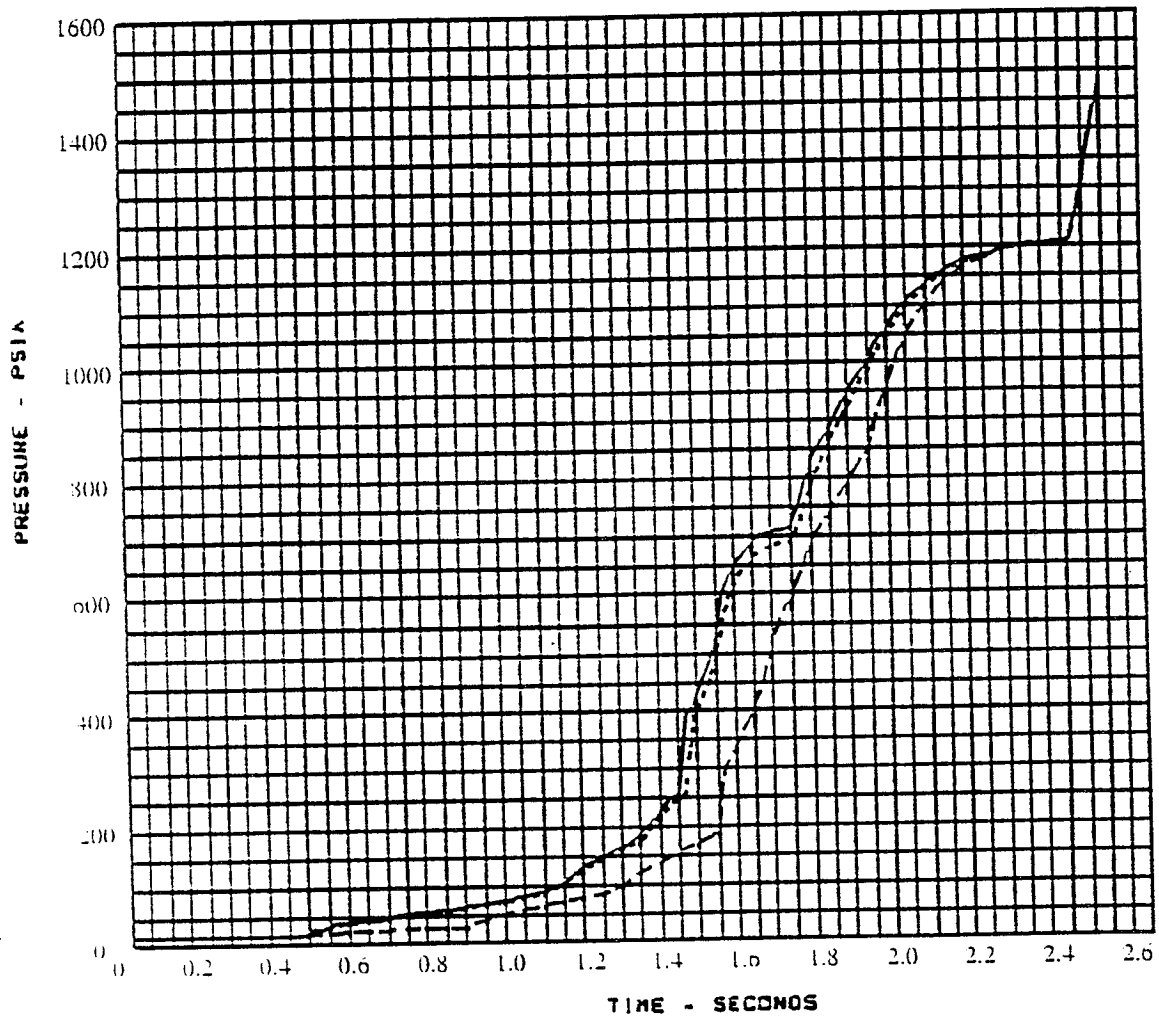
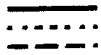


Figure 5-13d Simulation of Fuel Inlet Pressure Anomaly

TEMPERATURE OXIDIZER PREBURNER

29/ 8/90



arptm start run nominal 7/90
 start run 42.0 fuel in pr 8/17/90
 start run 42.0 fuel in pr with valve changes 8/17/90

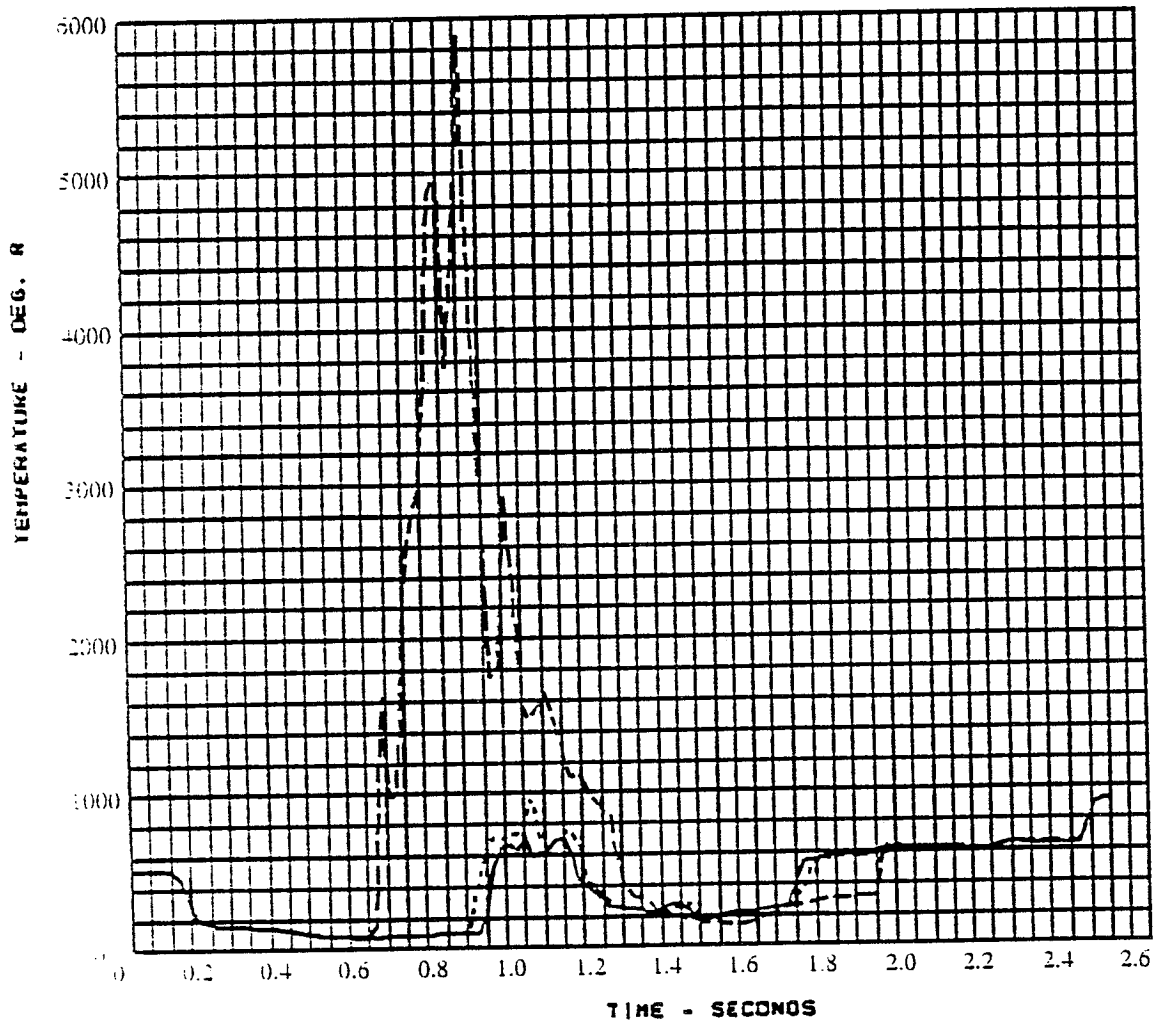


Figure 5-13e Simulation of Fuel Inlet Pressure Anomaly

C-2

RI/RD91-158

PRESSURE OXIDIZER PREBURNER

29/ 8/90

— DWGN atpdtm start run nominal 7/90
 - - - DWGN start run 42.0 fuel in pr 8/17/90
 - - - DWGN start run 42.0 fuel in pr with valve changes 8/17/90

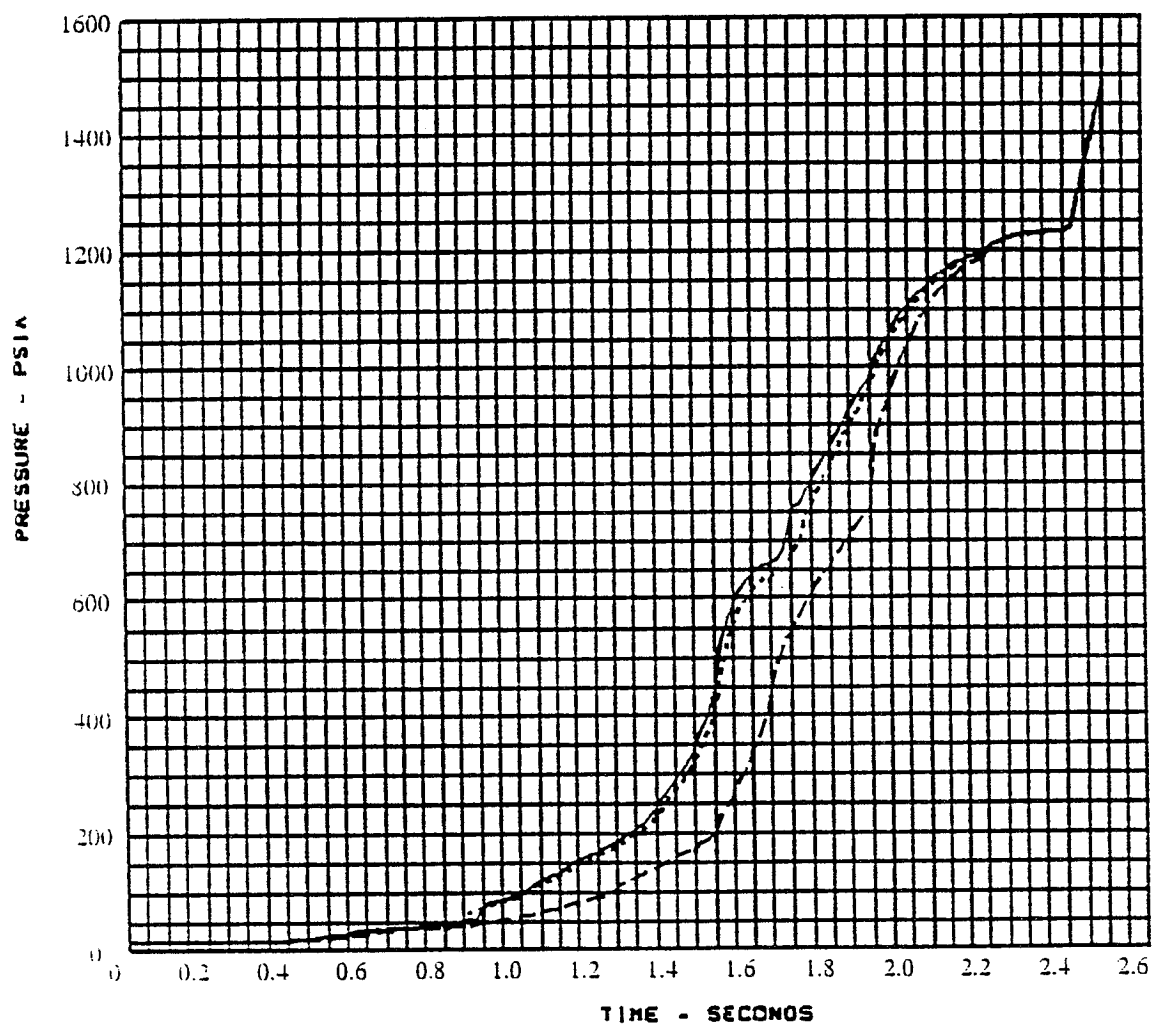


Figure 5-13f Simulation of Fuel Inlet Pressure Anomaly

MCC COMBUSTION CHAMBER PRESSURE

29/ 8/90

— F arpdtn start run nominal 7/90
 - - - F start run 42.0 fuel in pr 8/17/90
 - - - F start run 42.0 fuel in pr with valve changes 8/17/90

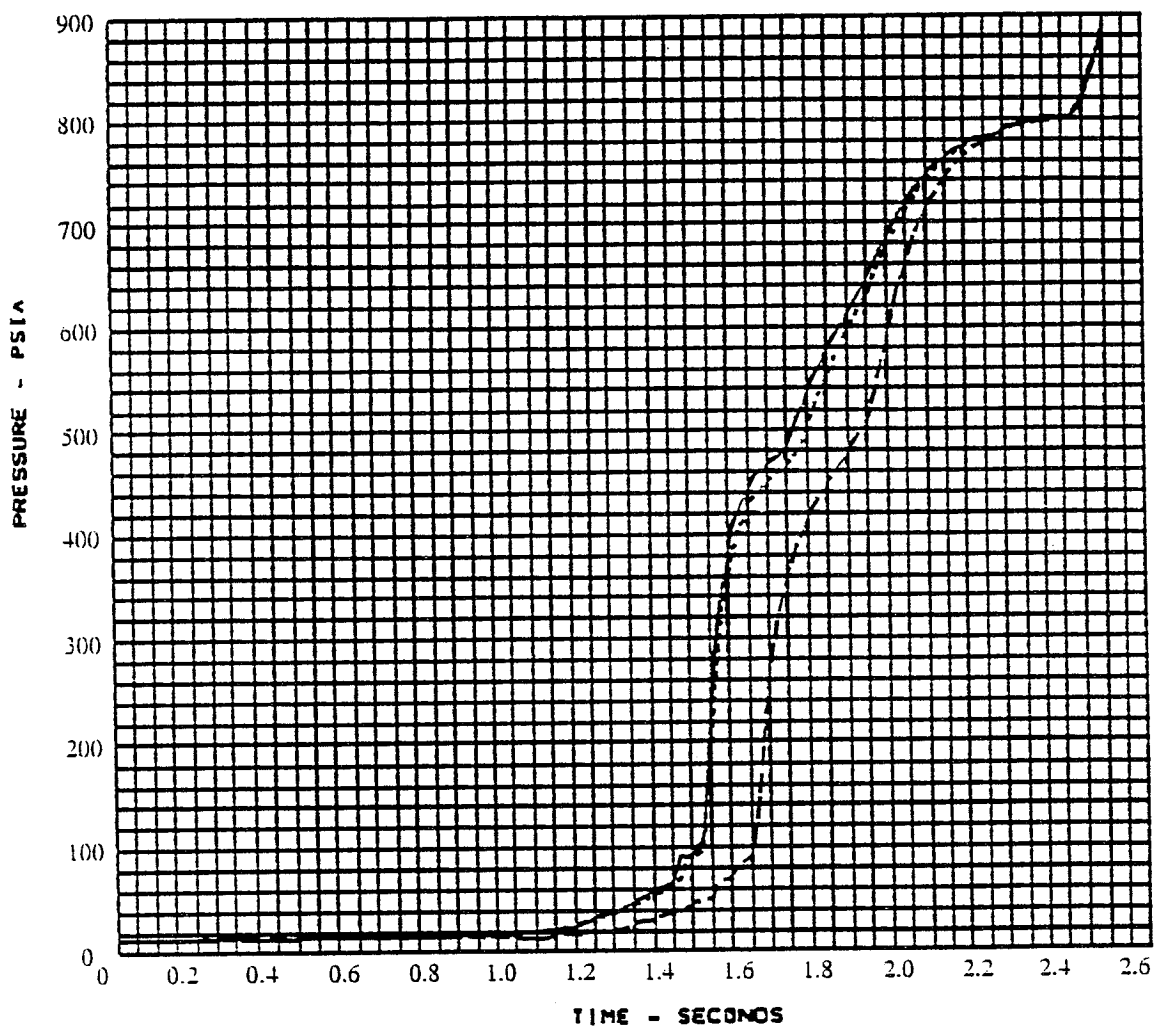


Figure 5-13g Simulation of Fuel Inlet Pressure Anomaly

HIGH PRESSURE FUEL PUMP SPEED

29/ 8/90

- DWHO arptm start run nominal 7/90
- - - DWHO start run 42.0 fuel in pr 8/17/90
- · - DWHO start run 42.0 fuel in pr with valve changes 8/17/90

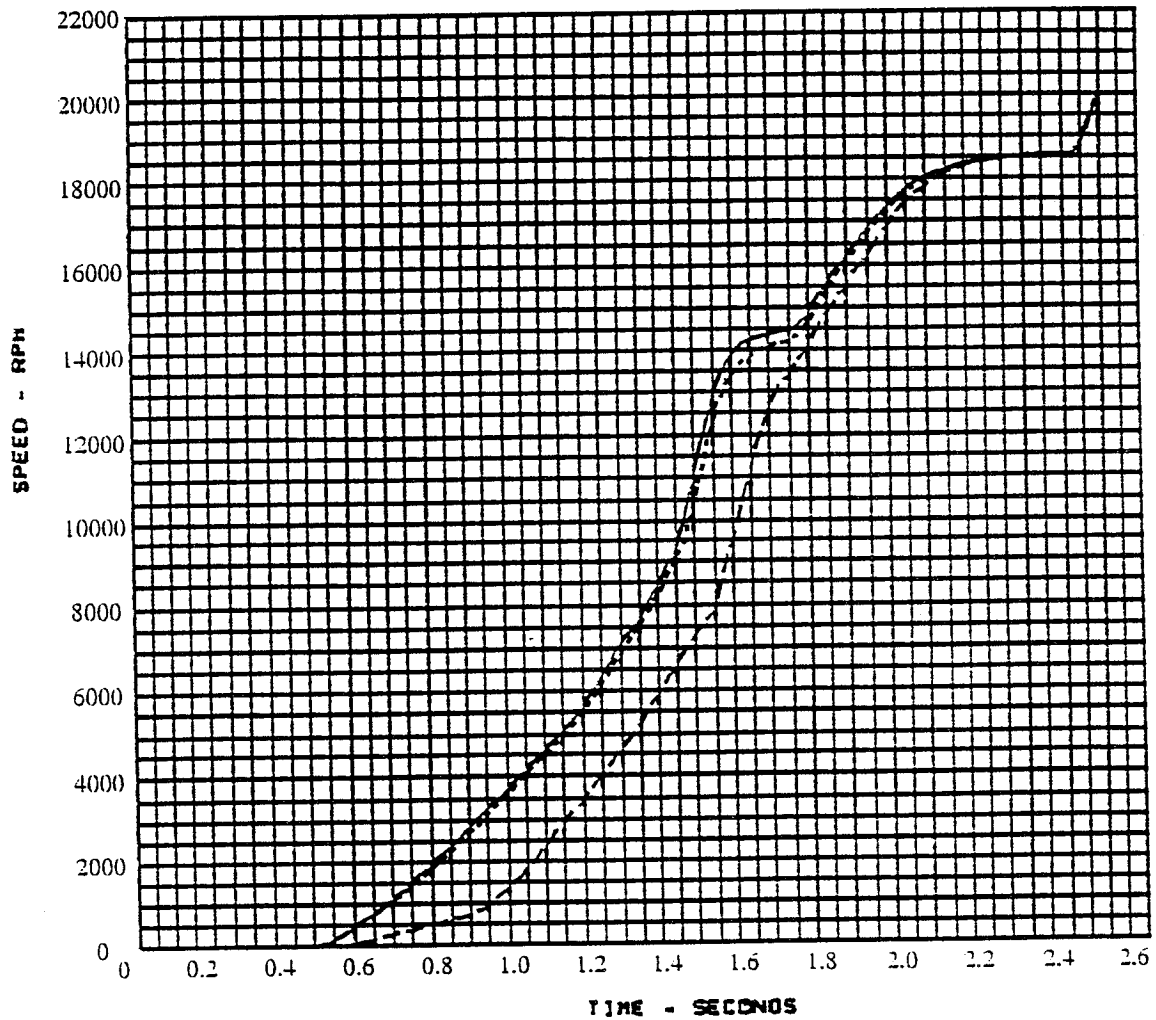


Figure 5-13h Simulation of Fuel Inlet Pressure Anomaly

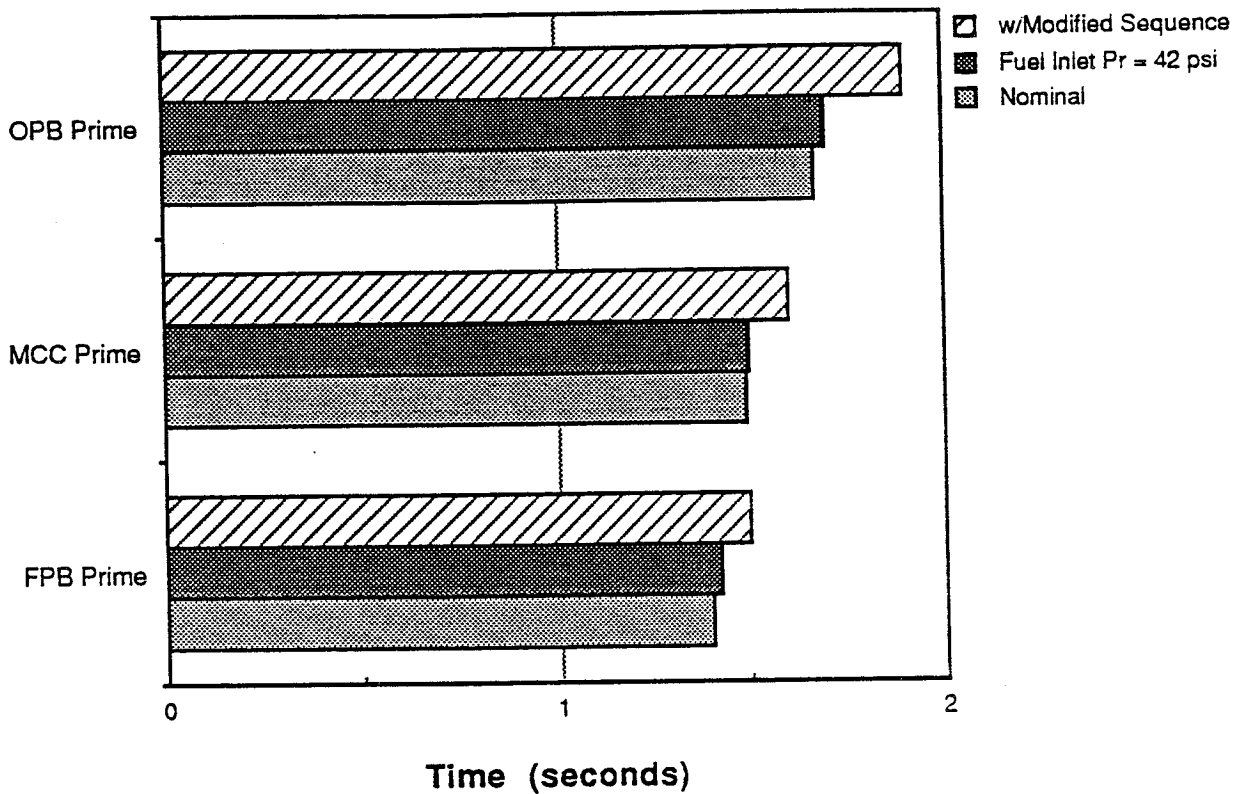


Figure 5-14a Summary of Fuel Pressure Anomoly & Accomodation Simulated Start Transient - LOX Dome Prime Times

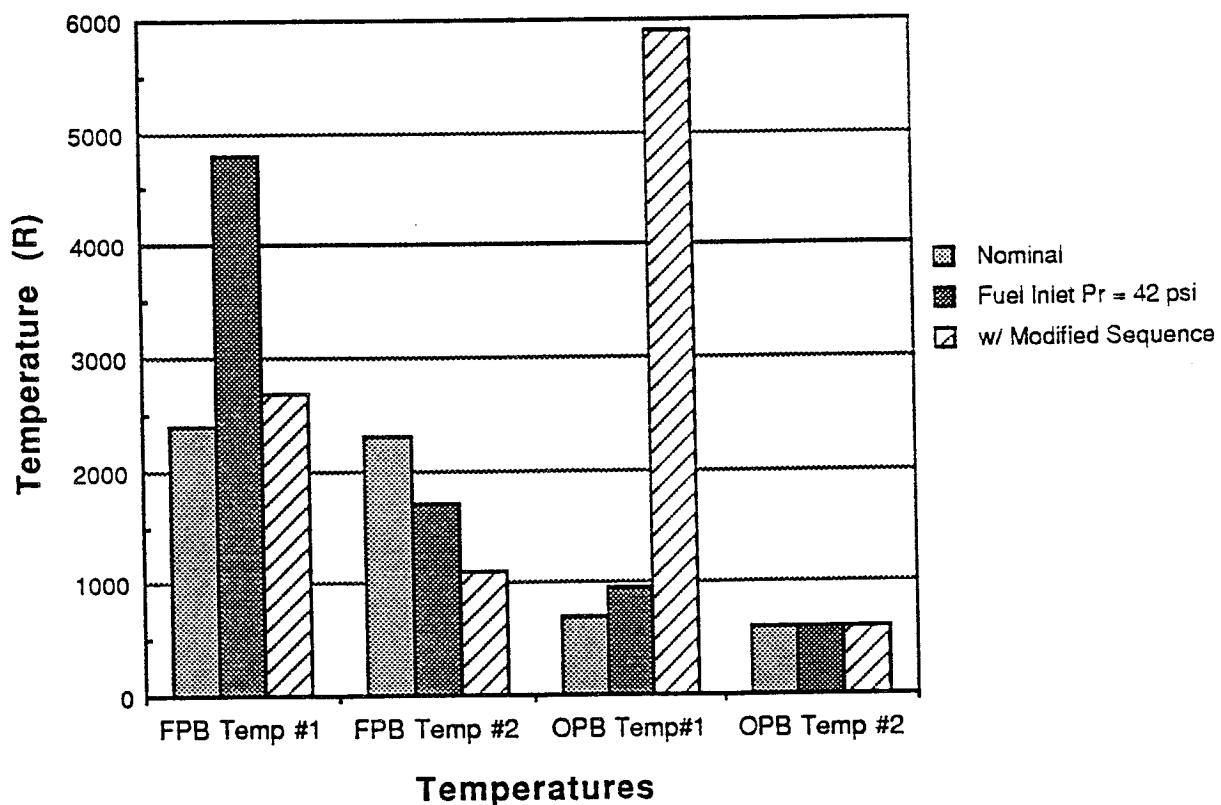


Figure 5-14b Summary of Fuel Pressure Anomoly & Accomodation Simulated Start Transient - Preburner Temperatures

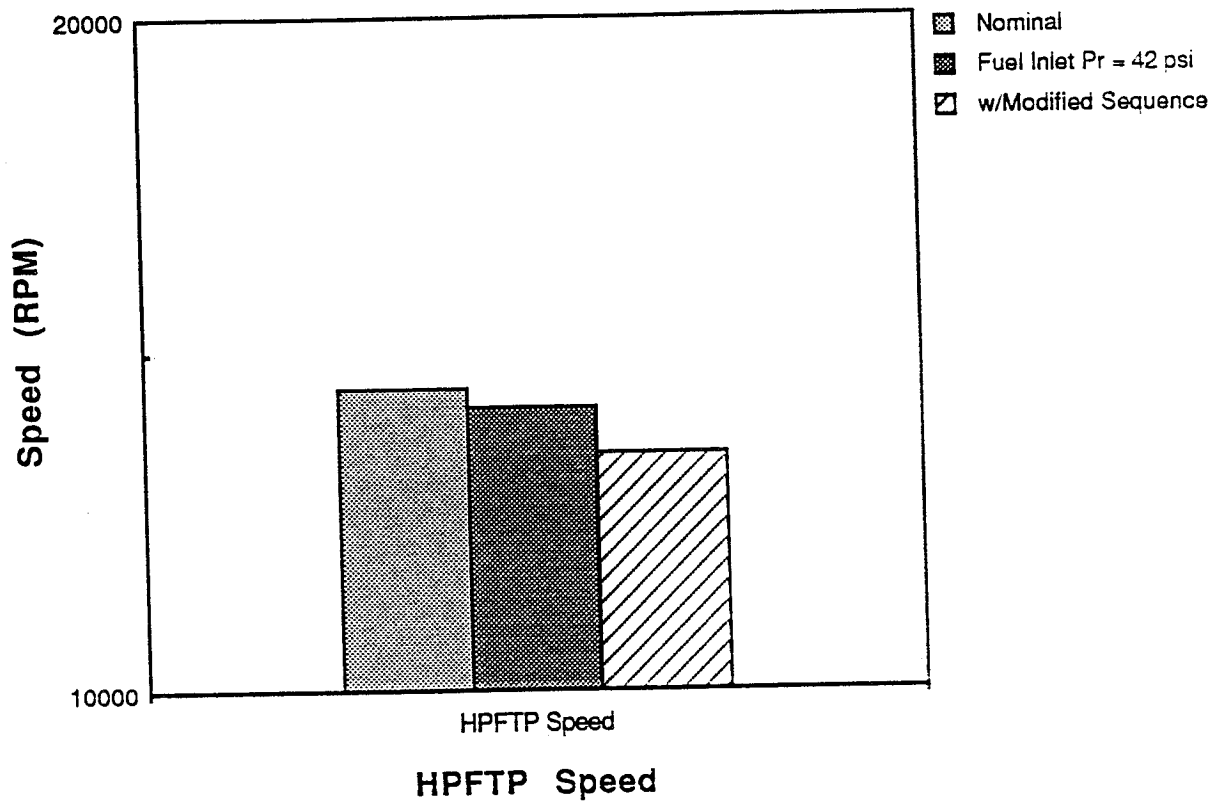


Figure 5-14c Summary of Fuel Pressure Anomaly & Accomodation Simulated Start Transient - HPFTP Speed

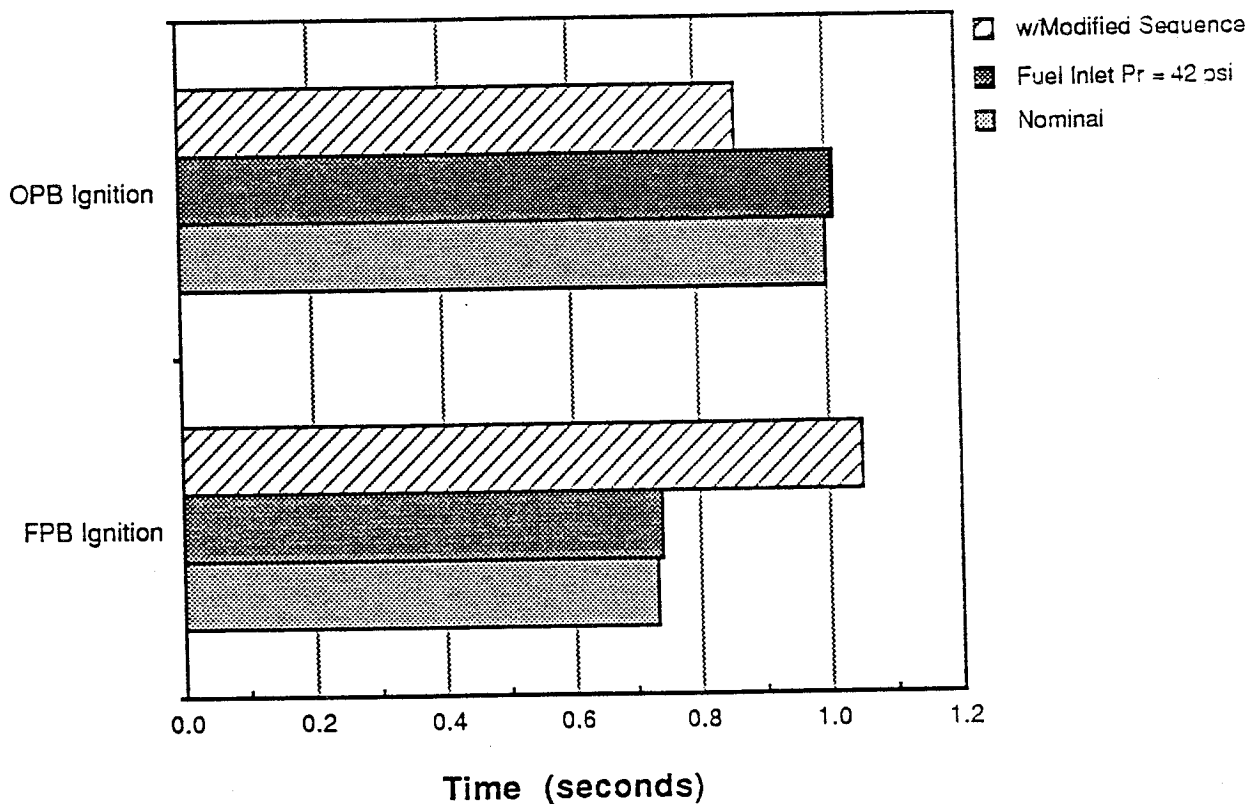


Figure 5-14d Summary of Fuel Pressure Anomaly & Accomodation Simulated Start Transient - Preburner Ignition Times

FUEL PREBURNER TEMPERATURE

7/9/90

- DWLO arpdmm start run nominal 7/90
- DWLO start run with mov at 55 9/04/90
- - - DWLO start run with mov area change and position fix 55 9/06/90

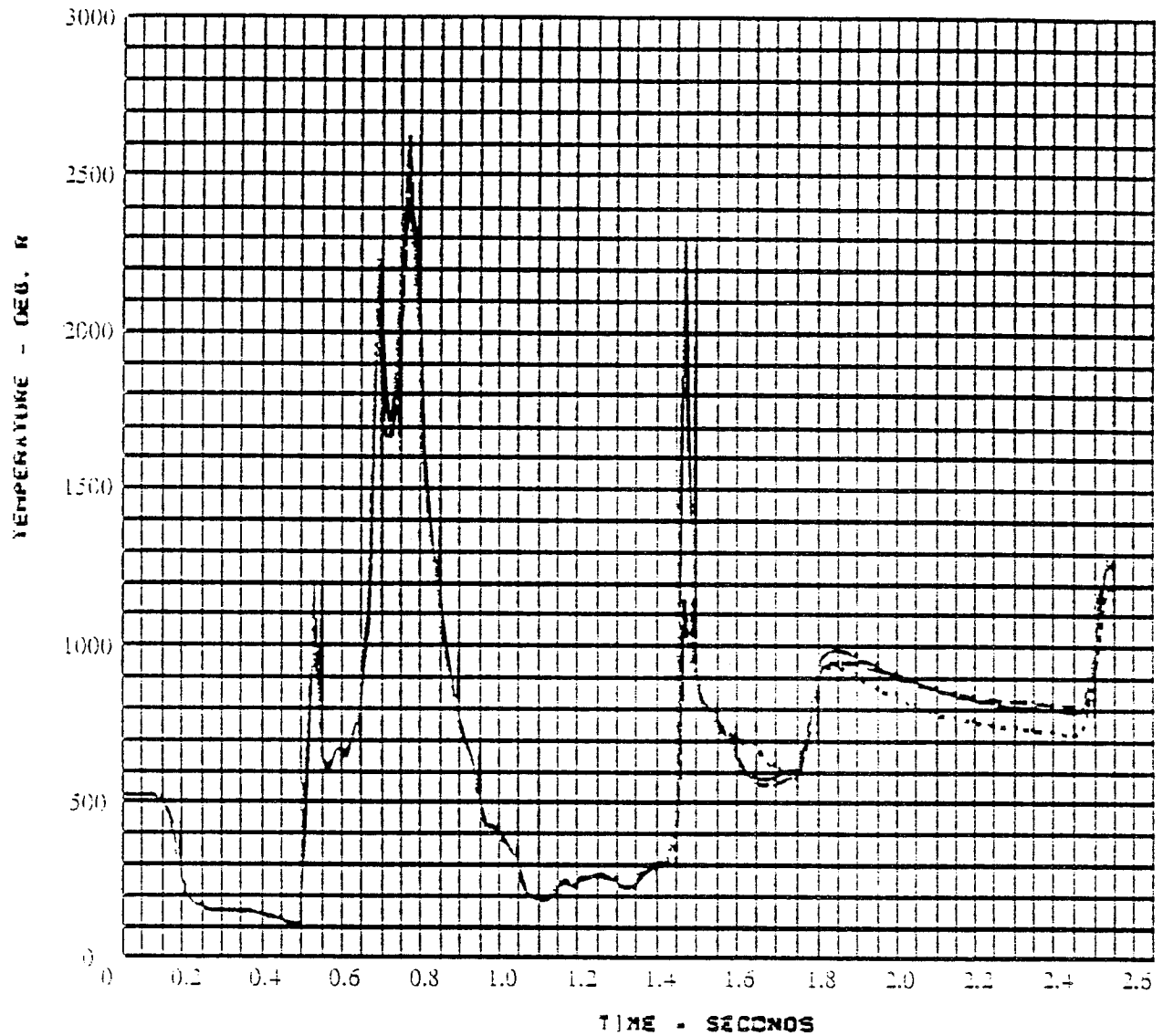


Figure 5-15a Simulation of MOV Anomaly

FUEL PREBURNER PRESSURE

7/9/90

- DWFP arpdtn start run nominal 7/90
- DWFP start run with mov at 55 9/04/90
- - - DWFP start run with mov area change and position fix 55 9/06/90

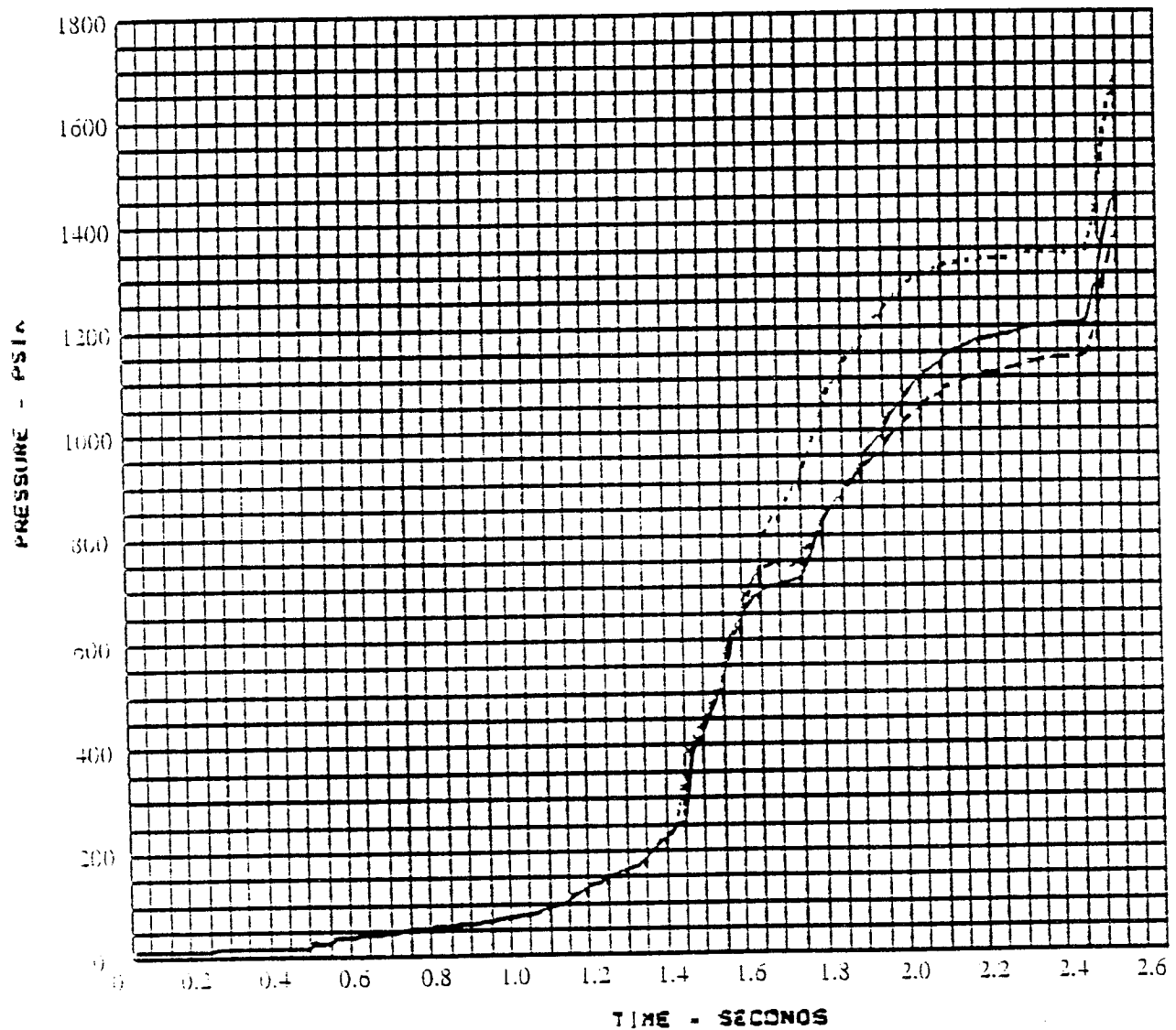
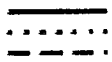


Figure 5-15b Simulation of MOV Anomaly



atpdtm start run nominal 7/90
start run with mov at 55 9/04/90
start run with mov area change and position fix 55 9/06/90

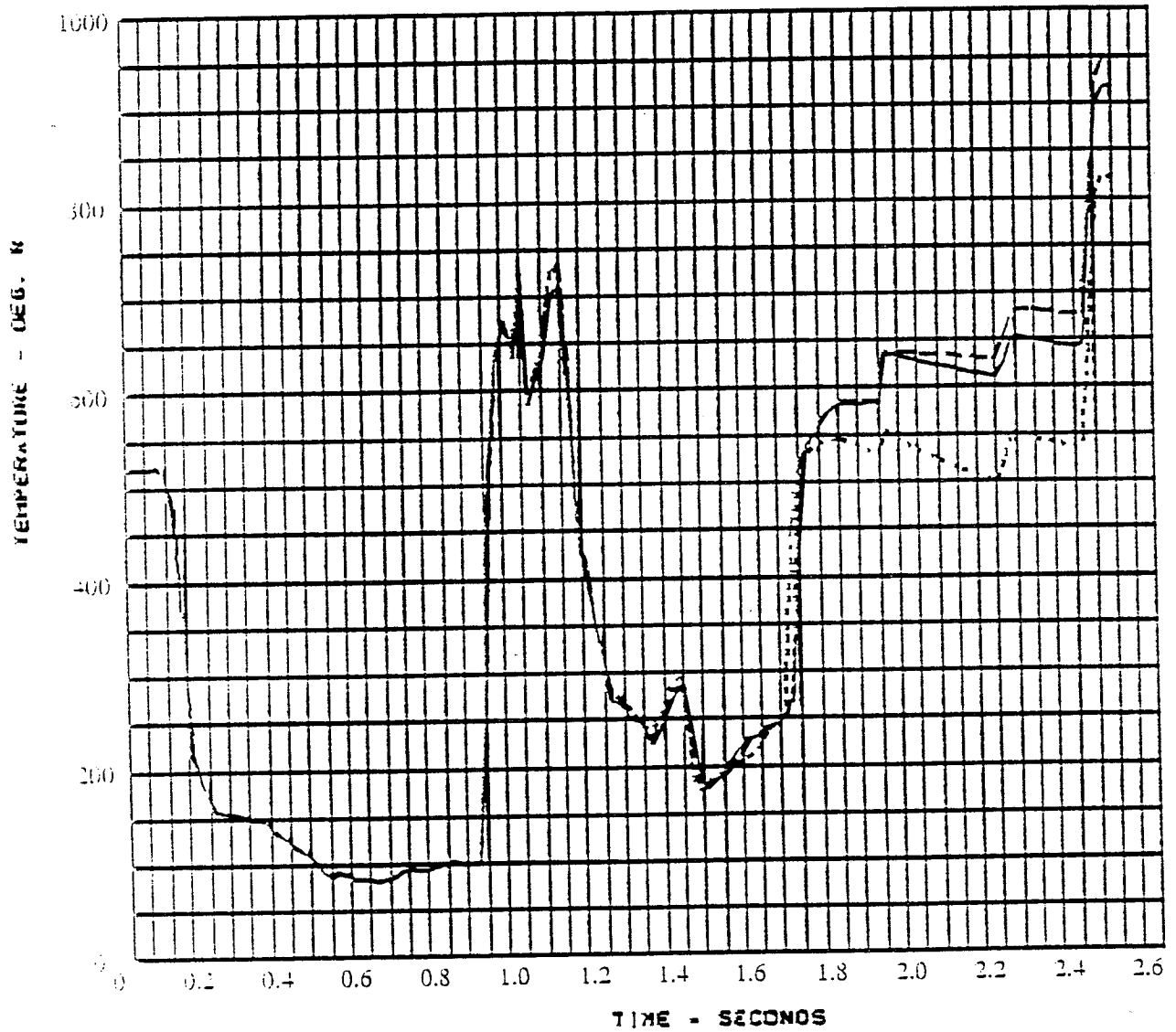


Figure 5-15c Simulation of MOV Anomaly

PRESSURE OXIDIZER PREBURNER

7/9/90

— DWGN arpdtn start run nominal 7/90
 - - - DWGN start run with mov at 55 9/04/90
 - - - DWGN start run with mov area change and position fix 55 9/06/90

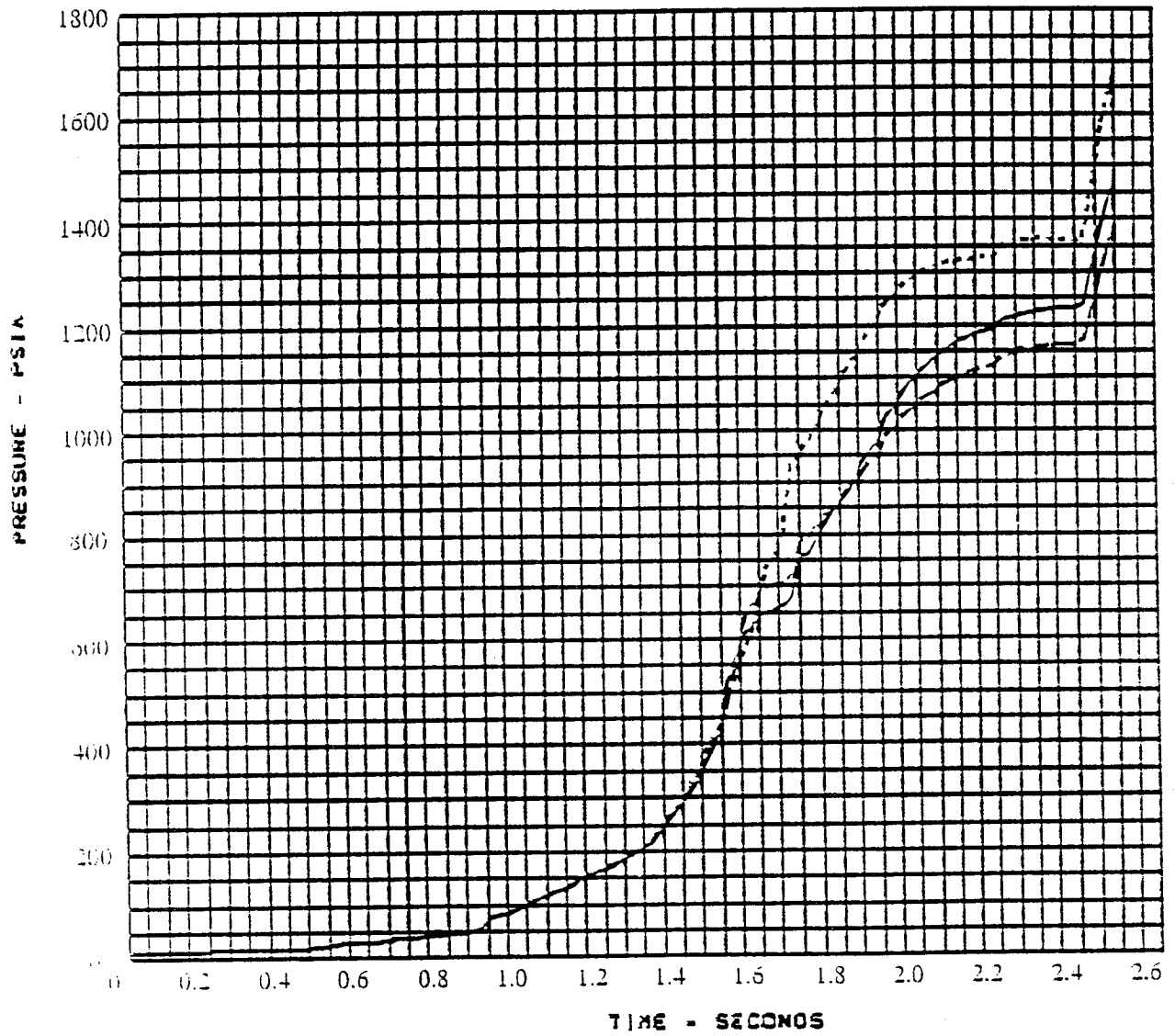


Figure 5-15d Simulation of MOV Anomaly

MCC COMBUSTION CHAMBER PRESSURE

7/9/90

— F
 - - - F
 - - - F

atpdtm start run nominal 7/90
 start run with mov at 55 9/04/90
 start run with mov area change and position fix 55 9/06/90

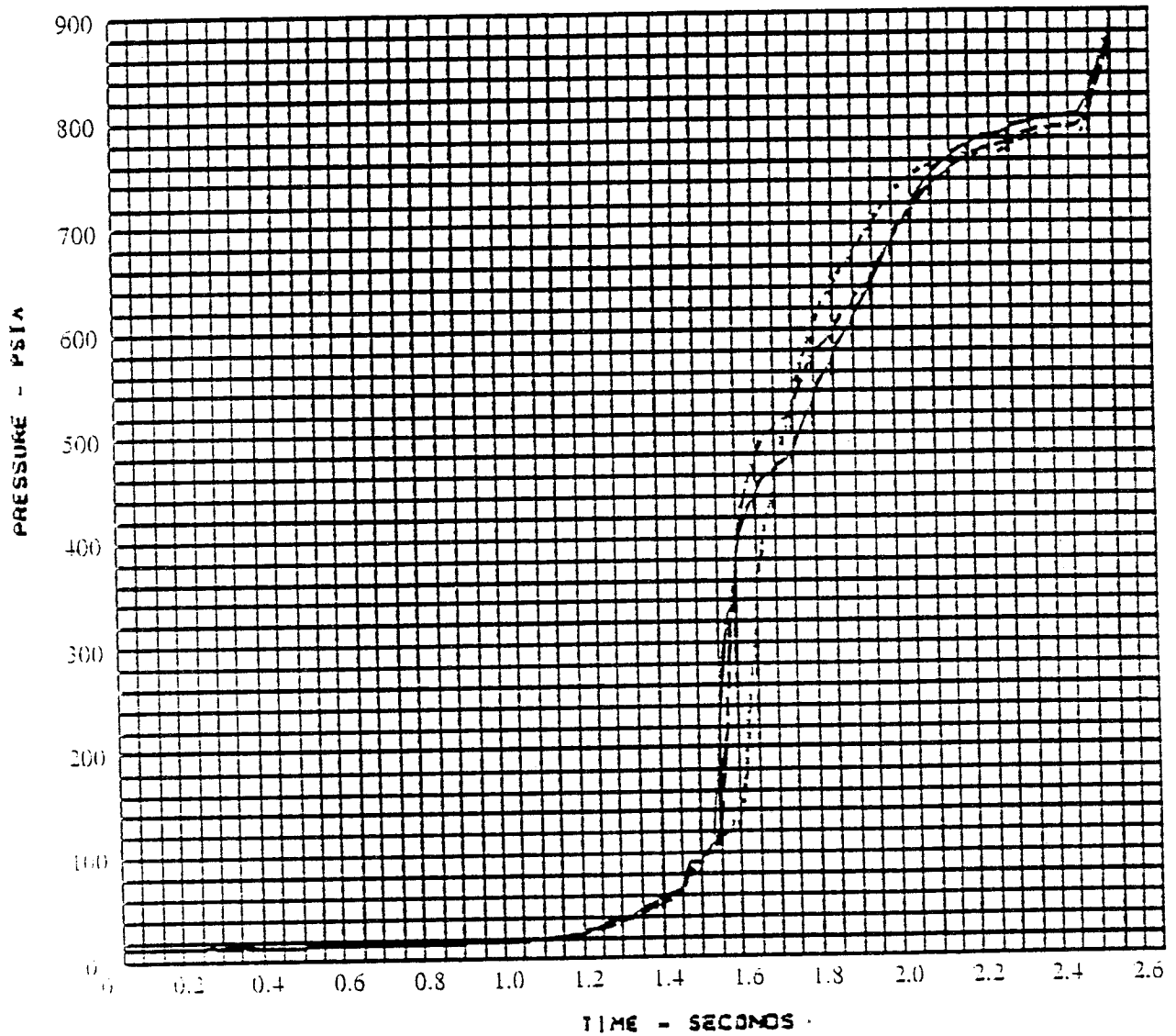


Figure 5-15e Simulation of MOV Anomaly

HIGH PRESSURE FUEL PUMP SPEED

7/ 9/90

- DWHO atpdtm start run nominal 7/90
- DWHO start run with mov at 55 9/04/90
- - - DWHO start run with mov area change and position fix 55 9/06/90

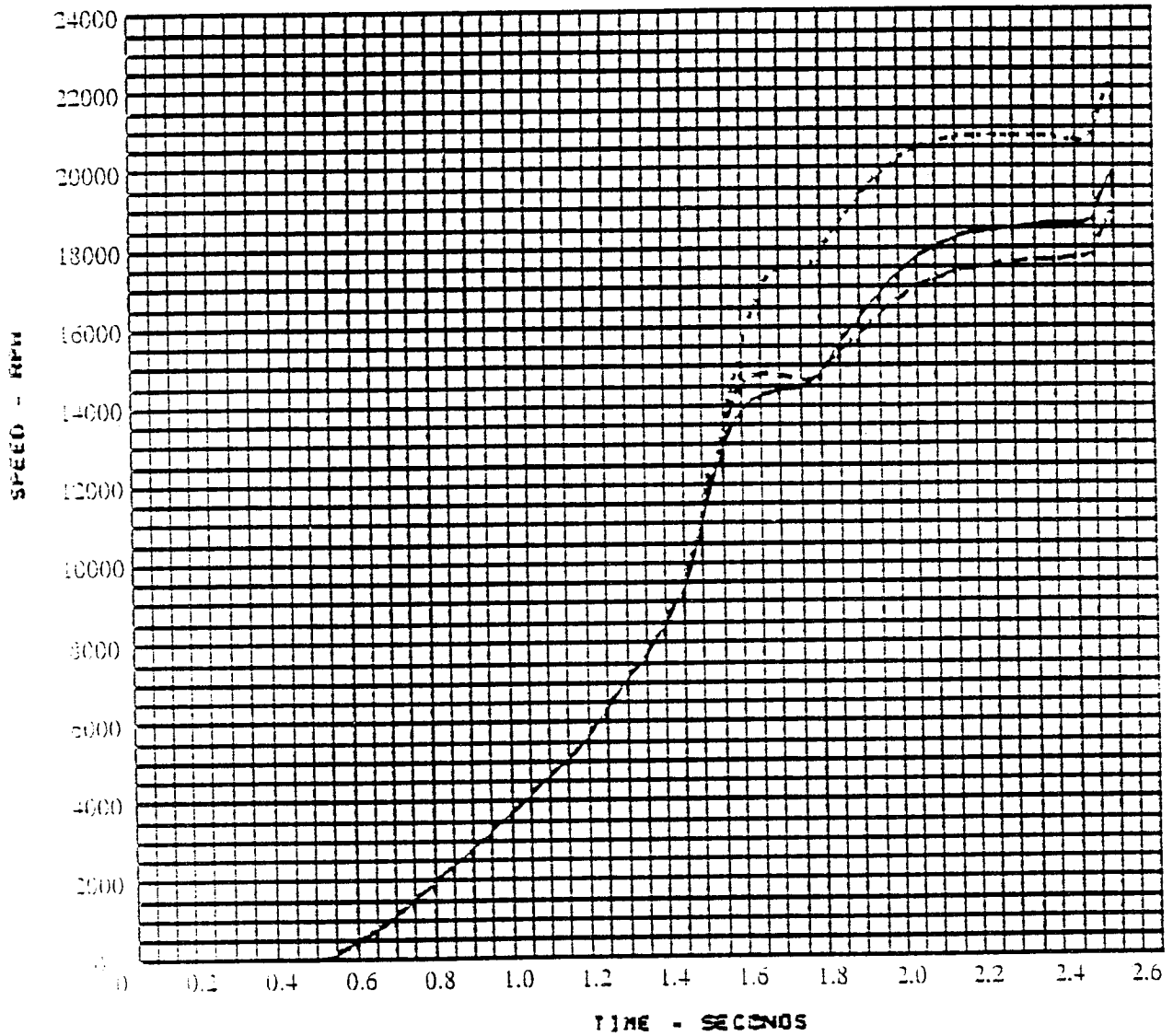


Figure 5-15f Simulation of MOV Anomaly

MAIN OXIDIZER VALVE POSITION

7/9/90

- CPV arpdtn start run nominal 7/90
- CPV start run with mov at 55 9/04/90
- - - CPV start run with mov area change and position fix 55 9/06/90

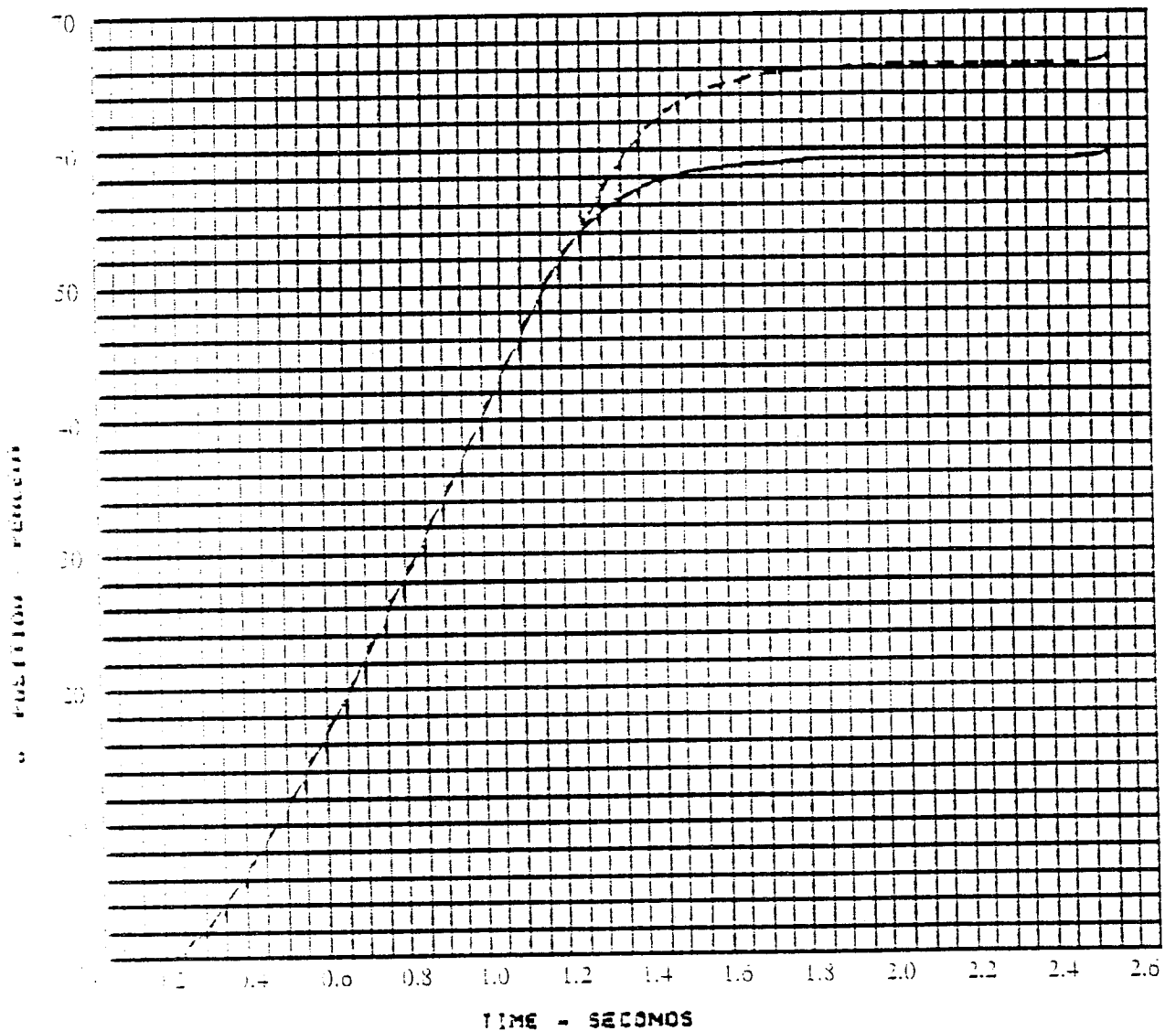


Figure 5-15g Simulation of MOV Anomaly

ORIGINAL PAGE IS
OF POOR QUALITY

MAIN CHAMBER MIXTURE RATIO

7/9/90

— COD1 arpdtn start run nominal 7/90
 - - - COD1 start run with mov at 55 9/04/90
 - - - COD1 start run with mov area change and position fix 55 9/06/90

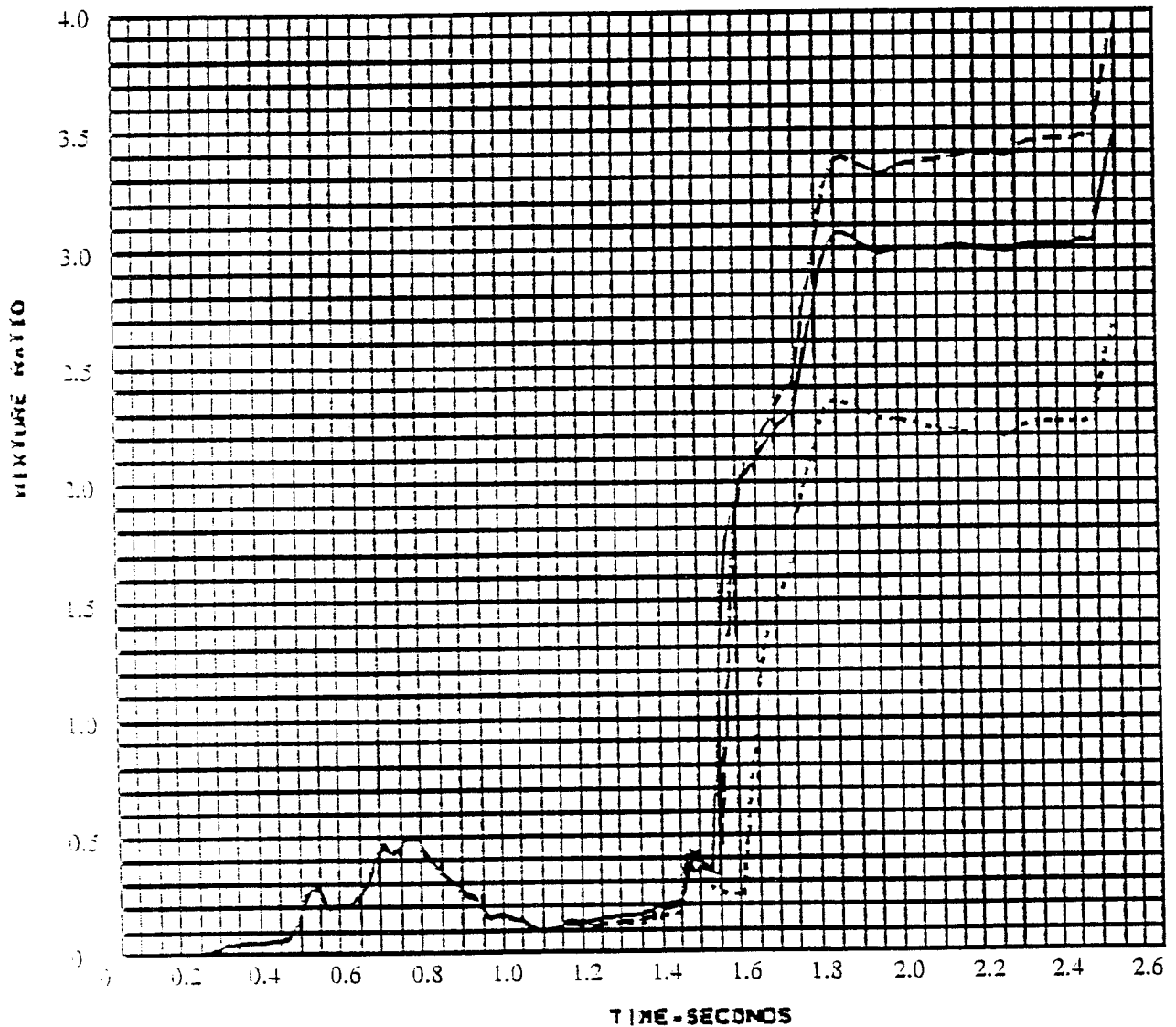


Figure 5-15h Simulation of MOV Anomaly

ORIGINAL PAGE IS
OF POOR QUALITY

Figure 5-16b Summary of MOV Anomaly & Accommodation
Simulated Start Transient - Preburner Temperatures

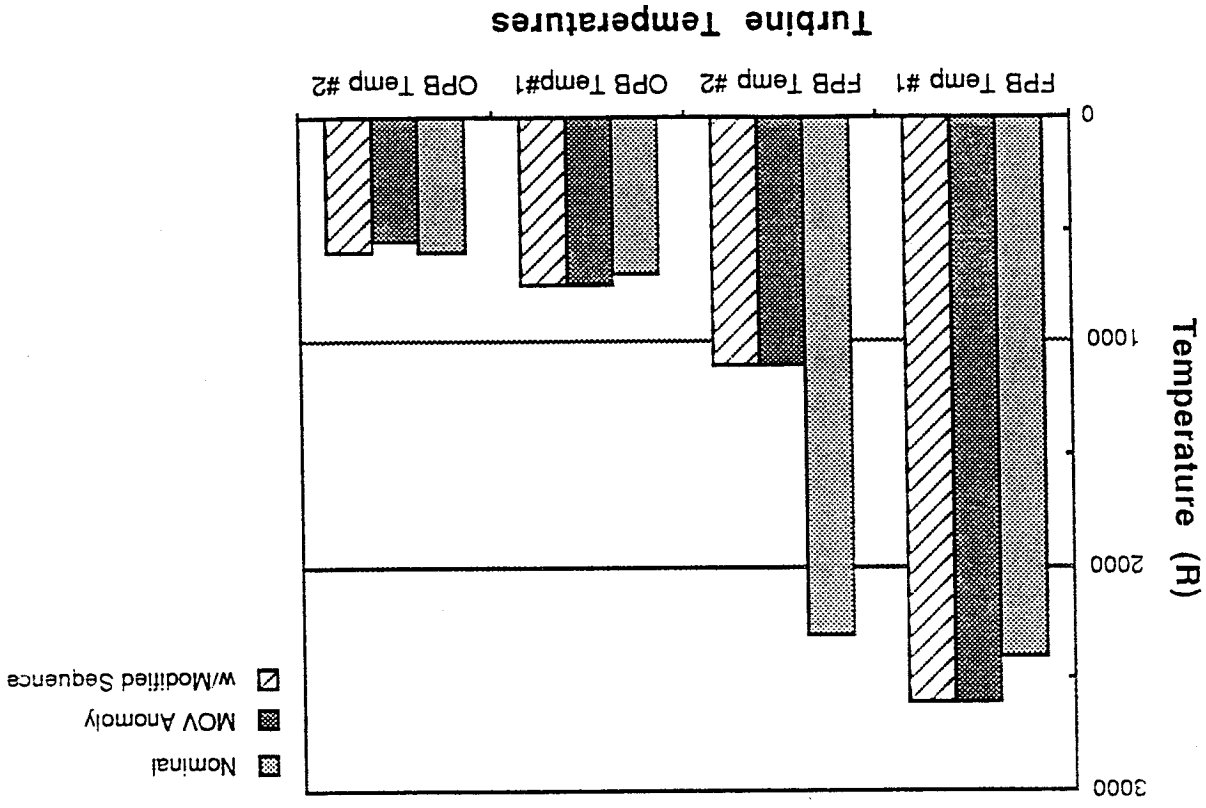
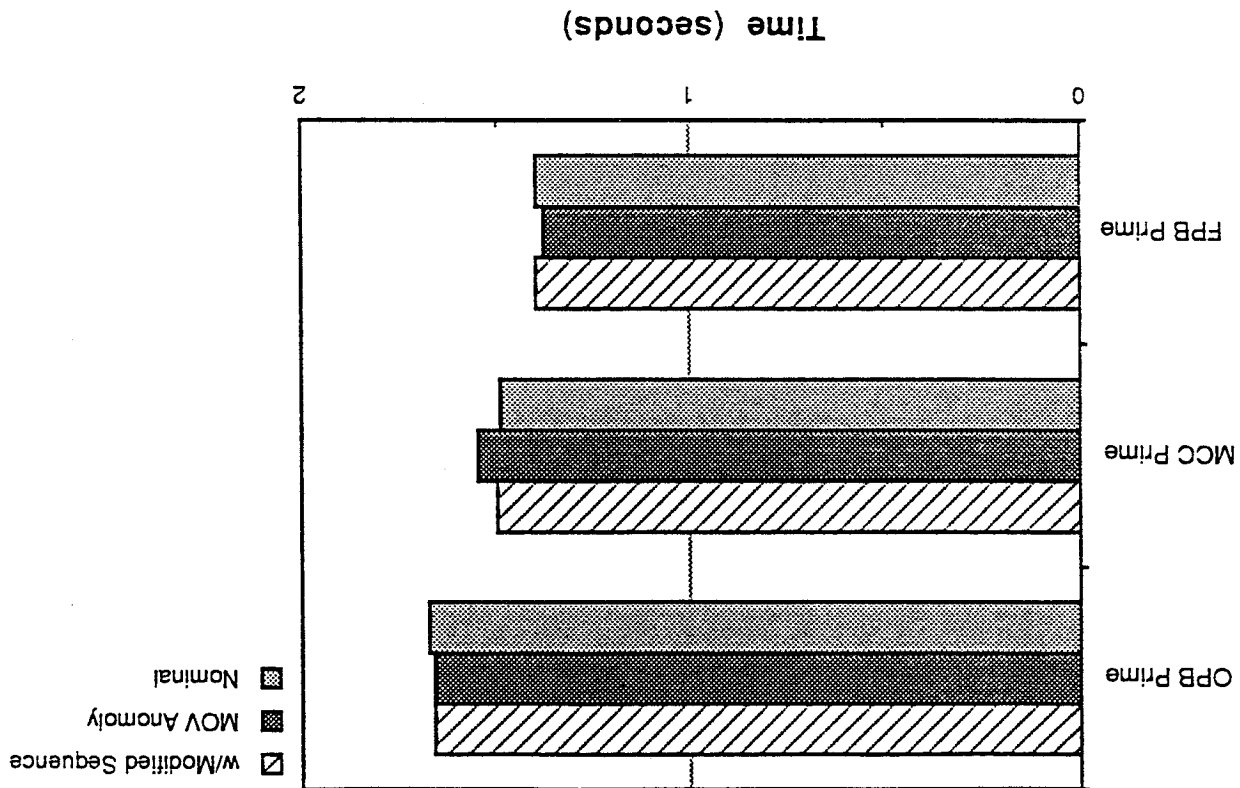
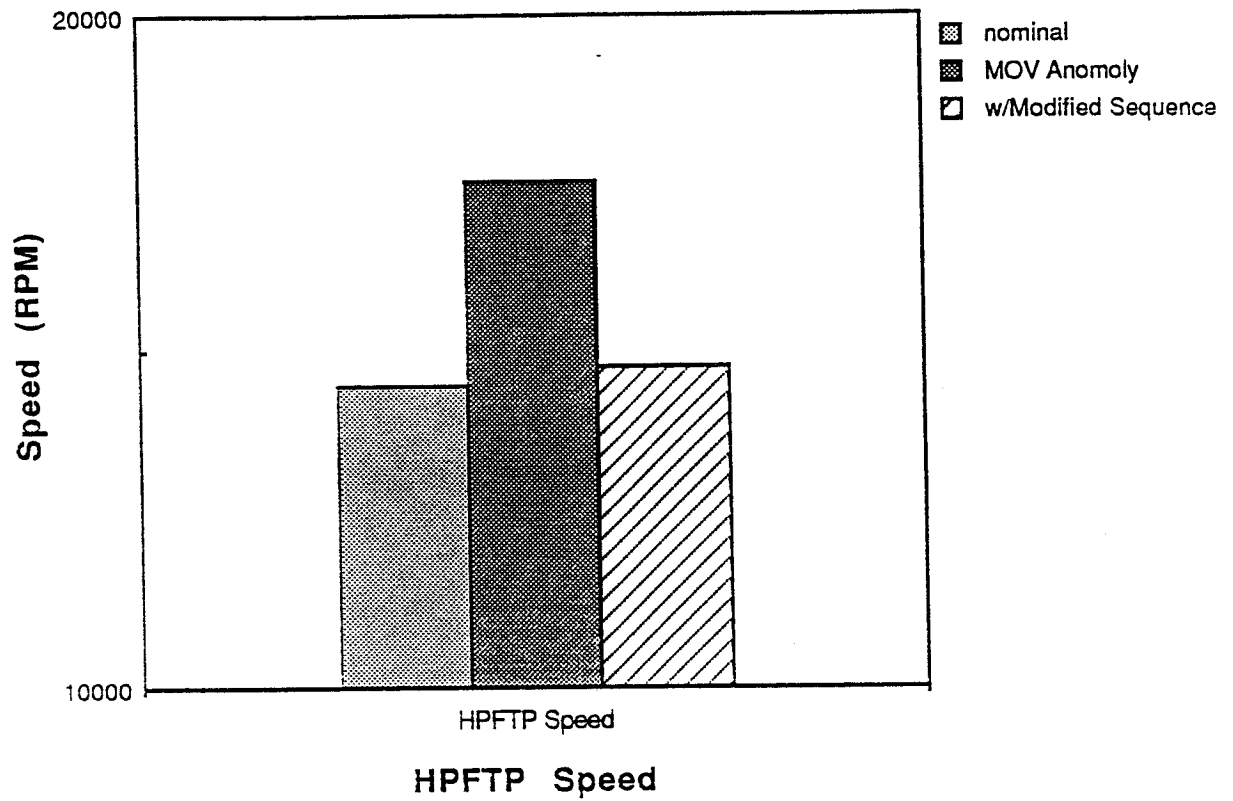
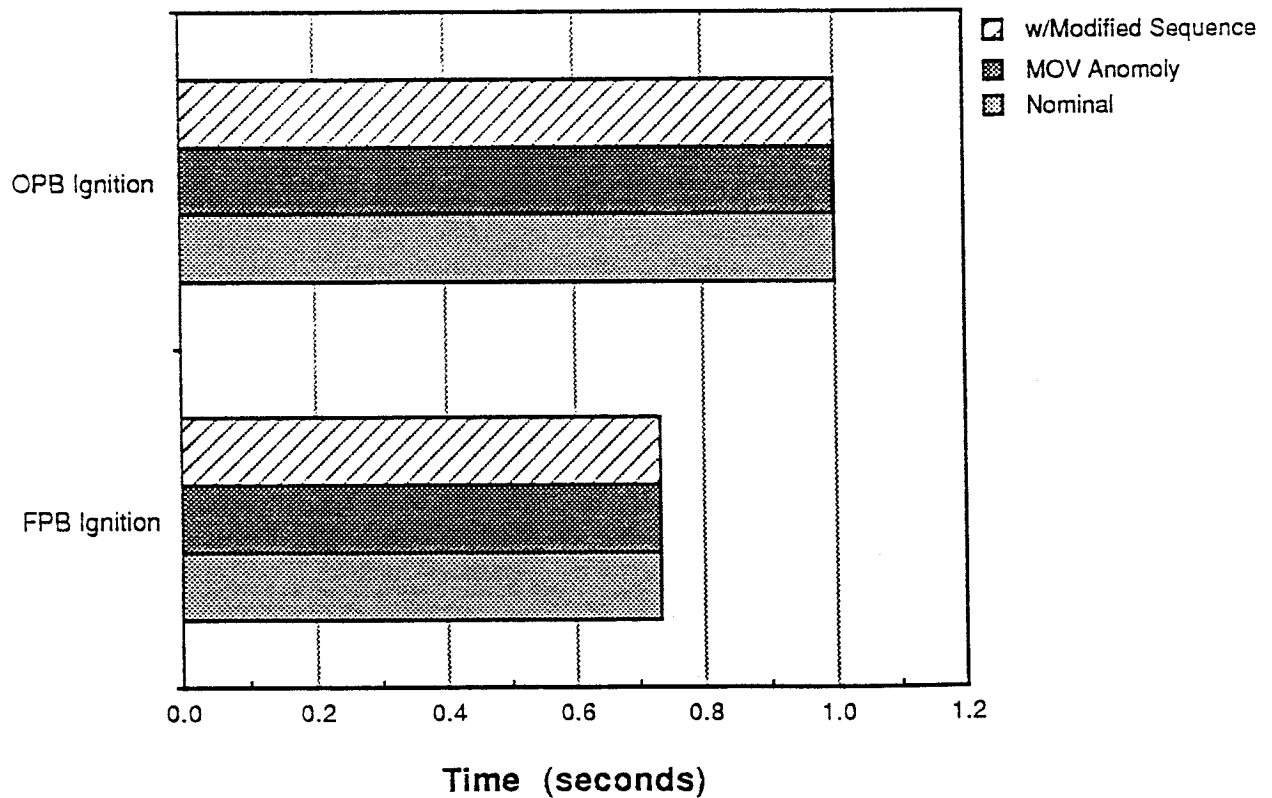


Figure 5-16a Summary of MOV Anomaly & Accommodation
Simulated Start Transient - LOX Dome Prime Times





**Figure 5-16c Summary of MOV Anomaly & Accomodation
Simulated Start Transient - HPFTP Speed**



**Figure 5-16d Summary of MOV Anomaly & Accomodation
Simulated Start Transient - Preburner Ignition Times**

SECTION 6 ICS FUNCTIONAL FRAMEWORK SIMULATION

The objective of the ICS functional framework simulations is to demonstrate the feasibility of key features of the framework. Key features demonstrated are: 1) the ability to control engine variables other than thrust and mixture ratio while maintaining a specified thrust and mixture ratio, 2) the ability to rapidly and smoothly change engine variables using a multivariable controller, and 3) the ability to coordinate a three engine cluster using downthrust factors as feedback. Similiar rocket engine control objectives have been demonstrated by NASA-LeRC and are presented in Reference 2. Since the goal of the simulation effort is to demonstrate feasibility, no effort to optimize the control gains was expended beyond that required to demonstrate the control feasibility.

The MATRIXx simulation environment was selected for this effort since a detailed simulation of the SSME dynamics was available in this environment. The detailed SSME dynamic model used in this effort was implemented in MATRIXx by NASA-LeRC based on equations provided by Rocketdyne and was made available by NASA-LeRC for this program.

The general control strategy employed in the ICS framework consists of a propulsion level controller and three engine level controllers. The propulsion level controller implements thrust control over the three engine cluster. The engine level controller implements additional engine variable control within the constraints set by the propulsion level controller.

The engine level controller is simulated to demonstrate the feasibility of controlling engine variables to desired values while maintaining mission thrust and mixture ratio constraints. Initially, a non-interacting multiple input controller is implemented as a proof of concept. Then the relationships between relevant engine variables is defined and an interacting multiple input/multiple output controller is implemented. Finally, the engine thrust and downthrust factor responses are characterized to define a simplified engine model.

The propulsion level controller simulation uses three simplified engine models to demonstrate thrust distribution between the engines in response to degradations as indicated by the downthrust factor. Several demonstration cases are run and an actual SSME failure case is simulated.

6.1 Engine Level Controller Simulations

6.1.1 Engine Level Simulation Overview and Goals

The goal of the ICS engine level controller simulation is to demonstrate the feasibility of controlling potentially degrading engine variables while maintaining mission requirements for engine thrust and engine mixture ratio.

To simplify the problem, only the fuel preburner oxidizer valve (FPOV), the oxidizer preburner oxidizer valve (OPOV), and the oxidizer preburner fuel valve (OPFV) were considered as control valves throughout the simulation. The FPOV and OPOV are currently used on the SSME and the OPFV is an additional valve proposed as part of the phase I ICS baseline functional framework that controls the distribution of fuel between the high pressure turbines. Additionally, only the thrust command is set by the propulsion level controller. The mixture ratio is controlled to a fixed value of 6.0.

The potentially degrading engine variables selected for control are the high pressure fuel turbine (HPFT) temperature and the high pressure oxidizer turbine (HPOT) temperature. The high pressure turbines are currently run at temperatures near the damage limits (redlines) during SSME mainstage operation. The HPFT temperature is especially high and contributes to the

life limits of turbine components such as turbine blades. The control strategy implemented is to force the ratio turbine temperature/temperature redline (T/R) to be equal for both high pressure turbines. The rationale for forcing T/Rs to equal values is:

- 1) The temperature redline value for each turbine indicates the temperature at which the damage rate is so great that the engine is expected to fail before mission completion.
- 2) The damage rate is estimated to be directly related to turbine temperature.
- 3) The relative damage rate for each turbine is therefore estimated as turbine temperature / temperature redline (T/R).
- 4) For a given set of engine fuel and oxidizer flowrates, the high pressure turbine temperatures are inversely related.
- 5) The goal of the controller is to maximize total engine life.
- 6) Total engine life is maximized when the damage rates for the high pressure turbines are equal.
(i.e. HPFT temperature/HPFT redline = HPOT temperature/HPOT redline)

The overview of the ICS engine level controller simulations is shown in Figure 6-1. The thrust level command (from the ICS propulsion level controller) and the mixture ratio command (fixed at 6.0) are converted into engine variable commands (fuel and oxidizer flowrates) that can be implemented by a combination of the FPOV, OPOV, and OPFV positions. Valve commands are issued that resolve errors in the commanded fuel and oxidizer flowrate while forcing the high pressure turbine T/Rs to be equal. Additionally, the main combustion chamber (MCC) pressure and the HPFT temperature/redline ratio are fed back to the propulsion level controller. The MCC pressure is used to estimate engine thrust and the HPFT temperature/redline ratio provides a simplified downthrust factor. The simulated functions represent the Engine Command Generator, the Primary Actuator Command Generator, and the high pressure turbine temperature function of the Engine Coordinator shown in Figure 3-1a. The propellant flowrates are used as the controlled variables at the engine level to reflect the RREICS framework philosophy of controlling each propulsion subsystem independently to meet the overall propulsion system requirements. Even though controlling the propellant feed system flowrates (instead of controlling thrust and mixture ratio directly) has little meaning in the case of the SSME, the applicability of controlling the propellant feed system to an integrated propulsion system warrants the additional effort.

6.1.2 Non-Interacting Multiple Input Control

The first simulation objective is a proof of concept of the ICS engine level control objectives for the SSME with the addition of the OPFV. The specific goals of the proof of concept simulation are to show that: 1) the high pressure turbine temperatures can be controlled to equal values of T/R and 2) the fuel and oxidizer flowrates can be maintained at the commanded values.

Figure 6-2a shows the proof of concept simulation layout. The superblock labeled "ssme" is the detailed ssme model and represents the dynamics of the engine and valves. The superblock labeled "e2" is the valve controller. External inputs to the simulation are the commanded engine fuel flowrate and the commanded oxidizer flowrate. Unity feedback of the simulated propellant flowrates is used to calculate the fuel flowrate error (Mf_ERROR) and the oxidizer flowrate error (Mo_ERROR). The temperature error is calculated as the difference between the

HPFT and the HPOT temperatures normalized by the inverse of the corresponding redline values (1905R for the HPFT, 1760R for the HPOT).

The valve controller is a non-interacting multiple input controller that consists of three independent control loops. The FPOV is commanded based on fuel flowrate errors. The OPOV is commanded based on oxidizer flowrate errors. The OPFV is commanded based on turbine temperature errors. Integral control is used for each valve control loop. The gain of each control loop is the sensitivity of the controlled parameter to the control valve as determined by baseline simulation runs.

Inputs to the proof of concept simulation are a constant 148 lbm/second for the engine fuel flowrate and a constant 893 lbm/second for the engine oxidizer flowrate. The input values represent the propellant flowrates required to achieve 100% of rated power level (RPL) for the SSME.

The results of the simulation are shown in Figures 6-2c, 6-2d, and 6-2e. Initial oscillations in the data are attributed to anomalies caused by initialization of the simulation and are not considered "real" data. Therefore, interpretation of the simulation results begins after the initial oscillations have settled out. Figure 6-2c shows that the temperature error was forced to 0.0 as expected. Figure 6-2d shows the commanded engine fuel flowrate (solid line) and the actual fuel flowrate (dashed line). The actual fuel flowrate oscillates around the commanded value and appears to be settling to the commanded value. Figure 6-2e shows the commanded engine oxidizer flowrate (solid line) and the actual oxidizer flowrate (dashed line). The actual oxidizer flowrate oscillates around the commanded value and appears to be settling to the commanded value.

With the proof of concept controller, the HPFT temperature reached a steady state value of about 1720R ($T/R = 0.903$) and the HPOT temperature reached a steady state value of about 1600R ($T/R = 0.909$) for a simulated 100% RPL. With the baseline SSME controller, the HPFT temperature at 100% RPL would be about 1810R ($T/R = 0.95$) and the HPOT temperature at 100% RPL would be about 1370R ($T/R = 0.78$). The engine life limiting damage rate is reduced from 0.95 for the baseline SSME to 0.90 for the SSME with the ICS control strategy.

Based on the proof of concept simulation, it appears that the high pressure turbine temperatures can be controlled while maintaining the commanded propellant flowrates using the SSME with the addition of an OPFV.

6.1.3 Interacting Multiple Input/Multiple Output Controller

The non-interacting multiple input controller implemented and described in Section 6.1.2 demonstrated the feasibility of the ICS engine level control strategy. Specifically, it was demonstrated that potentially damaging engine variables can be controlled within the constraints of mission thrust and mixture ratio constraints. However, the simple control scheme used in the proof of concept demonstration shows a slow response (the flowrates oscillate with a period of about 10 seconds) and a long settling time (the flowrate have not settled after 10 seconds). To demonstrate the feasibility of the proposed engine level control strategy for a real life application it is necessary to demonstrate that suitable engine responses to commanded inputs can be achieved. Therefore, a better (faster, less overshoot) engine response is implemented using a multivariable controller.

The first step in the interacting multiple input/multiple output controller development is to characterize the sensitivity of each controlled engine variable to each of the control valves. The sensitivities are determined using multiple simulation runs and the resulting data is used to

define a gain matrix that is implemented in the valve controller. The new valve controller is incorporated into the engine level controller model and a baseline control case is simulated.

6.1.3.1 Determination of the Gain Matrix

The relationship between the relevant SSME variables and the control valve positions was determined to facilitate implementation of an interacting multiple input/multiple output controller. The objective of this effort is to determine the relative changes in control valve positions required to resolve a measured error vector. The control valves investigated are the OPOV, FPOV, and OPFV. The SSME variables investigated are the engine fuel flowrate, the engine oxidizer flowrate, the HPFT temperature, and the HPOT temperature. Additionally, changes in the normalized turbine temperature difference were calculated by taking the difference between the HPFT temperature divided by the HPFT redline temperature (1905R) and the HPOT temperature divided by the HPOT redline temperature (1760R) as shown below:

$$T = T_HPFT/1905 - T_HPOT/1760, = \text{Temperature Error}$$

The sensitivity of each SSME variable to changes in control valve positions was determined for control valve perturbations around a 100% RPL nominal value. Seven simulation runs were generated and the relevant parameter values recorded. The results of the simulations are summarized in Table 6-1. The first column indicates the engine variables for the nominal 100% RPL. The remaining six columns show the engine variables for perturbations in a single valve position. The FPOV, OPOV, and OPFV were each perturbed by +/- 1% of the nominal value. Table 6-2 shows the valve to variable gains obtained by taking the difference between the +1% values and the -1% values.

Based on the simulation results, the engine response linearized around 100% RPL is represented by:

$$S = A \times V, \text{ where}$$

$$S = \frac{dMf}{dT}, \text{ error vector}$$

$$A = \begin{bmatrix} 175.6 & 149.2 & 1.26 \\ -428.2 & 2508 & 78.4 \\ 6.33 & -6.40 & 0.39 \end{bmatrix}$$

$$V = \begin{bmatrix} dP_FPOV \\ dP_OPOV \\ dP_OPFV \end{bmatrix}, \text{ changes in valve position}$$

To determine the relative changes in valve positions to resolve a measured error vector, the engine response equation is solved for V.

$$V = A^{-1} \times S, \text{ where}$$

$$A^{-1} = \begin{bmatrix} 0.005 & -0.0002 & 0.031 \\ 0.002 & 0.0002 & -0.053 \\ -0.026 & 0.004 & 1.88 \end{bmatrix}$$

6.1.3.2 Interacting Multiple Input/Multiple Output Controller Simulation and Results

The interacting multiple input/multiple output controller simulation has the same top level architecture as described in Section 6.1.2 and shown in Figure 6-2a. The difference is in the valve controller. The superblock labeled "e2" (the valve controller) is replaced with the valve controller shown in Figure 6-3a. The proportional gains correspond to the gain matrix A^{-1} described in Section 6.1.3.1. The integral gains are set to reduce the steady state error but are not optimized in any way.

The input to the simulation is initially a fuel flowrate command = 148 lbm/sec and an oxidizer flowrate command = 888 lbm/sec. At time = 1 second, a commanded step change to fuel flowrate command = 140 lbm/sec and oxidizer flowrate command to 840 lbm/sec is issued. At time = 2 seconds, a commanded step change back to the initial commanded values is issued. The input commands maintain a mixture ratio of 6.0 throughout the simulation and command the thrust from a nominal 100% RPL to about 94% RPL and back to 100% RPL.

The simulated thrust and downthrust factor for the interacting multiple input/multiple output controller using the input commands described above are shown in Figure 6-3b. The engine thrust settles to within 1/2 of a percent in about 0.15 seconds. The downthrust factor indicates some overshoot, but settles to steady state in about 0.15 seconds. Figures 6-3c and 6-3d show the propellant flowrate responses to the step inputs. Figure 6-3e shows the turbine temperature to redline temperature ratio for the HPFT and the HPOT. Figure 6-3e indicates a maximum HPFT temperature overshoot of about 75 R during the upthrust transient.

The interacting multiple input/multiple output controller (without gain optimization) simulation indicates that: 1) the HPOT and HPFT temperatures are controlled to the same value of T/R throughout the test, and 2) a thrust change rate of 40%/second is achieved. The interacting multiple input/multiple output controller simulation indicates an engine response 4 times faster than the current SSME which is thrust change rate limited to 10%/second. Therefore, the simulated controller results in an engine response that appears to exceed the requirements for a real life application and the feasibility of controlling the high pressure turbine temperatures while maintaining the thrust and mixture ratio at mission required values is demonstrated.

6.2 Propulsion Level Controller Simulations

6.2.1 Propulsion Level Simulation Overview and Goals

The ICS propulsion level controller controls the thrust and mixture ratio of each engine to achieve overall propulsion system thrust and mixture ratio commands issued by the ICS controller. The goal of the ICS propulsion level controller is to implement the overall propulsion system thrust and mixture ratio while maximizing the reliability, life, and performance of the engine cluster.

The objective of the ICS propulsion level controller simulation is to demonstrate that individual engine thrust values can be controlled to maximize engine cluster reliability, life, and performance (as indicated by the downthrust factor) within mission and engine constraints.

The ICS propulsion level controller simulation consists of three engine models and a single propulsion level controller that determines the thrust of each engine. The control objectives implemented in the ICS propulsion level simulation are:

- 1) The overall propulsion system thrust equals the mission level controller command
- 2) Individual engines are operated within an allowable operating range (65% to 109%)
- 3) The individual engine downthrust factors are equal

The first control objective is a requirement for mission completion. The second control objective is a requirement of the engine system. Implementation of the third control objective results in a thrust distribution between engines that extends the useful life of the weakest engine.

The first step in the simulation effort was to define a first order engine model to facilitate simulation of the ICS propulsion level controller. The first order engine model provides thrust and downthrust factor feedback to the ICS propulsion level controller.

The ICS propulsion level controller is implemented both in MatrixX and coded for use on an IBM PC using the Basic language. The PC version of the simulation includes features that could not be readily implemented in MatrixX within the time frame of this contract.

Three simulation cases (one using MatrixX and two using the PC) are presented to demonstrate the functions of the ICS propulsion level controller. Then a real SSME failure case is simulated and the engine cluster response using the ICS propulsion level controller is presented.

Finally, the detailed SSME dynamic model is integrated with the ICS propulsion level controller simulation in MatrixX.

6.2.2 Definition and Characterization of First Order Engine Model

The first order engine model is a greatly simplified model of the SSME that was used to provide the feedback necessary to demonstrate the propulsion level controller. Two engine feedbacks are required for the ICS propulsion level controller simulation, the engine thrust and the downthrust factor. Therefore, the first order model need only provide realistic indications of the thrust time response and the downthrust factor time response.

The first order engine model approximates the SSME response to thrust commands as a first order response with a time constant of 0.1 seconds. For simplicity and for the clarity of propulsion level controller responses, higher order effects and non-linearities were not included in the first order engine model. The time constant of 0.1 seconds is representative of the response demonstrated by the detailed engine simulations described in Section 6.1.3.2

The first order engine model approximates the downthrust factor as a function of thrust. In order to define the downthrust factor equation, the downthrust factor is represented by the high pressure fuel turbine temperature/redline ratio. HPFT T/R it is expected to be a major contributor to the overall downthrust factor in any ICS.

The downthrust factor function was quantified by forcing the detailed engine model to thrust values ranging from 100% RPL to 65% RPL and recording the HPFT T/R as shown in Figure 6-4. The downthrust factor oscillations at the lower thrust levels indicate that the detailed engine model is being overcontrolled. The reason for the overcontrol is that the gain matrix was derived for the controller around 100% and the valve response is not linear. The downthrust factor at the lower thrust levels was estimated as the mean value for those levels.

The detailed engine model downthrust factor was curve fit as a function of thrust to define the first order engine model downthrust factor function. The data fit a linear relationship well with the resulting equation being given by:

$$\text{Downthrust factor} = 1\text{e-}06 * \text{Thrust} + 0.43 \quad [6-1]$$

6.2.3 The Propulsion Level Controller Simulation

The ICS propulsion level controller strategy is described by the MatrixX version of the propulsion level controller simulation shown in Figure 6-5. The superblocks labeled "ideal_2" are the first order engine models described in Section 6.2.2. The superblock labeled "ideal_3" is the first order engine model with an engine degradation simulated. Input "1" is the propulsion system thrust command from the mission level controller.

In the outer control loop, the sum of engine thrusts is fed back to the ICS propulsion level controller and compared to the commanded propulsion level thrust to create a propulsion system thrust error. The engine thrusts are controlled using the propulsion system thrust error through a proportional-integral controller.

The inner loop modifies the outer loop thrust commands in response to variations in the engine downthrust factors. The average of the engine downthrust factors is compared to individual engine downthrust factors to create a downthrust error for each engine. Changes in each engines thrust command are defined by a proportional-integral controller based on the downthrust errors.

Finally, the thrust command for each engine is limited to values between 305 klbf and 512 klbf, the normal operating range of the SSME.

To understand the rationale for the ICS propulsion level controller strategy, an understanding of the downthrust factor is required. The downthrust factor represents the overall engine condition and is made up of multiple factors representing engine reliability, life usage, and performance degradation. Two types of effects contribute to the downthrust factor: 1) effects that are inherent to the engine operation and are related to engine thrust and mixture ratio (e.g. HPFT turbine speed), and 2) effects which represent a degradation or limitation of the engine (e.g. HPFT turbine blade cracks). Both types of effects are correlated to one of the downthrust factor elements, reliability for example, and contribute to the downthrust factor. Cracks in a the turbine blade are correlated to a reduction in the engine reliability. Decreased turbopump speed is correlated to an increase in turbopump reliability. The turbopump reliability is evaluated for the blade cracks and turbopump speed and the turbopump reliability is reflected in the downthrust factor. A higher reliability results in a lower downthrust factor.

The downthrust factor control strategy is to control the individual engine thrusts so that each engine has the same downthrust factor. The degradation accommodation scheme achieved by controlling engine downthrust factors to equal values is illustrated by the following example. If turbine blade cracks are detected in the HPFT of engine #1, the thrust of engine #1 is reduced and the thrusts of engines #2 and #3 are increased. Equilibrium is reached when the high pressure fuel turbopump of engine #1 has reduced its speed to the point where the reliability of the slow turbine with cracked blades (#1) is equal to the reliability of turbopumps #2 and #3 operating at higher speeds. This example considers only two of the factors making up the downthrust factor but accurately illustrates the concept.

The key to the downthrust error loop is the comparison to the average downthrust factor for the engine cluster. By comparing individual downthrust factors to the average downthrust factor

for the engine cluster, the sum of the individual engine thrust changes issued by the downthrust error loop is 0. Therefore, the propulsion system thrust control loop is not affected by the downthrust factor control loop

Evaluation of the ICS propulsion level controller showed that the propulsion system thrust control and downthrust factor control loops worked unless an engine degradation was simulated and one of the engines reached its thrust operating limit. When an engine thrust operating limit was reached, the downthrust factor control loop continued to detect a difference in individual engine downthrust factors and tried to modify the engine thrust commands to resolve the difference. Since one of the engines was unable to respond to the thrust command changes, the changes implemented did not add up to 0 and the propulsion system thrust level drifted away from the commanded value. To correct the thrust drift problem, the downthrust factor control loop was modified to ignore the downthrust factor if the engine thrust is at a thrust limit and the downthrust factor indicates the engine should be commanded beyond the limit. It was unclear how the downthrust factor control loop modifications could be implemented using MatrixX, so the simulation was coded in basic and implemented on a PC. The modified ICS propulsion level controller implemented on a PC is shown in Figure 6-6. The modifications are indicated by the inclusion of g-functions in the downthrust factor control loop. The g-function is defined in Figure 6-6 and is used to inhibit the downthrust factor control for an individual engine if that engine will be commanded beyond its thrust operating limit. Appendix 5 is the code of the PC version of the simulation.

6.2.4 Demonstration Cases

Simulations of the ICS propulsion level controller were run to demonstrate the feasibility of controlling individual engine thrusts to accommodate engine degradations within propulsion system and engine constraints. The demonstration cases run are summarized below.

MatrixX Demonstration

The ICS propulsion level controller simulation implemented in MatrixX and shown in Figure 6-5 was used for demonstration case A. The timeline for case A is:

t = 0.0	Propulsion system thrust command = 1,500,000 lbf
t = 2.0	Propulsion system thrust command = 1,200,000 lbf
t = 3.0	Engine #1 downthrust factor begins to ramp upward
t = 3.25	Engine #1 downthrust factor stops ramping
t = 4.0	Propulsion system thrust command = 1,400,000 lbf
t = 6.0	End of simulation

The simulation results are shown in Figure 6-7. The total thrust follows the commanded value throughout the test. The individual engine thrusts are identical until a degradation in engine #1 is indicated by an increasing downthrust factor at 3.0 seconds into the test. The ICS propulsion level controller responds by reducing the thrust of engine #1 to accommodate the degradation and simultaneously increasing the thrusts for engine #2 and #3 to maintain the commanded propulsion system thrust. At t = 3.25 the engine degradation has stabilized and the engine thrusts stop changing. When the propulsion system thrust is commanded upward at t = 4.0, all three engines respond but engine #1, which is indicating a stabilized degradation, is maintained at a lower thrust than engines #2 and #3.

PC Demonstration - Case 1

The ICS propulsion level controller simulation shown in Figure 6-6 was used for demonstration case 1. The timeline for case 1 is:

t = 0.0	Propulsion system thrust command = 1,000,000 lbf
t = 1.0	Propulsion system thrust command = 1,400,000 lbf
t = 3.0	Engine #1 downthrust factor begins to ramp upward
t = 8.0	Propulsion system thrust command begins to ramp downward
t = 10.0	End of simulation

In case 1, the degradation is assumed to be a gradual loss of high pressure fuel turbine efficiency resulting in a steady increase in the HPFT temperature.

Case 1 was run for three ICS propulsion level controller configurations. The first run provides a baseline to compare subsequent simulations against and was configured with the downthrust factor control loop not working. The first run implements the basic control strategy of the SSME, that is, all three engines are controlled to identical values. The second run has the downthrust factor control loop working but does not include the g-functions that inhibit engine commands beyond the engine thrust operating limits. The third case is with the full ICS propulsion level controller as shown in Figure 6-6.

RUN 1: The simulation results are shown in Figure 6-8. The total thrust follows the commanded propulsion system thrust except for a lag during the propulsion system downthrust. All three engines show identical responses throughout the test. It would be a surprise if they did not since no downthrust factor control is implemented for this run. The downthrust factors for each engine initially are identical. At $t = 3.0$, engine #1 begins to indicate a higher than normal HPFT temperature and its downthrust factor increases. The HPFT temperature crosses the redline at about $t = 5.0$ and continues to increase until engine #1 is downthrust with the others at $t = 8.0$. The maximum HPFT temperature indicated is about 2150R.

RUN 2: The simulation results are shown in Figure 6-9. The total thrust followed the commanded propulsion system thrust during the initial step at $t = 1.0$. All three engines indicated the same downthrust factor and have identical thrust profiles. At $t = 3.0$, engine #1 begins to indicate a degradation by an increase in the downthrust factor. The controller responds by downthrusting engine #1 to accommodate the degradation and simultaneously upthrusting engines #2 and #3 to maintain the propulsion system thrust at the commanded value. At about $t = 6.5$, engines #2 and #3 reach thrust levels of 512 klbf. The thrust operating limit for the engines is limited to 512 klbf and engines #2 and #3 are not upthrust any higher. However, the downthrust factor for engine #1 continues to increase and the downthrust factor control loop continues to attempt to downthrust engine #1 and make up the loss by upthrusting engines #2 and #3. However, the commands to engines #2 and #3 are inhibited by the thrust limiter. Therefore, only the downthrust of engine #1 is actually implemented, causing the propulsion system thrust to drift away from the commanded value. The propulsion system thrust control loop tries to force engine #1 back to a nominal value but only succeeds in reducing the downthrust rate of engine #1. Beyond $t = 6.5$, the propulsion system thrust continues to drift away from the commanded value.

RUN 3: The simulation results are shown in Figure 6-10. This run represents the fully implemented ICS propulsion level controller simulation. The propulsion system thrust follows the commanded value throughout the simulation except for a lag during the commanded downthrust. All three engines have the same thrust until $t = 3.0$ when the HPFT of engine #1 begins to lose efficiency. Engine #1 is downthrust to accommodate the loss of HPFT

efficiency and engines #2 and #3 are simultaneously upthrust to maintain the propulsion system thrust at the commanded value. The relationship between the downthrust of engine #1 and the upthrust of engines #2 and #3 is such that the HPFT temperature of each engine is near the same value. Engine #1 continues to lose HPFT efficiency and continues to be downthrust until engines #2 and #3 reach their maximum operating thrust of 512 klbf. When engines #2 and #3 are at their maximum allowable thrust, no further decrease in engine #1 thrust level is possible and engine #1 holds at its current thrust level. The engine #1 HPFT continues to lose efficiency at the same rate it has been and the HPFT temperature continues to rise. At $t = 8.0$, the propulsion system thrust is commanded to a downward ramp. The ICS propulsion level controller recognizes that engine #1 is indicating a higher degradation than the other engines and implements the entire propulsion system downthrust using engine #1 until engine #1 reaches its lower allowable thrust limit at about $t = 9.0$. The downthrust of engine #1 causes a lower HPFT temperature and results in a decrease in the engine #1 downthrust factor. When engine #1 reaches its lower thrust limit, the propulsion system downthrust is implemented using engines #2 and #3. If the engine #1 downthrust factor had been reduced to the same value as the engine #2 and #3 downthrust factors, all three engines would have been downthrust at proportions that keep the downthrust factors equal while implementing the propulsion system downthrust. The maximum HPFT temperature indicated is about 1920 R, over 200 R cooler than case 1 without downthrust factor control.

PC Demonstration - Case 2

The ICS propulsion level controller simulation shown in Figure 6-6 was used for demonstration case 2. The timeline for case 1 is:

$t = 0.0$	Propulsion system thrust command = 1,000,000 lbf
$t = 2.0$	Engine #1 downthrust factor steps to 110% of its nominal value
$t = 1.0$	Propulsion system thrust command = 1,400,000 lbf
$t = 3.0$	Propulsion system thrust command = 1,100,000 lbf
$t = 4.5$	Propulsion system thrust command = 1,400,000 lbf
$t = 4.6$	Engine #1 downthrust factor steps to 120% of its nominal value
$t = 6.0$	Engine #2 downthrust factor begins to ramp upward
$t = 8.0$	Propulsion system thrust command begins to ramp downward

In case 2, the degradation in engine #1 is assumed to be caused by a nozzle tube rupture at $t = 2.0$ resulting in fuel leakage and the further nozzle tube rupturing at $t = 4.6$ causing greater fuel leakage. The degradation in engine #2 is assumed to be a gradual loss of specific impulse degrading the engine performance.

The simulation results are shown in Figure 6-11. The propulsion system thrust follows the commanded value throughout the test. All three engines have identical thrusts until $t = 2.0$ when a nozzle tube ruptures on engine #1 causing a sudden increase in the engine #1 downthrust factor. The ICS propulsion level controller responds by downthrusting engine #1 and upthrusting engine #2 and #3 until the downthrust factors for each engine are equal indicating that the degradation of engine #1 is equivalent to the engine degradation caused by the higher operating thrust of engines #2 and #3. When the propulsion system thrust is given a step downthrust command at $t = 3.0$, all three engines decrease their thrust in a proportion that keeps the individual engine downthrust factors the same. At $t = 4.5$, the propulsion system thrust is given a step upthrust command and all three engines respond. During the upthrust transient, more nozzle tubes rupture on engine #1 and engine #1 is downthrust. Meanwhile, engines #2 and #3 have reached their maximum operating thrust and the engine #1 thrust settles to a value that maintains the commanded propulsion system thrust. At $t = 6.0$, engine #2

begins to lose specific impulse causing the engine #2 downthrust factor to increase. Initially, the ICS propulsion level controller takes no action since the engine #2 thrust cannot be decreased within the constraints of the propulsion system thrust command unless the engine #1 thrust is increased (engine #3 is at its upper thrust limit) and engine #1 is indicating greater problems than engine #2 (i.e. a greater downthrust factor). When the engine #2 downthrust factor exceeds the engine #1 downthrust factor, the propulsion level controller acknowledges that engine #2 has degraded as much as engine #1 and begins to trade engine #1 thrust for engine #2 thrust in proportion to make the downthrust factors equal. At $t = 8.0$ when the propulsion system thrust is commanded to ramp downward, engine #2 (which continues to degrade) continues to be downthrust, though at a slightly higher rate since the downthrust is no longer forcing engine #1 to higher thrust levels. Engine #1 is held at a constant thrust level. Engine #2 continues to be downthrust until it reaches its lower thrust limit and then the propulsion level controller begins to downthrust engine #1 to maintain the commanded propulsion system thrust.

Summary

The ICS propulsion level controller commands the individual engine thrusts to values that minimize the maximum downthrust factor while maintaining the commanded propulsion system thrust and keeping each engine within its safe operating thrust range.

6.2.5 Simulation of an SSME Failure Case

The feasibility of the ICS propulsion level controller strategy was demonstrated by the demonstration cases described in Section 6.2.4. To further demonstrate the utility of the ICS propulsion level controller, an SSME failure is simulated. The failure summary is taken from the SAFD phase I report.

Test 902-249: During stable operation at 109% of rated power level the test shut down prematurely due to a HPFTP accelerometer redline and associated massive failure of the HPFT first stage turbine blade. The sequence of events leading to the blade failure follows:

1. Initial turbine damage at $t = 3.0$ seconds. The FPB injectors non-uniform flow condition experienced in at least two previous tests may have persisted (despite rework) and worsened.
2. Engine fuel inlet temperature increases and the high pressure fuel pump begins to cavitate at $t = 108$ seconds. The temperature increase was brought about by a propellant transfer. The increased temperature lowers the fuel density causing an increase in the HPFP volumetric flowrate, speed, and power necessary to hold thrust constant. As the flow and speed increase, the HPFP approaches the conditions at which the suction capability of the hardware is exceeded and cavitation starts. Once cavitation is initiated, the efficiency of the pump degrades, causing the HPFTP speed to increase to maintain the fuel pump output to hold thrust constant, causing worsening cavitation conditions and causing an increase in the HPFT temperature.
3. A Kel-F rub ring flexes and melts at $t = 374$ seconds. The released Kel-F particles plug nozzle tubes causing them to rupture, contributing to the HPFT temperature increase.
4. The first stage turbine blade fails at $t = 450.52$ seconds.

Post firing inspection of the facility and engine revealed severe damage to the main combustion chamber including the injector and sidewalls, extensive burnthrough damage to the nozzle,

substantial damage to the HPFTP first and second stage turbines, and an approximately 12 inch long section of the HPFP inlet volute missing.

For the simulation, a typical STS flight thrust profile is used as the propulsion system thrust command. The failure is assumed to happen at the same time as the failure that occurred during test 902-249. The downthrust factor is assumed to follow a linear estimation of the HPFT temperature recorded during the test and shown in Figure 6-12.

The results of the simulation are shown in Figure 6-13. The individual thrust profiles using the ICS propulsion level controller are identical to the thrust profiles that would be expected with the current SSME controller until the HPFT temperature starts to rise. The current SSME controller would have held the engine at a constant thrust until the propulsion system thrust command was changed at about 460 seconds. The ICS propulsion level controller begins to reduce the degraded engine thrust at about 325 seconds and continues to reduce it until the other two engines reach the upper thrust limit of 512 klbf. At the time of failure, 450 seconds into the flight, the ICS propulsion level controller has reduced the degraded engine thrust to slightly under 94% of the rated power level whereas the current SSME controller would have maintained the engine at its nominal 104% thrust level. At 460 seconds, when the propulsion system thrust command is ramped down, the ICS propulsion level controller implements the entire downthrust using the degraded engine resulting in a rapid decrease in thrust level until the degraded engine reaches its lower thrust limit at 65% of RPL. Downthrusting the engine is clearly the correct response to the anomaly since downthrusting the engine reduces the output demanded of the HPFP. The HPFP speed decreases and reduces cavitation in the pump. Whether or not the downthrust is sufficient to have averted the failure is impossible to say. However, if the engine had still failed it would have failed at a reduced power level.

6.3 ICS Simulation Conclusions

The ICS simulations demonstrate that individual engine parameters can be controlled to reduce engine operating stresses within the constraints imposed by mission requirements (thrust and mixture ratio). Furthermore, the simulations demonstrate the capability to control an engine cluster to extend the propulsion system life using a calculated engine health parameter.

Table 6-1 SSME Characterization Results

FPOV Position, FPOV	0.7812	0.7734	0.7890	0.7812	0.7812	0.7812	0.7812	0.7812
OPOV Position, OPOV	0.6388	0.6388	0.6388	0.6388	0.6324	0.6452	0.6388	0.6388
OPFV Position, OPFV	0.6388	0.6388	0.6388	0.6388	0.6388	0.6324	0.6452	0.6452
Fuel Flow Rate, \dot{M}_f (lbm/sec)	148.57	146.89	149.63	147.36	149.27	148.5597	148.5759	
Oxidizer Flow Rate, \dot{M}_o (lbm/sec)	893.5	897.1	890.4	873.4	905.5	892.8386	893.8422	
HPFT Temperature, THPFT (R)	1811.4	1806	1814	1798	1819	1808.0	1813.2	
HPOT Temperature, THPOT (R)	1372.8	1423	1339	1314	1410	1375.0	1371.2	
Normalized Turbine Temperature Difference, $T_N = (THPFT/1905 - THPOT/1760)$	0.1709	0.1395	0.1914	0.1972	0.1537	0.1678	0.1728	

		dMf	dMo	dT
		Change in Fuel Flowrate	Change in Oxidizer Flowrate	Change in Temperature Error
<u>1</u> dP_FPOV	<u>1</u> Change in FPOV Position	<u>2.74</u> 0.0156	<u>-6.68</u> 0.0156	<u>0.0519</u> 0.0156
<u>1</u> dP_OPOV	<u>1</u> Change in OPOV Position	<u>1.91</u> 0.0128	<u>32.1</u> 0.0128	<u>-0.0435</u> 0.0128
<u>1</u> dP_OPFV	<u>1</u> Change in OPFV Position	<u>0.0162</u> 0.0128	<u>1.0036</u> 0.0128	<u>0.005</u> 0.0128

Table 6-2 Relationship Between Control Valves and Controlled Parameters

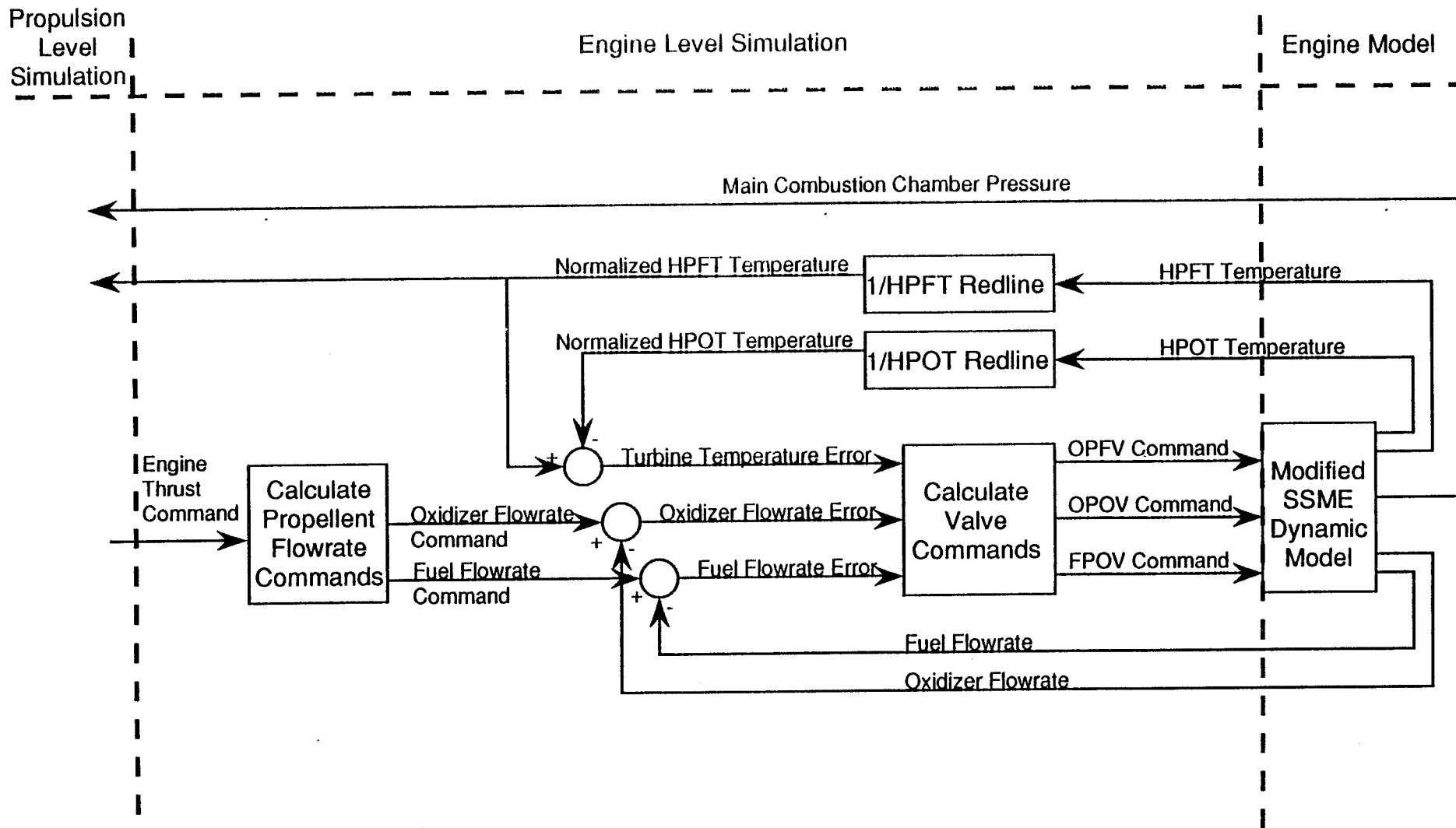


Figure 6-1 Overview of ICS Engine Level Simulation

11-DEC-90

Continuous Super-Block	Ext.Inputs	Ext.Outputs
ICS_4	5	10

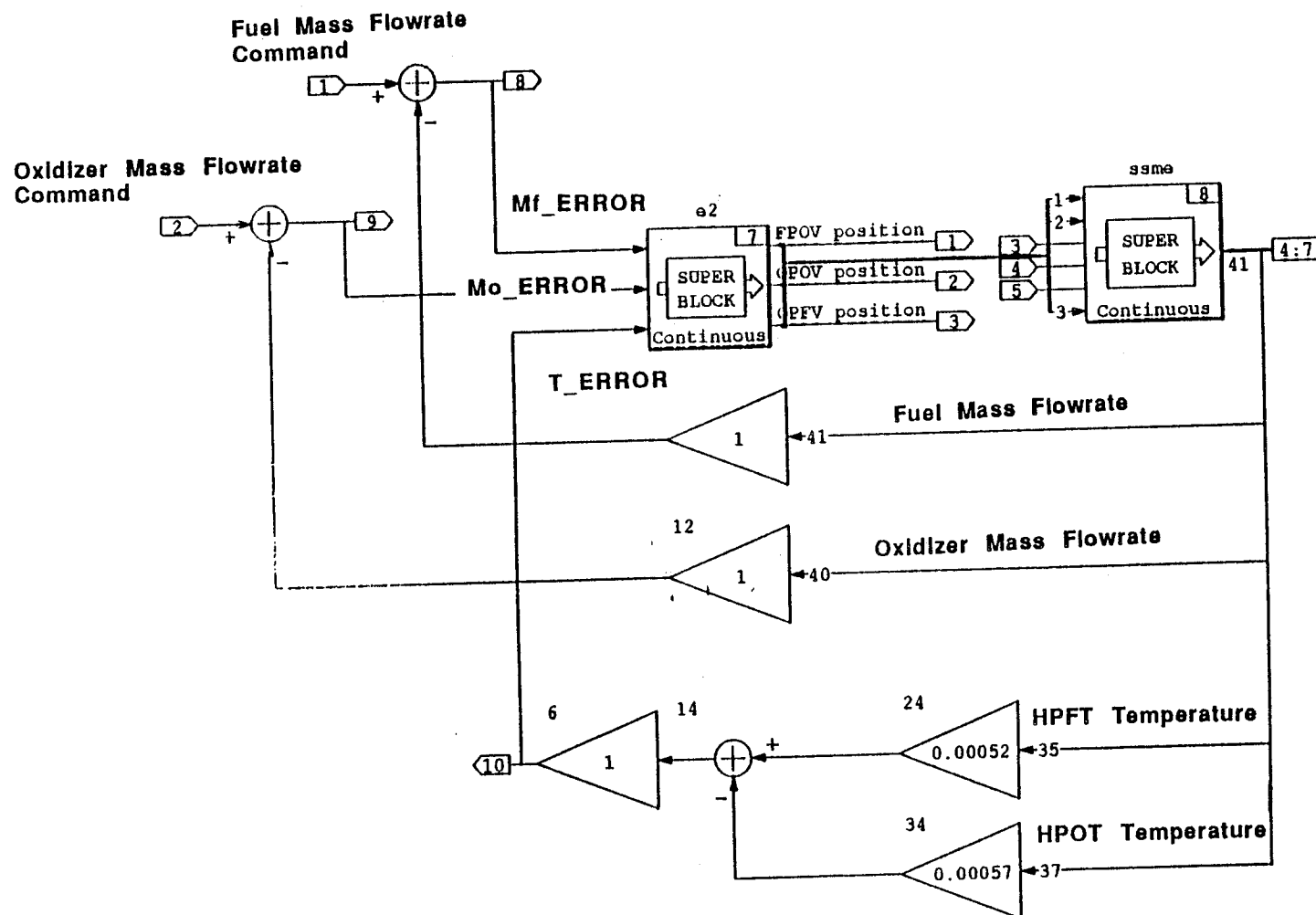


Figure 6-2a Proof Of Concept Controller - Top Level

RI/RD91-158

Continuous Super-Block
Ext. Inputs 3
Ext. Outputs 3

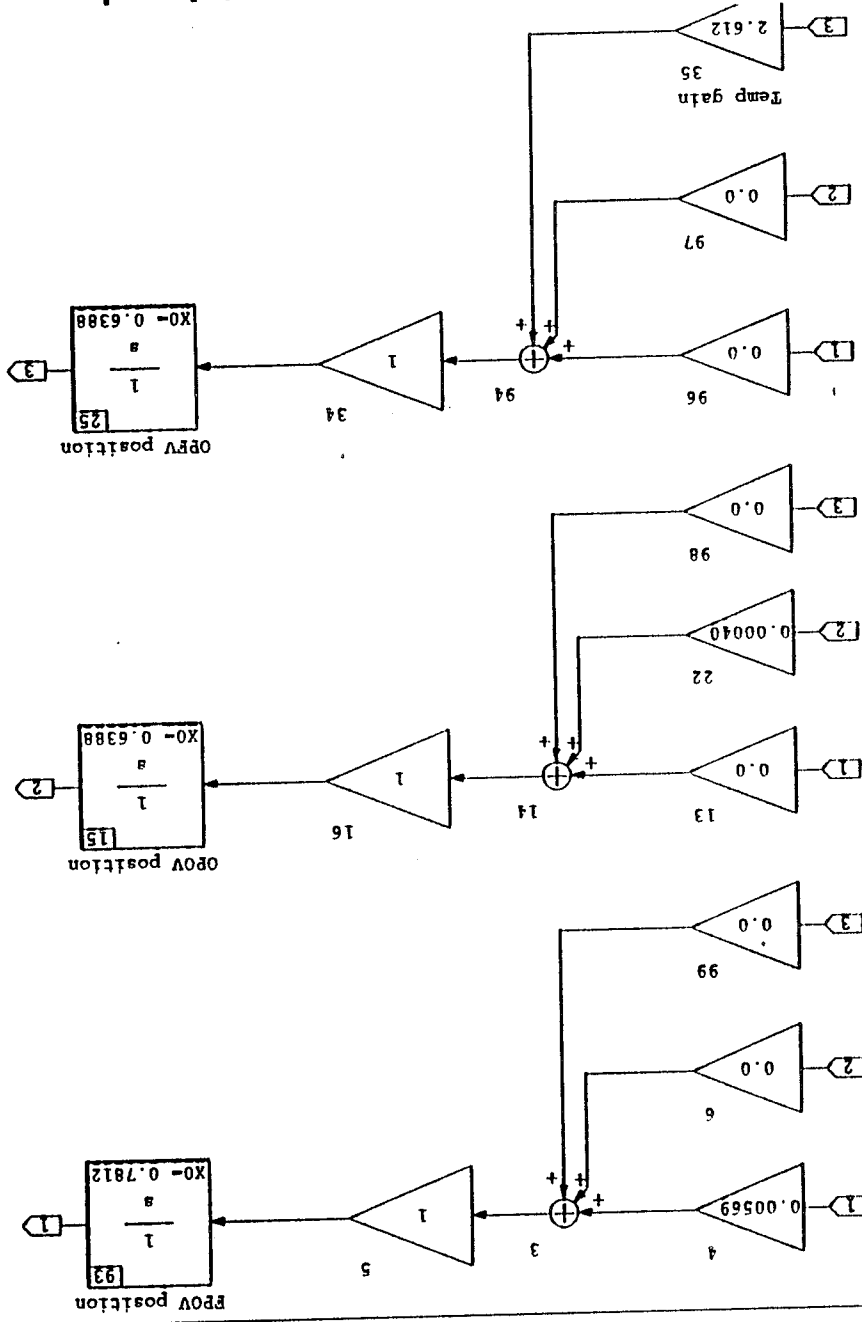


Figure 5-25 Proof Of Concept Controller - e2 Level

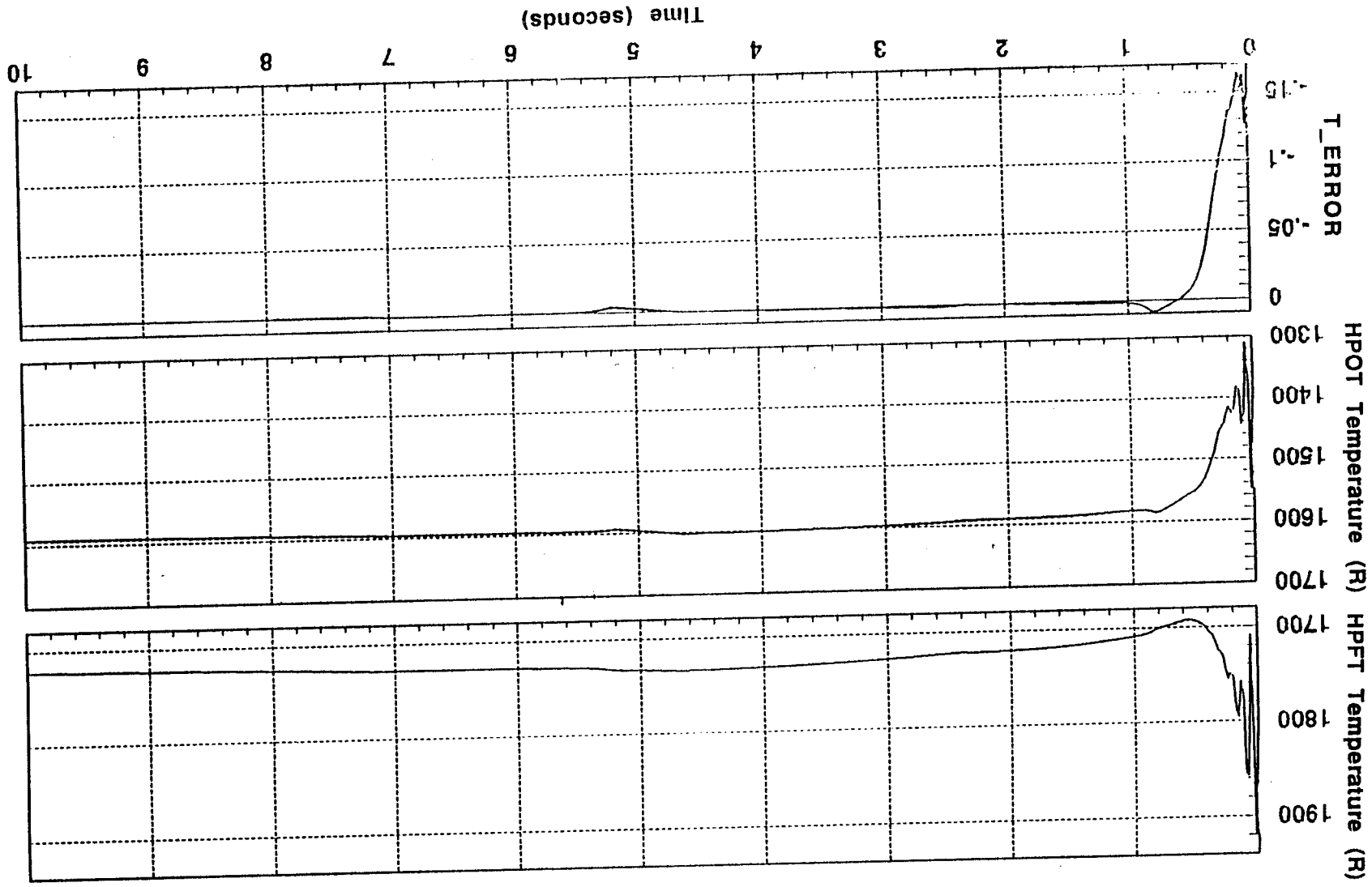


Figure 6-2c High Pressure Turbine Temperatures

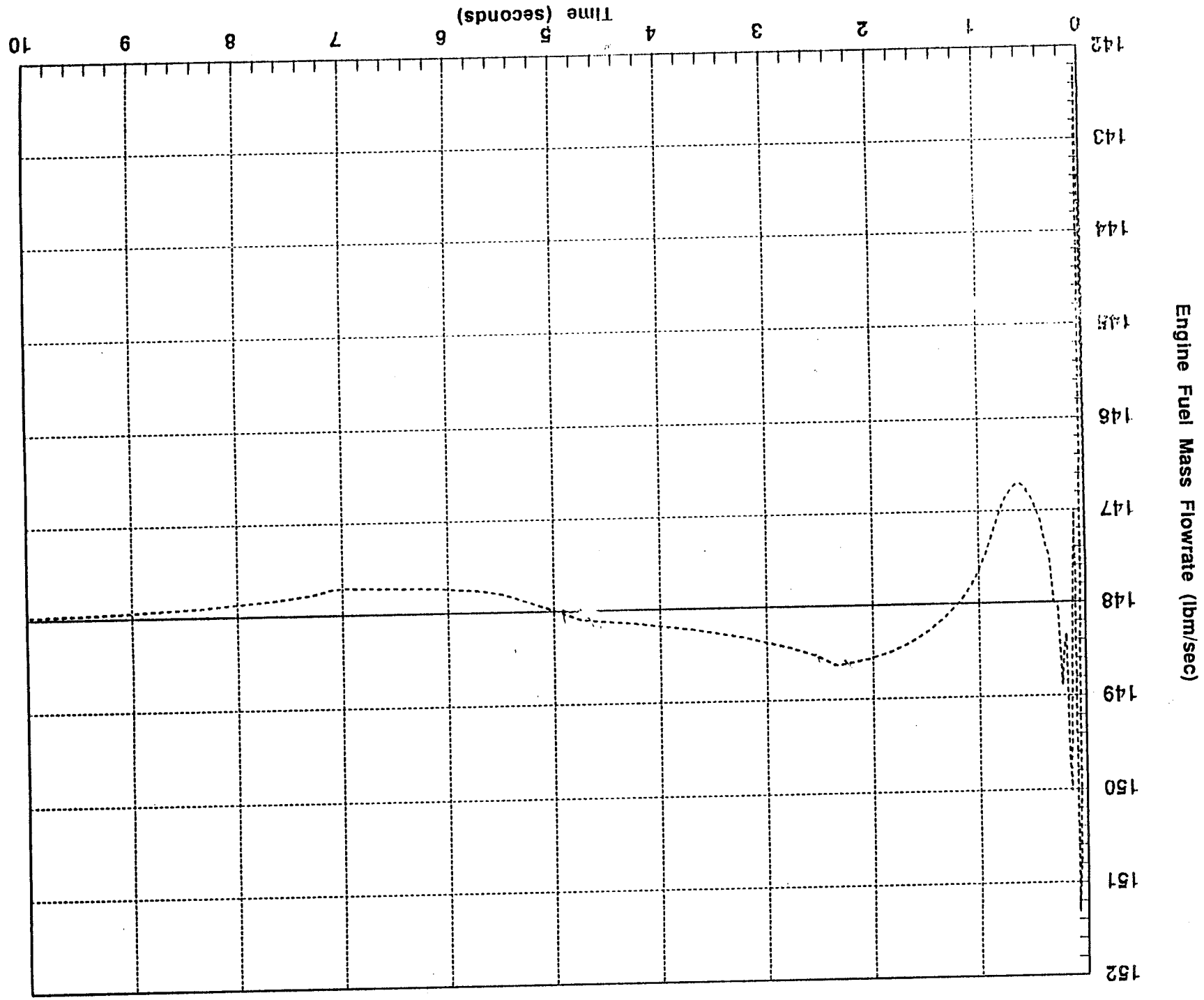


Figure 6-2d Engine Fuel Mass Flowrate

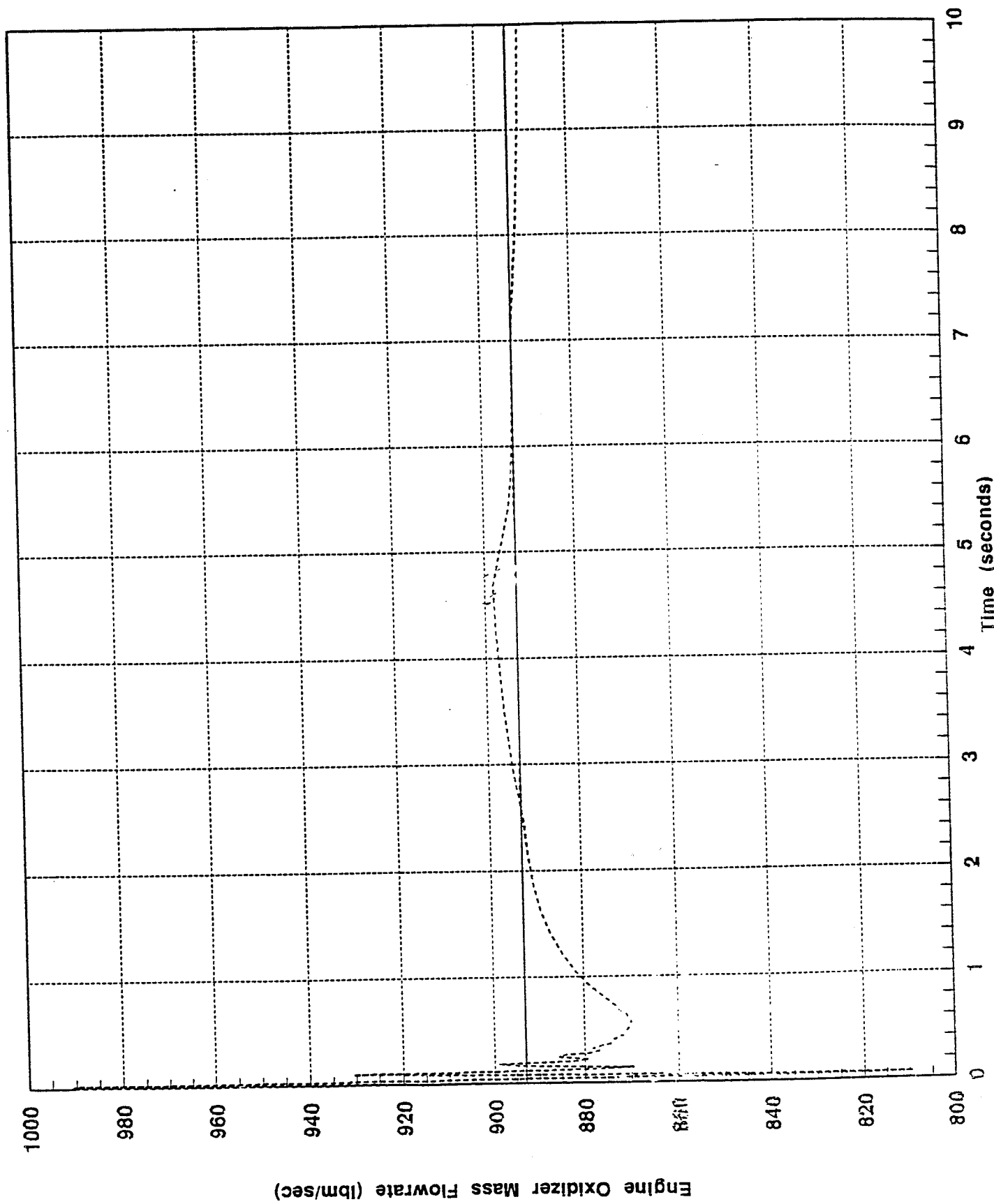


Figure 6.2a Engine Oxidizer Mass Flowrate

Continuous Super-Block
Ext.Inputs Ext.Outputs
e5 3 3

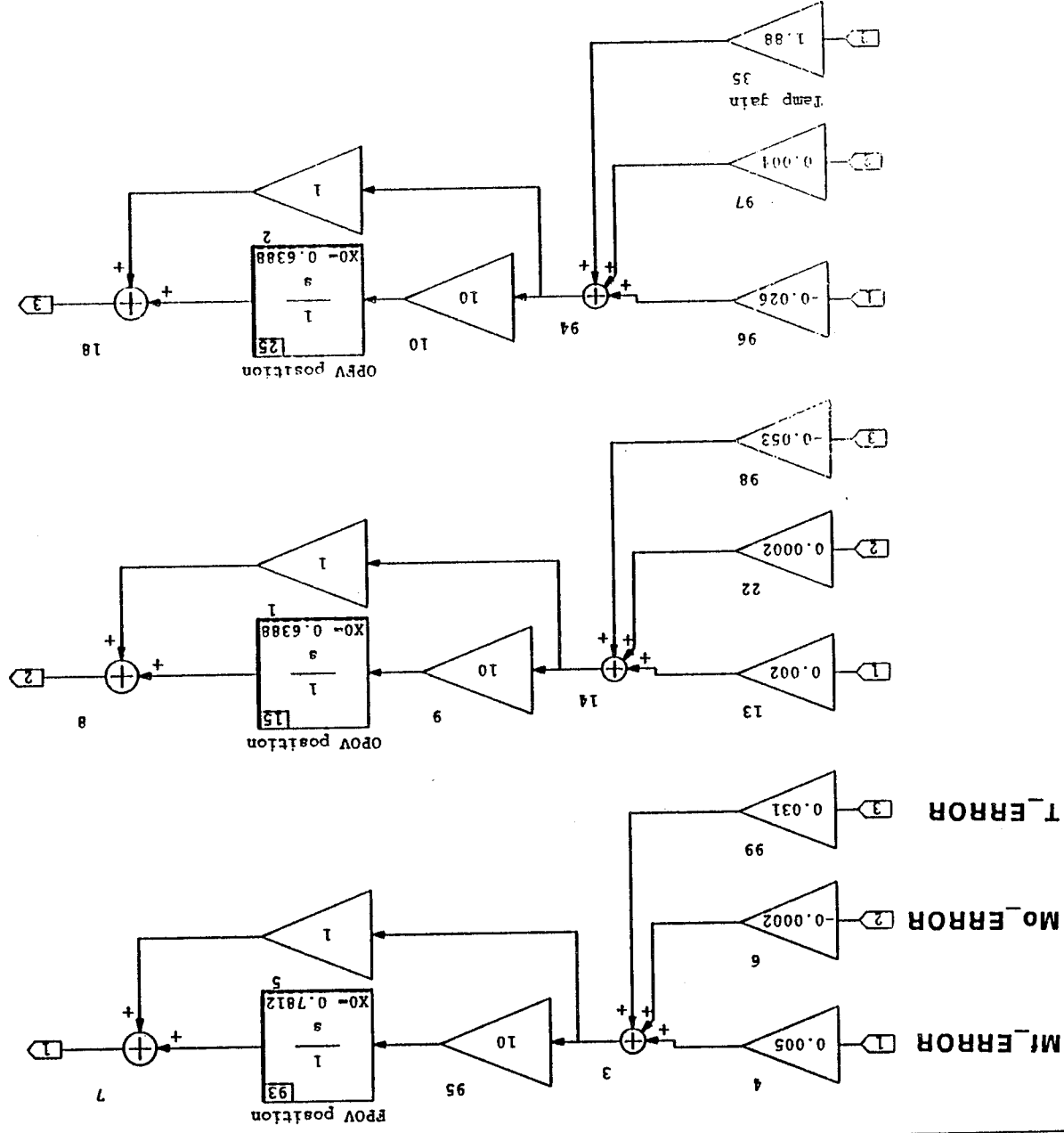


Figure 6-3a Multiple Input/Multiple Output Controller - Valve Controller Level (e2)

09:49:37

28-FEB-91

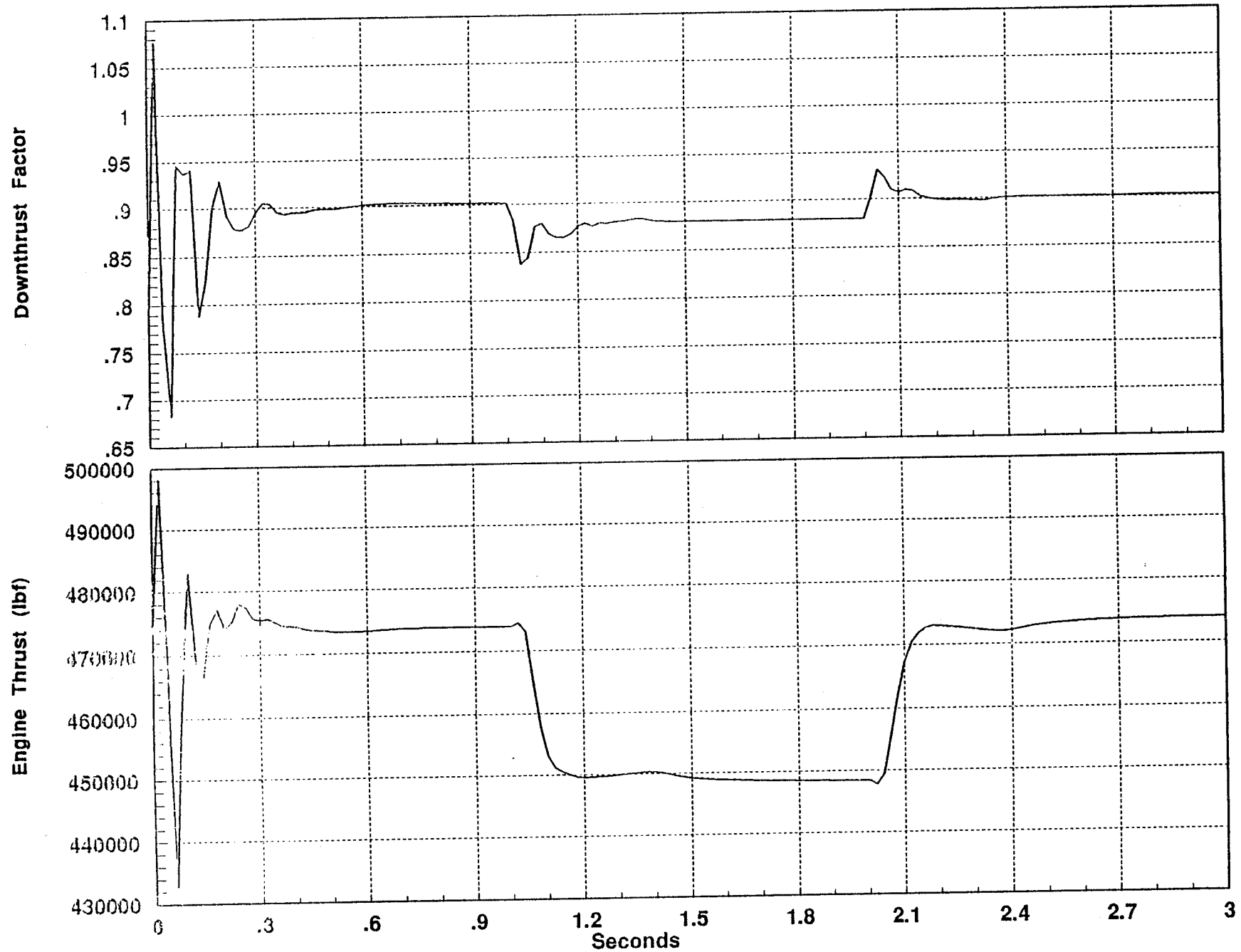


Figure 6-3b Engine Thrust and Downthrust Factor Responses to Step Inputs

09:49:29 28-FEB-91

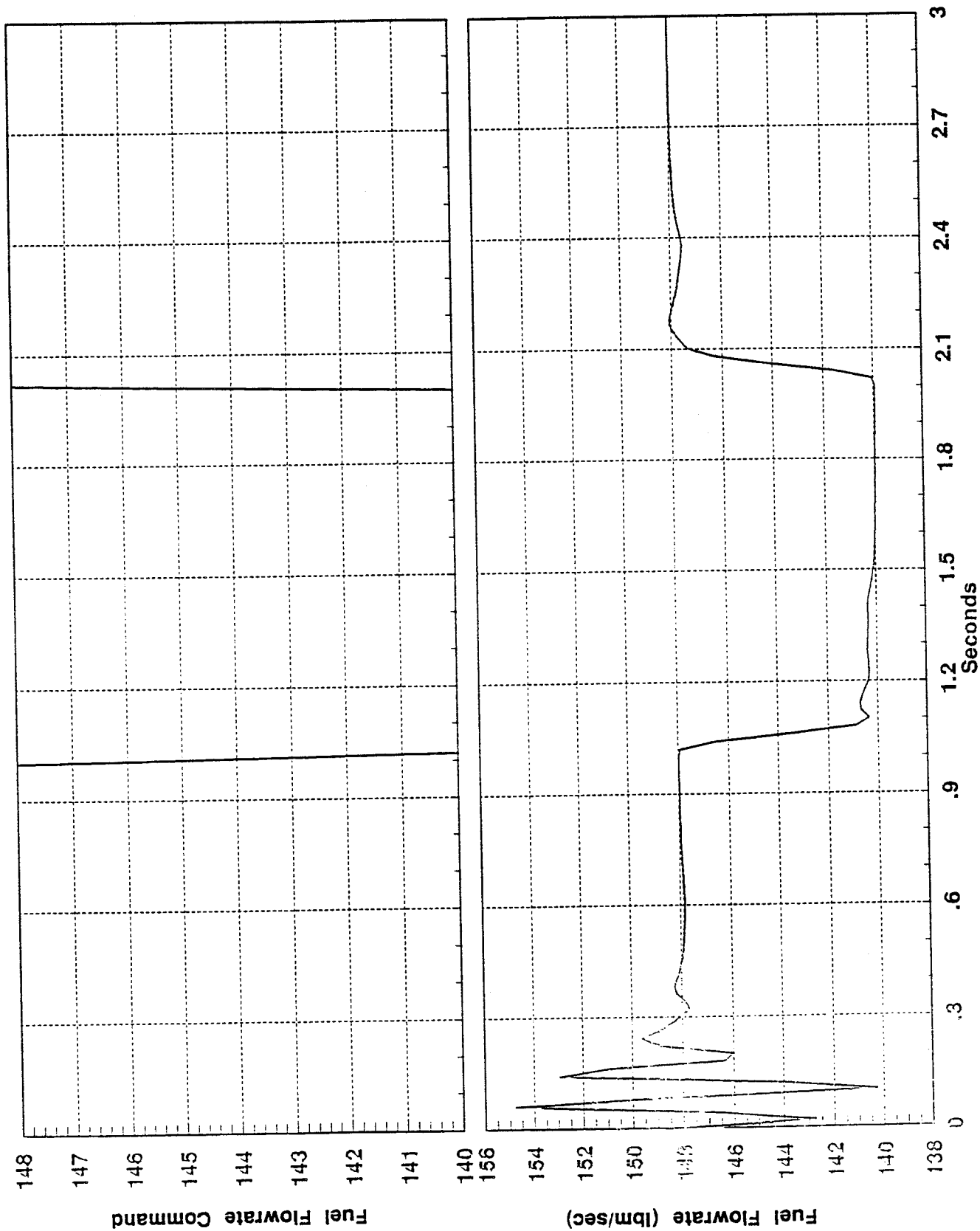


Figure 6-3c Engine Fuel Flowrate Response to Step Inputs

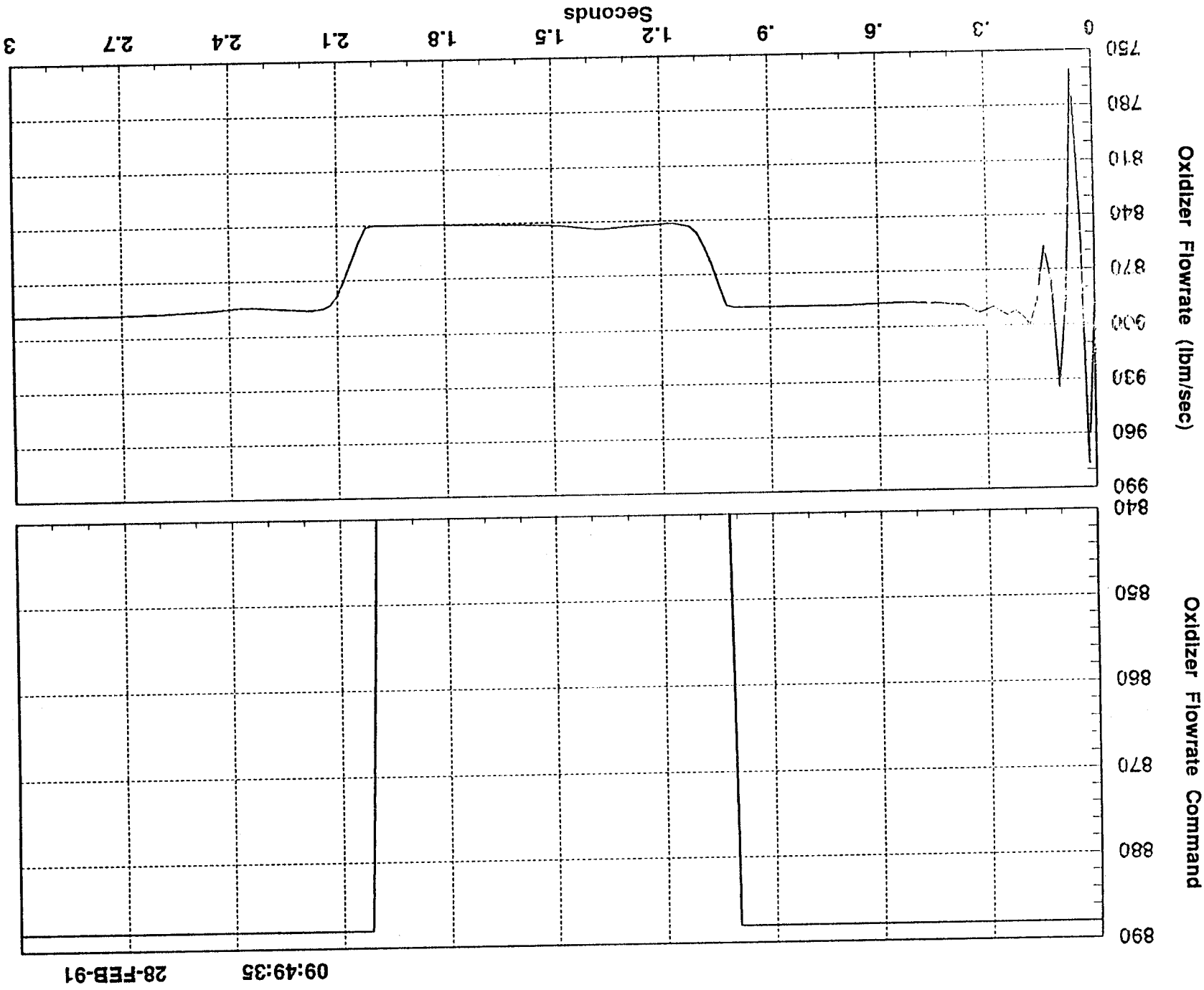


Figure 6-3d Engine Oxidizer Flowrate Response to Step Inputs

09:49:35 28-FEB-91

09:49:31 28-FEB-91

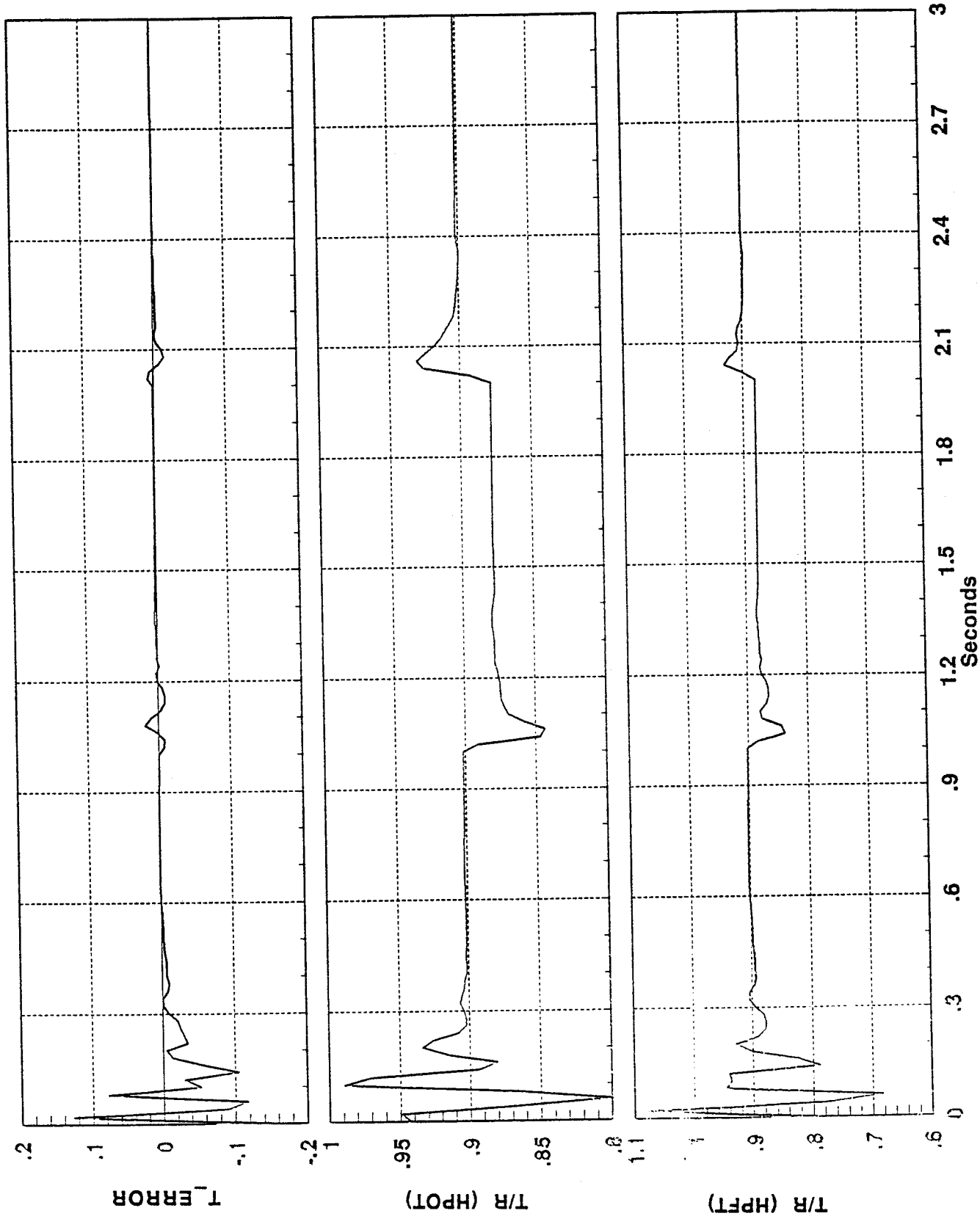
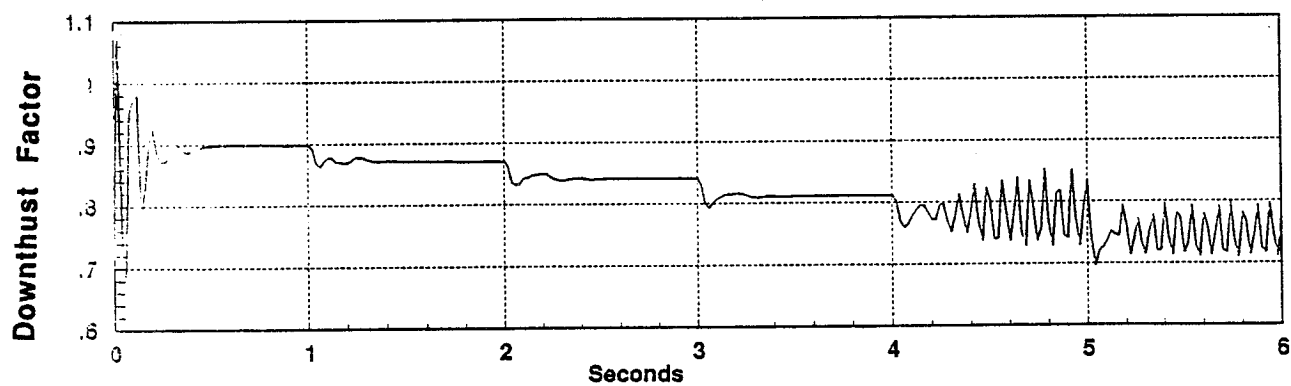
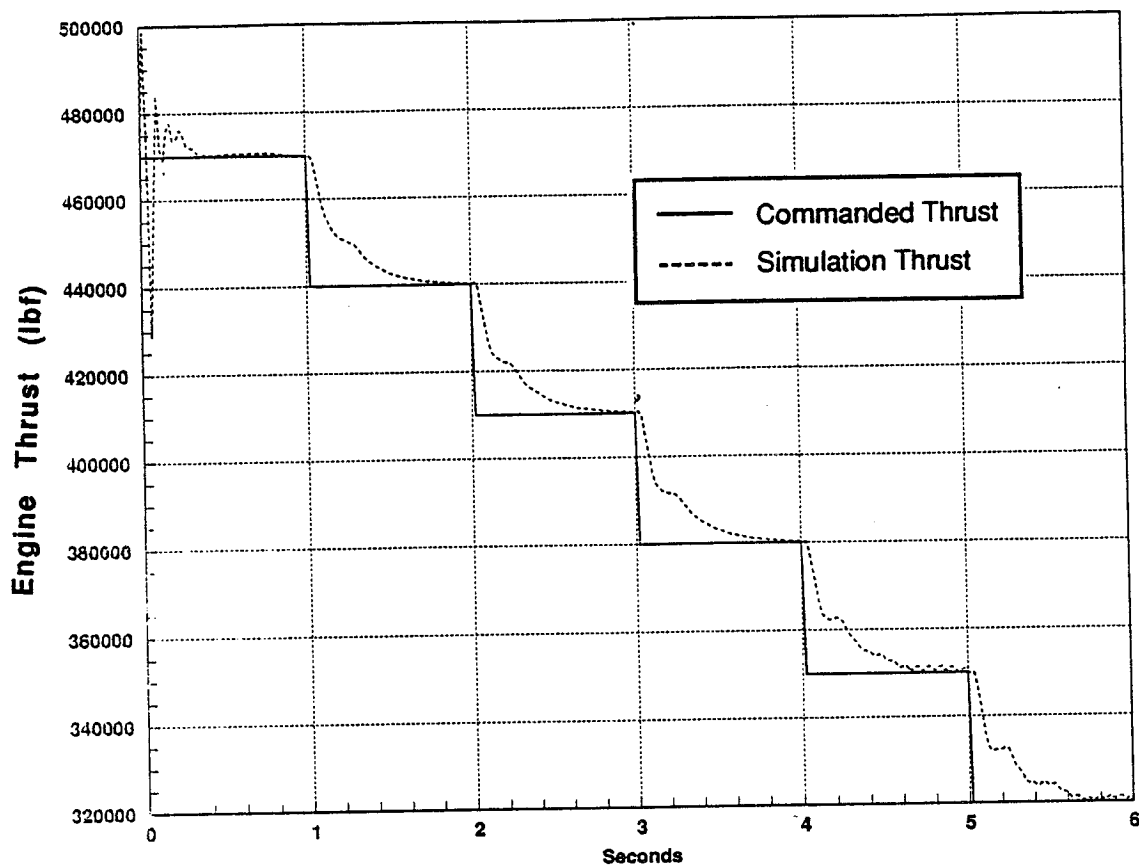


Figure 6-3e HPFT and HPOT Temperature/Redline Ratio response to Step Inputs



**Figure 6-4 Downthrust Factor Characterization
- Detailed Engine Model Results**

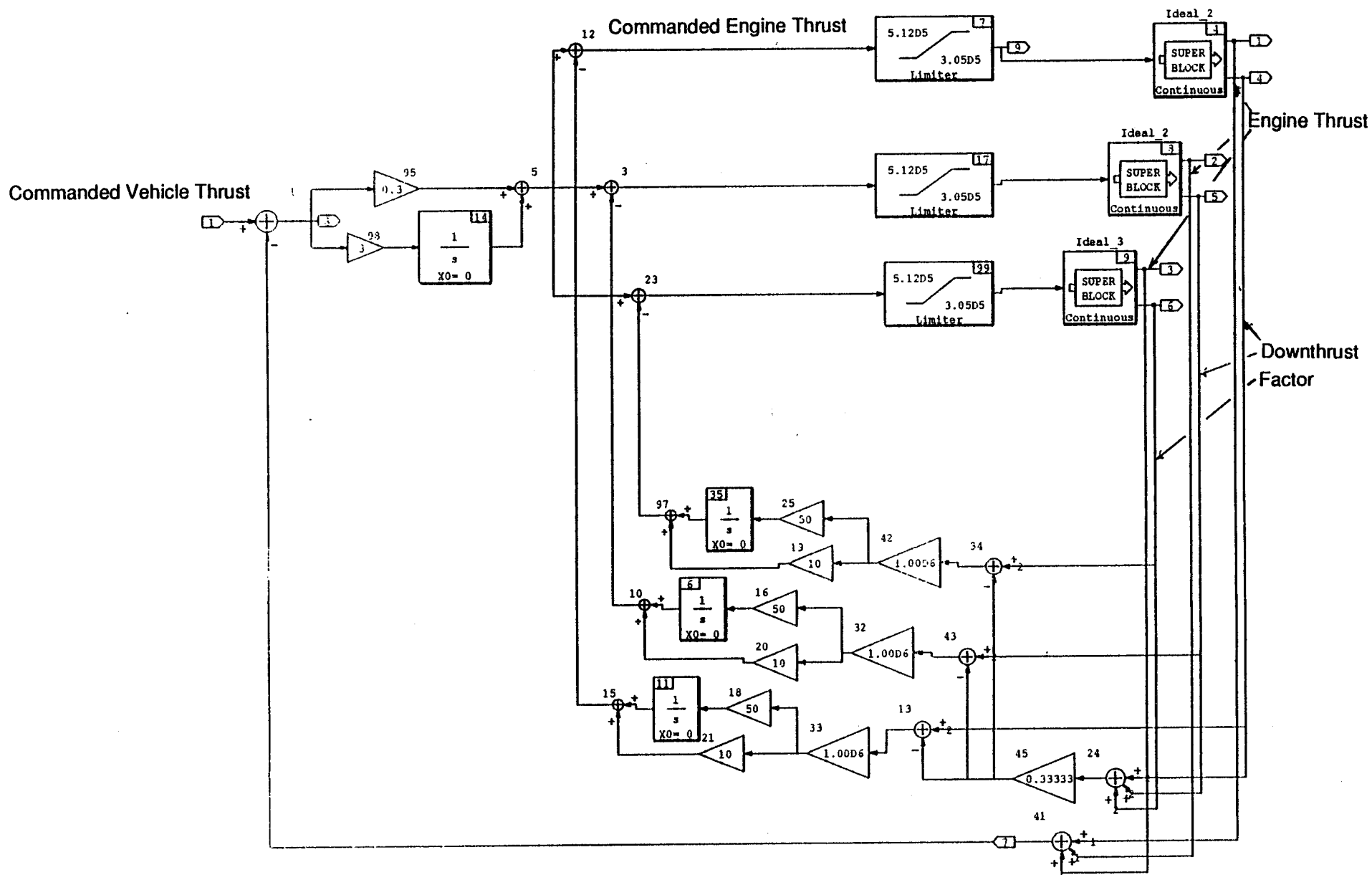


Figure 6-5 ICS Propulsion Level Simulation - MatrixX Version

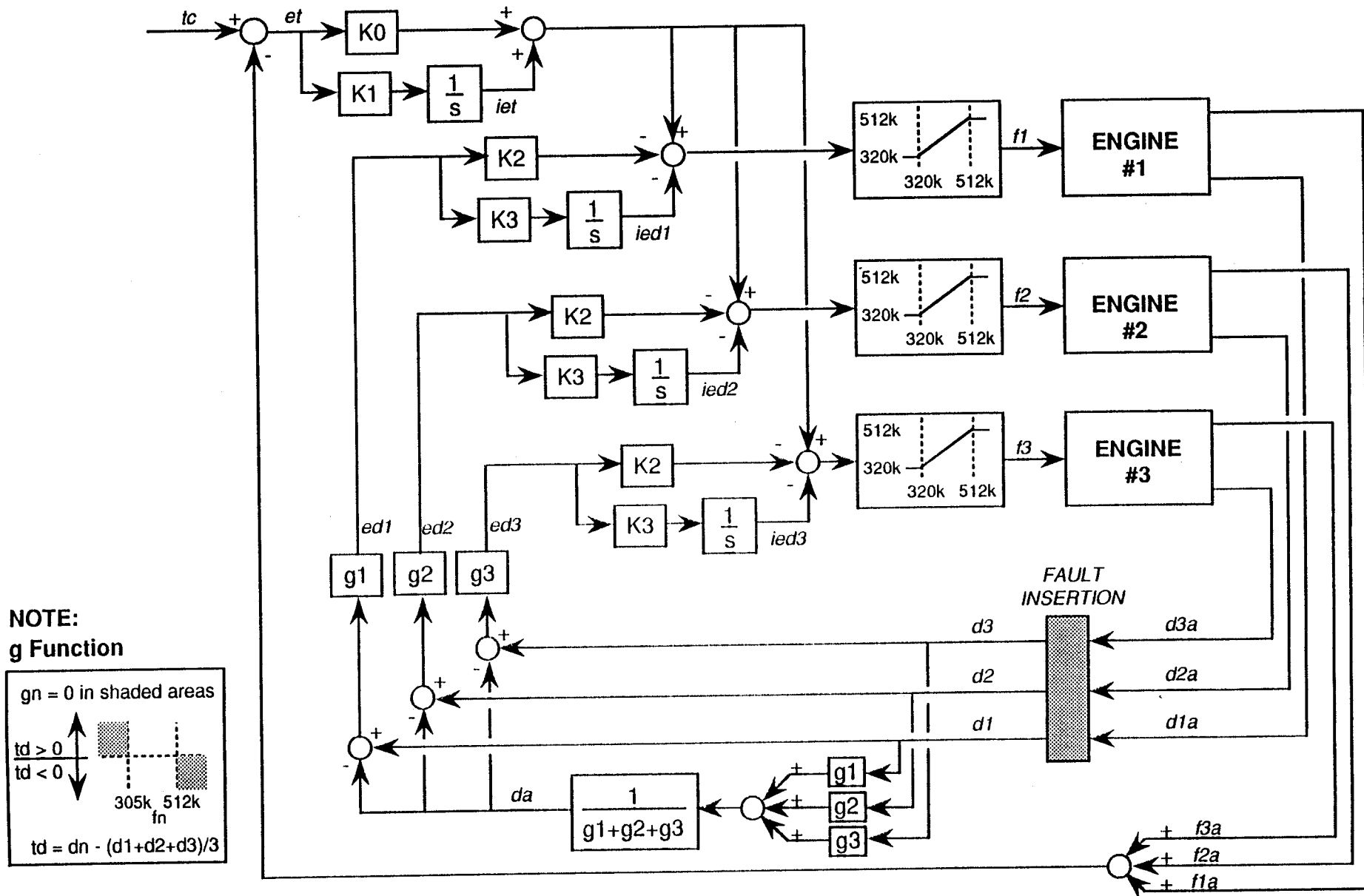
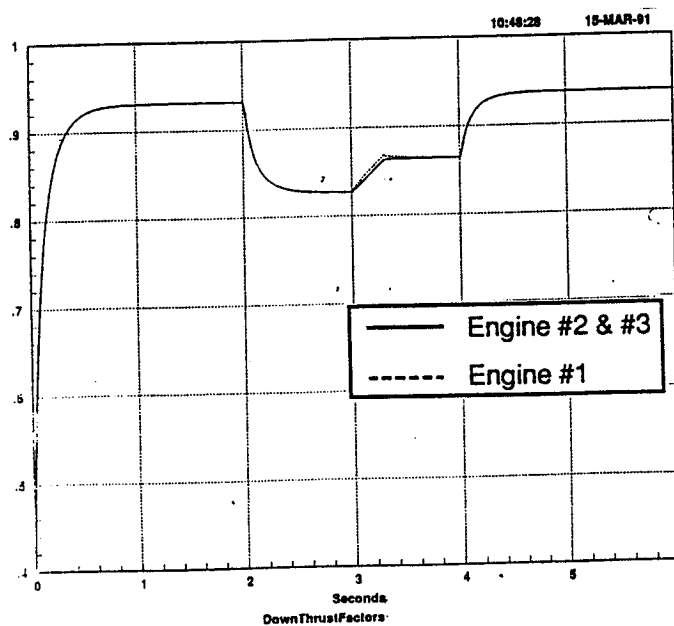
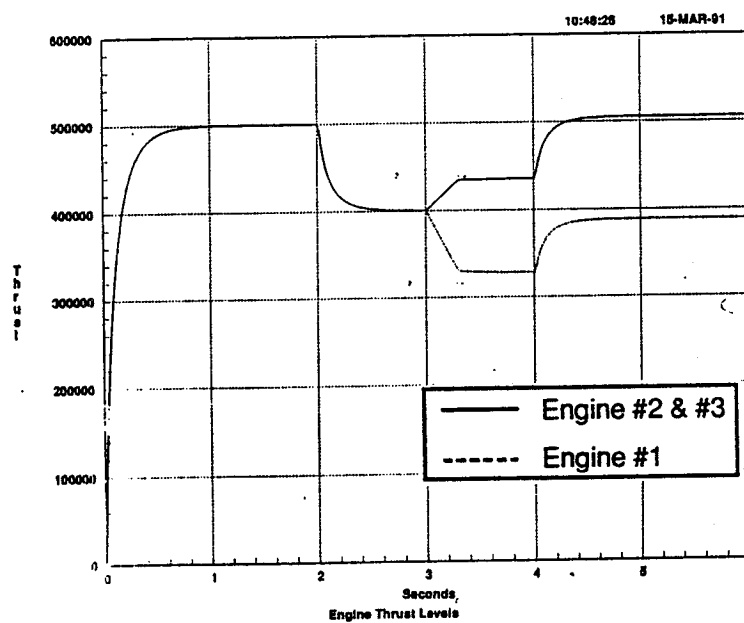
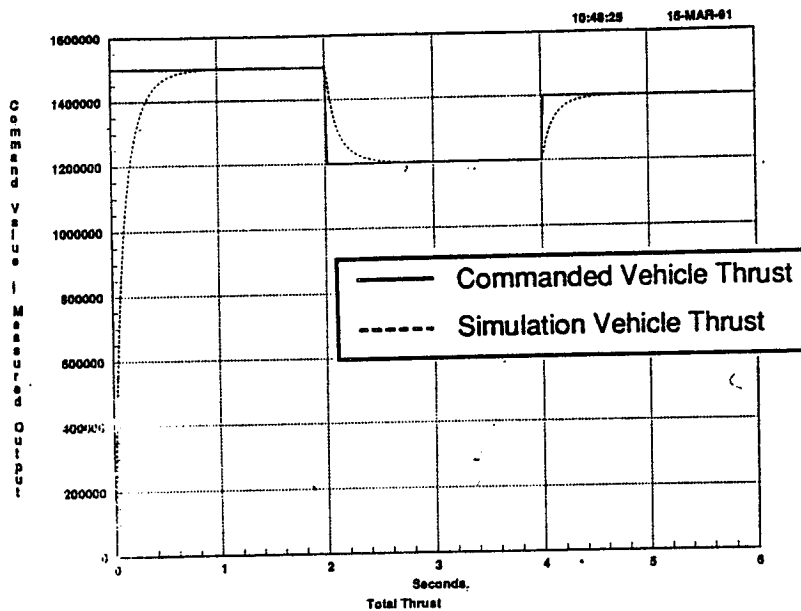
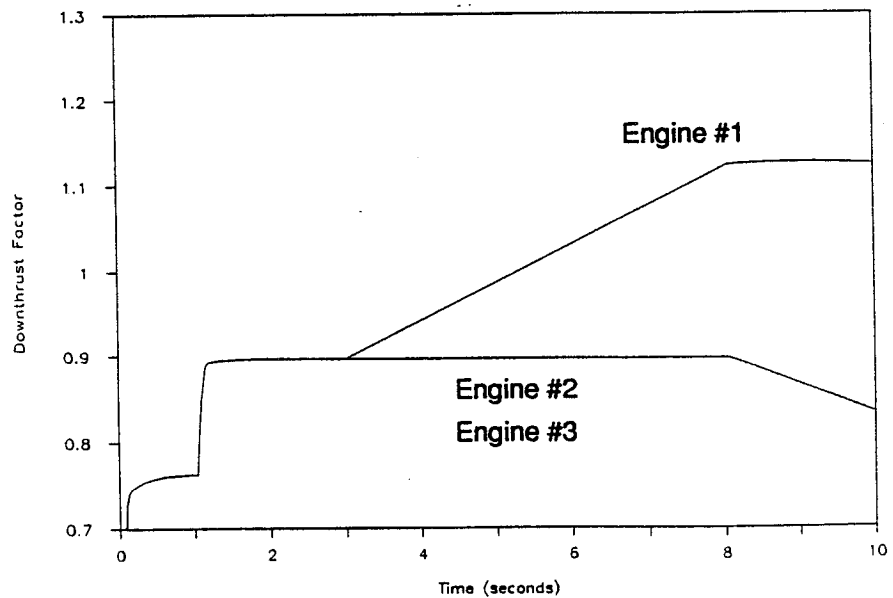
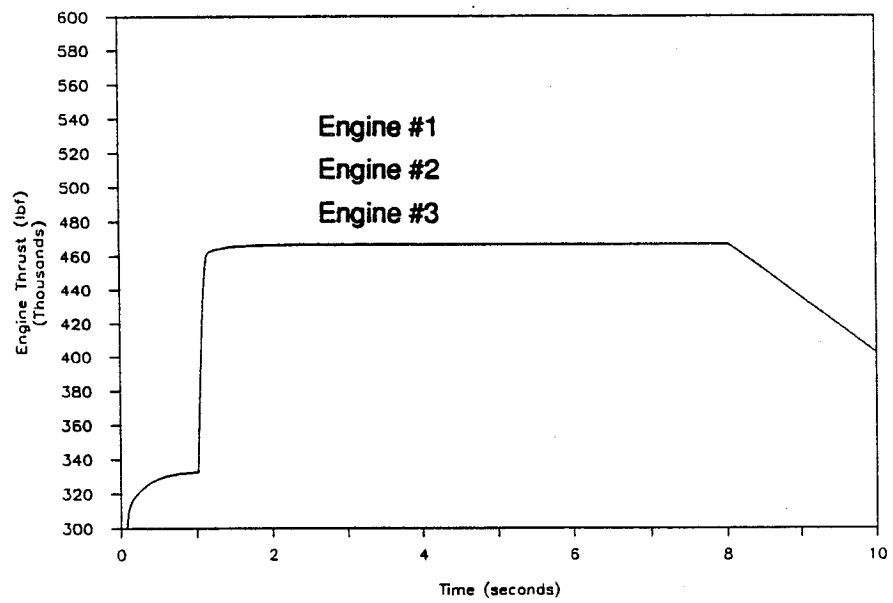
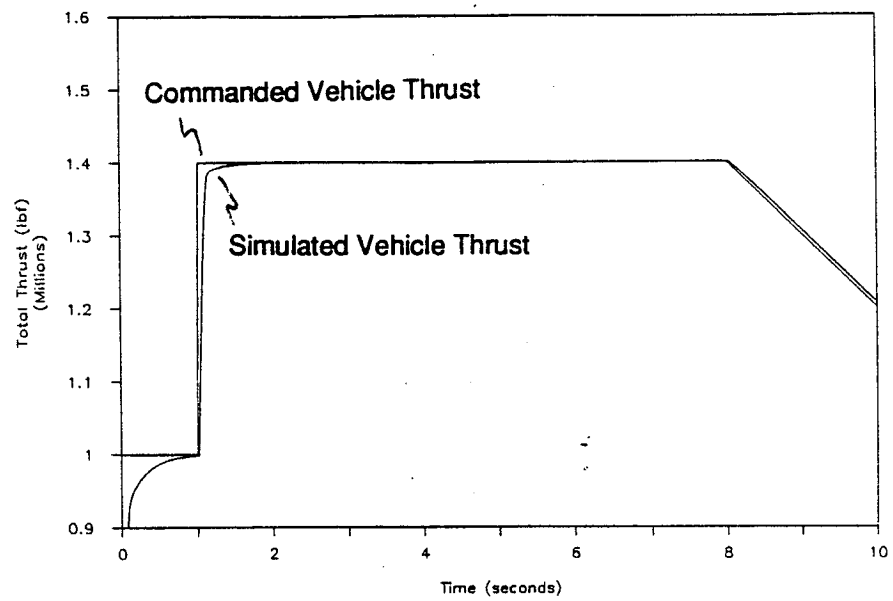


Figure 6-6 ICS Propulsion Level Simulation - PC Version



**Figure 6-7 ICS Propulsion Level Controller Simulation
MatrixX Model**



**Figure 6-8 ICS Propulsion Level Controller Simulation
Case 1, w/o Downthrust Factor Control**

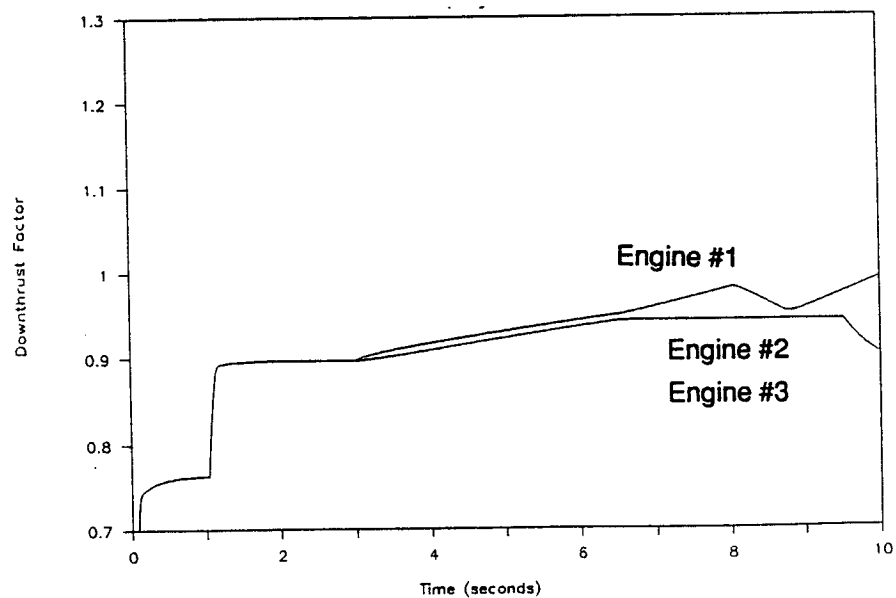
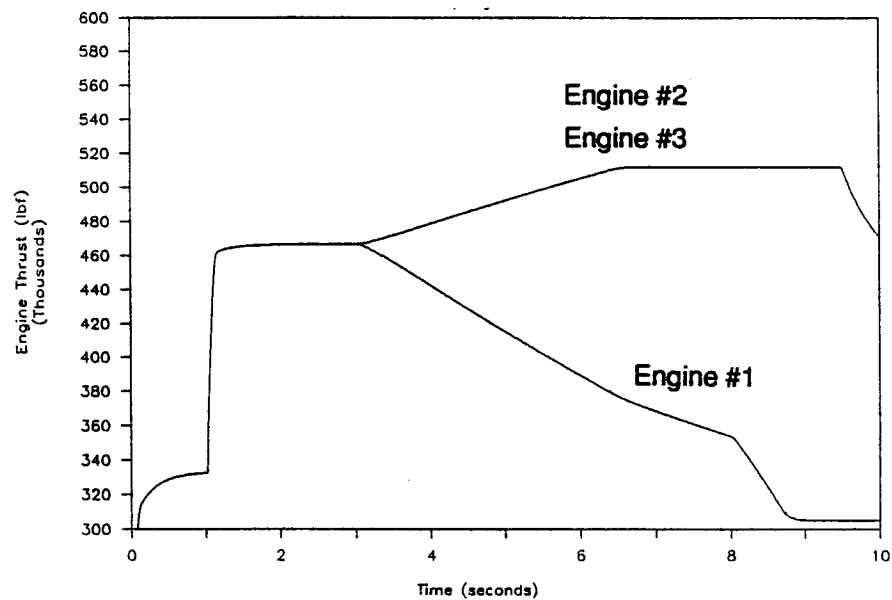
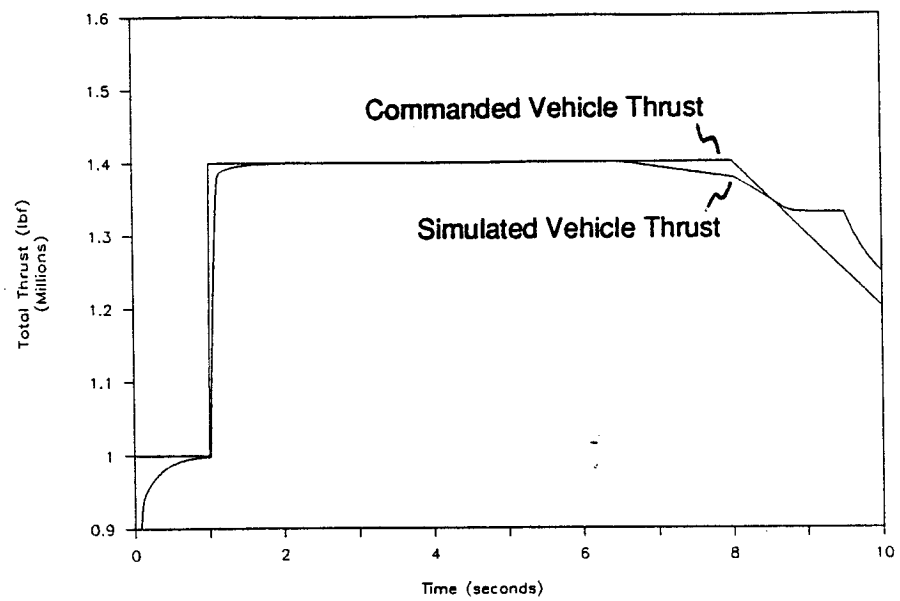


**Figure 6-9 ICS Propulsion Level Controller Simulation
Case 1, Downthrust Factor Control w/o gn Function**

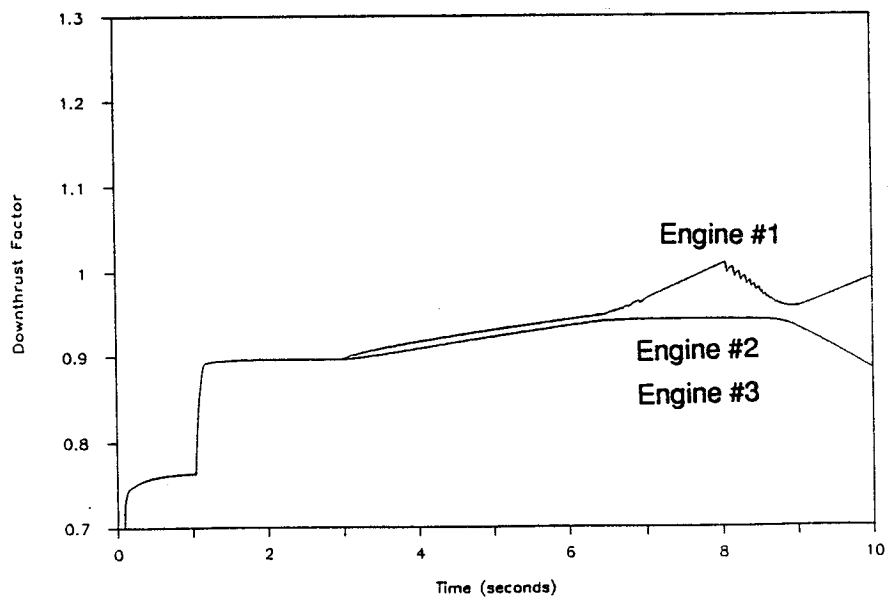
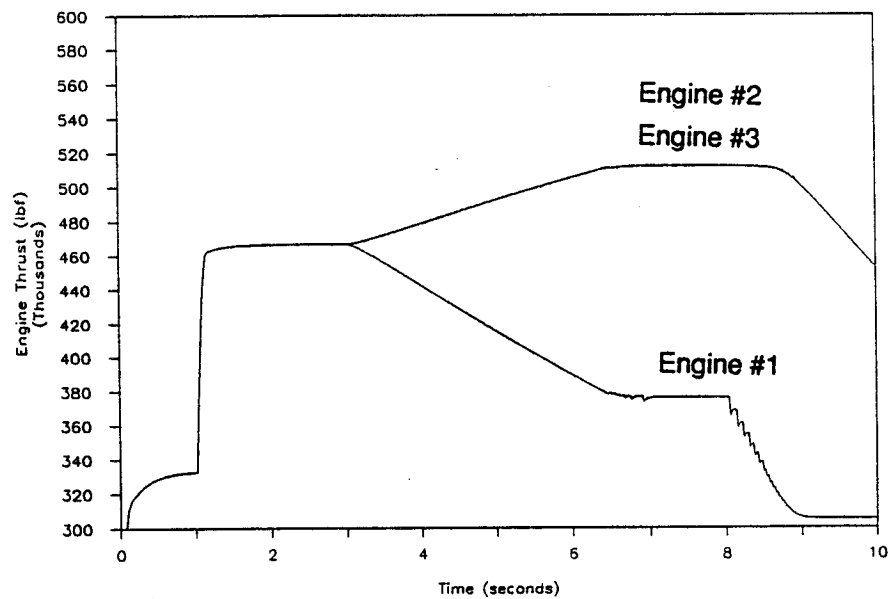
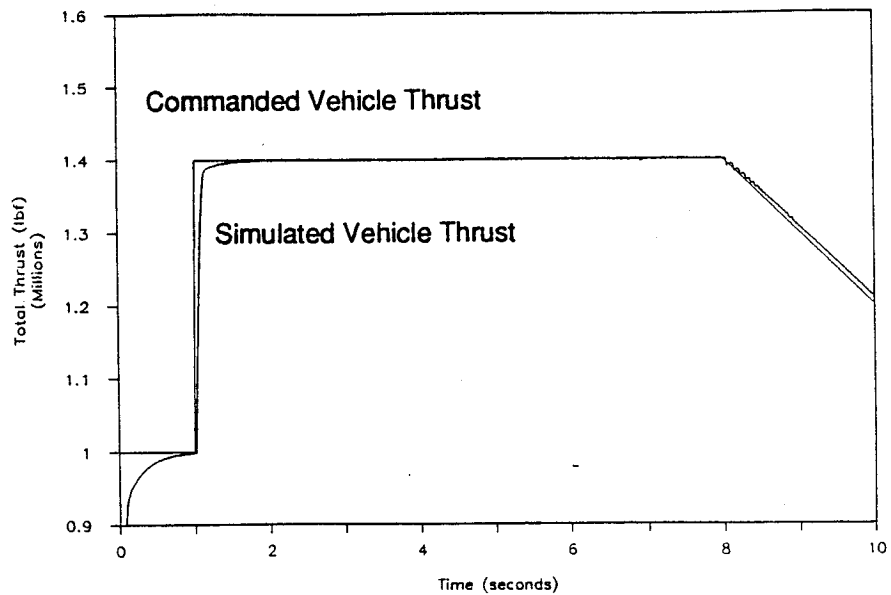
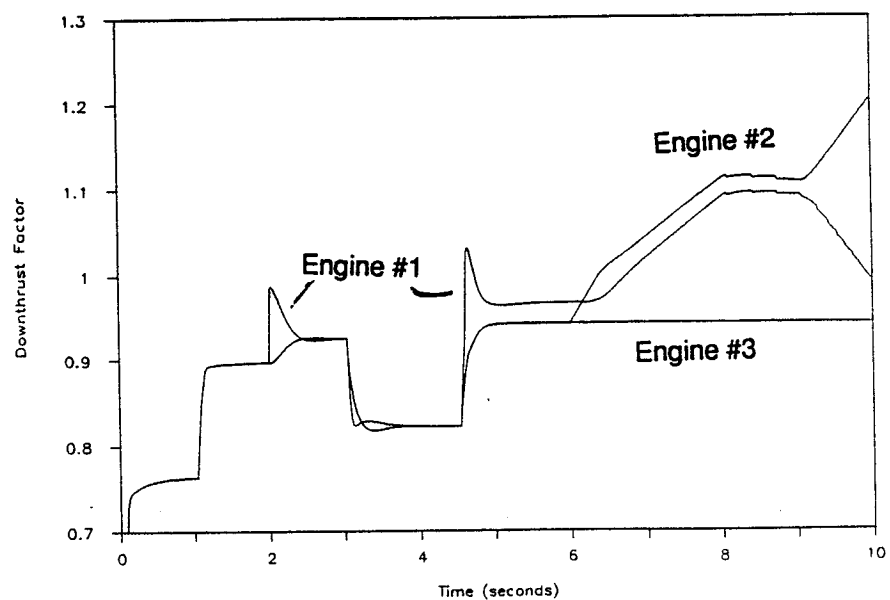
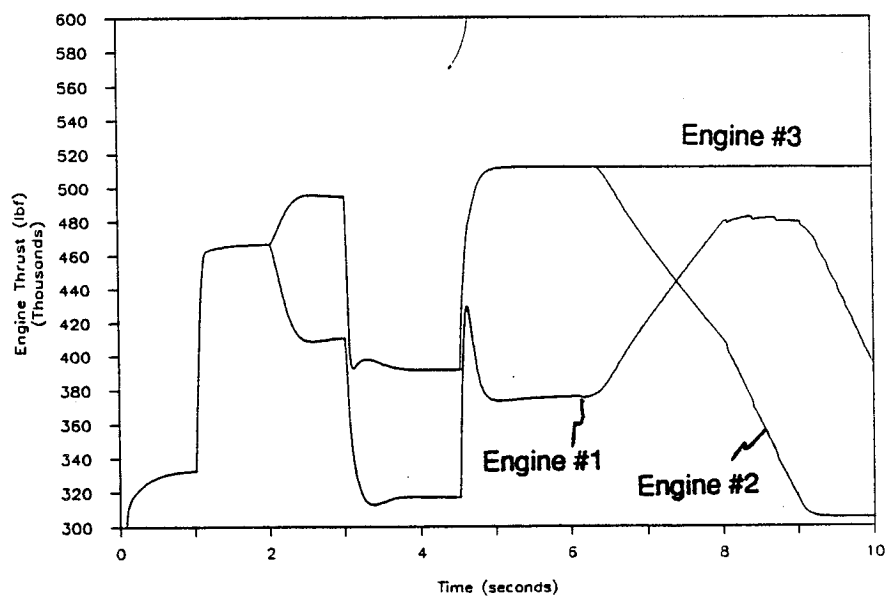
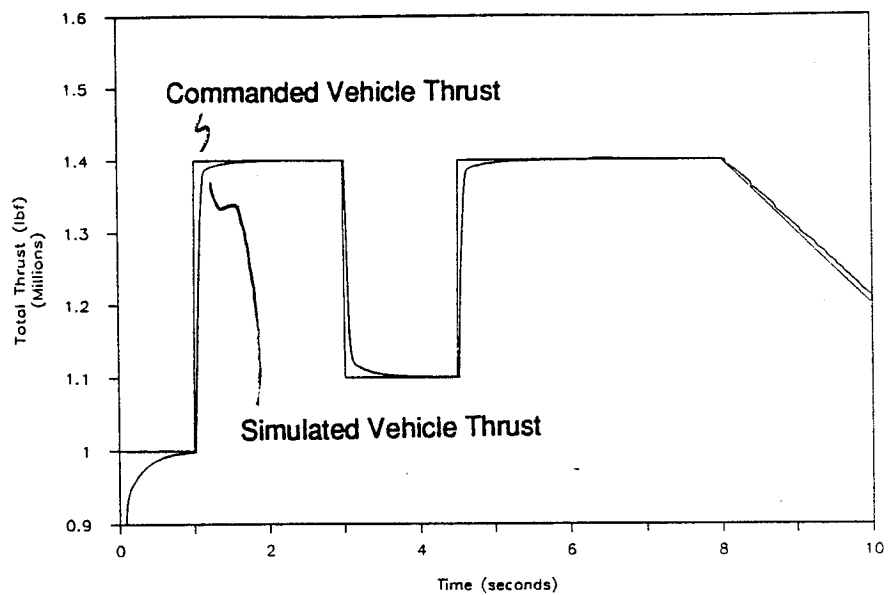


Figure 6-10 ICS Propulsion Level Simulation Case1



**Figure 6-11 ICS Propulsion Level Simulation
Case 2**

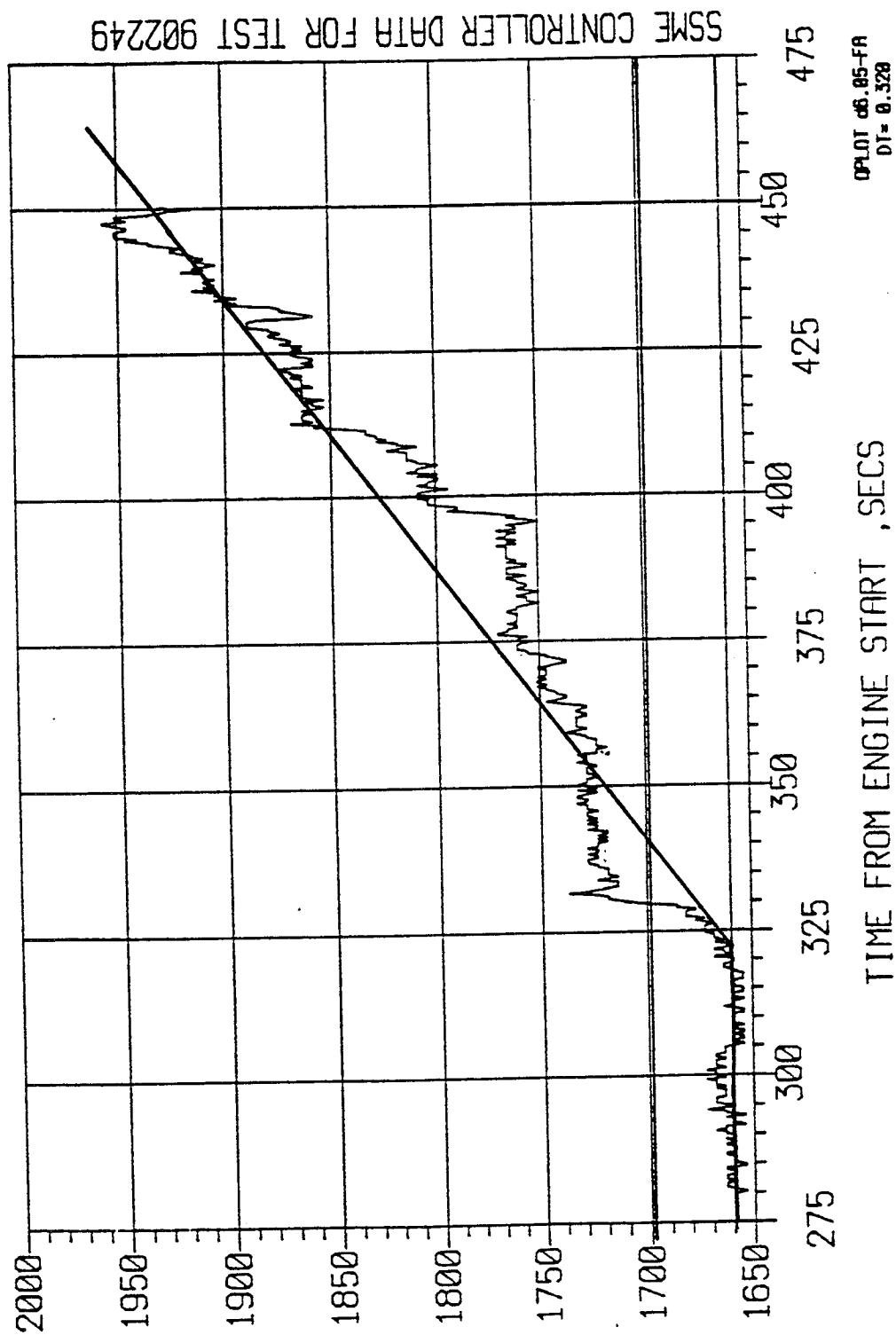


Figure 6-12 HPFT Temperature Recorded During SSME Test 902-249

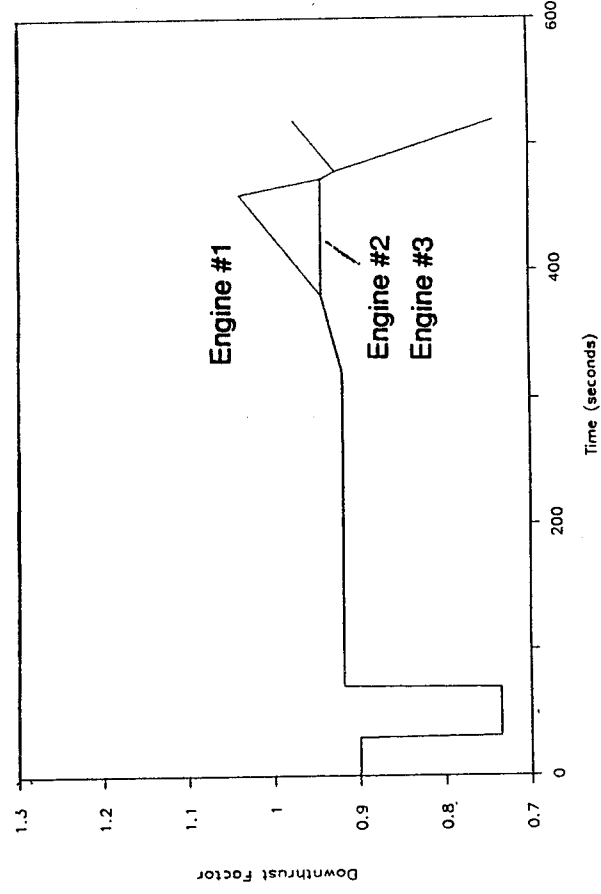
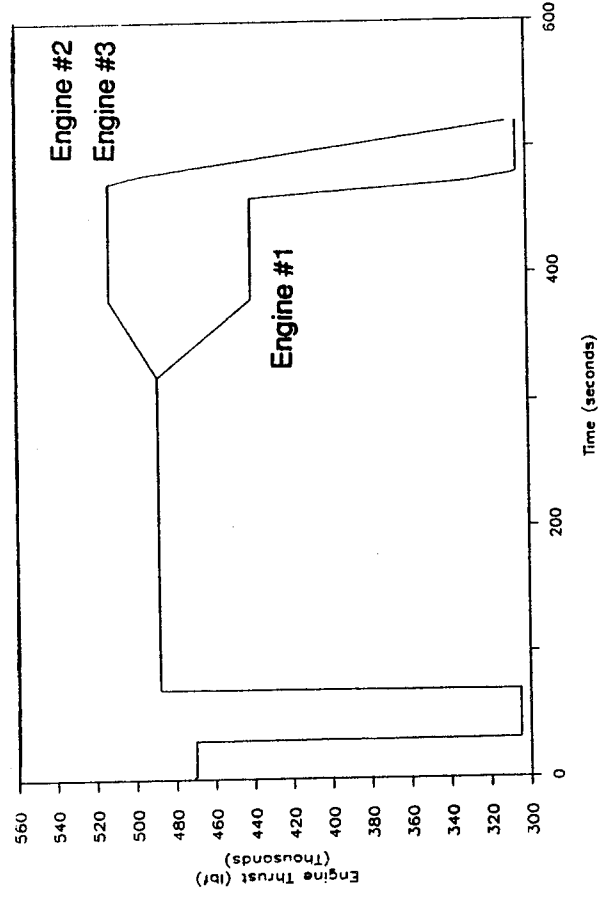
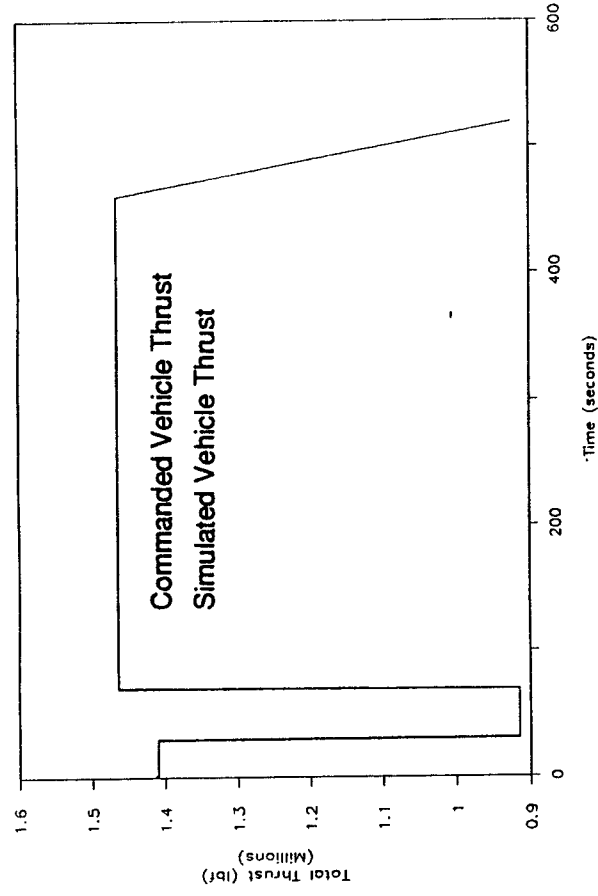


Figure 6-13 ICS Propulsion Level Controller Simulation
Test 902-249

SECTION 7 ICS ADVANCED FUNCTIONAL FRAMEWORK

The ICS advanced functional framework represents a control system that fully integrates the ICS control objectives of 1) maximum reliability, 2) minimum maintenance, and 3) maximum efficiency. The thrust and mixture ratio of each engine are controlled to meet the propulsion system thrust and mixture ratio requirements by a propulsion level controller. Individual engine control is limited to implementing the propulsion system commands in the manner that maximizes individual engine performance, efficiency, and life and includes feedback to the propulsion level. The propulsion system is controlled as an integrated system, rather than as a collection of individual engines (the approach used in current rocket engine propulsion systems). The integrated propulsion system is expected to increase the overall propulsion system reliability, performance, and useful life by enabling tradeoffs between individual engines and thereby mitigating the effects of the "weak link" in the system.

The proposed advanced functional framework is shown in Figure 7-1. The controller consists of a mission level controller that defines the requirements of the propulsion system, a propulsion level controller that coordinates implementation of the propulsion system requirements, and an engine level controller, for each engine, that implements the engine requirements in the most favorable manner for that engine. The mission level controller evaluates the requirements for mission completion and issues overall propulsion system thrust and mixture ratio commands. The propulsion level controller evaluates the propulsion system thrust and mixture ratio commands and controls each engine thrust and mixture ratio to implement the propulsion system thrust and mixture ratio. The distribution of thrust and mixture ratio between individual engines is determined based on the health, efficiency, and remaining life of each engine. The engine level controller implements the thrust and mixture ratio commands from the propulsion level controller by issuing position commands to the engine valves. Since only two engine variables are controlled to "hard" values, and seven control valves are available on the proposed engine configuration, multiple sets of valve commands result in implementation of the "hard" variables (thrust and mixture ratio). The engine level controller evaluates the sets of valve commands that can implement the commanded engine thrust and mixture ratio and selects the set that minimizes the cost to the engine. Unless otherwise specified, cost is defined in terms of engine wear, risk of engine failure, and performance losses.

The advanced functional framework is made up of two types of functions: 1) controller adaptation functions and 2) real time control loop functions. The real time control loop functions are implemented during every major cycle of the controller. The real time control loop functions implement and maintain the propulsion system thrust and mixture ratio according to the commands from the mission level controller. The controller adaptation functions modify parameters within the real time control loop to optimize control of the propulsion system in response to existing or predicted conditions that exist within the engine subsystems. Definitions of each functional element in the framework are provided below.

7.1 Controller Adaptation Functions

The controller adaptation functions are non-real time functions that evaluate engine conditions and modify the response of the real time control functions to optimize control of the propulsion system. The timing of the controller adaptation functions is not constant. The controller adaptation functions evaluate critical conditions on an interrupt basis and can quickly modify the real time control loop in response to a sudden engine degradation. Non mission critical conditions are evaluated at a slower rate. For example, during normal engine operation the remaining life of multiple turbopump components may be inferred from engine measurements and the real time control loop modified to reflect the new remaining life values every so often. However, if the HPFT temperature suddenly increases, the remaining life calculations are put

on hold and the real time control loop is immediately modified to accommodate the temperature rise. Once the temperature accommodation is implemented, the remaining life calculations are resumed.

Each of the controller adaptation functions and their supporting functions are described in the following sections.

Estimate Remaining Life of Critical Components

The purpose of this function is to estimate the remaining life of engine components. Four approaches to estimate component remaining life are proposed. They are: 1) direct measurement of remaining life, 2) direct measurement of life used, 3) estimation of damage accumulation based on detailed damage models, and 4) estimation of damage accumulation based on empirical data. The preferred method, where possible, is to directly measure the remaining life of a component, for example measuring the wall thickness of the MCC coolant channels. The second approach considered is to directly measure the damage that has occurred in a particular component. An example of direct damage measurement is to measure the radial displacement of a turbopump shaft to infer the amount of turbopump bearing wear. If no direct measurements are available, the next approach tried is to estimate the remaining life of a component based on the accumulated damage predicted by a detailed damage model using real time engine measurements (temperatures, pressures, vibrations, etc.). Finally, if there are no direct measurements and no damage model available, the remaining life of a component is estimated based on the number of engine starts, time at each power level, etc. The output of this function is an estimate of the remaining life and a standard deviation reflecting the certainty in the estimate for each specific component evaluated.

Engine Diagnostics

The purpose of this function is to identify specific conditions that exist within the engine. Examples of diagnostic capabilities include the identification of cracked turbine blades, failure of turbopump bearings, sensor failures, and nozzle fuel leaks. The technique used to identify each condition is specific to the condition being evaluated. The output of this function is a probability distribution for the magnitude of a specific condition if applicable, or the probability that a condition has been identified if there is no magnitude associated with the condition. For example, the output for a fuel leak would be the probability distribution that a specific magnitude fuel leak exists. The output for a sensor failure would be the probability that the sensor reading is correct.

Define Weighting Factors

The purpose of this function is to assign weights to critical engine parameters. Critical engine parameters include the high pressure turbine temperatures, turbopump vibrations, MCC temperatures, and the high pressure pump net pump suction heads. Engine parameters also include transient parameters such as changes in a high pressure turbine temperature. The probable remaining life of critical components and likely engine conditions are evaluated to define weights to each parameter. The parameter weights reflect the combination of all factors associated with that parameter and take into account both the severity and likelihood of each factor. As an example, a turbopump bearing with a high probability of little remaining life and a pump operating near its suction limit (where cavitation begins) both indicate that the weight associated with turbopump speed should be increased. The output of this function is a numerical value representing the weight associated with each engine parameter considered by the weighted cost calculation in the real time control loop.

Valve/Actuator Models

The valve/actuator models are dynamic models of each valve response. Engine valve commands issued by the real time control loop and the pressure drop across each valve are used as inputs to the valve models. The output of each model is the predicted time dependent position of each valve.

Valve/Actuator Diagnostics

The purpose of this function is to identify valves/actuators that have failed or that are likely to fail. The valve/actuator diagnostics compare the valve position predicted by the valve/actuator models with the positions indicated by engine sensors. Disagreements between the two position indications are evaluated to determine the health/availability of each valve. The output of this function is the probability of failure for each control valve.

Estimate Model Parameters

The purpose of this function is characterization of the engine operating state to anchor the engine model used in the real time control loop. Characterization includes the estimated efficiency of each high pressure turbine and each high pressure pump. Characterization also includes specific engine conditions which can change the effect of the control valves on the engine. For example, a nozzle fuel leak would cause the high pressure turbines to run abnormally hot and changes in the preburner oxidizer valve position would result in a greater temperature increase than normally expected. The output of this function is a numerical value for each model element characterized.

Propulsion System Diagnostics

The purpose of this function is to evaluate the condition of each engine and estimate the probability that the propulsion system is able to implement the overall thrust and mixture ratio required for mission completion or abort modes. The mission requirements (e.g. maximum thrust required for the flight profile, remaining mission time) are sent to the propulsion system diagnostics function by the mission controller for the current mission and possible abort modes. The propulsion system diagnostics evaluate the condition of each engine and estimates the probability that the propulsion system will be able to implement the mission requirements without a catastrophic failure in the propulsion system. The output of this function is a probability of success for the current mission and each abort mode possible. The mission level controller uses the success probabilities for the propulsion system (and those for other major subsystems) to evaluate the current mission and abort modes and decide on the course of action that has the highest likely payoff.

Determine Allowable Engine Thrust and Mixture Ratio Ranges

The purpose of this function is to determine the thrust and mixture ratio ranges that can be implemented by each engine. The allowable ranges are determined by the availability of engine control valves to implement changes. For example, if an engine's FPOV fails, the thrust and mixture ratio changes that can be implemented are severely limited. The output of this function is a range of allowable engine thrusts and mixture ratios. An example of the output thrust range for an individual engine is shown Figure 7-2. The solid line indicates the range for a nominal engine and the dashed line represents the allowable range for an engine with a failed actuator.

Determine Weighted Engine Thrust and Mixture Ratio Ranges Based on Engine Condition

The purpose of this function is to estimate the cost associated with operating the engine at each thrust or mixture ratio in its allowable range. Cost for this function is defined in terms of the risk of engine failure during the mission. In all cases, the cost of operating an engine is greater at higher thrust levels. Higher thrust levels result in higher failure risk in almost all cases. In addition to the nominal cost associated with each thrust and mixture ratio, specific engine conditions are evaluated to modify the "cost distribution" for each engine. For example, the cost of operating an engine at a given thrust with a degraded turbopump bearing is higher than the cost of operating a nominal engine at the same thrust. The probability and magnitude of specific engine conditions are used to define the likely cost at each thrust and mixture ratio. The output of this function is the cost associated with operating each engine at specific thrust and mixture ratios. Figure 7-3 shows the cost for an individual engine as a function of engine thrust if the cost distribution is linear. The solid line represents a nominal engine and the dashed line represents a degraded engine. Engine degradations are expected to increase the slope and height of the cost distribution.

Modify Weighted Engine Thrust and Mixture Ratio Ranges Based on Engine Efficiency

The purpose of this function is to modify the weighted engine thrust and mixture ratio ranges based on the cost associated with performance losses. Nominally, the engine performance is greatest at the rated thrust and drops off to either side. Engine performance also peaks at a specific mixture ratio and drops off to either side. Depending on the engine design, the nominal mixture ratio may not be the mixture ratio at which the highest engine performance is achieved. In addition to the nominal cost distribution, engine performance parameters (e.g. HPOP efficiency) are evaluated to determine the performance of each specific engine relative to a nominal engine. Changes in engine performance parameters are expected to effect the overall height of the cost distribution. Figure 7-4 shows the linear cost distribution from the weighted engine thrust example used in the previous example modified to reflect the cost associated with engine efficiency. The solid line is a nominal engine and the dashed line represents a less efficient engine.

Modify Weighted Engine Thrust and Mixture Ratio Ranges Based on Remaining Engine Life

The purpose of this function is to modify the weighted engine thrust and mixture ratio ranges based on the cost associated with remaining engine life. The cost, in terms of engine life, to operating an engine is greater at higher thrust and mixture ratios. The nominal cost distribution is modified by the estimated remaining engine component life probabilities. An engine that indicates little remaining life has a higher cost to operate than a nominal engine. Differences in remaining engine life change the slope and the height of the cost distribution. Figure 7-5 shows the linear cost distribution used in the previous example modified to reflect the remaining life of the engine. The output of this function is the total cost for operating each engine at specific thrust and mixture ratios.

7.2 Real Time Control Loop Functions

The real time control loop functions are the functions that produce outputs during every major cycle of the control system. These functions are responsible for achieving and maintaining the propulsion system thrust and mixture ratio at the values commanded by the mission coordinator. The real time control functions at the individual engine level evaluate the engine status and implement the propulsion level controller commands with the lowest cost to the individual engines. Additionally, the real time control loop functions initiate changes in the individual engine states in response to engine conditions.

Thrust and Mixture Ratio Estimator

The purpose of this function is to evaluate engine measurements and provide an estimate of the engine thrust and mixture ratio.

Issue Lowest Cost Set of Engine Thrusts and Mixture Ratios to Individual Engines

The purpose of this function is to evaluate errors in the propulsion level thrust and mixture ratio and issue thrust and mixture ratio command to each engine. The propulsion level controller distributes the thrust and mixture ratio between individual engines to minimize the maximum individual engine cost. Minimizing the maximum individual engine cost is proposed since the engine cluster is limited in life, reliability, and performance by its weakest member. Figure 7-6 shows conceptually how this function operates. The total cost distribution for three engines is shown. Engine #2 represents a nominal engine, engine #1 is degraded, and engine #3 has a failed control valve. If the measured thrust is lower than the commanded thrust the propulsion level controller issues an upthrust command. The thrust commands to individual engines reflect the associated cost for each engine. In the example shown in Figure 7-6, engine #2 is commanded to its maximum operating thrust and the remainder of the thrust error is corrected by engines #1 and #3 with engine #1 making up the majority of the error. Conceptually, the propulsion level controller moves the command line (dashed line in the Figure 7-6) up and down in response to measured propulsion system thrust errors.

If the cost distribution for an individual engine changes, the thrust command for that engine is changed which results in a propulsion system thrust error and the command line is adjusted to resolve the error. For example, take the case when all three engines are initially operating nominally and engine #2 suddenly develops a nozzle leak. The slope and height of engine #2s cost distribution suddenly increase changing the point at which engine #2s cost distribution crosses the command line. Engine #2 is downthrust causing an error in the propulsion system thrust. The command line is moved upward upthrusting all three engines until a new equilibrium is reached in which engines #1 and #3 are now operating at higher thrusts than engine #2 but the propulsion system thrust is at its original value.

Determine Possible Solutions

The purpose of this function is to determine the set of valve commands that implement the thrust and mixture ratio commands received from the propulsion level controller. The only external commands to the engine system are thrust and mixture ratio. Since seven control valves are used in the proposed system, multiple combinations of valve position changes are available to resolve the thrust and mixture ratio errors. The status of each valve/actuator is used to determine which valve position changes can be implemented. If the FPOV has failed and is locked in position, no combinations requiring a change in FPOV position will be output. The output of this function is the set of valve position commands that can be implemented to resolve the thrust and mixture ratio errors. Figure 7-7 shows an example of the data content of this functions output.

Estimate Engine Parameters for Each Solution

The purpose of this function is to estimate engine parameters expected to result from the implementation of each combination of valve position commands identified as possible solutions. Engine parameters are estimated for each possible solution by inputting the valve position commands to an engine model. The engine model is kept current with engine measurements and parameters estimated by the controller adaptation functions. The output of this function is a set of engine parameters for each combination of valve commands identified

as possible solutions. Figure 7-8 shows an example of the data content of this functions output.

Calculate Weighted Cost of Each Solution

The purpose of this function is to estimate the cost associated with implementing each set of valve commands identified as possible solutions. The weighted cost associated with each solution is determined by calculating the sum of the engine parameters multiplied by their weighting factors. The cost of a solution will change depending on engine conditions and remaining life. If an engine failure occurs and the parameter weighting factors change, a set of valve position commands different than the current set of valve positions may have the lowest cost. In this case the new valve commands will be implemented, changing the engine state but not affecting the engine thrust or mixture ratio. This function is shown conceptually in Figure 7-9.

Implement Solution With Lowest Cost

The purpose of this function is to implement the set of valve position commands that represents the lowest cost to the engine. In the example shown in Figures 7-7 to 7-9, solution #4 would be implemented.

7.3 Advanced Functional Framework Conclusions

The proposed framework is computationally intensive, but provides an integrated set of propulsion system functions that optimize propulsion system performance, increase propulsion system reliability, and extend the useful life of the propulsion system. The functions proposed enable the propulsion system controller to continuously evaluate individual engine statuses and implement the mission required thrust and mixture ratio commands in the manner that optimizes propulsion system life, reliability, and performance.

RI/RD91-158

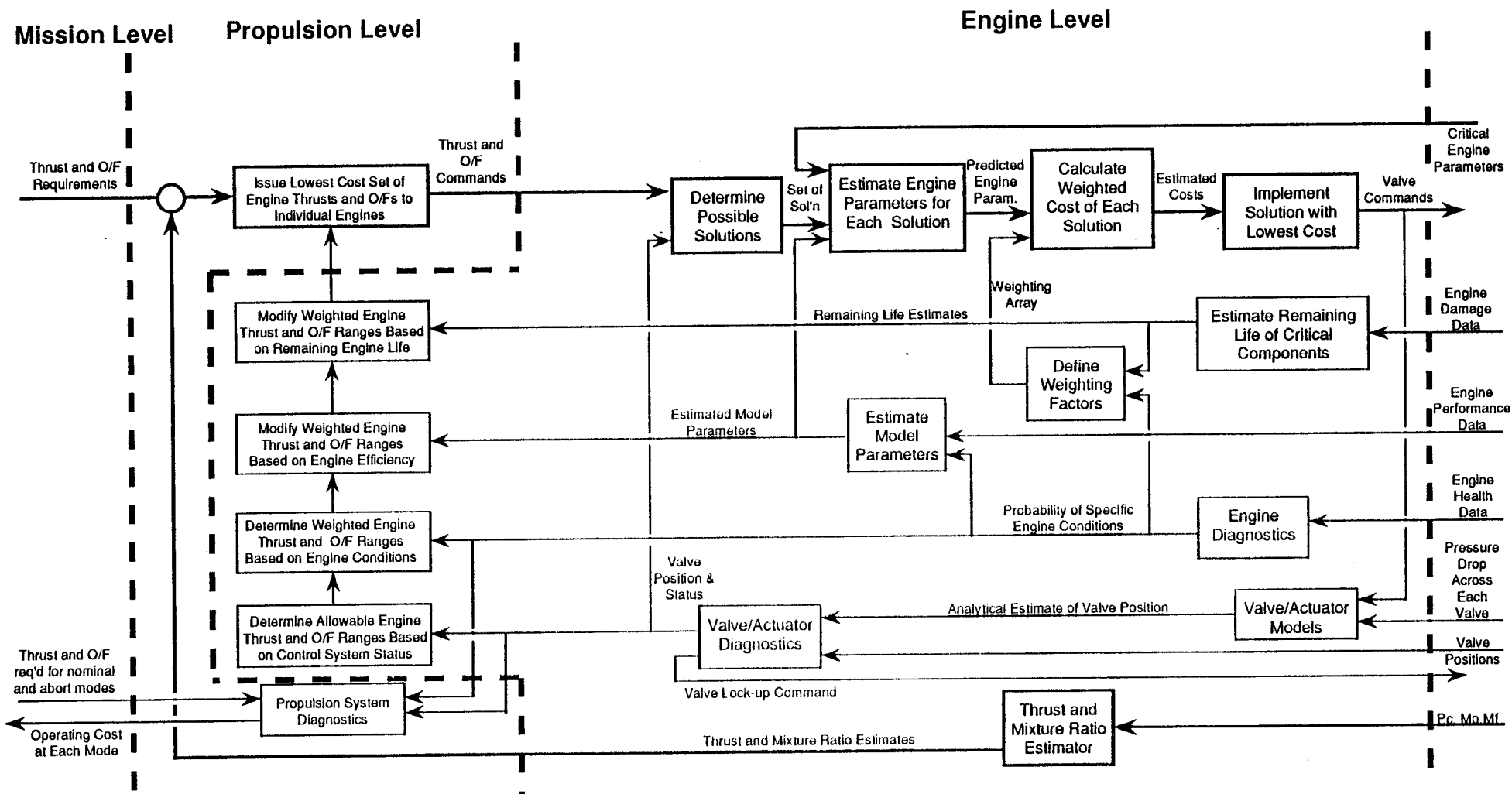


Figure 7-1 ICS Advanced Functional Framework

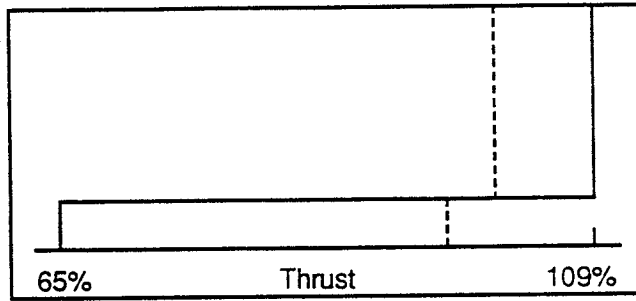


Figure 7-2 Allowable Thrust Range

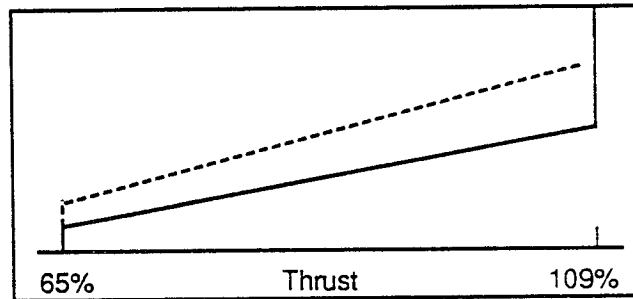


Figure 7-3 Weighted Engine Thrust

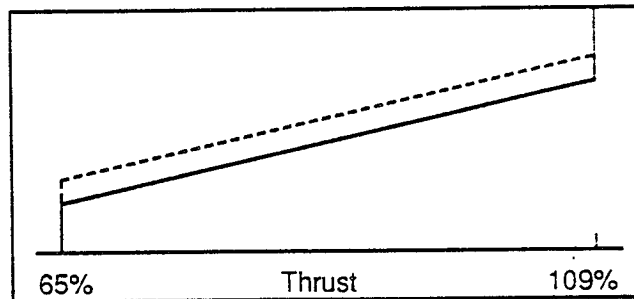


Figure 7-4 Engine Efficiency Modification To Weighted Engine Thrust

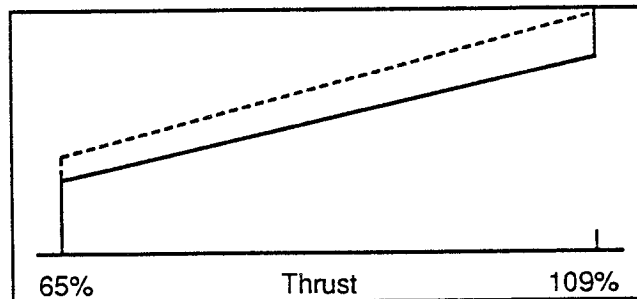


Figure 7-5 Remaining Engine Life Modification to Weighted Engine Thrust

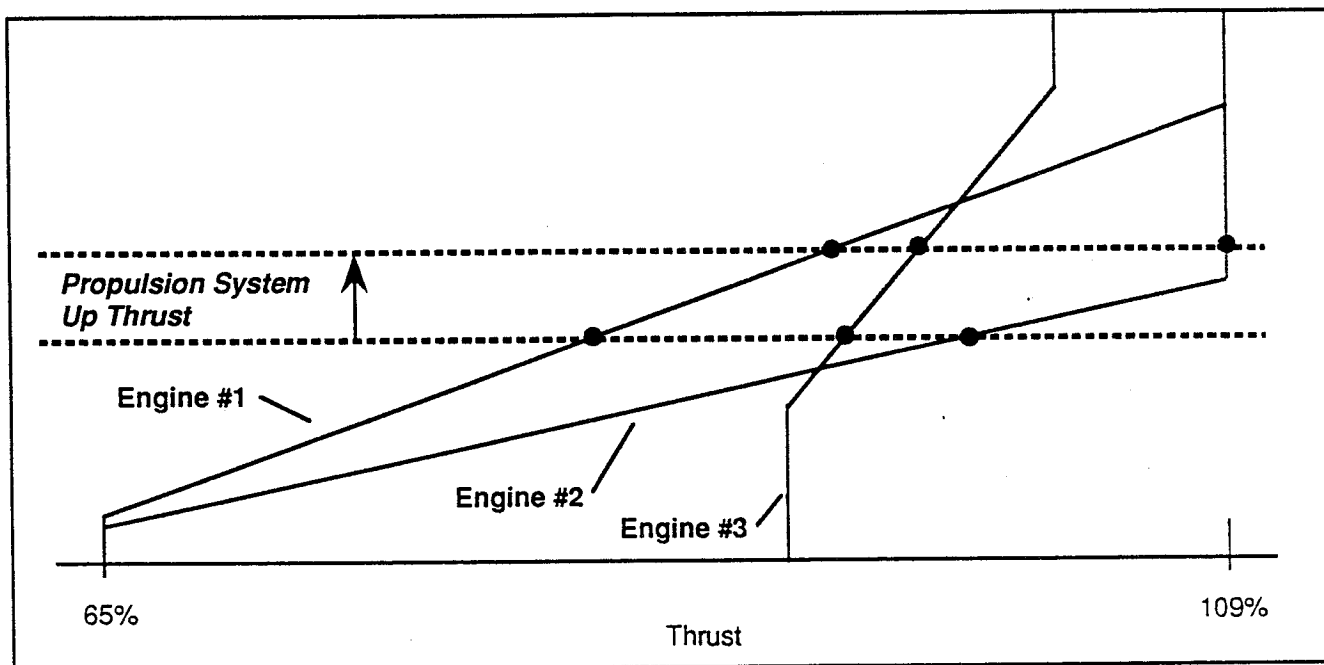


Figure 7-6 Three Engine Thrust Control Strategy

Solution ID	MFV	MOV	FPOV	OPOV	CCV	F7V	LPOTV
1	+0.01	-0.03	+0.01	-0.02	+0.135	-0.003	-0.013
2	-0.013	+0.001	-0.003	+0.001	+0.001	+0.01	+0.135
3	+0.01	-0.02	+0.034	+0.01	+0.034	-0.03	+0.01
4	0.0	+0.001	-0.005	-0.003	+0.001	-0.002	+0.001
5	-0.002	+0.001	-0.03	+0.135	+0.001	0.0	+0.001

Figure 7-7 Possible Solutions

Solution ID	HPFT Temp	HPOT Temp	LPFP Vibration	HPFT Δ TEMP
1	1850	1600	100	50
2	1825	1520	125	25
3	1700	1750	87	100
4	1768	1525	101	32
5	1800	1630	110	0

Figure 7-8 Estimated Engine Parameters

Solution ID	HPFT Temp	HPOT Temp	LPFP Vibration	HPFT Δ TEMP	Weighted Cost
1	1850	1600	100	50	21150
2	1825	1520	125	25	20265
3	1700	1750	87	100	21924
4	1768	1525	101	32	20037
5	1800	1630	110	0	20630
Weighting Factors	5	7	2	10	

Figure 7-9 Weighted Cost of Each Solution

References

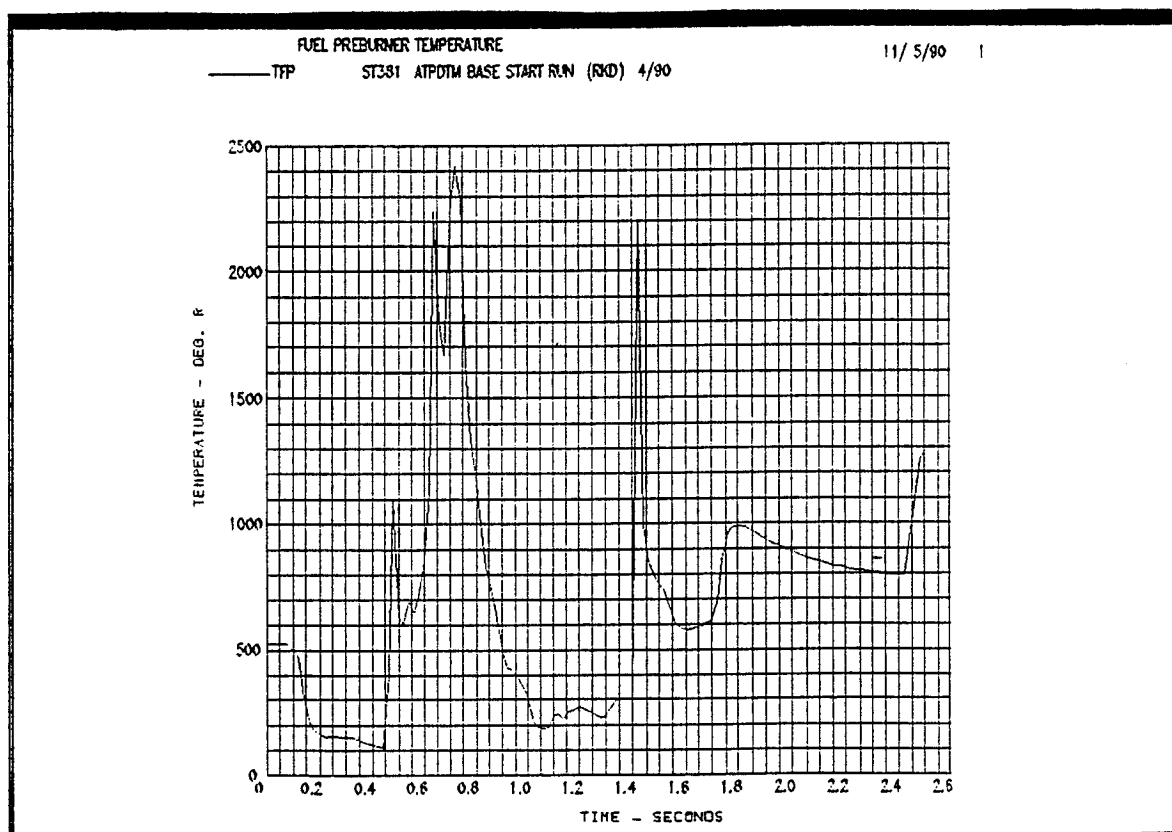
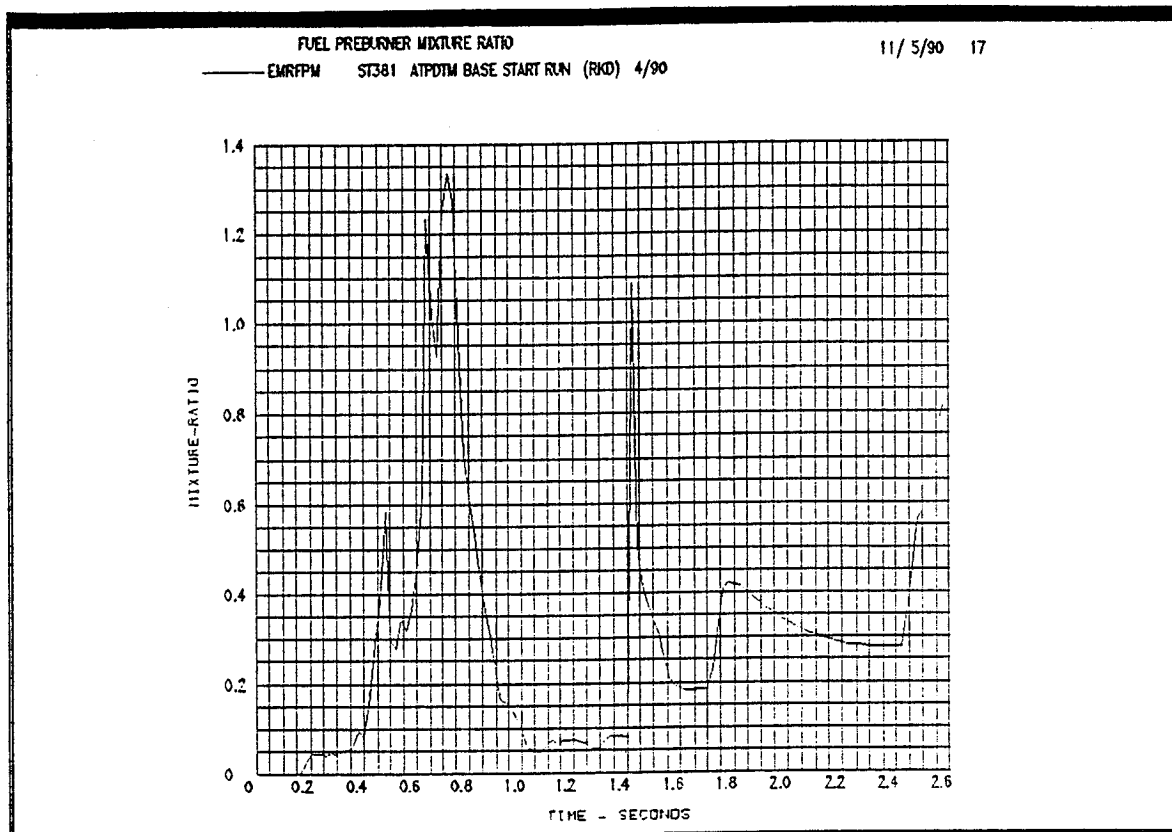
1. Reusable Rocket Engine Intelligent Control System Framework Design - Phase I,
Ed Nemeth, Rockwell International,
NASA Contractor Report CR187043
2. Advanced Control Modes for The Space Shuttle Main Engine
J. L. Musgrave, NASA Lewis Research Center,
Advanced Earth-to-Orbit Propulsion Technology Conference 1990
NASA Conference Publication 3092, Volume I

Appendix 1

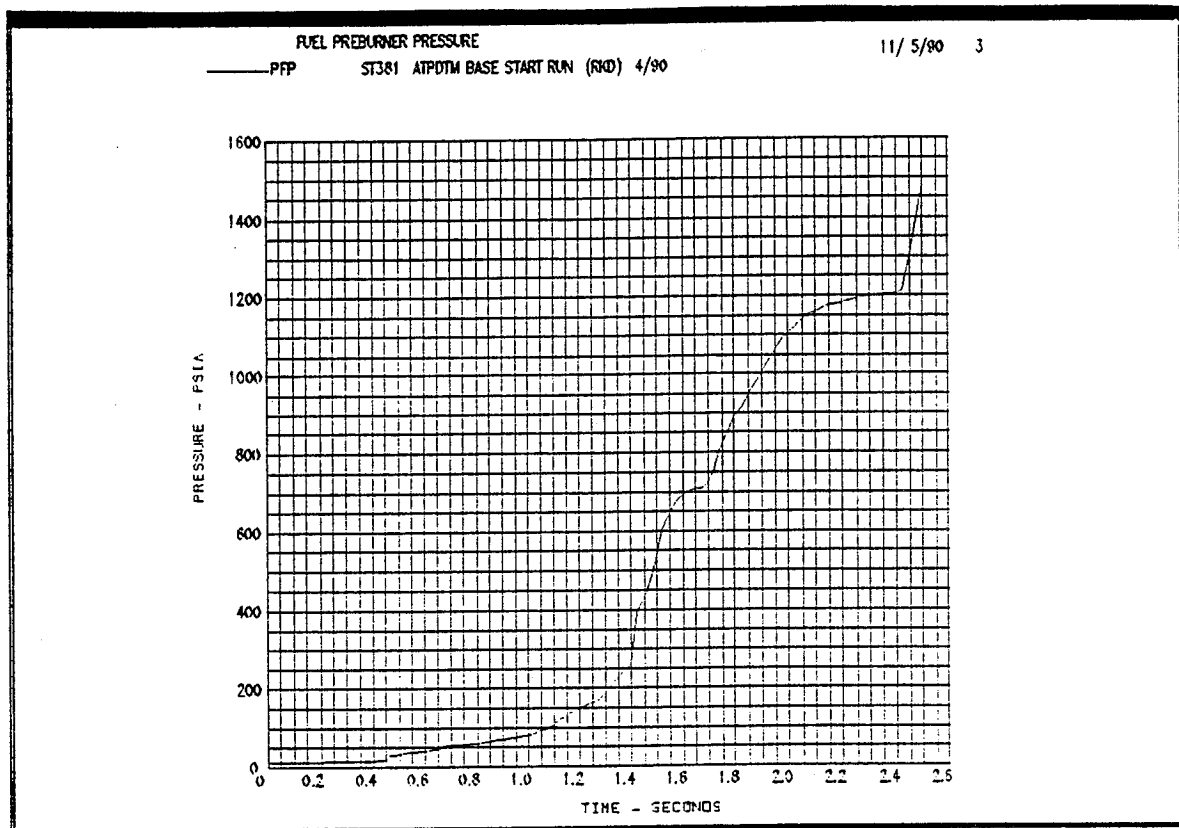
SSME Start Transient Simulation Results

Nominal Case

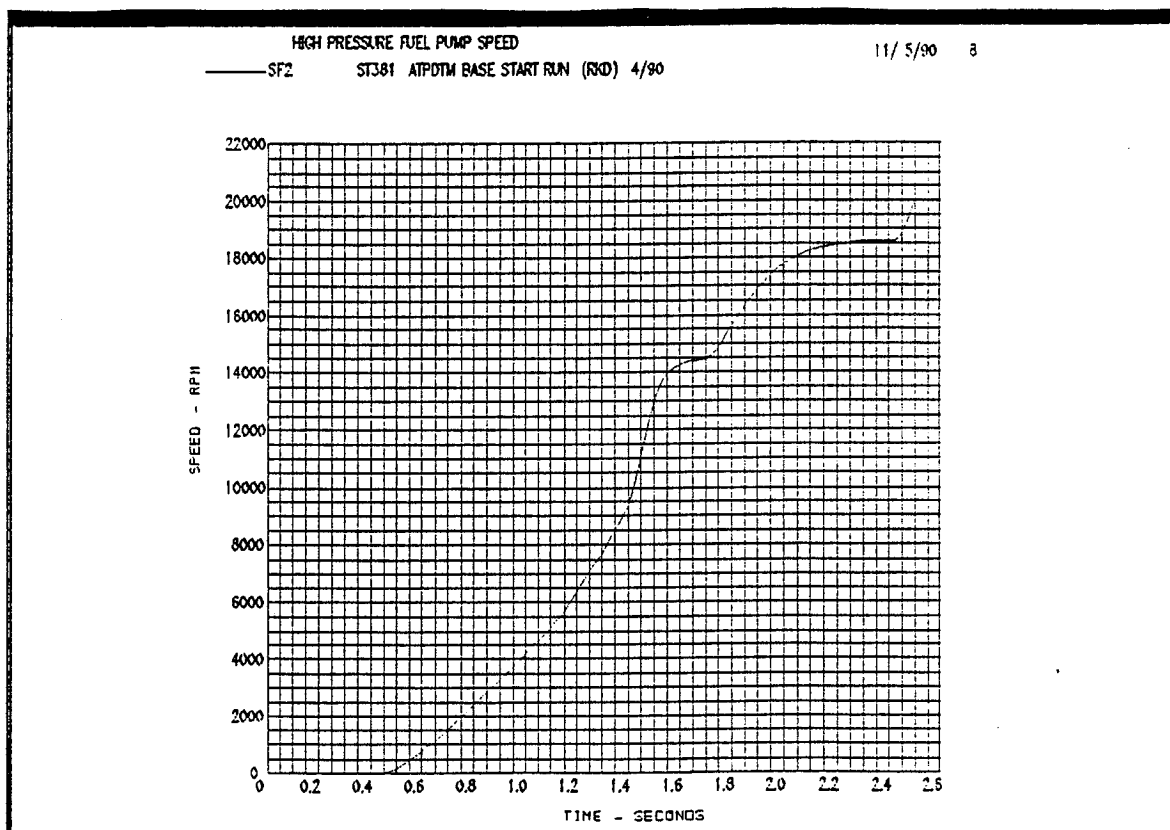
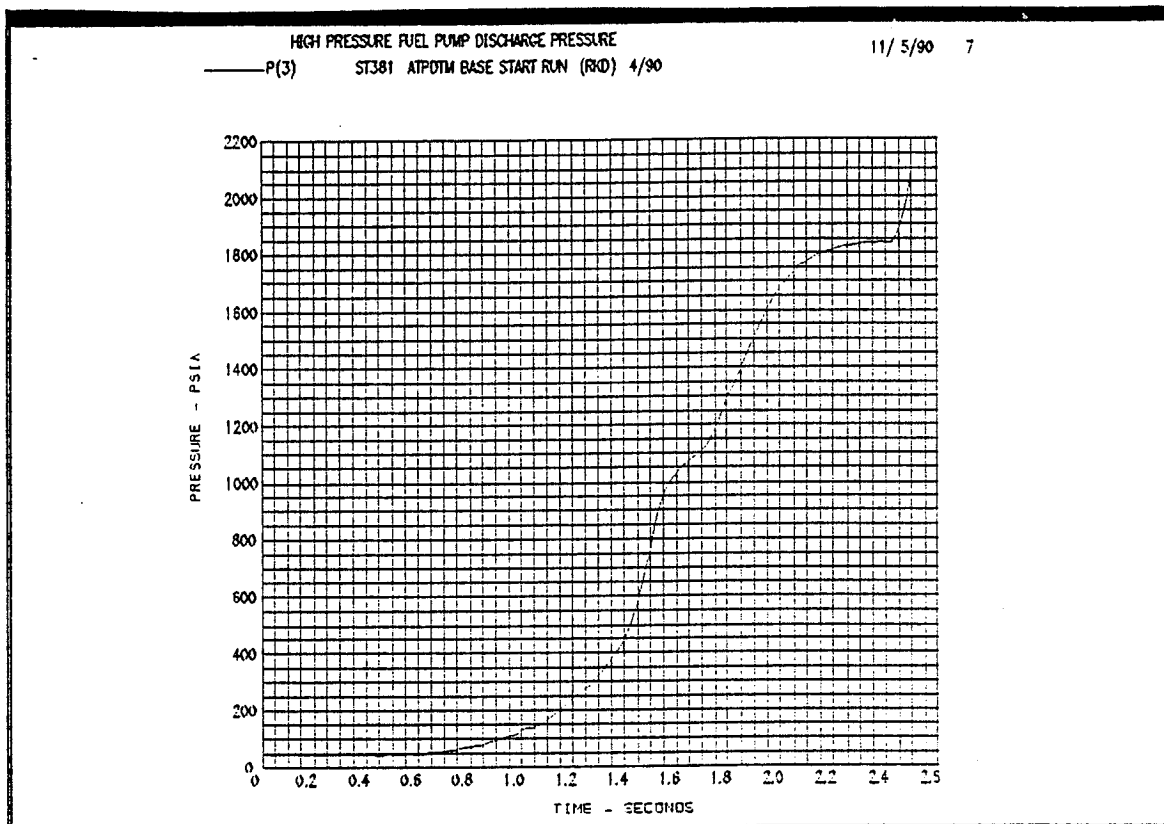
APPENDIX 1



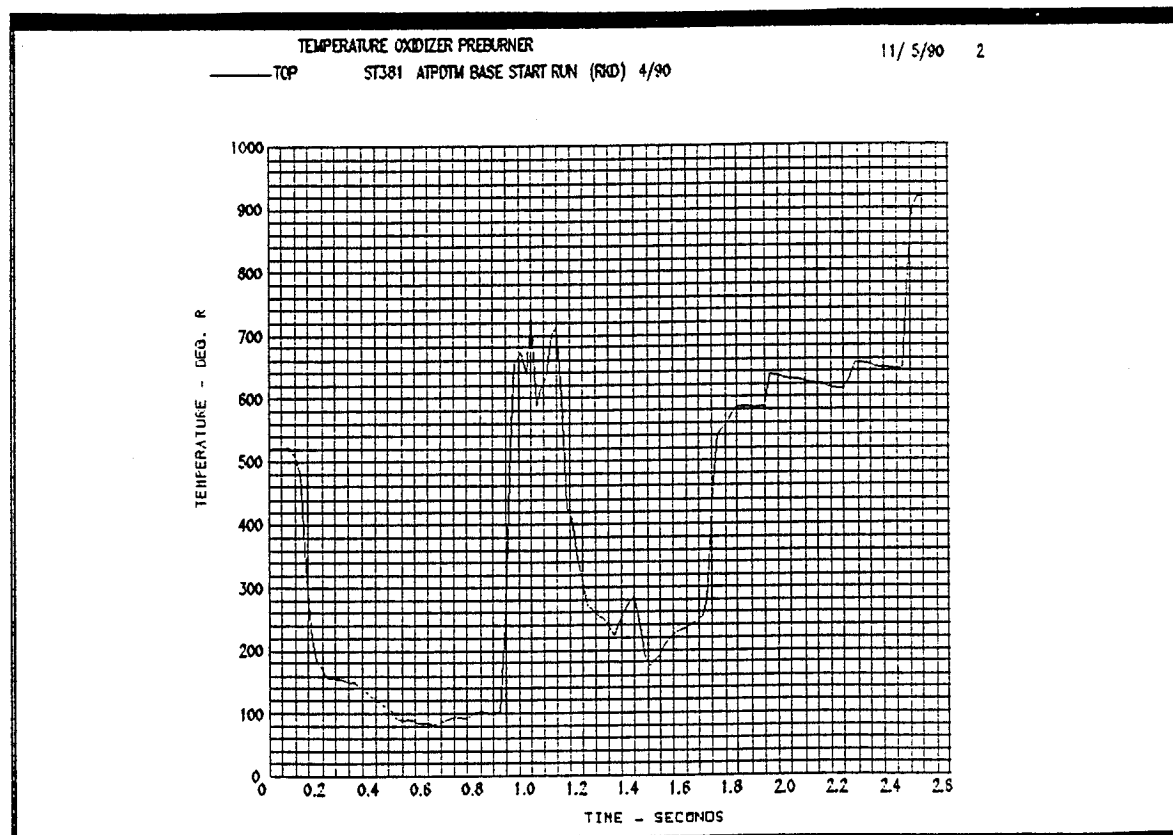
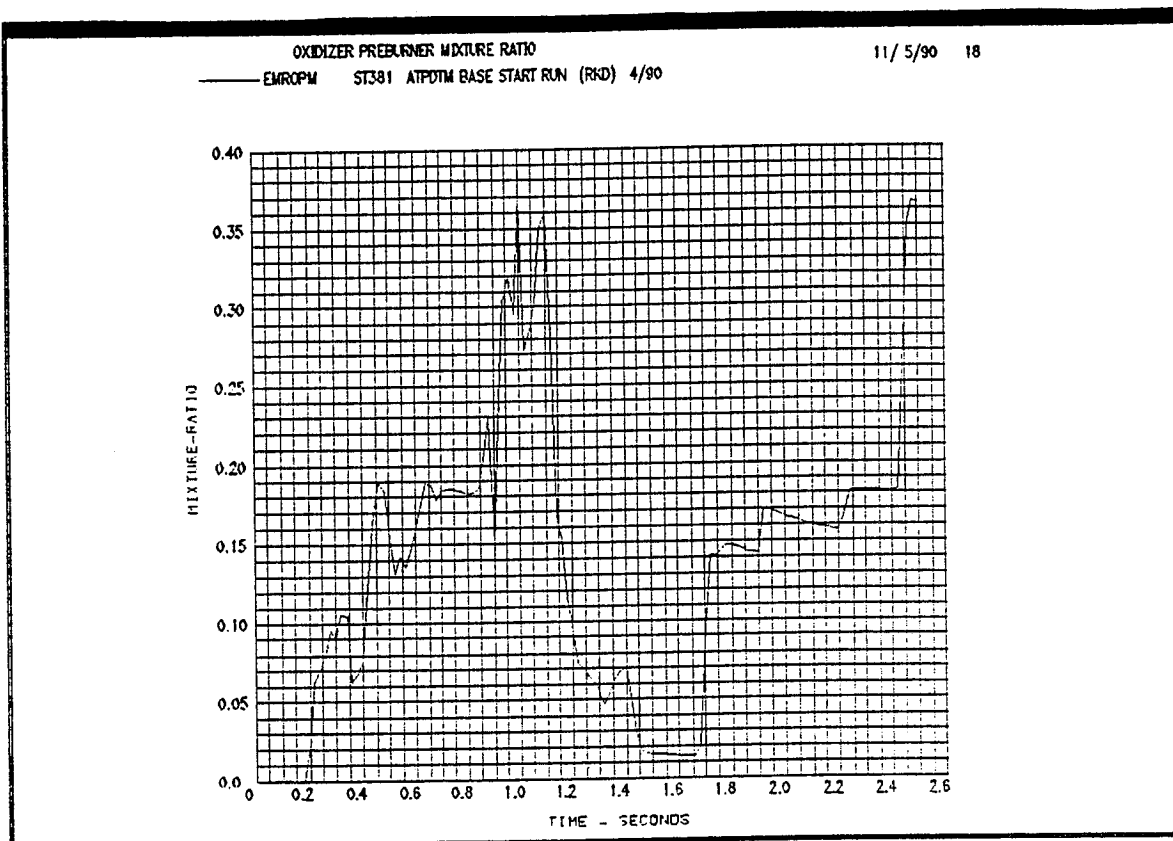
APPENDIX 1



APPENDIX 1



APPENDIX 1

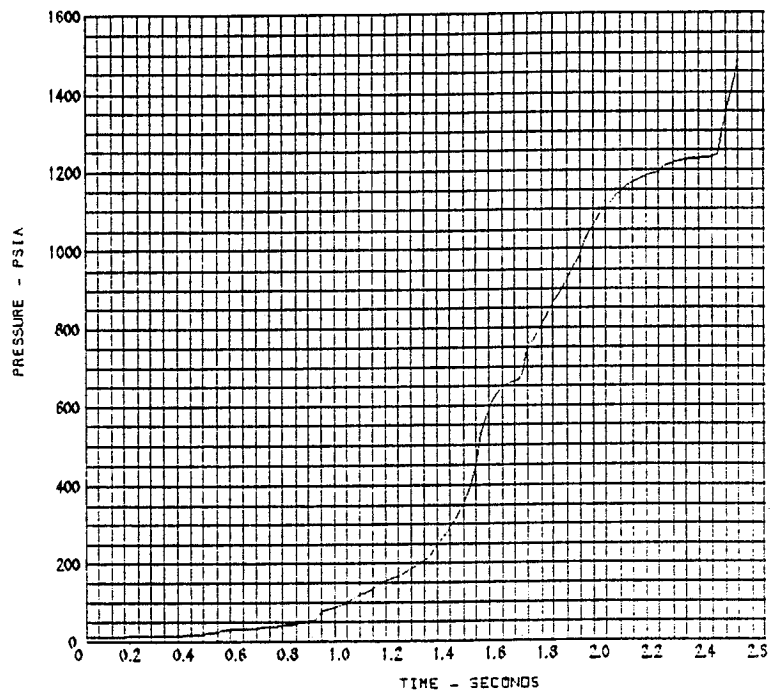


APPENDIX 1

PRESSURE OXIDIZER PREBURNER

11/ 5/90 4

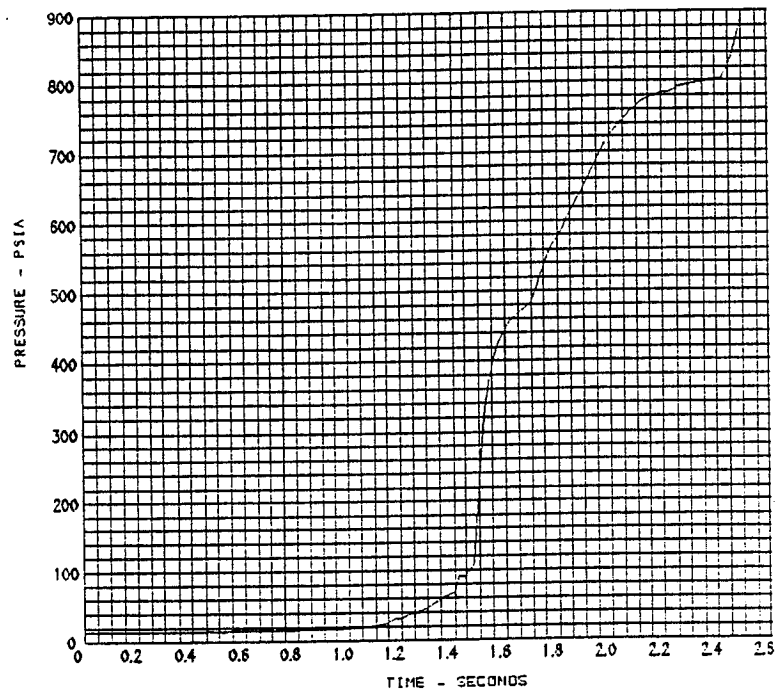
POP ST381 ATPDTM BASE START RUN (R00) 4/90



APPENDIX 1

MCC COMBUSTION CHAMBER PRESSURE
—— PCIE ST381 ATPDTM BASE START RUN (RND) 4/90

11/ 5/90 5

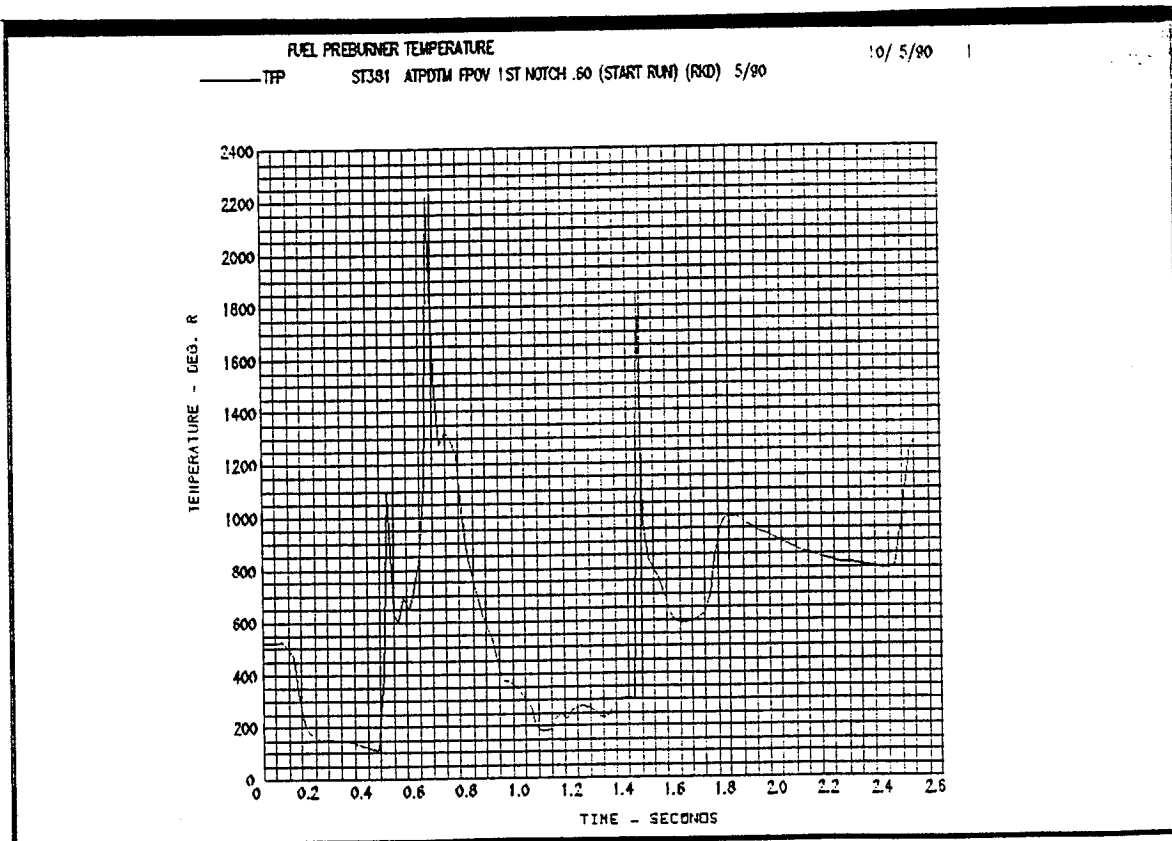
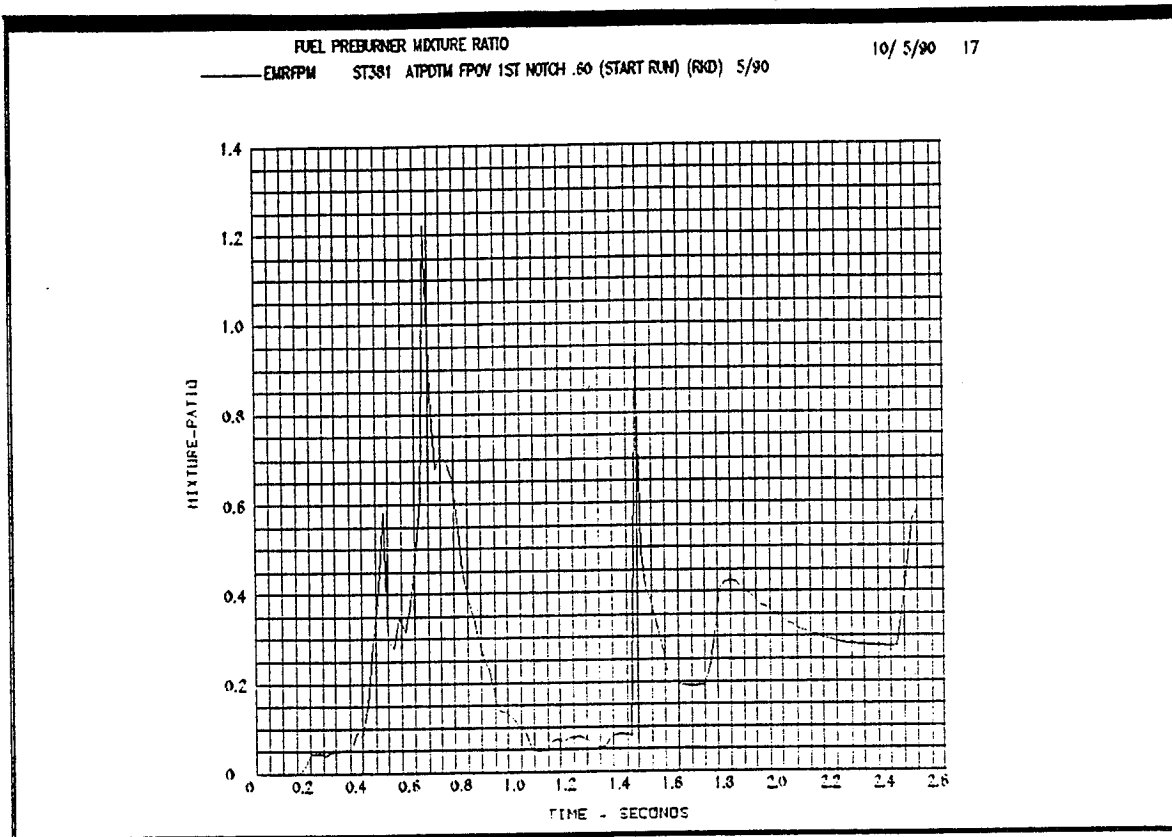


Appendix 2

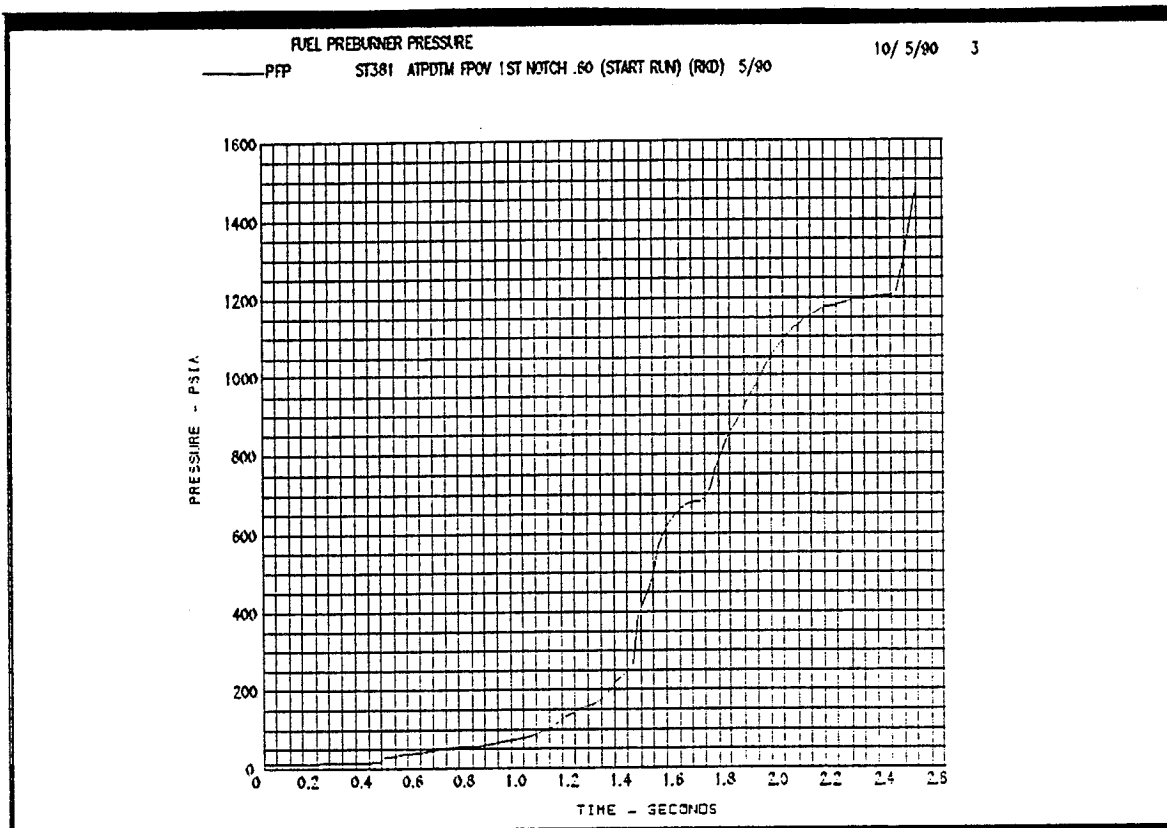
SSME Start Transient Simulation Results

FPOV 1st Notch @ 0.60 seconds

APPENDIX 2



APPENDIX 2

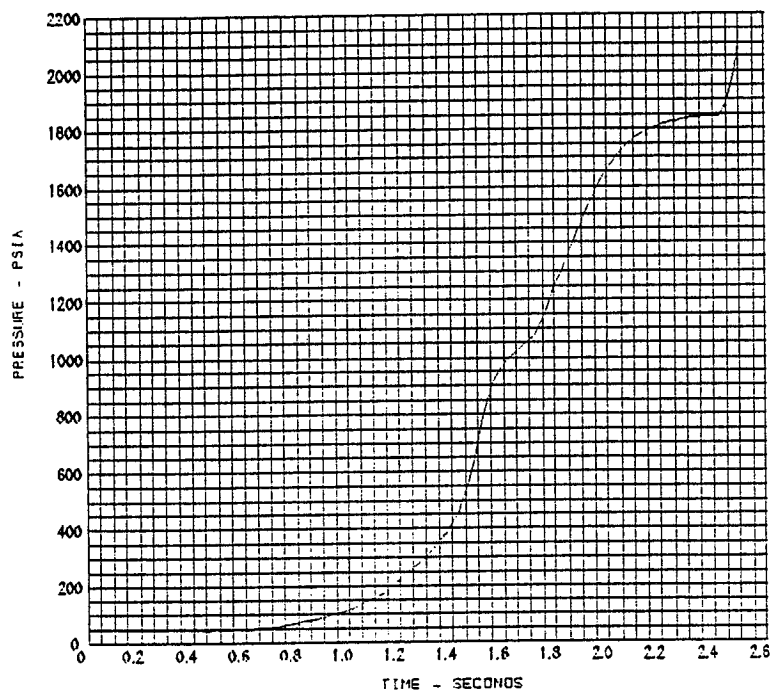


APPENDIX 2

HIGH PRESSURE FUEL PUMP DISCHARGE PRESSURE

— P(3) ST381 ATPDTM FPOV 1ST NOTCH .60 (START RUN) (RND) 5/90

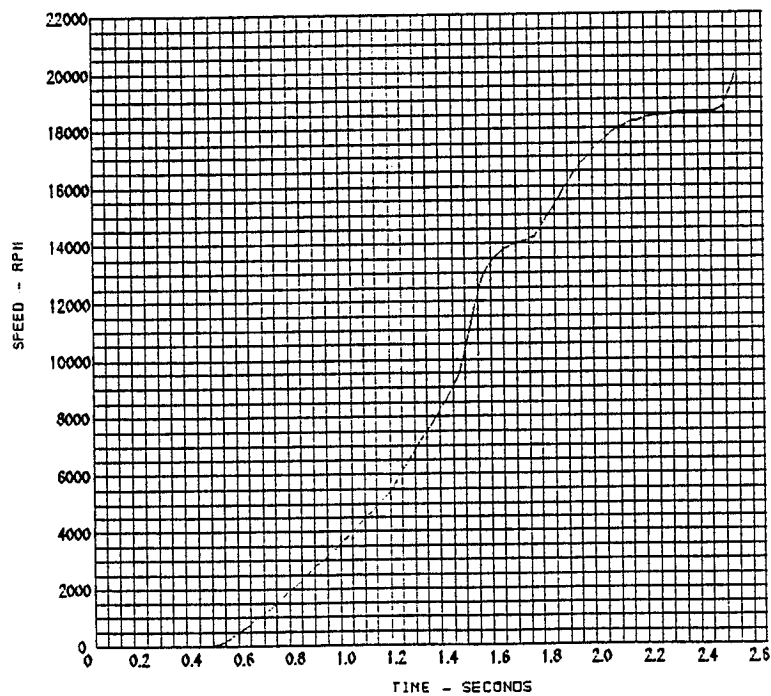
10/ 5/90 7



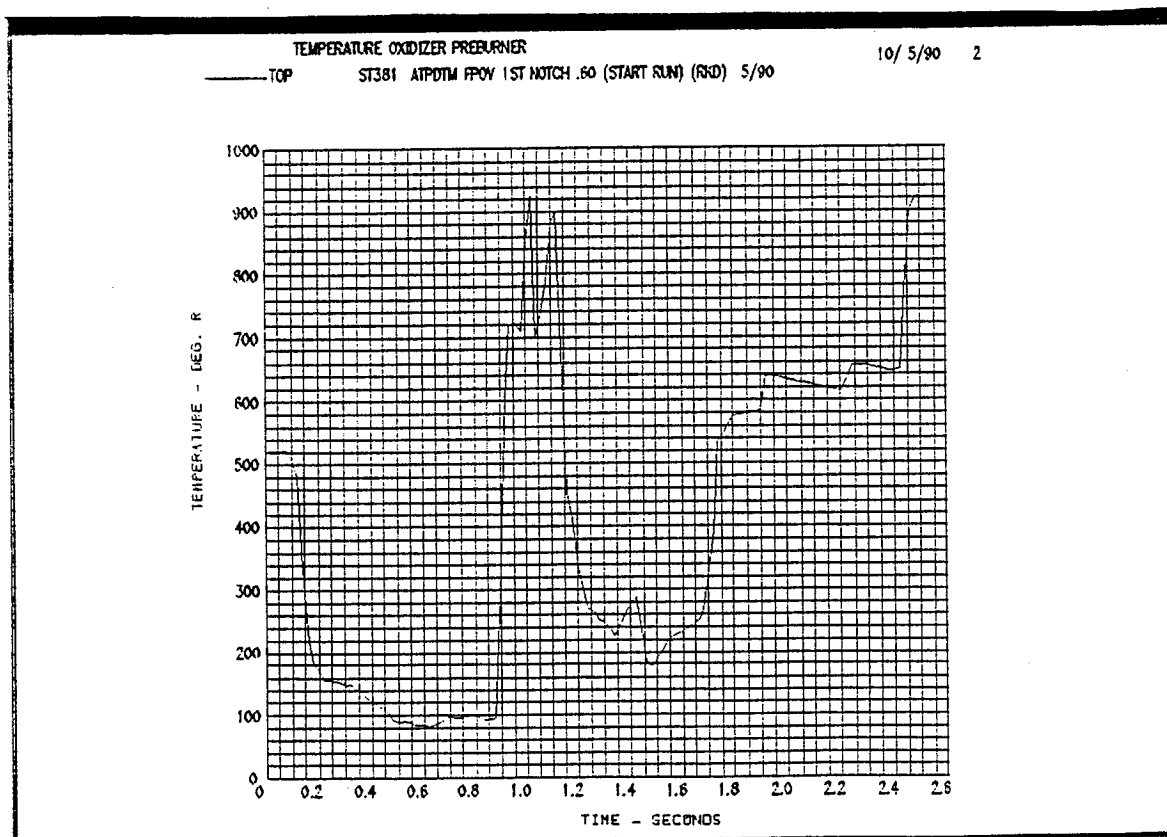
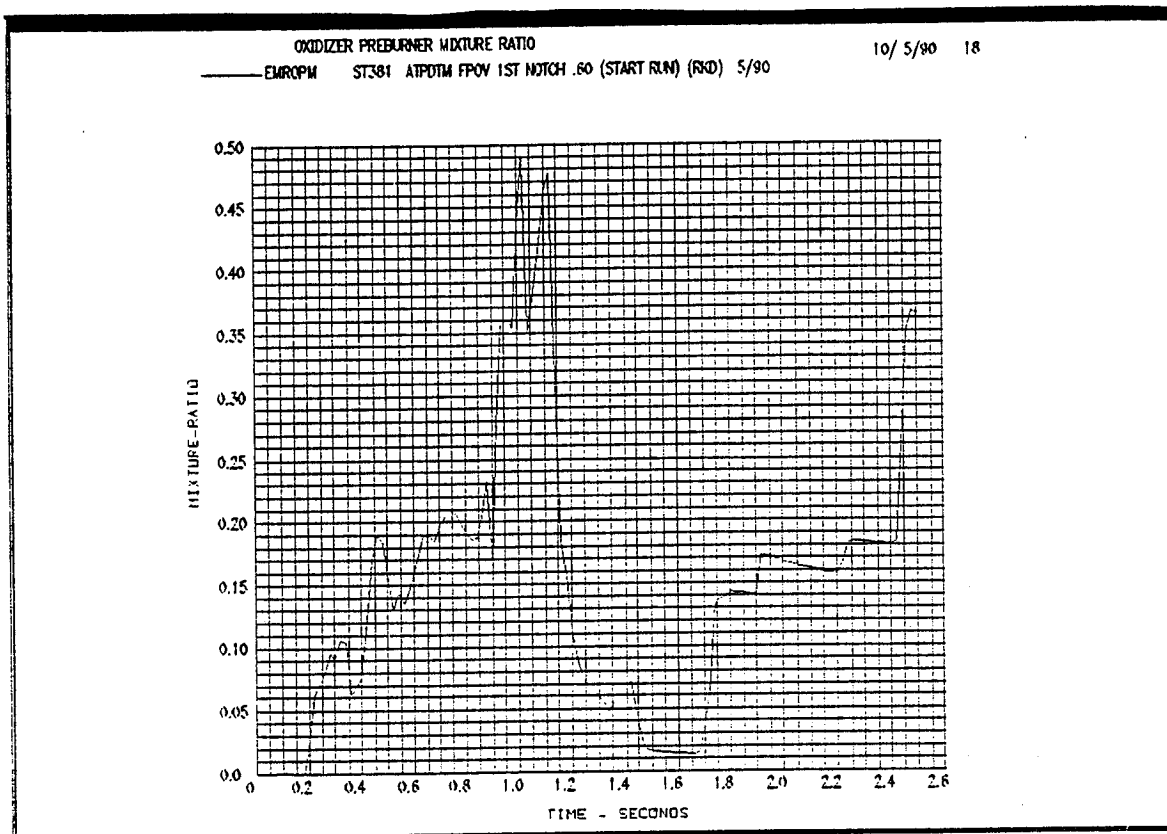
HIGH PRESSURE FUEL PUMP SPEED

— SF2 ST381 ATPDTM FPOV 1ST NOTCH .60 (START RUN) (RND) 5/90

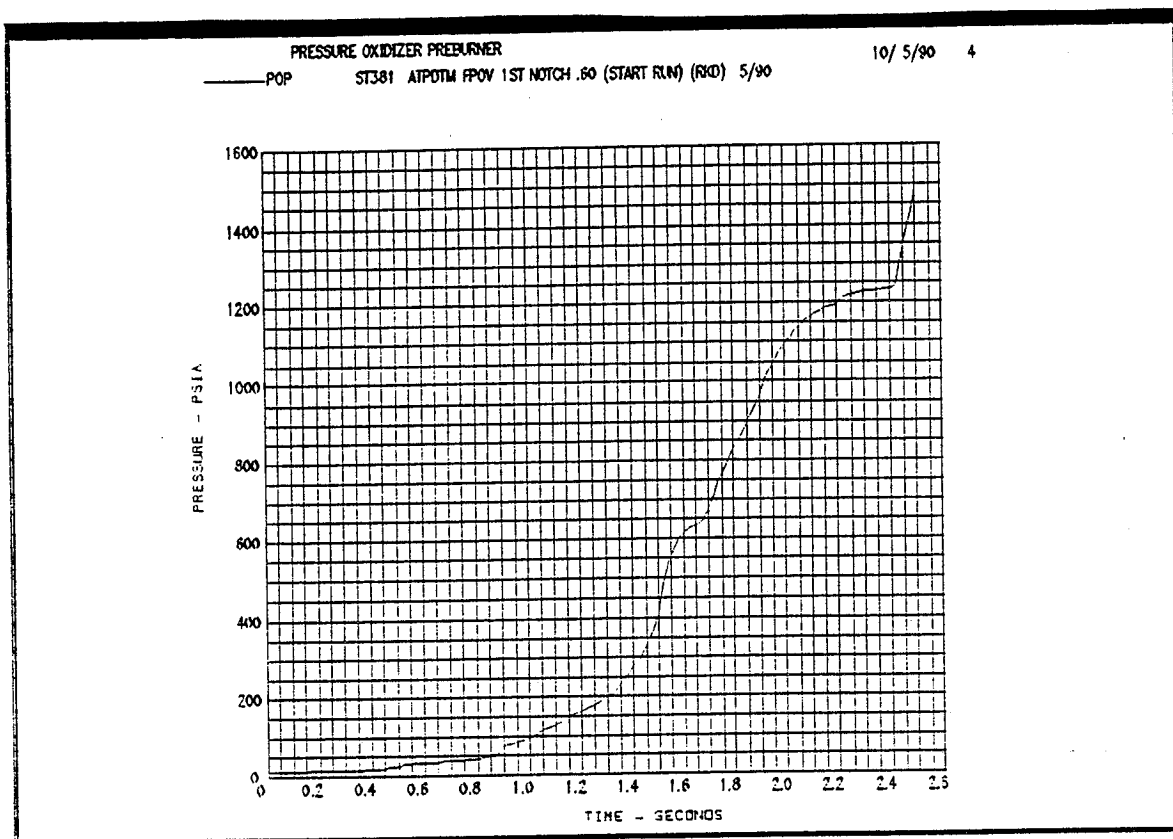
10/ 5/90 8



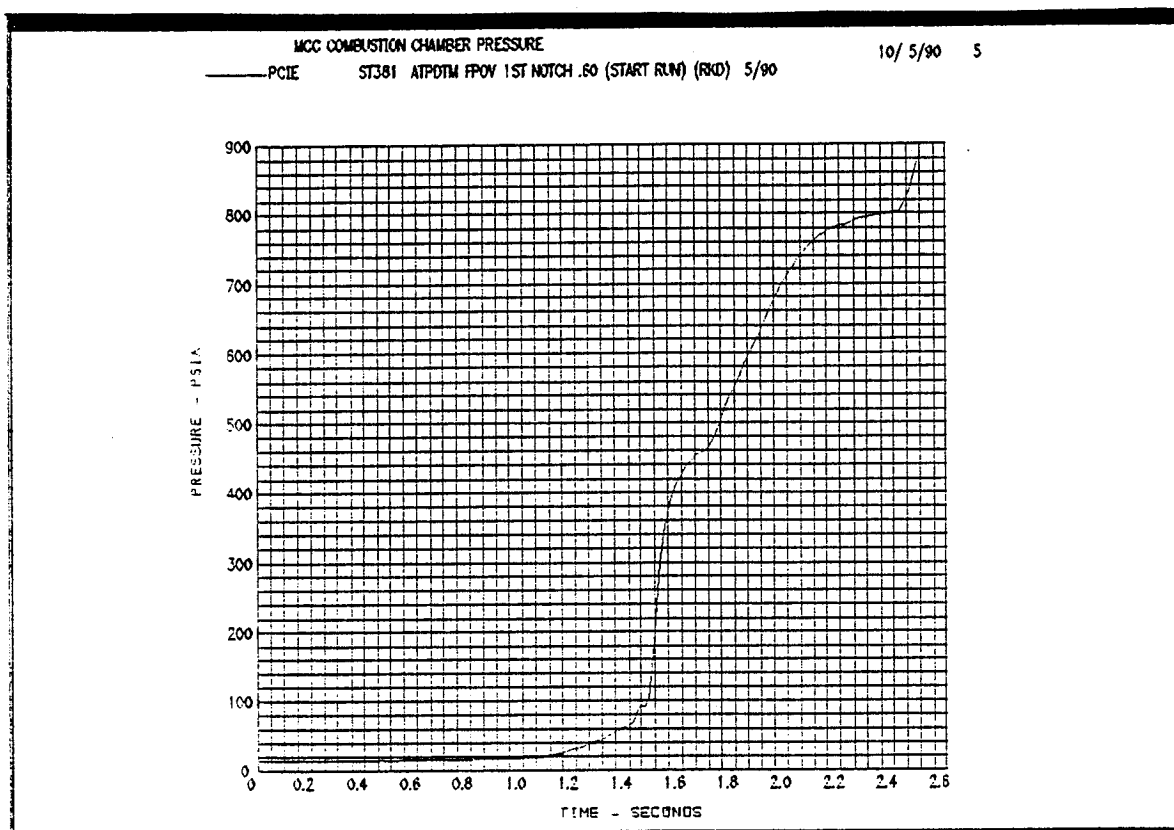
APPENDIX 2



APPENDIX 2



APPENDIX 2

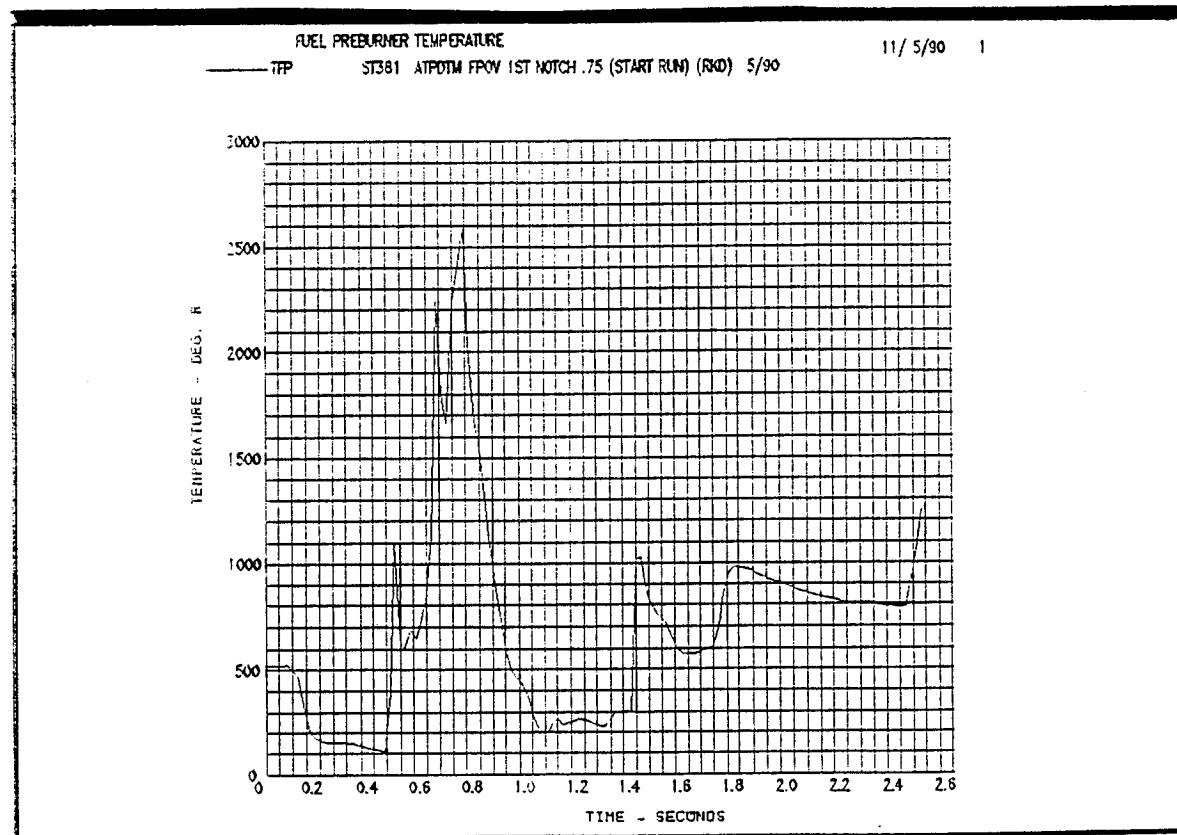
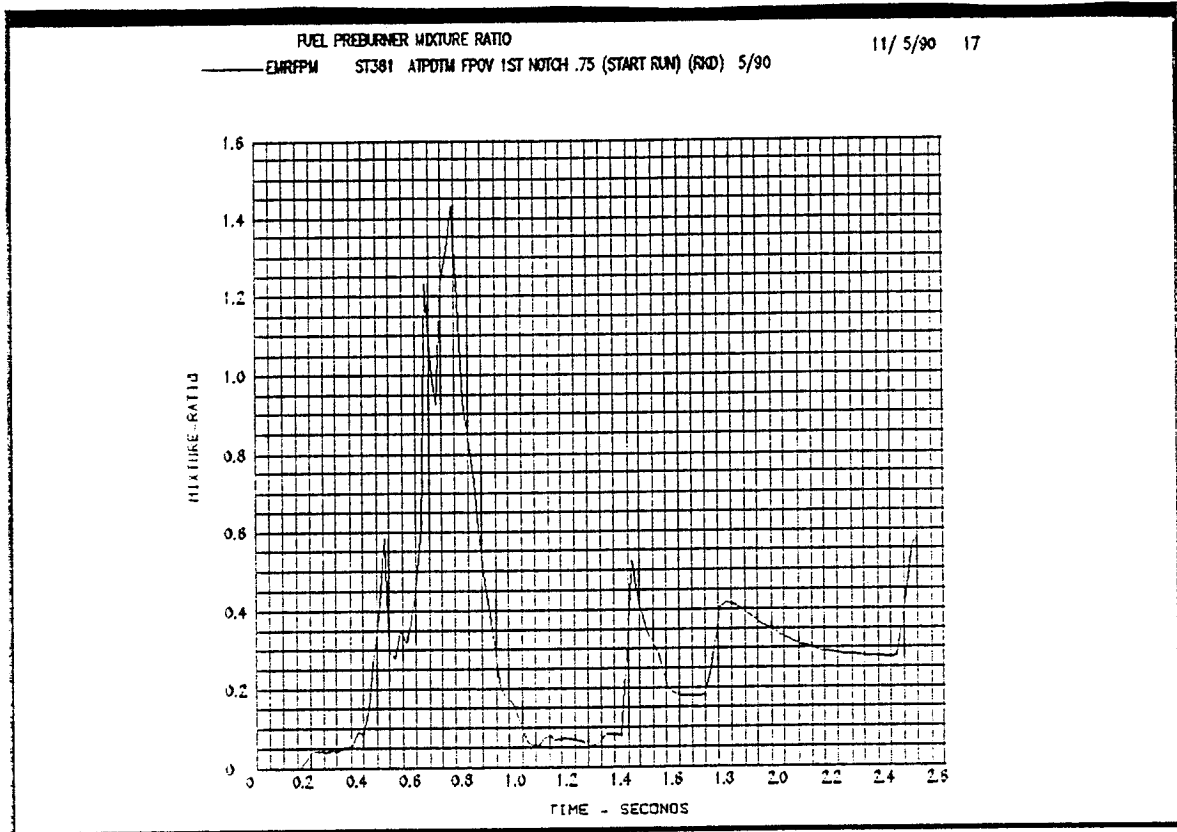


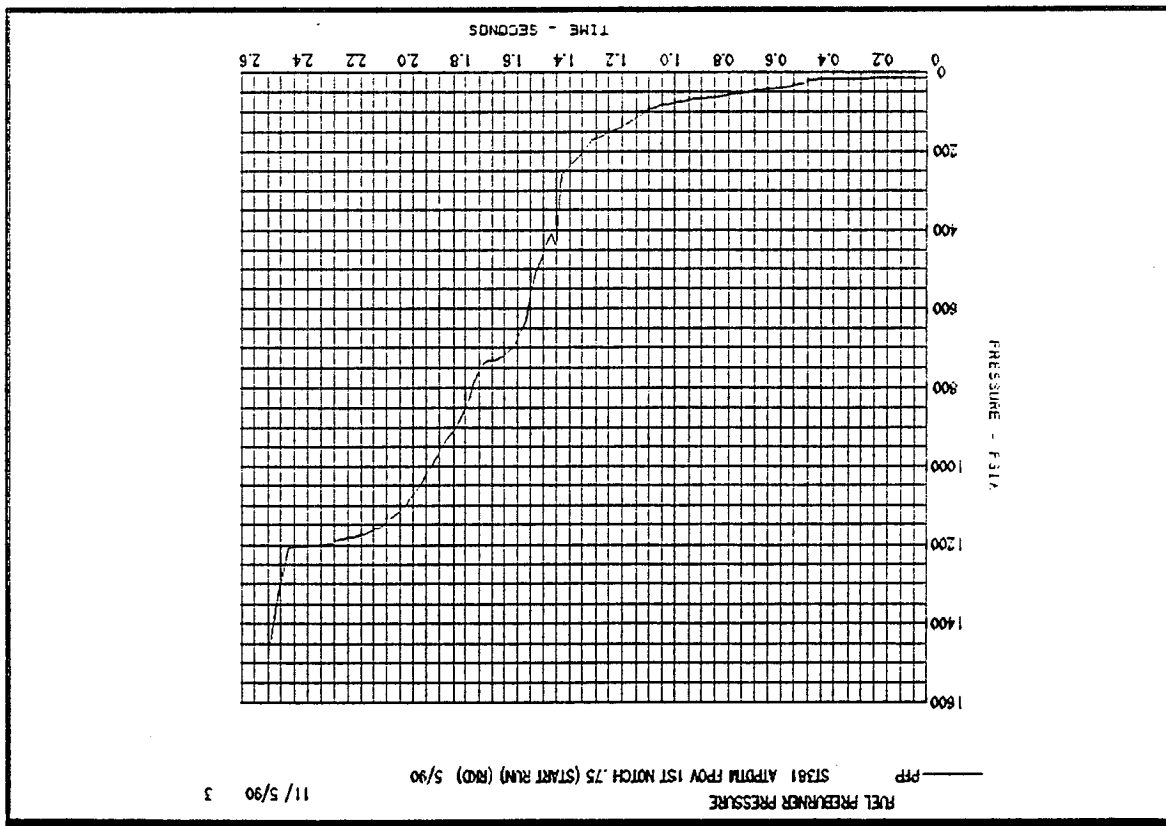
Appendix 3

SSME Start Transient Simulation Results

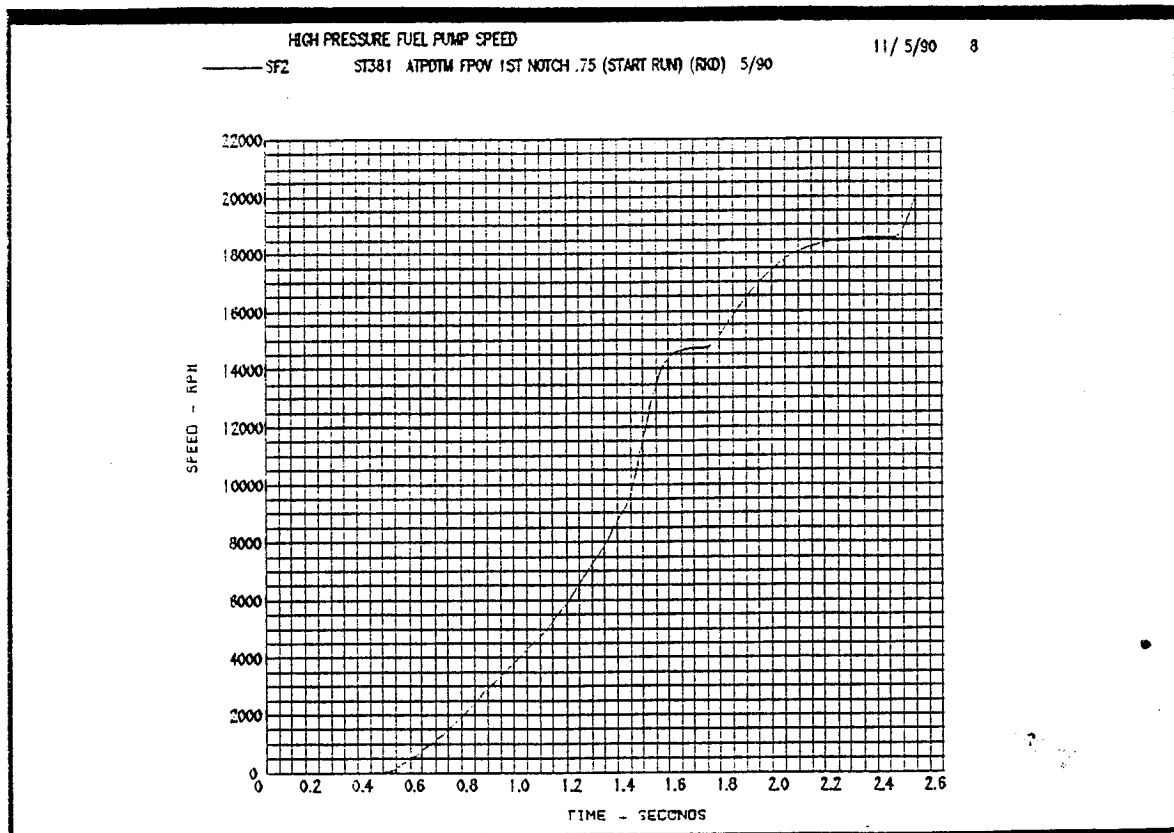
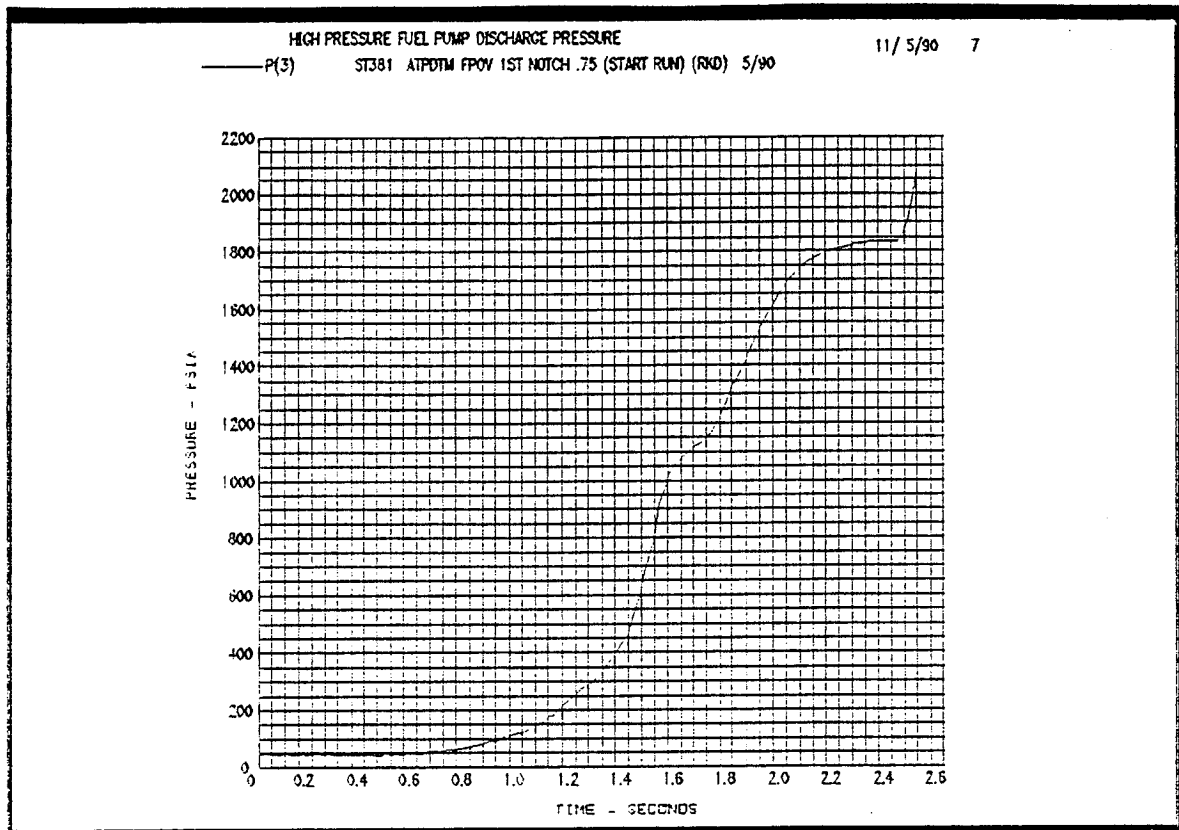
FPOV 1st Notch @ 0.75 seconds

APPENDIX 3

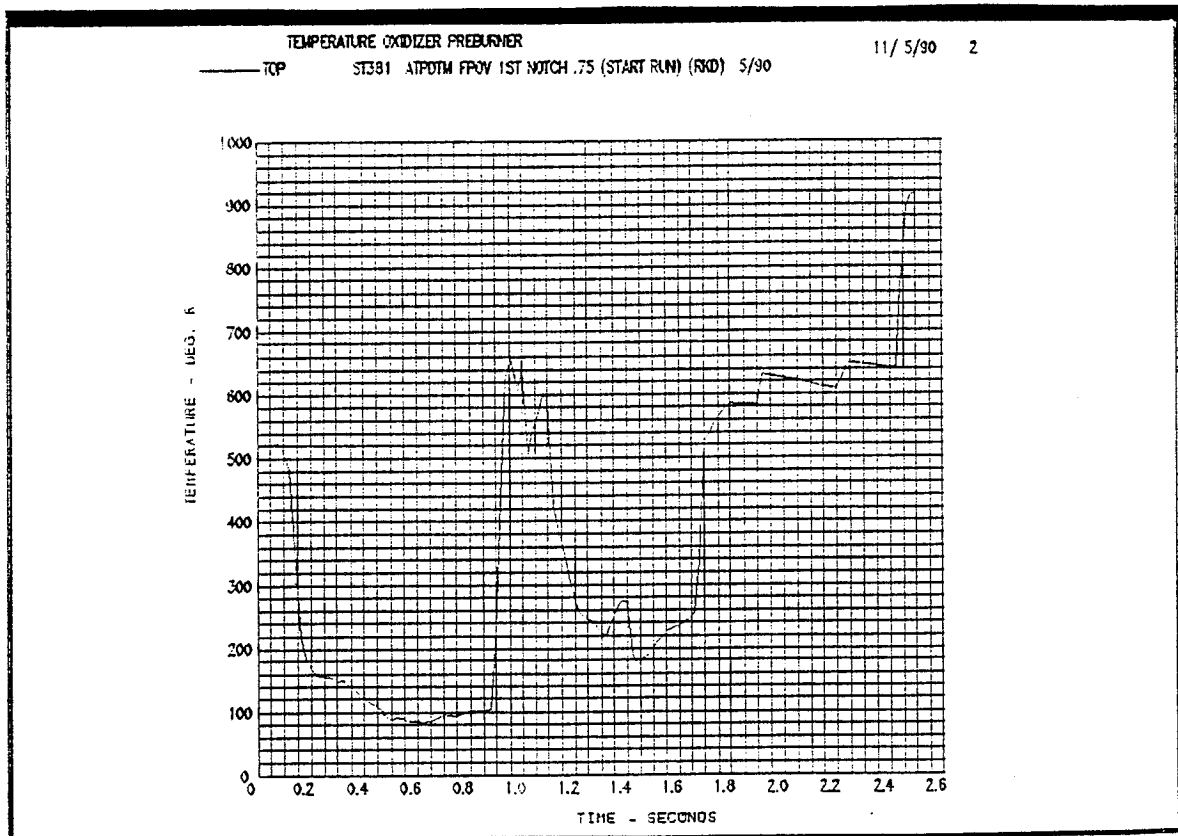
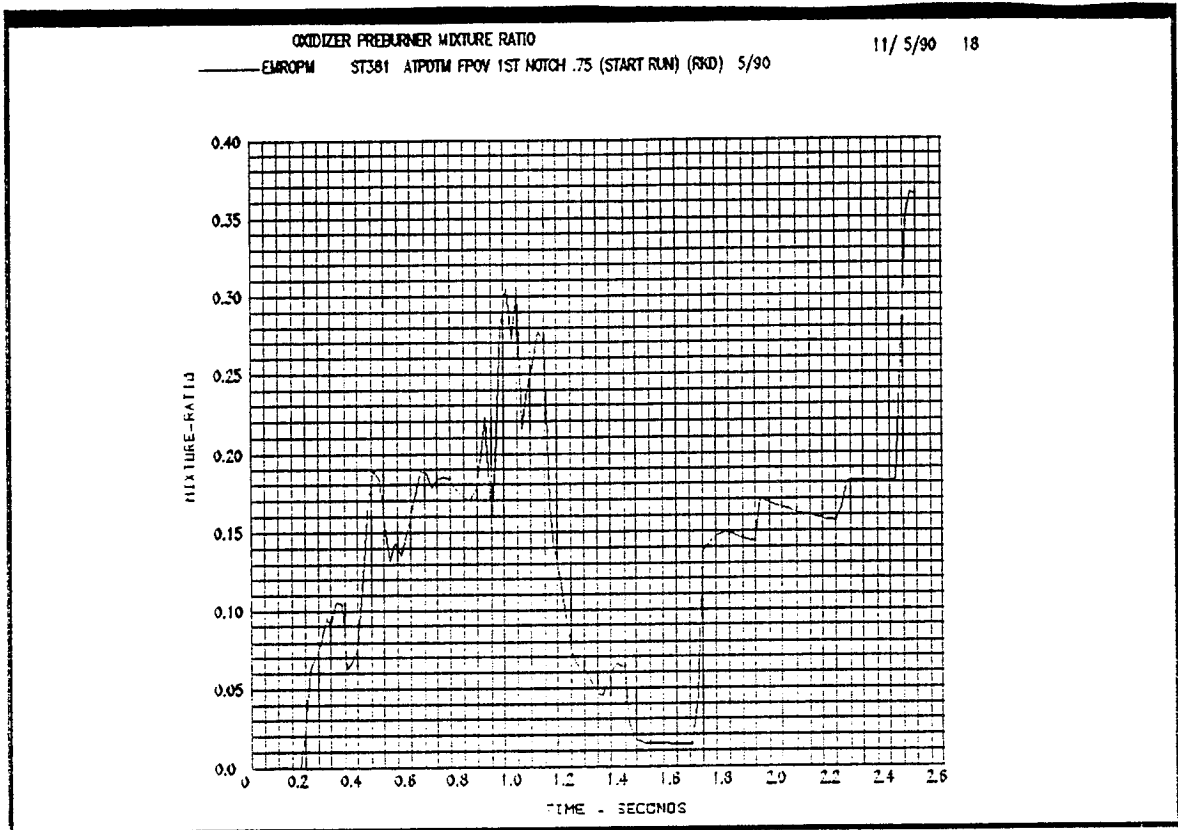




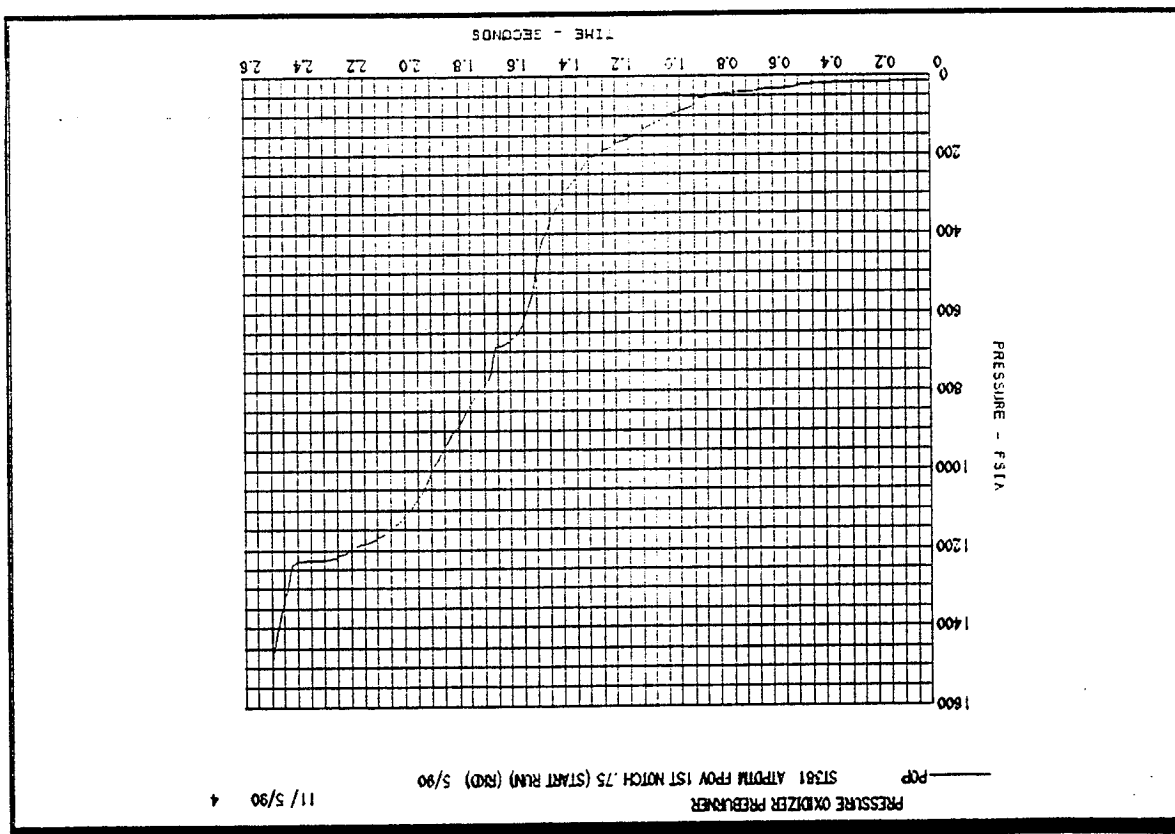
APPENDIX 3



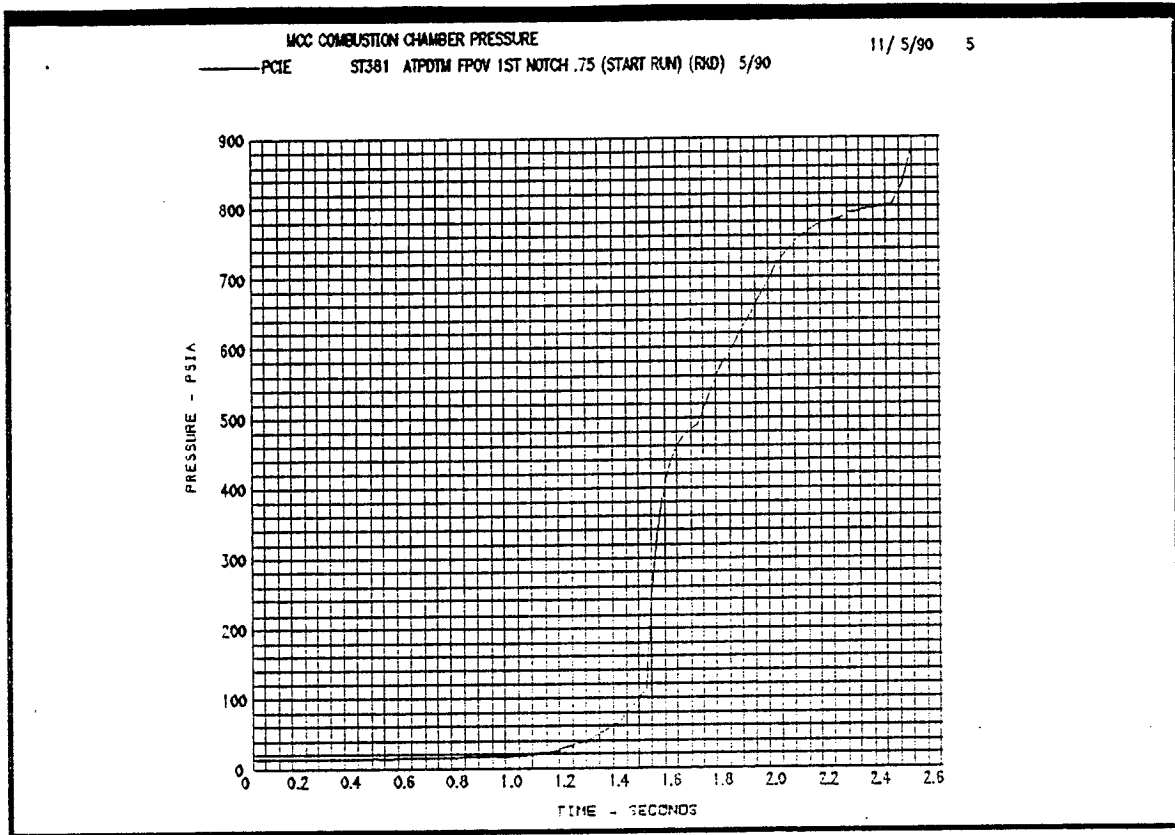
APPENDIX 3



APPENDIX 3



APPENDIX 3



Appendix 4

Listing of SSME Start Transient Control Actions

<u>Step</u>	<u>Action</u>	<u>Time (seconds)</u>
1	Update Engine Status Word to Start Initiation mode of Start phase.	0
	Limit OPOV command to 70% and FPOV command to 56.1%. Set initial OPOV Delta Power Level to 9.65517%. NOTE - For FRT limit OPOV command to a constant 100% throughout START/MAINSTAGE.	
2	Reset TIME REFERENCE to Zero.	--
3	Initial conditions of propellant and pneumatic valves assumed per ending status of Start Preparation phase (except for Engine Fuel Purge). Energize all igniters.	--
4	Set MCC Pressure Reference at 731 psia.	--
5	De-energize Fuel System Purge Control Valve Channel A and Channel B.	--
6	Initiate Shutdown Limit Monitoring for HPOP Intermediate Seal Purge, and HPOT Secondary Seal Cavity Pressures.	--
7	Initiate Sensor Qualification Monitoring for HPOT Turbine Discharge Temperature. Initiate Shutdown Limit Monitoring for Preburner S/D Purge Pressures.	--
8	Ramp MFV to 100% actuator position at 150%/second actuator rate.	--
9	Set Sequence for Shutdown from Start.	--
	(a) Set FPOV shutdown compare position No. 3 to 43% open.	
	(b) Set FPOV shutdown actuator rate No. 2 to 14%/second.	

<u>Step</u>	<u>Action</u>	<u>Time (seconds)</u>
9	(Continued)	
	(c) Set OPOV shutdown actuator rate No. 3 to 70%/second.	
	(d) Set OPOV shutdown actuator rate (effective at Shutdown+1.42 sec) to 70%/sec.	
	(e) Set Preburner Shutdown purge ON time equation to accommodate time = 2.2 sec at RPL and time = 1.8 sec at 65% RPL.	
10	Ramp MOV to 59.3% actuator position at 60%/sec actuator rate.	0.10
11	Ramp FPOV to 30% actuator position at 200%/sec actuator rate.	--
12	Ramp OPOV to 30% actuator position at 200%/second actuator rate.	0.12
13	Ramp FPOV to 56.1% actuator position at 200%/sec actuator rate.	0.26
14	Ramp OPOV to 48.0% actuator position at 20.0%/sec actuator rate.	0.28
15	Ramp FPOV to 47.0% actuator position at 200%/sec actuator rate.	0.68
16	Change FPOV and OPOV ramp rates to 100 percent per second and 100 percent per second respectively.	0.74
17	Initiate closed-loop MCC Pressure control (proportional error control only). In addition continue to completion the OPST schedule. Initial value of proportional error control gain = 0.01444 percent/psia	.74

<u>Step</u>	<u>Action</u>	<u>Time (seconds)</u>
18	Ramp MCC Pressure reference to 406 psia at 8.0 psi/20 msec.	--
19	Set FPOV crossfeed gain to 0.4596% per % and ramp to 1.15% per % at 0.5676% per % per second. In addition continue to completion the FPST schedule.	0.80
20	Ramp FPOV to 51.5 percent actuator position at 200 percent per second actuator rate.	0.88
21	Ramp OPOV to 38.5 percent actuator position at 200 percent per second actuator rate.	1.10
22	Ramp FPOV to 49.0 percent actuator position at 200 percent per second actuator rate.	1.16
23	Check HPFP Shaft Speed within limits for ignition confirmation.	1.24
24	Ramp CCV to 70 percent actuator position at 100 percent per second.	1.46
25	Ramp OPOV to 38.5 percent actuator position at 200 percent per second actuator rate.	1.50
26	Ramp FPOV to 54.6 percent actuator position at 200 percent per second actuator rate.	1.68
26a	Verify Main Combustion Chamber Pressure is within ignition confirm limits.	1.70
27	Ramp OPOV to 48.5 percent actuator position at 200 percent per second actuator rate.	2.10
28	Initiate channel qualification monitoring of MCC Pressure as a function of Pc Reference Value.	--
29	Monitor for DCU switchover or PFI/PRI sequence for Anriflood valve monitoring delay.	2.26
29a	Latest time to perform Shutdown Limit Monitoring on Preburner Shutdown Purge Pressures.	2.28

<u>Step</u>	<u>Action</u>	<u>Time (seconds)</u>
30	Verify Main Combustion Chamber Pressure is within limits and Antiflood Valve is open for ignition confirmation.	2.30
31	Initiate Shutdown Limit Monitoring of HPOT Turbine Discharge Temperature Upper Limit.	--
32	Change FPOV command limit to 102%. Retain OPOV command limit 70%.	--
33	Terminate monitoring for DCU switchover or PFI/PRI sequence.	--
34	Set Backup DCU ignition confirmation for MCC Pc and AFV.	2.40
35	Ramp OPOV to 49.1 percent actuator position and change OPOV ramp rate limit to 100% per second.	--
36	Ramp FPOV to 56.85 percent actuator position and change FPOV ramp rate limit to 100% per second.	--
37	Switch to Mainstage gain value of proportional error control and <u>activate integral error control for MCC Pressure.</u>	2.40
38	Activate POGO Precharge Control Valve Channel A and Channel B	--
39	Step MCC Pressure reference to 737 psia, then ramp MCC Pressure reference to command level at 34.46 psi/20 msec rate.	--
40	De-energize all igniters.	--
41	Ramp MOV to 100% actuator position at 31.50%/sec actuator rate.	--
42	Ramp CCV to 52% actuator position at 45.0%/second actuator rate.	--
43	Update Engine Status Word to indicate Thrust Buildup mode, if Hydraulic or Electrical Lockup not in effect.	2.42

<u>Step</u>	<u>Action</u>	<u>Time (seconds)</u>
44	Terminate channel qualification monitoring of MCC Pressure as a function of Pc Reference value.	--
45	Initiate channel "band test" qualification monitoring of MCC Pressure as a function of Pc Reference value.	--
46	Initiate scheduled operation of CCV as a function of MCC Pressure Reference (CCV = 52% at 50% RPL; CCV = 100% at RPL)	2.80
46a	Initiate Fuel Flowrate individual sensor qualification tests and inter-channel test	3.50
47	Initiate OPOV command limiting as a function of Pc Reference.	3.60
48	Initiate closed-loop mixture ratio control (proportional plus integral control)	3.6
49	Initiate both MCF Limit monitoring and Lower Shutdown Limit monitoring for HPOT Turbine Discharge Temperature	3.80
50	De-activate POGO Precharge Control Valve Channel A and Channel B	4.40
51	Verify POGO Precharge pressure is within limits.	4.94
52	Last time to monitor POGO Precharge pressure.	4.98
53	Reinitialize control-loop integrators to zero as required. Reinitialize OPST and FPST so that OPOV command and FPOV command remain unchanged by reinitialization. Set Mainstage Pc Reference Rate Limit to 6 psi/20 msec. Set maximum rate limits for FPOV and OPOV total valve command positions to 200%/second.	--
54	Initiate scheduled operation of MOV as a function of MCC Pressure Reference. (MOV = 100% at 50% RPL; MOV = 100% at RPL).	--
55	Initiate scheduled operation of MFV as a function of MCC Pressure Reference. (MFV = 100% at 50% RPL; MFV = 100% at RPL.)	--

<u>Step</u>	<u>Action</u>	<u>Time (seconds)</u>
56	Set Sequence for Shutdown from Mainstage	--
	(a) Set FPOV Shutdown compare position No. 3 to 40% open.	
	(b) Set FPOV Shutdown actuator rate No. 2 to 18%/second.	
	(c) Set OPOV Shutdown actuator rate No. 3 to 30%/second.	
	(d) Set OPOV Shutdown actuator rate (effective at Shutdown + 1.42 sec) to 200%/second.	
	(e) Set Preburner Shutdown Purge ON time equation to accommodate time = 1.8 sec at RPL and at 65% RPL (i.e., zero slope).	
57	Change engine phase of Engine Status Word to Mainstage. If in Hydraulic Lockup, Electrical Lockup, or Fixed Density then report the corresponding mode in the Engine Status Word, else report Normal Control in the Engine Status Word.	5.00
58	Change crossfeed gain schedule.	
59	Discontinue "band test" and initiate "delta test" to qualify MCC Pressure channels as a function of Pc Reference value.	
60	Initiate monitor for OPOV position.	5.02
61	Initiate both Sensor Qualification and Shutdown Limit Monitoring for HPFT TDT, HPFP Coolant Liner Pressure, and MCC Pc.	5.04
62	Terminate monitor for maximum OPOV position.	5.5
	Calculate OPOV Delta Power Level using the maximum OPOV position observed between 5.02 and 5.5 seconds. Use OPOV Delta Power Level and Pc Reference to determine a dynamic OPOV Command Limit each Major Cycle.	--

Appendix 5

ICS Propulsion Level Simulation

BASIC code listing

'ics propulsion level simulation, icsp9

screen 1

ied1=0

ied2=0

ied3=0

iet=0

' define output file

open "icsp2.out" for output as 1

tmax=10

dt=.02

for t=0 to tmax step dt

'----- Input Parameters -----

'thrust command

tc=1000000

if t>1 then tc=1400000

if t>3 then tc=1100000

if t>4.5 then tc=1400000

if t>8 then tc=1400000-(t-8)*100000

'downthrust deviations

d1=d1a

d2=d2a

d3=d3a

if t>2 then d1=1.1*d1a

if t>4.5 then d1=1.2*d1a

if t>6 then d2=d2a*(1-(t-6)/5*0.8)

'-----engine models-----

df1a=(f1-f1a)/0.1

f1a=f1a+df1a*dt

d1a=0.000001*f1a+0.43

df2a=(f2-f2a)/0.1

f2a=f2a+df2a*dt

d2a=0.000001*f2a+0.43

df3a=(f3-f3a)/0.1

f3a=f3a+df3a*dt

d3a=0.000001*f3a+0.43

-----controller-----
k0=1:'Thrust Error Proportional Gain
k1=5:'Thrust Error Integral Gain
k2=100000:'Downthrust Factor Proportional Gain
k3=5000000:'Downthrust Factor Integral Gain

da=(d1+d2+d3)/3

g1=1

g2=1

g3=1

if f1<305001 then if d1-da>0 then g1=0

if f1>511999 then if d1-da<0 then g1=0

if f2<305001 then if d2-da>0 then g2=0

if f2>511999 then if d2-da<0 then g2=0

if f3<305001 then if d3-da>0 then g3=0

if f3>511999 then if d3-da<0 then g3=0

if g1+g2+g3=0 then ed1=0:ed2=0:ed3=0:goto 10

da=(g1*d1+g2*d2+g3*d3)/(g1+g2+g3)

ed1=g1*(d1-da)

ed2=g2*(d2-da)

ed3=g3*(d3-da)

10

et=tc-f1a-f2a-f3a

ied1=ied1-(k3*ed1)*dt

ied2=ied2-(k3*ed2)*dt

ied3=ied3-(k3*ed3)*dt

iet=iet-(k1*et)*dt

f1=iet+k0*et-ied1-k2*ed1

f2=iet+k0*et-ied2-k2*ed2

f3=iet+k0*et-ied3-k2*ed3

if f1<305000 then f1=305000

if f1>512000 then f1=512000

if f2<305000 then f2=305000

if f2>512000 then f2=512000

if f3<305000 then f3=305000

if f3>512000 then f3=512000

----- screen output -----

```
locate 1,1:print int(f1a);int(f2a);int(f3a);int(f1a+f2a+f3a),int(1000*d2)/1000
```

```
ptc=tc/165  
pf1a=f1a/165  
pf2a=f2a/165  
pf3a=f3a/165
```

```
circle (t*300/tmax,60-(ptc-5000)*60/6000),.1,1  
circle (t*300/tmax,60-(pf1a+pf2a+pf3a-5000)*60/6000),.1,2
```

```
circle (t*300/tmax,120-(pf1a-1600)*60/1600),.1,1  
circle (t*300/tmax,120-(pf2a-1600)*60/1600),.1,2  
circle (t*300/tmax,120-(pf3a-1600)*60/1600),.1,3
```

```
circle (t*300/tmax,180-(d1)*60),.1,1  
circle (t*300/tmax,180-(d2)*60),.1,2  
circle (t*300/tmax,180-(d3)*60),.1,3
```

-----file output-----

```
print#1,t,int(tc),int(f1a+f2a+f3a),int(f1a),int(f2a),int(f3a),d1,d2,d3
```

```
next t  
close #1
```